Doctoral Thesis
Stockholm, Sweden 2014

On the Dynamics and Statics of Power System Operation

Optimal Utilization of FACTS Devices and Management of Wind Power Uncertainty

Amin Nasri

On the Dynamics and Statics of Power System Operation

Optimal Utilization of FACTS Devices and Management of Wind Power Uncertainty

Amin Nasri

Doctoral thesis supervisors:

Prof. Mehrdad Ghandhari, Kungliga Tekniska Högskolan

Members of the Examination Committee:

Prof. Lars Nordström,	Kungliga Tekniska Högskolan
Prof. Luis Rouco,	Universidad Pontificia Comillas
Dr. Marjan Popov,	Technische Universiteit Delft
Prof. Elling W. Jacobsen,	Kungliga Tekniska Högskolan
Dr. Stefan Arnborg,	Svenska kraftnät

This research was funded by the European Commission through the Erasmus Mundus Joint Doctorate Program, and also partially supported by the KTH Royal Insititute of Technology.

TRITA-EE 2014:048
ISSN 1653-5146
ISBN 978-91-7595-302-1

Printed by: US-AB 2014

On the Dynamics and Statics of Power System Operation

Optimal Utilization of FACTS Devices and Management of Wind Power Uncertainty

PROEFSCHRIFT

ter verkrijging van de graad van doctor
aan de Technische Universiteit Delft,
op gezag van de Rector Magnificus prof. ir. K.C.A.M. Luyben,
voorzitter van het College voor Promoties,
in het openbaar te verdedigen
op donderdag 13 november 2014 om 14:00 uur

door

Amin Nasri

geboren te Mashhad, Iran

Dit proefschrift is goedgekeurd door de promotoren:

Prof.dr. Mehrdad Ghandhari,	Kungliga Tekniska Högskolan
Prof.dr.ir. Paulien M. Herder,	Technische Universiteit Delft, promotor

Samenstelling promotiecommissie:

Prof.dr. Lars Nordström,	Kungliga Tekniska Högskolan
Prof.dr. Luis Rouco,	Universidad Pontificia Comillas
Dr. Marjan Popov,	Technische Universiteit Delft
Prof.dr. Elling W. Jacobsen,	Kungliga Tekniska Högskolan
Dr. Stefan Arnborg,	Svenska kraftnät

Keywords: Trajectory sensitivity analysis (TSA), transient stability, small signal stability, flexible AC transmission system (FACTS) devices, critical clearing time (CCT), optimal power flow (OPF), ac unit commitment (ac-UC), wind power uncertainty, wind power spillage, stochastic programming, Benders' decomposition.

ISBN 978-91-7595-302-1

Printed by: US-AB 2014

SETS Joint Doctorate

The Erasmus Mundus Joint Doctorate in **Sustainable Energy Technologies and Strategies**, SETS Joint Doctorate, is an international programme run by six institutions in cooperation:

- Comillas Pontifical University, Madrid, Spain
- Delft University of Technology, Delft, the Netherlands
- Florence School of Regulation, Florence, Italy
- Johns Hopkins University, Baltimore, USA
- KTH Royal Institute of Technology, Stockholm, Sweden
- University Paris-Sud 11, Paris, France

The Doctoral Degrees issued upon completion of the programme are issued by Comillas Pontifical University, Delft University of Technology, and KTH Royal Institute of Technology.

The Degree Certificates are giving reference to the joint programme. The doctoral candidates are jointly supervised, and must pass a joint examination procedure set up by the three institutions issuing the degrees.

This Thesis is a part of the examination for the doctoral degree.

The invested degrees are official in Spain, the Netherlands and Sweden respectively.

SETS Joint Doctorate was awarded the Erasmus Mundus **excellence label** by the European Commission in year 2010, and the European Commission's **Education, Audiovisual and Culture Executive Agency**, EACEA, has supported the funding of this programme.

The EACEA is not to be held responsible for contents of the Thesis.

Abstract

Nowadays, power systems are dealing with some new challenges raised by the major changes that have been taken place since 80's, e.g., deregulation in electricity markets, significant increase of electricity demands and more recently large-scale integration of renewable energy resources such as wind power. Therefore, system operators must make some adjustments to accommodate these changes into the future of power systems.

One of the main challenges is maintaining the system stability since the extra stress caused by the above changes reduces the stability margin, and may lead to rise of many undesirable phenomena. The other important challenge is to cope with uncertainty and variability of renewable energy sources which make power systems to become more stochastic in nature, and less controllable.

Flexible AC Transmission Systems (FACTS) have emerged as a solution to help power systems with these new challenges. This thesis aims to appropriately utilize such devices in order to increase the transmission capacity and flexibility, improve the dynamic behavior of power systems and integrate more renewable energy into the system. To this end, the most appropriate locations and settings of these controllable devices need to be determined.

This thesis mainly looks at (i) rotor angle stability, i.e., small signal and transient stability (ii) system operation under wind uncertainty. In the first part of this thesis, trajectory sensitivity analysis is used to determine the most suitable placement of FACTS devices for improving rotor angle stability, while in the second part, optimal settings of such devices are found to maximize the level of wind power integration. As a general conclusion, it was demonstrated that FACTS devices, installed in proper locations and tuned appropriately, are effective means to enhance the system stability and to handle wind uncertainty.

The last objective of this thesis work is to propose an efficient solution approach based on Benders' decomposition to solve a network-constrained ac unit commitment problem in a wind-integrated power system. The numerical results show validity, accuracy and efficiency of the proposed approach.

Keywords: Trajectory sensitivity analysis (TSA), transient stability, small signal stability, flexible AC transmission system (FACTS) devices, critical clearing time (CCT), optimal power flow (OPF), network-constrained ac unit commitment (ac-UC), wind power uncertainty, wind power spillage, stochastic programming, Benders' decomposition.

Sammanfattning

Numera bemöter dagenskraftsystem nya utmaningar på grund av de stora förändringar som har börjat ske sedan 80-talet, till exempel, avregleringar på elmarknaden, betydande ökning av efterfrågan för el och på senare tid storskalig integrering av förnybara energikällor som vindkraft. Därför måste systemansvariga göra vissa justeringar för att tillgodose dessa förändringar i framtiden för kraftsystem.

En av de största utmaningarna är att upprätthålla stabiliteten i systemet eftersom de extra system på frestningar som orsakas av ovanstående förändringar minskar stabilitetsmarginalen, och kan leda till uppkomsten av många oönskade fenomen. Den andra viktiga utmaningen är att hantera produktionsosäkerhet och variationer i förnybara energikällor som gör kraftsystem att bli mer stokastiska i naturen, och mindre kontrollerbar.

Flexible AC Transmission Systems (FACTS) har vuxit fram som en lösning för att hjälpa kraftsystem med dessa nya utmaningar. Avhandlingen syftar till att på lämpligt sätt utnyttja sådana styrbara komponenter för att öka överföringskapaciteten och flexibiliteten, förbättra det dynamiska beteendet hos kraftsystem och integrera mer förnybar energi i systemet. För detta ändamål de lämpligaste platserna och inställningarna för dessa styrbara komponenter måste bestämmas.

Denna avhandling tittar främst på (i) rotorvinkelstabilitet, dvs små signal och transient stabilitet (ii) systemdrift vid osäkerhet i vindkraftsproduktion. I den första delen av denna avhandling, tillämpas trajektoriakänslighetsanalys för att fastställa den lämpligaste placeringen av FACTS-komponenter för att förbättra rotorvinkelstabilitet, medan den andra delen ska optimala inställningar för FACTS-komponenter hittas för att maximera nivån av vindkraft integration. Som en allmän slutsats, visades att FACTS-komponenter installerade i rätt lägen och lämpliga inställningar, är effektiva medel för att stärka systemets stabilitet och för att hantera osäkerhet i vindkraftsproduktion.

Det sista målet av denna avhandling är att föreslå en effektiv lösning baserad på "Benders' decomposition" för att lösa korttidsdriftplanering problematiken i ett kraftsystem med vindkraft. De numeriska resultaten visar giltighet, noggrannhet och effektivitet av den föreslagna lösningen.

Acknowledgments

I deeply thank my supervisor Professor Mehrdad Ghandhari for his expert guidance, wise advise and help during the last four years. I would also like to thank Professor Lennart Söder for his support, and also for providing an outstanding research atmosphere at Electric Power System department, KTH Royal institute of Technology.

I am truly grateful to Professor Antonio J. Conejo for his excellent supervision and guidance through our collaboration over the last two years of my PhD. Working with him has been a fruitful experience for me. I would like to thank my friends, Doctor Seyyedjalal Kazempour and Associate Professor Robert Eriksson, for the helpful advices and stimulating discussions regarding technical and mathematical aspects of this work.

I also appreciate the technical support I gained from the research group of Professor Luis Rouco at Pontificia Comillas University, Madrid, Spain, during my research mobility from September 2012 to June 2013.

I would like to express my gratitude towards all partner institutions within the SETS programme as well as the European Commission for its financial support.

My gratitude goes to my colleagues at the division of Electric Power System at KTH for the friendly and multi-cultural atmosphere, interesting conversations, lunches and coffee breaks!

Finally, many thanks, from the bottom of my heart, to my lovely wife Behnaz and my parents for their endless love and all their support.

Contents

Chapter 1

Introduction

1.1 Background

Evolution is not just a biological concept. Everything in this world even nonliving things are subject to change. The electric power system is not also exempted from this law, and indeed it has been changed significantly over the last decades. Among these changes, restructuring of the electric power industry and the advent of renewable energy resources are of higher importance [1].

The restructuring of the electric power industry was initiated in the 80's in order to unbundle the vertically integrated utilities, and establish competitive electricity markets with private players [2]. Previously, power systems worldwide were run by regulated monopolies where the regulations were generally imposed by the government authorities. Rapid technology changes in the mid 70's drove real prices down and gave the opportunity to private players to independently generate power. Moreover, critical thoughts have emerged regarding the performance of monopoly utilities in providing incentive for efficient operation. The factors identified above are among the most important ones contributing to the deregulation of power industry and creation of modern electricity markets [3]. Basically, an electricity market consists of three main parts: (i) power producers who submit their production offers aiming to maximize their profits, (ii) consumers who submit their demand bids, with the goal to maximize their utilities and (iii) market operator which is a non-profit entity whose duty is to clear the market, with the objective of maximizing the social welfare. With this open market for electricity, producers and consumers have more freedom for trading energy with each other. Obviously, every costumer wants to buy power from the cheapest generator available, regardless of relative geographical location of costumer and producer. As a result, destructive phenomena may happen, e.g., transmission lines transferring powers from cheaper generators would become fully loaded or the amount of power provided by critical generators may increase. Moreover, the liberalization in the electricity sector led power systems to be more interconnected, and have increased cross-border trades

through long distance transmission lines [4]. Considering all the above factors, the new competitive environment puts an extra stress on the system which may lead to rise of many undesirable phenomena.

The other major change in today's power systems is the dramatic growth in share of renewable energy sources in the generation portfolio. According to renewables 2013 global status report, total renewable power capacity worldwide, after increasing 21.5% in 2012, exceeded 480 *GW* (not including hydro power) [5]. Renewable energy is the key solution to manage diminishing fossil fuel reserves, and to combat with climate change and global warming. Wind power and solar PV are those renewable resources with utmost growth. In the European Union, almost 70% of the newly installed electric capacity in 2012 is related to solar PV and wind power. Among the renewable energy sources, wind power is relatively cheaper, and technologically more mature. The total capacity of solar PV world-wide is 100 *GW* by 2012, while such a capacity for wind power is 283 *GW* . Denmark and Italy have more than 30% penetration of wind power in their grids [5]. As a result of inherent variability and uncertainty of these resources, the power injection into the grid becomes more stochastic in nature, and less controllable by the system operator. Thus, the large-scale integration of wind power and solar PV into an electric power system poses new challenges which will require system operators to make adjustments to accommodate these into the future.

At the same time, a number of other technologies, especially applications of power electronics in power system, have been also evolved which help power systems to cope with the changes described above. Power electronic based controllable devices such as Flexible AC Transmission Systems (FACTS) and High Voltage DC transmissions have emerged for increasing the transmission capacity and flexibility, improving the dynamic behavior of power systems, integrating more renewable energy into the system, etc [6]. In addition, power system monitoring and measurement have been upgraded with the appearance of new technologies, e.g., Phasor Measurement Units (PMU) and Wide Area Measurement Systems (WAMS) helping the system in managing the increased grid complexity due to the aforementioned evolutions.

1.2 Challenges and motivations

1.2.1 Power system stability

Deregulation in electricity markets, increasing electricity demands and high penetration of renewable energy sources on one hand, and insufficient construction of new transmission lines due to the economical and environmental concerns, on the other hand, have pushed the existing transmission systems to be operated close to their stability limits. Therefore, nowadays, there is a higher risk of instability in power systems after being subjected to disturbances [7]. The dynamic performance of power systems is important from both economic and reliability point of view, i.e., the power system should remain stable and be capable of withstanding a

wide range of disturbances in order to supply reliable service to consumers. Therefore, it is crucial that the system stability is improved in today's heavy-loaded and interconnected power systems.

In general, power system stability is defined as the ability of a power system to remain in a state of operating equilibrium point under normal operating conditions and to regain an acceptable state of equilibrium after being subjected to a disturbance [8]. Stability of power systems is classified into three different categories. First classification is rotor angle stability dealing with the ability of interconnected machines of a power system to remain in synchronism after being subjected to a disturbance. The second stability classification is voltage stability which refers to the ability of a power system to maintain steady acceptable voltages at all the buses in the system after the incidence of disturbance. Finally, the third category called frequency stability discusses the ability of a power system to maintain steady frequency following a severe system upset which results in a significant imbalance between generation and load.

The rotor angle stability itself which is one of the main subjects under study in this thesis is divided into two subcategories [9]:

1. Small-signal stability which is concerned with the ability of power system to keep its synchronism under small disturbances such as small variations in loads and generation. The disturbances are considered to be sufficiently small that linearization of system equations is allowed for the purpose of analysis.

2. Transient stability which refers to the ability of power system to maintain its synchronism when subjected to a severe transient disturbance, e.g., a short-circuit on a transmission line. Transient stability depends on the initial operating state of the system as well as the type, severity and location of the disturbance.

Assessment of rotor angle stability is essential to study the dynamic behavior of power system. The analysis of small signal stability is more straightforward compared to transient stability since it deals with disturbances which are small enough that the system may be linearized for the purpose of study [10–13]. Small signal analysis are based on linear techniques such as modal analysis and prony analysis, and provides valuable information about the inherent dynamic characteristics of the power system [9].

On the other hand, transient stability is influenced by the nonlinear characteristics of the power system which makes it mathematically complicated. The methods proposed in the technical literature for transient stability assessment may be characterized as follows (in chronological order):

1. Time domain simulation method which is the traditional way for transient stability assessment. The main advantage of this method is its unlimited modeling capability, while it has two significant shortcomings, namely time-consuming computation requirement and incapability to provide any information regarding the stability margin [14].

2. Transient Energy Function (TEF) method (also known as the direct method) which is based on Lyapunov's second or direct method. This method gives an estimate of the actual stability region without explicitly solving the system differential equations [15–17]. The significant advantage of this method is its capability to provide a stability index [14]. Despite all the advantages of the TEF based methods, the main shortcoming of them is their high complexity in the following situations: (i) dealing with the detailed models of the system components, (ii) when a number of system parameters have to be taken into account for the sensitivity analysis, [18, 19] and the references therein.

3. SIngle Machine Equivalent (SIME) method, a hybrid-temporal transient stability approach which aims to combine the advantages of time domain simulation and TEF methods [20, 21]. In this method, the system machines are separated to two groups, namely critical and non-critical machines, and then, these two groups are replaced by a single machine equivalent system, to which it applies the equal-area criterion (EAC). SIME method does not have the modeling limitations of TEF method, and provide additional information such as stability margin, identification of the mode of instability and corresponding critical machines [22, 23]. In spite of all the advantages of this method, it is not able to provide an effective sensitivity approach to determine the impacts of system parameters on transient stability, except for some immature works [24, 25] that considered very simple modeling of system components.

4. Trajectory Sensitivity Analysis (TSA) method which calculates directly the sensitivities of dynamic trajectories of power system with respect to changes in parameters, or initial conditions. This analysis is based on linearizing the system around a trajectory, rather than around an equilibrium point [26]. This technique has all the advantages of other techniques, e.g., providing stability margin [27], no restriction on complexity of the model while providing security margin [28] and possibility to be extended to systems with discrete events [26, 29]. Additionally, this method provides valuable insight into the the impact of parameters on the stability of power system which can be used for study of parameter uncertainty in system behavior [30], dynamic security-constrained rescheduling of power systems [31], allocating power electronic based controllable devices [19], and etc. However, the cost to be paid for such advantages is the increased computational cost.

In Part I of this thesis, trajectory sensitivity analysis is used for assessment of rotor angle stability of power system. The main objective is to maximize the benefits of using FACTS devices in order to enhance the rotor angle stability. Note that these power electronic based devices have significant impacts on operational flexibility and controllability of power system. Using these devices, the power flow through the system can be controlled dynamically in a way to increase the transient stability margins, and make the system more secure [32–38]. These devices, equipped with the proper controller, can also be used to improve the small signal stability [39–44].

Since the impact of FACTS devices on the system stability is strongly dependent on their locations, it is required to provide useful information to the system planners regarding the best possible locations to install them. In this thesis, an effective approach based on analytical formulation of TSA is proposed to identify the most suitable placement of series and shunt compensators for improving the transient and small signal stability of power system.

1.2.2 Power system operation under wind uncertainty

In most real-world electricity markets, the share of wind power penetration in total installed generation capacity is rapidly increasing. Power systems with significant penetration of wind power need to be flexible to cope with uncertainties in wind generation.

Short-term trading of electricity is carried out through the day-ahead market and balancing market, which in most real-world markets take place from one day to one hour ahead of energy delivery [45–49]. By noon of the day prior to energy delivery, the day-ahead market is cleared and preliminary values for active power productions and consumptions are determined. Then, about 1 hour prior to power delivery, the "balancing market" (also called "real-time market") is cleared and "final" values for active power productions and consumptions are assigned to each generating unit and to each demand, respectively. This market is particularly relevant for stochastic producers such as wind power producers that cannot accurately predict their production levels in the day-ahead market [1]. In other words, the balancing market adjusts the results of the day-ahead market and compensates deviations. In general, a market clearing process under uncertainty is normally formulated as an optimization problem (decision-making problem) with uncertain parameters [50]. Different techniques, e.g., stochastic programming and robust optimization, can be used to handle such problems. The implementation of day-ahead market and balancing market under wind uncertainty has been widely investigated in the technical literature [51–53]. However, there are still lots of opportunities for research in this area. Part II of this thesis addresses the following challenges:

1. **Minimizing wind power spillage using FACTS devices:** wind power spillage refers to the amount of the wind power production which cannot not be used due to inherent variability of wind power and also technical reasons, e.g., insufficient transmission capacity. FACTS devices are capable to improve the operational flexibility of the system and help integrating increasing amounts of wind power. The fast operation of FACTS devices makes them appropriate tools to cope with the deviations of wind power production. In this thesis, an Optimal Power Flow (OPF) model with FACTS devices is proposed to minimize wind power spillage, i.e., maximize wind power integration. The proposed OPF model is used by the system operator after clearing the balancing market, and determine optimal reactive power outputs of gener-

ating units, voltage magnitude and angles of buses, deployed reserves, and optimal setting of FACTS devices.

2. **Solving a network-constrained ac unit commitment (ac-UC) problem under wind uncertainty:** the problem of unit commitment (UC) is carried out within day-ahead market, and determines the least-cost dispatch of available generation resources to meet the electrical load. This problem is not continuous since there is a binary variable related to each generating unit specifying if that unit is scheduled to be committed or not. A unit commitment problem becomes mathematically so complicated considering the detailed ac representation of the transmission system and wind uncertainty. Problems of this type are generally termed stochastic Mixed-Integer Nonlinear Programming (MINLP) problems [54], and no reliable off-the-shelf solver is available to guarantee their convergence or optimality. In this thesis, a decomposition-based approach is proposed to make the stochastic ac-UC problem efficiently solvable.

1.3 Objective and scope

The main objective of this thesis is to use FACTS devices for more efficient utilization of current transmission systems in order to enhance the system stability and integrate more wind power. Some challenges are to find the most appropriate locations and settings of these controllable devices. Accordingly, this thesis mainly looks at (i) rotor angle stability, i.e., small signal and transient stability (ii) system operation under wind uncertainty. In the first part of this thesis, trajectory sensitivity analysis is used to determine the most suitable placement of FACTS devices for improving rotor angle stability, while in the second part, optimal settings of such devices are found to maximize the level of wind power integration. The other objective of the second part of this thesis work is to propose an efficient solution approach based on Benders' decomposition to solve a network-constrained ac unit commitment problem in a wind-integrated power system. Note that no FACTS devices are considered in the work focusing on the network-constrained ac-UC problem. The assumptions considered in each study are reported in its corresponding chapter.

1.4 Contributions

The main contributions of this thesis are listed below:

1. **Rotor angle stability improvement**

   a) To propose a novel approach based on analytical formulation of TSA for suitable placement of series compensators in order to improve both the transient and small signal stability of power system. The proposed approach is formulated as a two-stage problem analyzing the pre-fault and post-fault behaviors of power system [Papers J1].

b) To find suitable placement of shunt compensators based on TSA in order to improve the transient stability of power system [Paper C3].

c) To appropriately allocate multiple series compensators based on TSA in order to improve dynamic behavior of power system [Paper C2].

d) To demonstrate the cases where installing series compensators in certain locations deteriorates the system stability [Papers J1, C4].

e) To show the impacts of inertia reduction of synchronous generators on the transient stability [Paper C1].

2. **Minimizing wind power spillage using FACTS devices**

a) To propose an OPF model with FACTS devices, compatible with the structure of most real-world electricity markets, whose objective is minimizing wind power spillage. This OPF model is run by the system operator once the final values of the active power productions and consumptions are assigned after market clearing [Paper J2].

b) To model the uncertainty of wind power production through a set of plausible wind power scenarios and to formulate the proposed OPF model using a two-stage stochastic programming problem [Paper J2].

c) To derive the optimal deployment of active and reactive power reserves, and to optimally identify the FACTS device's settings corresponding to each wind scenario, which result in minimum wind power spillage [Paper J2].

3. **Network-constrained ac unit commitment model under wind uncertainty**

a) To propose a stochastic ac-UC problem for a power system including significant wind power production [Paper J3].

b) To derive a way to decompose the proposed ac-UC problem by scenario and time period, which ease the computational burden [Paper J3].

c) To implement Benders' decomposition, which allows decomposing the original mixed-integer and non-linear ac-UC problem to (i) a mixed-integer linear master problem, and (ii) a set of non-linear, but continuous subproblems [Paper J3].

1.5 List of publications

The following articles were published during this project:

Papers in science citation index (JCR) journals:

Paper J1

A. Nasri, R. Eriksson and M. Ghandhari, "Using trajectory sensitivity analysis to find suitable locations of series compensators for improving rotor angle stability," *Electric Power System Research*, vol. 111, pp. 1-8, Jun. 2014.

Paper J2

A. Nasri, A. J. Conejo, S. J. Kazempour, and M. Ghandhari, "Minimizing wind power spillage using an OPF with FACTS devices," *IEEE Transactions on Power Systems*, vol. 29, no. 5, pp. 2150-2159, Sep. 2014.

Paper J3

A. Nasri, A. J. Conejo, S. J. Kazempour, and M. Ghandhari, "Network-constrained AC unit commitment under uncertainty: a Benders' decomposition approach," *IEEE Transactions on Power Systems*, provisionally accepted.

Conference papers:

Paper C1

A. Nasri, H. Chamorro and M. Ghandhari, "Multi-parameter trajectory sensitivity approach to analyze the impacts of wind power penetration on power system transient stability," *CIGRE AORC Technical meeting 2014*, Tokyo, Japan, May. 2014.

Paper C2

A. Nasri, R. Eriksson and M. Ghandhari, "Suitable placements of multiple FACTS devices to improve the transient stability using trajectory sensitivity analysis," *North American Power Symposium*, Manhattan, KS, Sep. 2013.

Paper C3

A. Nasri, M. Ghandhari, and R. Eriksson, "Transient stability assessment of power systems in the presence of shunt compensators using trajectory sensitivity analysis," *IEEE Power and Energy Society General Meeting (PES)*, Vancouver, BC, Jul. 2013.

Paper C4

A. Nasri, M. Ghandhari, and R. Eriksson, "Appropriate placement of series compensators to improve small signal stability of power system," *Energy Conference and Exhibition (ENERGYCON)*, Florence, Italy, Sep. 2012.

Paper C5

A. Nasri, M. Ghandhari, and R. Eriksson, "Appropriate placement of series compensators to improve transient stability of power system," *Innovative Smart Grid Technologies-Asia (ISGT Asia)*, Tianjin, China, May 2012.

1.6 Thesis outline

The studies carried out throughout this thesis work are divided to two main parts:

Part I Rotor angle stability improvement including chapters 2 and 3.

Part II Power system operation under wind uncertainty comprising chapters 4, 5 and 6.

The chapters of this thesis are organized as follows:

Chapter 2 gives a brief description of power system modeling and theoretical foundation of trajectory sensitivity analysis.

Chapter 3 proposes an approach based on trajectory sensitivity analysis to determine the most suitable placement of series and shunt compensators for improving rotor angle stability. In this chapter, the impacts of inertia reduction of the system on the transient stability are also analyzed.

Chapter 4 reviews briefly the application of stochastic programming for solving a decision-making problem under uncertainty. The theoretical background on Benders' decomposition technique is also addressed in this chapter.

Chapter 5 proposes an optimal power flow model with FACTS devices to minimize wind power spillage.

Chapter 6 presents an efficient solution approach based on Benders' decomposition to solve a network-constrained ac unit commitment (UC) problem in a wind-integrated power system.

Chapter 7 provides the conclusions of this dissertation, and suggests some topics for future research.

For the sake of clarity, the various subjects considered in each chapter of this dissertation are shown in Table 1.1.

Table 1.1: Items considered in various chapters

	Part I		Part II		
	Chapter 2	Chapter 3	Chapter 4	Chapter 5	Chapter 6
Rotor angle stability	✓	✓			
Trajectory sensitivity analysis	✓	✓			
FACTS devices		✓		✓	✓
Wind power		✓		✓	✓
Stochastic modeling			✓	✓	✓
Optimization			✓	✓	✓
Benders' decomposition			✓		✓

Part I

Rotor Angle Stability Improvement

Chapter 2

Power System Modeling and Trajectory Sensitivity Analysis

This chapter provides a brief overview on the modeling of the main components of power system. It also gives the theoretical foundation of trajectory sensitivity analysis.

2.1 Power system modeling

An electric power system is basically divided into three main sections: generation, transmission and distribution. The electricity is first produced by the generating units, and then it is feeded into the transmission system via the step-up transformers. The generated power is conveyed by the transmission lines to the point where it is delivered to the distribution system via step-down transformer. Finally, the distribution system feeds the power to nearby homes and industries. In this path, there are several components such as synchronous generators, transmission lines and electrical loads that should be modeled appropriately in order to analyze the interconnected power system as a whole.

In general, a power system can be modeled by the following differential algebraic equations (DAE) [26]

$$\dot{x} = f(x, y; \lambda) \tag{2.1}$$

$$0 = g(x, y; \lambda) \tag{2.2}$$

$$x(t_0) = x_0,\ y(t_0) = y_0 \tag{2.3}$$

where x is a vector containing the state variables, y is a vector of algebraic variables, λ is a vector of system parameters, f is a vector-valued function and g is the set of algebraic equations. Rotor angles of the generators, magnitude and angle of bus voltages and reactances of the transmission lines are the examples

of the state variables, algebraic variables and parameters of the power system, respectively. Vectors x_0 and y_0 are the initial conditions of state and algebraic variables. Note that in this thesis, equation (2.1) is used to model the dynamics of equipments such as synchronous generators while equation (2.2) consists of the network equations based on Kirchhoff's current law, i.e. the sum of all current (or powers) flowing into each bus must be equal to zero.

This chapter presents briefly the dynamic models of the main equipments which constitute equation (2.1) as well as their corresponding algebraic equations in a multi-machine power system which forms equation (2.2). When the system components are modeled properly, set of equations (2.1)-(2.3) is used for the assessment of power system stability.

2.1.1 Synchronous generators

A synchronous generator can be modeled at different levels for rotor angle stability studies. In this thesis, classical model which is the simplest one is considered for analyzing the dynamics of this component [55]. However, more detailed models such as one-axis model or two-axis model can also be easily incorporated. The classical model is also called "the constant voltage behind the transient reactance x'_d model" as shown in Fig. 2.1. The dynamic of synchronous generator k represented by this model is described by (2.4) and (2.5).

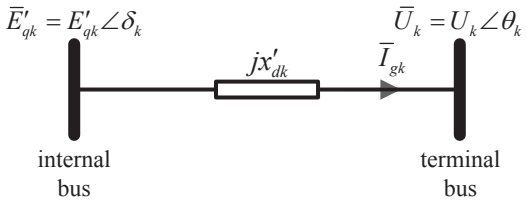

Figure 2.1: Dynamic circuit of a synchronous generator

for $k = 1, 2, \ldots n$

$$\dot{\delta}_k = \omega_k \tag{2.4}$$

$$\dot{\omega}_k = \frac{1}{M_k}(P_{mk} - \frac{E'_{q_k} U_k}{x'_{d_k}} \sin(\delta_k - \theta_k) - D_k\omega_k) \tag{2.5}$$

where n is the number of generators, and the state variables are:

- δ_k: the rotor angle of generator k
- ω_k: the rotor speed deviation of generator k from the synchronous speed

The algebraic variables are:

- U_k: the magnitude of the voltage of the generator terminal bus where the synchronous generator k is connected
- θ_k: the phase angle of U_k

and the vector of parameters includes:

- M_k: the inertia of generator k
- D_k: the shaft damping constant of generator k
- E'_{qk}: the voltage magnitude at the internal bus of generator k
- x'_{dk}: the d-axis transient reactance of generator k
- P_{mk}: the mechanical power applied to the shaft of generator k

Additionally, the complex power supplied by generator k, injected into its terminal bus k is defined by:

$$P_{gk} = \mathrm{Re}(\overline{U}_k \overline{I}^*_{gk}) = \frac{E'_{qk} U_k \sin(\delta_k - \theta_k)}{x'_{d_k}} \tag{2.6}$$

$$Q_{gk} = \mathrm{Im}(\overline{U}_k \overline{I}^*_{gk}) = \frac{E'_{qk} U_k \cos(\delta_k - \theta_k) - U_k^2}{x'_{d_k}} \tag{2.7}$$

2.1.2 Static load

The exponential model of load is considered in this thesis [56]. In this model, active and reactive components of the load as shown in Fig. 2.2 are expressed by (2.8) and (2.9).

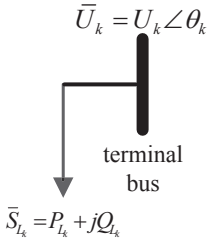

Figure 2.2: Static load connected to the grid

for $k = 1, 2, \ldots N$

$$P_{L_k} = P_{L0_k} \left(\frac{U_k}{U_{0_k}}\right)^{mp} \tag{2.8}$$

$$Q_{L_k} = Q_{L0_k} \left(\frac{U_k}{U_{0_k}}\right)^{mq} \tag{2.9}$$

where N is the total number of buses in the grid, and the only algebraic variable is:

- U_k: the magnitude of the voltage of the terminal bus where the load k is connected

In addition, the vector of parameters includes:

- mp, mq: the voltage exponents corresponding to active and reactive components of load k, respectively
- U_{0_k}: the steady-state pre-fault value of U_k
- P_{L0_k}, Q_{L0_k}: the steady-state pre-fault values of the active and reactive power components of load k, respectively

Obviously, the load model consists of only algebraic variables and parameters, and does not include any state variables.

2.1.3 Transmission line

The transmission lines are modeled using the Π model depicted in Fig. 2.3 [9].

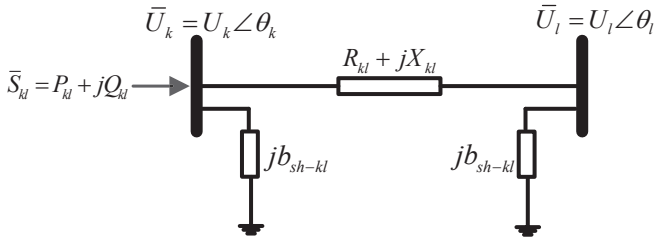

Figure 2.3: Equivalent Π circuit of a transmission line

Let

$$Z_{kl} = \sqrt{R_{kl}^2 + X_{kl}^2} \tag{2.10}$$

$$\theta_{kl} = \theta_k - \theta_l \tag{2.11}$$

$$g_{kl} + jb_{kl} = \frac{1}{R_{kl} + jX_{kl}} = \frac{R_{kl}}{Z_{kl}^2} + j\frac{-X_{kl}}{Z_{kl}^2} \tag{2.12}$$

The active and reactive power P_{kl} and Q_{kl} in the sending end k is given by [55]:

$$P_{kl} = g_{kl}U_k^2 - U_kU_j[g_{kl}\cos(\theta_{kl}) + b_{kl}\sin(\theta_{kl})] \tag{2.13}$$

$$Q_{kl} = (-b_{sh-kl} - b_{kl})U_k^2 - U_kU_j[g_{kl}\sin(\theta_{kl}) - b_{kl}\cos(\theta_{kl})] \tag{2.14}$$

Obviously, there is no state variables in the modeling of transmission line, and the algebraic variables are:

- U_k, U_l: the magnitude of the voltages at terminal buses on two sides of transmission line connecting bus k to bus l
- θ_k, θ_l: the phase angle of U_k and U_l

and the vector of parameters includes:

- R_{kl}: resistance of transmission line connecting bus k to bus l
- X_{kl}: reactance of transmission line connecting bus k to bus l
- b_{sh-kl}: shunt conductance of transmission line connecting bus k to bus l

Note that transformers are modeled as constant impedances and are not further described here.

2.1.4 Multi machine power system

Let us consider a multi-machine power system shown in Fig. 2.4 with n generators and a transmission network with N buses [55]. Considering classical model of generators, the dynamic of the k^{th} generator is given by (2.4) and (2.5).

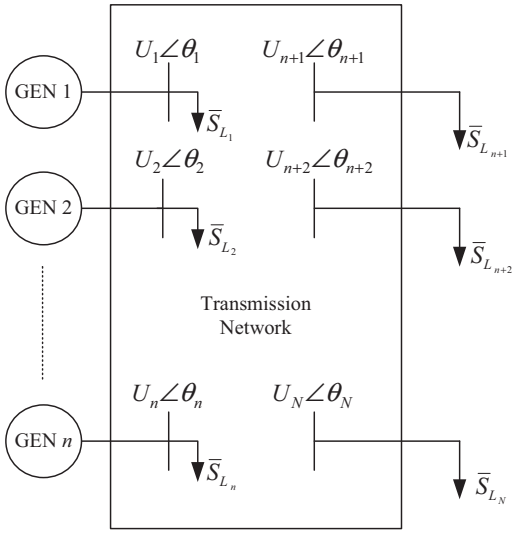

Figure 2.4: A multi-machine power system

Next, let Y_{bus} of order $(N \times N)$ be the admittance matrix of transmission network, and the $kl-th$ element of the admittance matrix be defined by

$$\overline{Y}_{bus_{kl}} = G_{kl} + jB_{kl} \tag{2.15}$$

Note that

$$G_{kl} = -g_{kl}, \quad B_{kl} = -b_{kl} \qquad \forall k, l \;\; if \; k \neq l \tag{2.16}$$

$$G_{kk} = \sum_{l \in \Omega_k} g_{kl}, \quad B_{kk} = \sum_{l \in \Omega_k} (b_{kl} + b_{sh-kl}) \qquad \forall k \tag{2.17}$$

where Ω_k is a set of system buses adjacent to bus k.

Concerning the transmission network, the complex power injected into bus k is given by:
for generator buses, i.e., $k = 1, ..., n$

$$P_k = U_k \sum_{l=1}^{N} [G_{kl} U_l \cos(\theta_k - \theta_l) + B_{kl} U_l \sin(\theta_k - \theta_l)] + \frac{E'_{qk} U_k \sin(\delta_k - \theta_k)}{x'_{d_k}} \tag{2.18}$$

$$Q_k = U_k \sum_{l=1}^{N} [G_{kl} U_l \sin(\theta_k - \theta_l) - B_{kl} U_l \cos(\theta_k - \theta_l)] + \frac{E'_{qk} U_k \cos(\delta_k - \theta_k) - U_k^2}{x'_{d_k}} \tag{2.19}$$

and for non-generator buses, i.e., $k = (n+1), ..., N$

$$P_k = U_k \sum_{l=1}^{N} [G_{kl} U_l \cos(\theta_k - \theta_l) + B_{kl} U_l \sin(\theta_k - \theta_l)] \tag{2.20}$$

$$Q_k = U_k \sum_{l=1}^{N} [G_{kl} U_l \sin(\theta_k - \theta_l) - B_{kl} U_l \cos(\theta_k - \theta_l)] \tag{2.21}$$

Finally, let P_{L_k} and Q_{L_k} be the active and reactive loads at bus k. Then, for $k = 1, ..., N$ the power flow equations (2.18)-(2.21) can be written as

$$0 = P_k + P_{L_k} \tag{2.22}$$

$$0 = Q_k + Q_{L_k} \tag{2.23}$$

Note that equations (2.22) and (2.23) represent the set of algebraic equations described in (2.2). Taking into account all the equations given above, the vector of state variables x and algebraic variables y considered in this thesis are:

$$x = [\delta_1 ... \delta_n, \omega_1 ... \omega_n]^T \tag{2.24}$$

$$y = [\theta_1 ... \theta_N, U_1 ... U_N]^T \tag{2.25}$$

2.2 Trajectory sensitivity analysis

Trajectory sensitivity analysis (TSA) calculates the sensitivity of state variable trajectories with respect to system parameters or initial conditions. To formulate TSA, the equations (2.1)-(2.3) are written in a more organized way, as described by (2.27)-(2.28), using vectors $\underline{x}$, $\underline{f}$ and $\underline{x}_0$ defined below:

$$\underline{x} = \begin{bmatrix} x \\ \lambda \end{bmatrix} \qquad \underline{f} = \begin{bmatrix} f \\ 0 \end{bmatrix} \qquad \underline{x}_0 = \begin{bmatrix} x_0 \\ \lambda \end{bmatrix} \tag{2.26}$$

and

$$\dot{\underline{x}} = \underline{f}(\underline{x}, y) \tag{2.27}$$
$$0 = g(\underline{x}, y) \tag{2.28}$$

To calculate the trajectory sensitivities analytically, the derivatives of (2.27)-(2.28) are calculated with respect to $\underline{x}_0$ which is a vector including the system parameters as well as the initial conditions of state variables

$$\dot{\underline{x}}_{\underline{x}_0} = \underline{f}_{\underline{x}}(t)\underline{x}_{\underline{x}_0} + \underline{f}_y(t)y_{\underline{x}_0} \tag{2.29}$$
$$0 = g_{\underline{x}}(t)\underline{x}_{\underline{x}_0} + g_y(t)y_{\underline{x}_0} \tag{2.30}$$

The initial conditions for $\underline{x}_{\underline{x}_0}$ and $y_{\underline{x}_0}$ are obtained by differentiating (2.3) with respect to $\underline{x}_0$. It is obvious that the initial value for the trajectory sensitivities of state variables is an identity matrix. Using this identity matrix, the initial values for the trajectory sensitivities of algebraic variables can be also computed from (2.30).

$$\underline{x}_{\underline{x}_0}(t_0) = I, \quad y_{\underline{x}_0}(t_0) = -(g_y(t_0))^{-1} g_{\underline{x}_0}(t_0) \tag{2.31}$$

Note that $\underline{f}_{\underline{x}}$, $\underline{f}_y$, $g_{\underline{x}}$ and g_y are time varying functions which are calculated along the system trajectories. To find the trajectory sensitivities, the DAEs (2.27)-(2.30) should be solved simultaneously considering the initial conditions described above as explained in the next section.

2.2.1 Trapezoidal approach for trajectory sensitivity computation

The trapezoidal approach is a common method used for transient analysis of power systems [57]. Using this method, explained in detail in [58], two sets of algebraic **difference** equations coupled to the original DAEs (2.27)-(2.30) are introduced as follows [26]:

$$0 = \begin{bmatrix} F_1(\cdot) \\ F_2(\cdot) \end{bmatrix} = \begin{bmatrix} \frac{\eta}{2}\underline{f}(\underline{x}^{k+1}, \underline{y}^{k+1}) - \underline{x}^{k+1} + \frac{\eta}{2}\underline{f}(\underline{x}^k, \underline{y}^k) + \underline{x}^k \\ g(\underline{x}^{k+1}, \underline{y}^{k+1}) \end{bmatrix} \tag{2.32}$$

$$0 = \begin{bmatrix} F_3(\cdot) \\ F_4(\cdot) \end{bmatrix} = \begin{bmatrix} \underline{x}^{k+1}_{\underline{x}_0} - \underline{x}^{k}_{\underline{x}_0} - \frac{\eta}{2}(\underline{f}^{k}_{\underline{x}}\underline{x}^{k}_{\underline{x}_0} + \underline{f}^{k}_{y}y^{k}_{\underline{x}_0} + \underline{f}^{k+1}_{\underline{x}}\underline{x}^{k+1}_{\underline{x}_0} + \underline{f}^{k+1}_{y}y^{k+1}_{\underline{x}_0}) \\ g^{k+1}_{\underline{x}}\underline{x}^{k+1}_{\underline{x}_0} + g^{k+1}_{y}y^{k+1}_{\underline{x}_0} \end{bmatrix} \quad (2.33)$$

where η is the integration time-step, and the superscript k indexes the time instant t_k.
Note that (2.32) is a set of implicit nonlinear algebraic equations which is solved using Newton-Raphson iterative algorithm. The set of equation (2.32) has the form $F(\varkappa) = 0$ which is solved iteratively based on

$$\varkappa_{i+1} = \varkappa_i - F_{\varkappa}(\varkappa_i)^{-1}F(\varkappa_i) \quad (2.34)$$

where $F_{\varkappa}$ is the Jacobian of F with respect to $\varkappa$, and the index i is the Newton-Raphson iteration step. So, the solution to the nonlinear set of equations (2.32) is obtained by solving the following linear problem

$$\begin{bmatrix} \underline{x}^{k+1} \\ y^{k+1} \end{bmatrix}_i = \begin{bmatrix} \underline{x}^{k} \\ y^{k} \end{bmatrix}_i - \underbrace{\begin{bmatrix} \frac{\eta}{2}\underline{f}^{k+1}_{\underline{x}} - I\frac{\eta}{2}\underline{f}^{k+1}_{y} \\ g^{k+1}_{\underline{x}} \quad g^{k+1}_{y} \end{bmatrix}^{-1}_i}_{F_{\varkappa}} \begin{bmatrix} F_1(\cdot) \\ F_2(\cdot) \end{bmatrix}_i \quad (2.35)$$

Once (2.35) has converged, the trajectory sensitivities are calculated by rearranging the set of linear equations (2.33) as given in (2.36)

$$\begin{bmatrix} \underline{x}^{k+1}_{\underline{x}_0} \\ y^{k+1}_{\underline{x}_0} \end{bmatrix} = \underbrace{\begin{bmatrix} \frac{\eta}{2}\underline{f}^{k+1}_{\underline{x}} - I\frac{\eta}{2}\underline{f}^{k+1}_{y} \\ g^{k+1}_{\underline{x}} \quad g^{k+1}_{y} \end{bmatrix}^{-1}}_{F_{\varkappa}} \begin{bmatrix} -\frac{\eta}{2}(\underline{f}^{k}_{\underline{x}}\underline{x}^{k}_{\underline{x}_0} + \underline{f}^{k}_{y}y^{k}_{\underline{x}_0}) - \underline{x}^{k}_{\underline{x}_0} \\ 0 \end{bmatrix} \quad (2.36)$$

Note that the coefficient matrix in the right side of (2.36) is exactly the same Jacobian used in solving final iteration of (2.35).

2.2.2 Numerical formulation of trajectory sensitivity analysis

Numerical formulation of TSA gives an estimation of trajectory sensitivity of state variable x to the parameter λ [38]. In this method, a small perturbation of $\triangle\lambda$ over the nominal parameter λ_0 is considered such that $\lambda = \lambda_0 + \triangle\lambda$. Time domain simulations need to be carried out for the original and perturbed systems, and then, the numerical estimation of sensitivity is obtained as follows

$$x_{\lambda} = \frac{x(\lambda) - x(\lambda_0)}{\triangle\lambda} \quad (2.37)$$

Obviously, the TSA calculation for a system with n_{λ} number of parameters, using numerical formulation, needs $(n_{\lambda} + 1)$ number of time domain simulations. Note that similar calculation using analytical formulation requires only one time domain simulation regardless of the number of parameters taken into account.

Chapter 3

Assessment of Rotor Angle Stability Using Trajectory Sensitivity Analysis

This chapter briefly explains the application of TSA to determine the impacts of different system parameters on the rotor angle stability.

3.1 Rotor angle stability assessment using trajectory sensitivity analysis

Power systems may become transiently unstable after being subjected to large disturbances. The result of transient instability appears in the form of increasing rotor angles of some generators which leads to their loss of synchronism with other generators. Under small disturbances, rotor angle oscillations show if the system is small signal stable or not. If their oscillation are positively damped and decay with time, the power system is stable. Otherwise, there will be a negative damping in electromechanical oscillation which results in oscillatory instability.

Therefore, it is possible to check both the transient and small signal stability using rotor angles of generators (state variables δ). To improve the transient stability, power system parameters can be controlled (if applicable) in a way to have positive impacts on the variation of rotor angles of generators when the system is subjected to a fault, and prevent power system from being transiently unstable. These parameters can also be controlled for improving the power oscillation damping, and ensuring the small signal stability of power system.

Nowadays with the presence of FACTS devices, it is possible to change the system parameters dynamically, control the power flows through lines, and improve the rotor angle stability of power system. For instance, a series compensator such as Thyristor Controlled Series Capacitor (TCSC) is able to change the reactance of a transmission line dynamically and a shunt compensator such as static synchronous

compensator (STATCOM) is capable of injecting a controllable amount of reactive power into a grid node [6]. Due to the heavy costs of these devices, it is necessary to find the appropriate locations to install minimum numbers of them needed for the stability enhancement. In this chapter, trajectory sensitivities of rotor angles of generators with respect to the parameters of interest, e.g., reactance of transmission lines are used for suitable placement of series and shunt compensators.

Additionally, inertia of generators can also be selected as a system parameter for studying the impact of inertia reduction on the system stability. In the real-world power systems, wind generation is growing rapidly, and consequently, the conventional fuel-based generating units are gradually substituted with these renewable resources. This results in reduction of the total kinetic energy stored in power systems through rotating masses since wind generators are decoupled from the grid by power electronic converters, and cannot contribute to the inertia of the grid. The resulting reduction of grid inertia may cause higher risk of transient instability. In this chapter, TSA is also used to analyze the impacts of inertia reduction on the transient stability of power system.

In general, equations (3.1) and (3.2) show the vector of power system parameters and the trajectory sensitivities of dynamical states, which are rotor angles of generators in this study, to these parameters:

$$\lambda = [\lambda_1 \ ... \ \lambda_p \ ... \ \lambda_{n_p}] \tag{3.1}$$

$$\frac{\partial \delta}{\partial \lambda} = \begin{bmatrix} \frac{\partial \delta_1}{\partial \lambda_1} \cdots \frac{\partial \delta_1}{\partial \lambda_p} \cdots \frac{\partial \delta_1}{\partial \lambda_{n_p}} \\ . \ . \ . \ . \ . \\ . \ . \ . \ . \ . \\ \frac{\partial \delta_i}{\partial \lambda_1} \cdots \frac{\partial \delta_i}{\partial \lambda_p} \cdots \frac{\partial \delta_n}{\partial \lambda_{n_p}} \\ . \ . \ . \ . \ . \\ . \ . \ . \ . \ . \\ \frac{\partial \delta_n}{\partial \lambda_1} \cdots \frac{\partial \delta_n}{\partial \lambda_p} \cdots \frac{\partial \delta_n}{\partial \lambda_{n_p}} \end{bmatrix} \tag{3.2}$$

where λ_p is the p^{th} parameter, δ_i is the rotor angle of the i^{th} generator, n_p is the number of parameters, and n is the number of generators. The first part of this thesis consists of several sensitivity-based analyses in which the following parameters (λ_p) are considered:

- **Suitable placement of series compensator:** $\lambda_p = x_{L_l}$, the reactance of the l^{th} transmission line
- **Suitable placement of shunt compensator:** $\lambda_p = Q_{inj_m}$, the reactive power injected into the m^{th} node
- **Analyzing the impacts of inertia reduction:** $\lambda_p = H_i$, the inertia of i^{th} synchronous generator

3.1.1 Equivalent rotor angles for stability studies

In a large scale power system, it is very time-consuming to check all the rotor angles of generators in order to assess the rotor angle stability of the system. Hence, two equivalent angles, δ_{eq_s} and δ_{eq_t} consisting all the rotor angles, are introduced to simplify the evaluation of the small signal and transient stability of the system, respectively.

The equivalent rotor angle δ_{eq_s} for small signal stability study is based on the modal analysis corresponding to the mode of interest. The mode of interest which is the one with poorest damping and a low frequency is determined from the eigenvalues of the state matrix of the system. Based on the compass plot corresponding to the mode of interest, generators are divided to two groups which are oscillating against each other. Then, these two groups are replaced by a single machine equivalent system.

To define the equivalent rotor angle δ_{eq_t} for transient stability study generators are separated to two groups, depending if their rotor angles after fault occurrence, in center of inertia (COI) reference, are accelerating or decelerating. These two groups are then substituted by a single machine equivalent system.

The more detailed definitions of these two equivalent angles are given in Paper J1 for the case that reactance of transmission line is selected as the parameter of interest, but it is quite straightforward to extend these definitions to include other system parameters.

3.2 Suitable placement of series and shunt compensators to improve rotor angle stability stability

In this section, a method is proposed to find the suitable placement of FACTS devices for improving rotor angle stability. As previously stated, rotor angle stability is divided into two categories, small signal stability and transient stability. The time framework of this study is characterized as follows:

1. Before fault occurrence ($t_0 < t < t_f^-$): this time frame pertains to small signal stability enhancement since there is no disturbances in the system, and linearization is permissible for the purpose of analysis.

2. After fault occurrence ($t_f^+ < t < t_{end}$): this time frame is concerned with transient stability improvement since the power system is subjected to several large disturbances.

3.2.1 Small signal stability improvement ($t_0 < t < t_f^-$)

Despite the fact that before the fault occurrence, the power system works in its operating point with fixed state and algebraic variables, the trajectory sensitivities will oscillate around their operating points as a result of non-zero initial values

described in (2.31) until their steady-state values will be reached. The trajectory sensitivities are computed based on (2.36) with this explanation that matrices $\underline{f}_{\underline{x}}$, $\underline{f}_{y}$, $g_{\underline{x}}$ and g_y are time-invariant since there is no change in the system. Equation (3.3) describes the evolution of the trajectory sensitivities $\underline{x}_{\underline{x}_0}$, $y_{\underline{x}_0}$ within this time frame (t_0-t_f^-) [26, 59].

$$\begin{bmatrix} \underline{x}_{\underline{x}_0}^{k+1} \\ y_{\underline{x}_0}^{k+1} \end{bmatrix} = \underbrace{\begin{bmatrix} \frac{\eta}{2}\underline{f}_{\underline{x}}^0 - I\frac{\eta}{2}\underline{f}_{y}^0 \\ g_{\underline{x}}^0 \quad g_y^0 \end{bmatrix}^{-1}}_{F_{\varkappa}} \begin{bmatrix} -\frac{\eta}{2}(\underline{f}_{\underline{x}}^0 \underline{x}_{\underline{x}_0}^k + \underline{f}_{y}^0 y_{\underline{x}_0}^k) - \underline{x}_{\underline{x}_0}^k \\ 0 \end{bmatrix} \tag{3.3}$$

These pre-fault oscillations of trajectory sensitivities show how sensitive state and algebraic variables are with respect to the system parameters under the assumption that the system is subjected to a very small disturbance such that the state and algebraic variables can be considered constant. In Papers J1 and C4, an approach is proposed for suitable placement of series compensators to enhance the small signal stability of the system. Additionally, to evaluate the well-functioning of the proposed approach, it is compared with the Residue technique described in [60].

3.2.2 Transient stability improvement ($t_f^+ < t < t_{end}$)

First, a set considering the most probable and severe faults with the clearing times close to their critical clearing time is selected. Then, vector of system parameters is chosen depending on the type of analysis, i.e., including all the reactances of transmission lines for allocating series compensators, or the injected reactive powers into the grid nodes for suitable placement of shunt compensators. To find the trajectory sensitivities after fault occurrence, the sets of equations (2.35) and (2.36) should be solved simultaneously. The obtained sensitivities show how effective a certain parameter is for improving the transient stability of the system. These sensitivities are then used to appropriately allocate FACTS devices. Several weighting factors are considered in this allocation, e.g., a term which weights the sensitivities obtained with respect to a certain parameter based on the maximum allowed change of that parameter, i.e., maximum possible series/shunt compensation, and another term taking into account the severity and occurrence probability of each selected fault. In this vein, Paper J1 proposes an algorithm for suitable placement of series compensators in order to improve the transient stability. The same study is carried out in Paper C3 considering shunt compensators. In addition, Paper C2 deals with appropriate allocation of multiple series compensators for transient stability enhancement.

3.2.3 Results and Discussion

The proposed methods are evaluated using three test systems (i) IEEE 3-machine 9-bus [57] (ii), IEEE 10-machine 39-bus [61] and (iii) Nordic-32 [62]. Papers C1-C3

analyze the transient stability, Paper C4 discusses the small signal stability while Paper J1 addresses both. In each case study, the most appropriate locations to install either the series or shunt compensators for improving the system stability were found using the proposed TSA-based methods.

To verify the results, commercial software SIMPOW®11, is used for modeling and simulation of the considered test systems containing series/shunt FACTS devices. The numerical results show validity, accuracy and efficiency of the proposed methodologies.

In addition, the proposed methods not only determine the most effective placement of FACTS devices, but also explains why installing such devices in certain locations could worsen the power system stability, e.g., Paper J1 demonstrates a situation where series compensation of a transmission line has negative impacts on the transient stability of the system after the occurrence of a specific disturbance.

It is worth mentioning that in Paper J1, both the transient and small signal stability assessments are incorporated into a single problem which is formulated as a two-stage model, whose first-stage describes prior to fault occurrence, and whose second-stage represents the power system behavior involving a set of severe faults. The first-stage focuses on small signal stability, while the second-stage deals with transient stability of power system.

Regarding computational time viewpoint, the proposed methods are more efficient compared to the similar works which used numerical formulation of TSA since solving the TSA equations with the analytical method needs fewer number of time domain simulations, see Section 2.2.2.

3.3 Analyzing the impacts of inertia reduction of generators on the transient stability

In the final stage of part II of this thesis, a new research work has been initiated which focuses on the impacts of inertia reduction of generators on the transient stability of the system. The inertia reduction can be the result of penetrating high amount of wind power into the power system. Trajectory sensitivity analysis technique is used in Paper C1 to calculate the dynamic sensitivities of rotor angles with respect to the inertia of generators. This paper shows that depending on the type and location of the disturbance and also the location of inertia reduction, the transient stability is either improved or weakened. Note that this research is currently in its early stages, and further analyses will not be included in this dissertation. The future study is considering both the mechanical power and inertia of the generators in the sensitivity analysis, analyzing small signal stability as well as implementing the detailed model of wind power for verification of the results.

3.3.1 Improving the transient stability by deployment of series compensators after inertia reduction in the grid

In this subsection, the results obtained in Paper C1 have been extended considering the following issues: (i) analyzing the impacts of inertia reduction which can be caused by replacing a synchronous generator with its equivalent wind power on the results obtained from the former study (Paper J1) whose objective was to determine the appropriate placement of series compensators for improving the transient stability in a power system without any renewable source of generation, and (ii) deployment of series compensators to enhance the transient stability after inertia reduction in the grid due to high penetration of wind power.

In this vein, the IEEE 10-machine 39-bus test system introduced in Paper C1 and the Fault $z = 3$ given in Table 1 of this paper are considered. The critical clearing time of this fault is 203 ms. Fig. 3.1 shows the rotor angles of generators in the center of inertia (COI) reference corresponding to this fault. According to Table 2 of Paper C1 and for this fault, reducing inertia of Generators 2, 3, 5, 4, 7, 6, 9 and 8 have the worst impact on the transient stability, respectively, while such inertia reduction in Generator 1 slightly improves the transient stability of this test system.

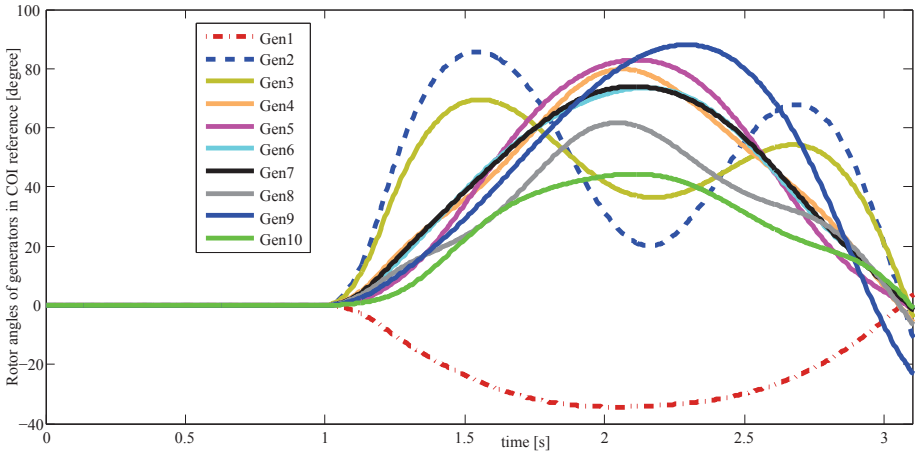

Figure 3.1: Rotor angles of the generators in the original system - Fault $z = 3$.

A sensitivity analysis, according to Section 4.2 of Paper J1, has been carried out for the original system (without inertia reduction) to determine the suitable locations for installing a series compensator in order to improve the transient stability. Fig. 3.2 shows the trajectory sensitivities of the equivalent rotor angle, see Subsection 3.1.1, with respect to the impedance of different transmission lines. It is observed that Line 11-12, Line 11-1, Line 18-19, Line 19-1 and Line 16-17 have the highest positive peak values of trajectory sensitivities while Line 16-21, Line 20-21 and Line 14-15 have the most negative ones, respectively. Based on Section 5.3 of

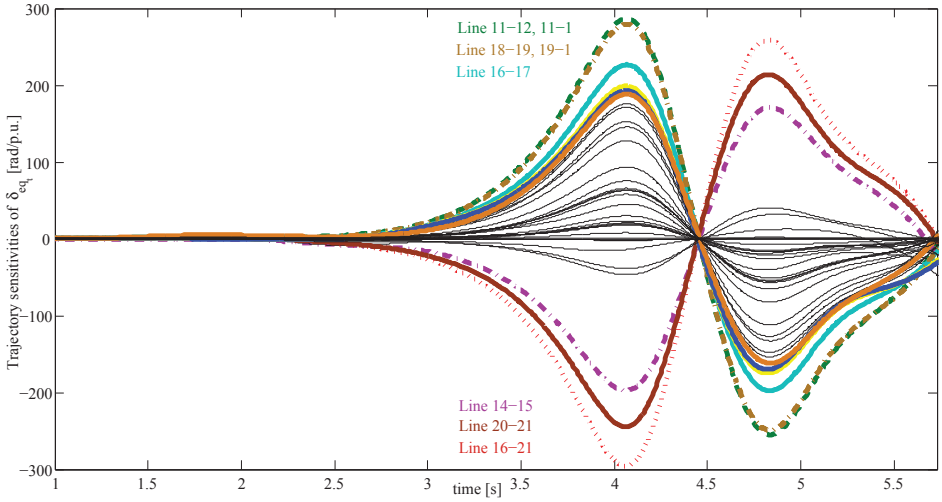

Figure 3.2: Trajectory sensitivities of δ_{eq_t} to the reactances of transmission lines in the original system - Fault $z = 3$.

Paper J1, Line 11-12 is the most suitable place for installing the series compensator since between the lines with positive impacts, this line is the most sensitive one (highest peak value), and it also has a larger reactance value, and therefore larger possible amount of series compensation.

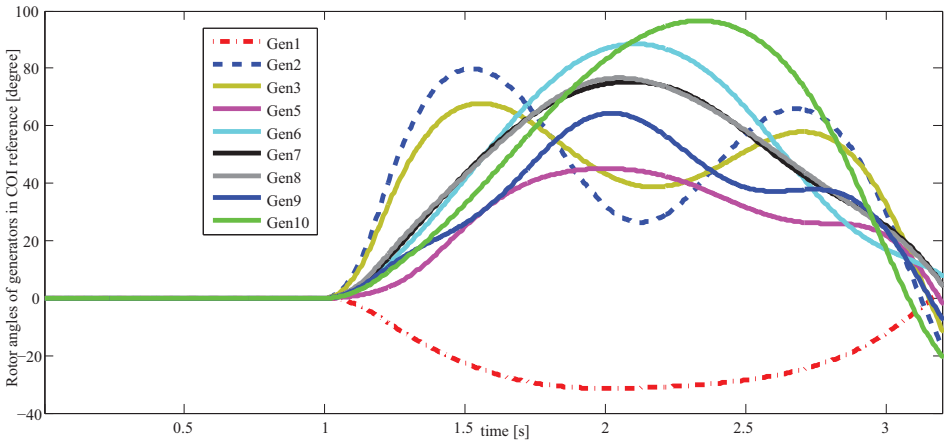

Figure 3.3: Rotor angles of the generators in the modified system after replacing Generator 4 - Fault $z = 3$.

After appropriate placement of series compensator in the original system, Generator 4 which is one of the generators with negative impacts of inertia reduction on the transient stability is replaced by its equivalent wind power. It is assumed

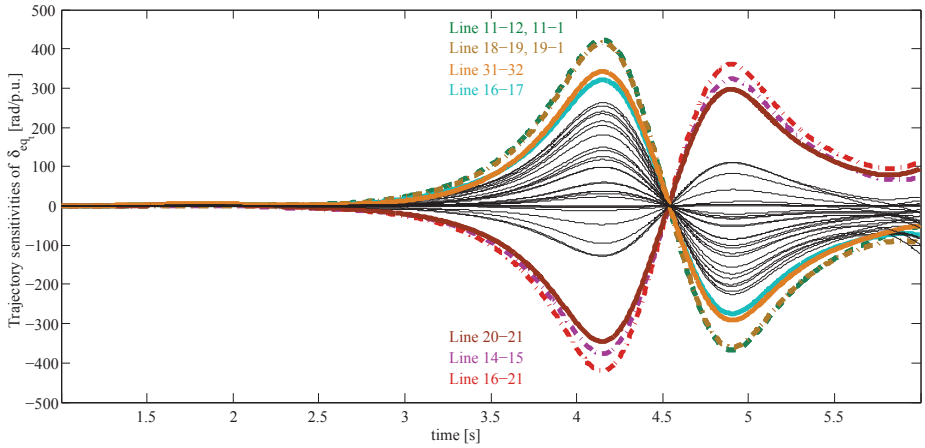

Figure 3.4: Trajectory sensitivities of δ_{eq_t} to the reactances of transmission lines in the modified system after replacing Generator 4 - Fault $z = 3$.

that wind generator is completely decoupled from the grid by power electronic converters, and cannot contribute to the inertia of the grid. Therefore, it is modeled as a fixed static load with the same amounts of active and reactive powers as the ones that the original Synchronous generator 4 produced, but with the opposite signs. The new critical clearing time corresponding to Fault $z = 3$ after such replacement is calculated via time domain simulations, and is equal to 193 ms which is lower than the previous value (203 ms), as expected. Fig. 3.3 shows the rotor angles of generators in the modified system. It is observed that the grouping of generators after fault occurrence have not changed, i.e., similar to the original system, Generator 1 is decelerating while the rest of generators are accelerating. A sensitivity analysis with respect to the impedances of different transmission lines has been carried out for appropriate placement of series compensator in the modified system, and the results are given in Fig. 3.4. It can be seen that there is no considerable change in the placement results, and Line 11-12 is still the most suitable place for series compensation. The next step is to check if a series compensation is able to recompense the deterioration of transient stability caused by the inertia reduction due to penetration of wind power. In this regard, a Fixed Series Capacitor (FSC) is installed in transmission line 11-12. The reactance of FSC is set to 50% capacitive of the original reactance of the line. The new critical clearing time of Fault $z = 3$ after series compensation is calculated via time domain simulation, and is equal to 203 ms. Hence, it is concluded that installing series compensators can be considered as a remedy for stability deterioration due to high penetration of wind power.

The same analysis has been done replacing Generator 1 by its equivalent wind power. There are two main differences in this case compared to the case where Generator 4 has been replaced: (i) on the contrary to Generator 4, reducing inertia

of Generator 1 has a positive impact on the transient stability corresponding to Fault $z = 3$ (according to Table 2 of Paper C1) and (ii) Generator 1 has the highest value of inertia between all the generator (almost ten times the rest of generators), and therefore, eliminating it from the grid may totally change the system dynamics. Fig. 3.5 shows the rotor angles of generators after replacing Generator 1 by its equivalent wind power.

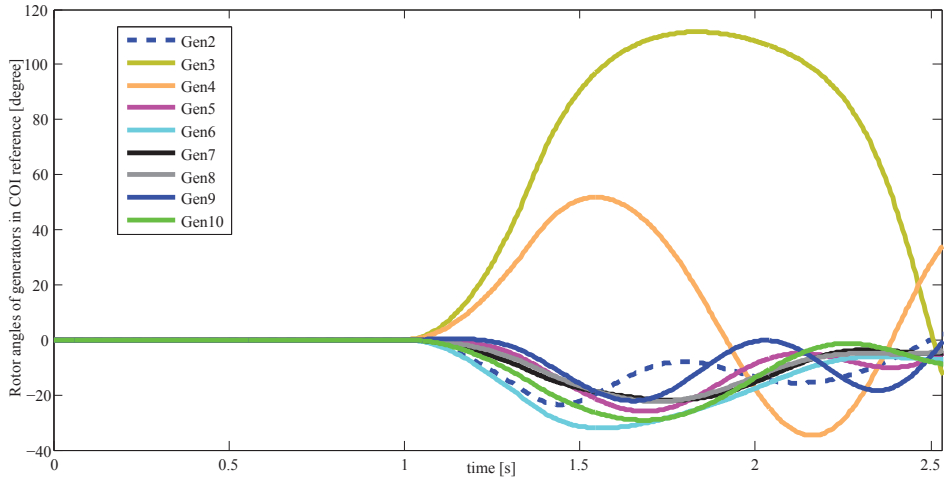

Figure 3.5: Rotor angles of the generators in the modified system after replacing Generator 1 - Fault $z = 3$.

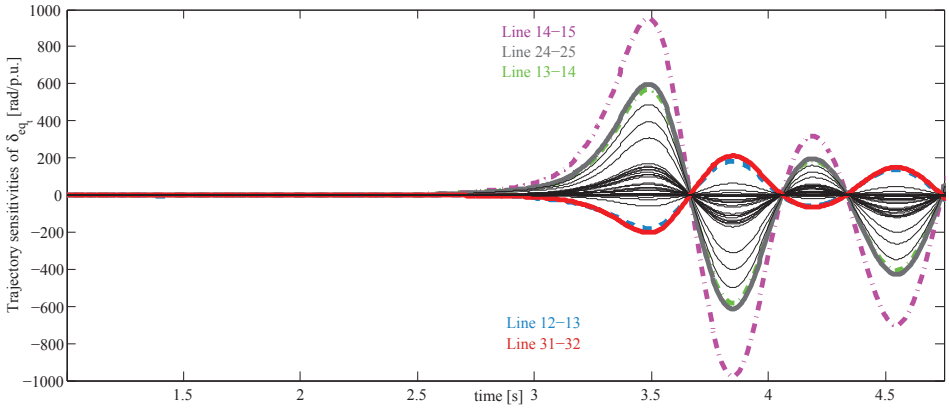

Figure 3.6: Trajectory sensitivities of δ_{eq_t} to the reactances of transmission lines in the modified system after replacing Generator 1 - Fault $z = 3$.

In this case compared to the original system, the grouping of generators after fault occurrence has been totally changed. As it can be seen from Fig. 3.5, in this case, Generators 3 and 4 are accelerating while the rest of generators are deceler-

ating. The critical clearing time corresponding to Fault $z = 3$ after replacement of Generator 1 has been significantly improved, as expected, and is equal to 367 ms. The main reason behind such significant improvement is the very high inertia reduction at Generator 1 where reducing inertia is beneficial to the transient stability, according to Table 2 of Paper C1.

Similar to the previous cases, a sensitivity analysis has been carried out to find the appropriate locations for installing a series compensator in order to improve the transient stability, and the obtained results are depicted in Fig. 3.6. It is observed that the results are different compared to the original system or the case where Generator 4 is replaced (Figs. 3.4 and 3.2). This difference is mainly due to eliminating Generator 1 which is a very high-inertia generator, and has a significant impact on the system dynamics.

Part II

Power System Operation under Wind Uncertainty

Chapter 4

Stochastic Programming and Benders' Decomposition

This chapter briefly reviews the application of stochastic programming for solving a decision-making problem under uncertainty. Additionally, Benders' Decomposition technique is introduced to make such problems computationally convenient.

4.1 Stochastic programming

Stochastic programming is a technique to model decision-making problems involving uncertainty. Most decision-making problems are often modeled as an optimization problem. The first step to formulate an optimization problem is to collect all the input data (parameters), e.g., in the field of power system studies could be collecting generator and load data in solving an optimal power flow (OPF) problem. If theses parameters are clearly stated and deterministic, the optimal solution is obtained by solving the formulated optimization problem. However, in most real-world problems, there are also sets of uncertain parameters which are not deterministic, and described through probability functions. For instance, in one day prior to the real-time operation of power system when the "day-ahead market" is cleared, the output powers of wind generators are considered uncertain since such outputs are strongly dependent on the real-time wind speed which is uncertain.

There are different approaches to deal with optimization problems under uncertainty. One possibility is to eliminate the uncertainty by considering the minimum, maximum or expected value of the uncertain parameter, and therefore, make the optimization problem deterministic. Obviously, the solution obtained by this approach is not optimal and can be even infeasible since it does not model appropriately the uncertain nature of the problem.

The other possibility to model an uncertain parameter is by considering a set of plausible scenarios with different probabilities of occurrence. Stochastic programming uses such modeling approach and considers a given set of possible values for

the uncertain parameter in order to find a single solution which is optimal with respect to all possible values of the uncertain parameter, but not to any one of them particularly [50]. Note that despite having uncertain parameters, the objective function of an optimization problem should be specific. Hence, a deterministic representation of the objective function, such as its expected value, should be considered.

Stochastic programming is used in chapter 5 and 6 of this thesis to deal with operational problems under uncertainty, e.g., optimal power flow and network-constrained unit commitment in a power system with high penetration of wind power.

4.1.1 Random variable

Stochastic programming models each uncertain parameter of an optimization problem as a random variable which is represented through a finite set of scenarios. Each scenario is a single realization of the random variable. In general, the uncertain parameter λ is represented by the random variable $\lambda(s), s = 1, ..., N_{\mathcal{S}}$ where s is the index for scenarios, $N_{\mathcal{S}}$ is the number of plausible scenarios and $\mathcal{S}$ is a set consisting all the possible scenarios of random variable λ. In addition, the occurrence probability of scenario s is given by ρ_s. Note that sum of the probabilities corresponding to the scenarios considered for random variable λ should be equal to one as described by (4.1)

$$\sum_{s} \rho_s = 1 \qquad \forall s \in \mathcal{S} \tag{4.1}$$

To appropriately model the uncertainty, it is crucial to generate adequate number of scenarios in order to cover all the plausible realizations of the uncertain parameter λ. However, a stochastic programming problem with a very large number of scenarios may become computationally intractable. Note that scenario generation and scenario reduction techniques are beyond of the scope of this thesis.

4.2 Multi-stage stochastic programming problem

In the decision-making problems under uncertainty, there exists a decision horizon where the optimal decisions are made. This decision horizon is normally divided to several stages where each stage refers to a point in time that some decision are made or the uncertainty partly or completely disappears [50]. The input data to the decision-making problem alters stage by stage. Note that this thesis deals with two-stage stochastic programming problems.

4.2.1 Two-stage problems

In this type of problems, two stage of decision making are considered. If the uncertain parameter is represented by a set of scenarios, the first-stage variables con-

stitute *here-and-now* decisions, i.e., scenario-independent decisions that are made before the realization of any scenario, but they are adapted to all the scenarios. On the other hand, the second-stage variables constitute *wait-and-see* decisions, i.e., decisions which are related to the conditions involving each scenario. To formulate the problem, two decision variable vectors, namely a and b, are considered. The uncertain parameter λ is also represented by a set of scenarios $\lambda_{\mathcal{S}}$. The variable a represents the first-stage decisions which are made prior to uncertainty realization while the variable b is related to the second-stage decision taking place after realization of the uncertain parameter λ.

The two-stage stochastic programming problem applied to the cases of this thesis can be generally formulated as below:

$$\underset{a\in\mathcal{A},b(s)\in\mathcal{B}}{\text{Minimize}} \quad \{p(a) + \sum_{s} \rho_s \left[q(b,s)\right]\} \tag{4.2}$$

s.t.

$$h(a) \quad = c \tag{4.3}$$

$$r(a) \quad \leq d \tag{4.4}$$

$$f(a) \quad + w(b,s) = m(s) \tag{4.5}$$

$$g(a) \quad + v(b,s) \leq n(s) \tag{4.6}$$

where $p(a)$ is the objective function component of the first-stage variables, $q(b,s)$ is the objective function component of the second-stage variables corresponding to scenario s, ρ_s is the occurrence probability of scenario s. Equations (4.3) and (4.4) specify constraints on the first-stage decisions while Equations (4.5) and (4.6) are the stochastic constraints in the second-stage of the problem. The participation of first-stage decisions in the second-stage constraints are considered through functions $f(a)$ and $g(a)$.

The main drawback for using a stochastic programming approach is a significant increase in the size of the problem to be solved, which if not handled properly may cause intractability. Decomposition techniques such as Benders' decomposition can be used to overcome the mentioned shortcoming, and make the model tractable for cases with many scenarios. In chapter 6 of this thesis, an efficient solution approach based on Benders's decomposition is proposed to solve a two-stage ac unit commitment problem under wind power uncertainty. In this regard, a basic introduction to Benders' decomposition is given in the next section.

4.3 Benders' decomposition

This section describes briefly the theoretical foundation of Benders' decomposition [63]. Within optimization problem (4.2)-(4.6), note that a is complicating variable, so that fixing that variable (i.e., fixing functions $p(a)$, $h(a)$ and $r(a)$) to given values renders decomposing the original optimization problem (4.2)-(4.6) to smaller ones,

one per s, which are easier to be solved. Each decomposed problem is as follows:

$$\left\{ \underset{b(s)\in\mathcal{B}}{\text{Minimize}} \;\; \rho_s \left[q(b,s)\right] \right. \tag{4.7}$$

s.t.

$$w(b,s) \;\; = m(s) - f(a) \tag{4.8}$$

$$\left. v(b,s) \;\; \leq n(s) - g(a) \right\} \quad \forall s \tag{4.9}$$

To take the computational advantages of Benders' decomposition, its algorithm is explained below. However note that such an algorithm works well only if the objective function of original optimization problem (4.2)-(4.6) as a function of the complicating variable has a "sufficient convex" envelope.

4.3.1 The Benders' decomposition algorithm

Step 0: Initialization. Build master problem based on (4.2)-(4.6), and then start the algorithm by initializing the iteration counter, $\nu = 0$. The initial master problem below needs to be solved to find the optimal value for complicating variable a in this iteration.

$$\underset{a^0\in\mathcal{A},\sigma^0}{\text{Minimize}} \;\; \{p(a^0) + \sigma^0\} \tag{4.10}$$

s.t.

$$h(a^0) \;\; = c \tag{4.11}$$

$$r(a^0) \;\; \leq d \tag{4.12}$$

$$\sigma^0 \;\; \geq \sigma^{down} \tag{4.13}$$

where superscript 0 referes to $\nu = 0$, and σ^ν represents $\sum_s \rho_s \left[q(b,s)\right]$. The solution of initial master problem above fixes the value of complicating variable a in the subproblem corresponding to $\nu = 0$, i.e., $a^{0,fixed} \leftarrow a^0$. The parameter σ^{down} is a lower bound of σ^ν that can be determined from physical or economical considerations pertaining to the problem under study or it can be easily considered to be a very large negative value, e.g. -1e10. Appropriate value selection for σ^{down} can accelerate the convergence of the algorithm.

Step 1: Subproblems solution. Each following subproblem corresponding to iteration ν, one per s, is solved while the value of a^ν is fixed to the one obtained from the master problem (if $\nu = 0$ such value is coming from Step 0, otherwise it

is coming from Step 3).

$$\underset{b^\nu(s)\in\mathcal{B}}{\text{Minimize}} \;\; \rho_s\left[q(b^\nu, s)\right] \tag{4.14}$$

$$\text{s.t.} \tag{4.15}$$

$$w(b^\nu, s) = m(s) - f(a^\nu) \tag{4.16}$$

$$v(b^\nu, s) \leq n(s) - g(a^\nu) \tag{4.17}$$

$$a^\nu \quad = a^{\nu,fixed} \quad : \quad \lambda^\nu \tag{4.18}$$

Note that λ^ν is the dual variable corresponding to the fixing constraint (4.18).

Step 2: Convergence checking. Compute upper and lower bounds for the optimal value of the objective function of the original problem:

$$z^\nu_{up} \; = p(a^\nu) + \sum_s \rho_s\left[q(b^\nu, s)\right] \tag{4.19}$$

$$z^\nu_{down} = p(a^\nu) + \sigma^\nu \tag{4.20}$$

if $z^{(\nu)}_{up} - z^{(\nu)}_{down} \leq \varepsilon$, stop the algorithm, the optimal solution is a^ν and b^ν. Otherwise, the algorithm continues with the next step.

Step 3: Master problem solution. Update the iteration counter $\nu = \nu + 1$, and solve the master problem

$$\underset{a^\nu\in\mathcal{A},\sigma^\nu}{\text{Minimize}} \;\; \{p(a^\nu) + \sigma^\nu\} \tag{4.21}$$

$$\text{s.t.}$$

$$\sum_s \rho_s\left[q(b^k, s)\right] + \lambda^k(a^\nu - a^k) \leq \sigma^\nu; \quad k = 1, ..., \nu - 1 \tag{4.22}$$

$$h(a^\nu) = c \tag{4.23}$$

$$r(a^\nu) \leq d \tag{4.24}$$

$$\sigma^\nu \geq \sigma^{down} \tag{4.25}$$

Constraints (4.22) are Benders' cuts, i.e., inequality constraints which link the master problem and the subproblems. Note that at every iteration, a new cut is added to the master problem (4.22)-(4.25). The solution of master problem above updates the value of complicating variable a in the subproblem, i.e., $a^{\nu,fixed} \leftarrow a^\nu$, and then the algorithm continues in Step 1.

Chapter 5

Minimizing Wind Power Spillage Using an OPF With FACTS Devices

This chapter proposes an optimal power flow (OPF) model with FACTS devices based on a two-stage stochastic programming problem whose main objective is to minimize wind power spillage, while the second priority is to minimize active power losses in the network.

5.1 Motivation and aim

Over the last decade, the share of wind power in the generation portfolio of power systems has significantly grown. However, the inherent variability of wind power and also the technical constraints due to long-distance power transmission may limit the integration of wind power production into the system. On the other hand, FACTS devices can significantly improve the operational flexibility of the system and help integrating increasing amounts of wind power.

The fast operation of FACTS devices makes them appropriate tools to cope with the variability and uncertainty of wind power production by altering the reactance of transmission lines and/or nodal voltages. Note that the uncertainty of wind power production in this work is modeled through a set of plausible scenarios, i.e., stochastic programming is used. To this end, the optimal reactance setting of such devices needs to be determined per wind scenario, which results in reduced wind power spillage. Wind power spillage refers to the amount of the wind power production which is not used due to technical reasons, e.g., insufficient transmission capacity.

This chapter proposes an optimal power flow (OPF) model with FACTS devices based on a two-stage stochastic programming problem to optimally determine the

setting of such devices. The main objective is to minimize wind power spillage, while the second priority is to minimize active power losses in the network.

5.2 Decision framework

The framework considered consists of two consecutive stages as depicted in Fig. 5.1: market and operation.

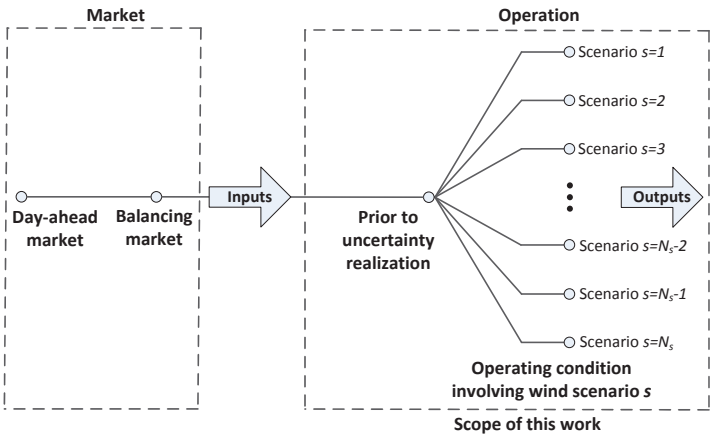

Figure 5.1: Decision framework of the proposed model.

1. *Market:*
   By noon of day $D-1$, the "day-ahead market" for day D is cleared and preliminary values for active power productions and consumptions are determined. Then, about 1 hour prior to power delivery, the "balancing market" (also called "real-time market") is cleared and "final" values for active power productions and consumptions are assigned to each generating unit and to each demand, respectively. The balancing market adjusts the results of the day-ahead market and compensates deviations. Note that this framework is consistent with most real-world markets [45–49]. Note also that this market stage is outside the scope of this work; however, its final outcomes are in fact the inputs for the OPF problem considered. Such inputs are:

   a) Power production of each generating unit.

   b) Active power consumption by each load.

   c) Maximum downward reserve of active power that can be provided by each generating unit.

   d) Maximum upward reserve of active power that can be provided by each generating unit.

e) Power production of each wind farm dispatched in the market.

2. *Operation*:
After clearing the balancing market, the proposed OPF model is used by the system operator to minimize wind power spillage. It is important to note that the OPF proposed does not represent the market stages, i.e., the system operator runs such an OPF after closing the last market, i.e., the balancing or real-time market. Thus, the time frame of this OPF spans from the closing of the balancing market to power delivery. In most real-world electricity markets this time period is smaller than one hour. This model is cast as a two-stage stochastic programming problem in which the first-stage refers to the decisions "prior to uncertainty realization", while the second-stage represents the "operating conditions involving wind scenarios". In the first-stage, the market operator makes "scheduling decisions" appropriate for any plausible wind production scenario, while in the second-stage, "operating decisions" corresponding to each individual scenario are made.

The outputs of the proposed model are of two types, first-stage and second-stage. Variables pertaining to the first-stage are:

a) Voltage magnitude at each bus prior to uncertainty realization.

b) Voltage angle at each bus prior to uncertainty realization.

c) Scheduled reactive power output of each generating unit prior to uncertainty realization.

Additionally, variables corresponding to the second-stage include:

a) Voltage magnitude at each bus in the operating condition involving wind scenario.

b) Voltage angle at each bus in the operating condition involving wind scenario.

c) Reactance of the Thyristor Controlled Series Capacitor (TCSC) installed in the operating condition involving wind scenario.

d) Deployed reserve of active power by each generating unit in the operating condition involving wind scenario.

e) Deployed reserve of reactive power by each generating unit in the operating condition involving wind scenario.

f) Wind power spillage of wind each farm in the operating condition involving wind scenario.

g) Involuntarily active load shedding of each load in the operating condition involving wind scenario.

Regarding the scheduling decisions made in the first-stage of the proposed model, note that the first-stage variables constitute *here-and-now* decisions,

i.e., scenario-independent decisions that are made before the realization of any scenario, but they are adapted to all the scenarios. On the other hand, the second-stage variables constitute *wait-and-see* decisions, i.e., decisions which are related to the operating conditions involving each wind power production scenario.

5.3 Modeling assumptions

The assumptions considered in this chapter are as follows:

1. A detailed ac representation of the transmission system is embedded within the considered OPF model.

2. The proposed OPF model is run after clearing the last market (e.g., the balancing or real-time market). This implies that the active power productions of all generating units have been dispatched, and are fixed at the time of running the proposed OPF model. In fact, the values of active power productions and consumptions provided by the market clearing process are the inputs of the proposed OPF model, whose mechanisms for minimizing wind power spillage are (i) optimal setting of the FACT devices, and (ii) optimal deployment of active and reactive power reserves. Therefore, since the decisions obtained with the proposed OPF model do not change the cleared quantities in the market, a financial analysis is not generally required.

3. For the sake of simplicity, only wind power production uncertainty is taken into account. However, other uncertainties such as generators' availability can be incorporated into the model. The uncertainty of wind power production is modeled through a set of plausible wind power scenarios based on the available forecasted data prior to running the proposed OPF. Note that scenario generation techniques are beyond of the scope of this work.

4. Wind power production of each farm corresponding to each scenario remains fixed over the time period considered. Note that periods smaller than one hour can be considered.

5. The power factors of wind producers are considered to be equal to one.

6. Among the available FACTS devices, the thyristor controlled series capacitor (TCSC) is selected in this work. However, the proposed methodology can be straightforwardly extended to consider any other type of FACTS devices.

7. The injection model of the TCSC [64, 65] is used in this work since it provides an appropriate representation of TCSC functioning and can be easily incorporated into an OPF formulation.

5.4 Formulation

The considered two-stage OPF problem is formulated in detail in Paper J2. Equation (5.1) shows the objective function of the proposed problem:

$$\underset{\Xi}{\text{Minimize}} \quad \sum_{s} \rho_s \left[\sum_{k \in \mathcal{K}} \alpha_k^{\text{SP}} W_{ks}^{\text{SP}} + \sum_{d \in \mathcal{D}} \alpha_d^{\text{SH}} L_{ds}^{\text{SH}} + \sum_{n(m \in \Omega_n)} \alpha_{nm}^{\text{L}} P_{nms}^{\text{L}}(\cdot) \right] \tag{5.1}$$

where W_{ks}^{SP} is wind power production spillage of wind farm k, L_{ds}^{SH} is involuntarily active load shedding of load d and Function $P_{nms}^{\text{L}}(\cdot)$ gives the value of active power loss of the transmission line (n,m) in the operating condition involving wind scenario s. Moreover, ρ_s is the occurrence probability of scenario and s.

The main goal of objective function (5.1) is to minimize wind power spillage, while the second priority is to minimize active power losses in the network. In addition, load shedding is also considered to avoid load curtailment. Thus, this objective function consists of three terms: (i) wind power spillage, (ii) unserved load, and (iii) active power losses in the network. Weighting factors α_k^{SP}, α_d^{SH} and α_{nm}^{L} specify the degree of importance of their corresponding terms.

Note that the proposed OPF problem is subject to two sets of constraints: (i) first-stage constraints (prior to uncertainty realization), (ii) second-stage constraints (operating conditions involving wind scenarios), see Paper J2.

5.5 Results and discussions

The proposed OPF model is applied to a case study based on the IEEE one-area reliability test system (RTS) [66]. In this study three different cases are analyzed:

Case A) No FACTS device is installed in the system (no series compensation).

Case B) A single fixed series capacitor (FSC) is installed in transmission line 14-16, whose reactance is capacitive and equal to 80% of the original reactance of the line.

Case C) A single TCSC is installed in same location as Case B. The limitation of the effective reactance of the TCSC is set to 80% capacitive and 50% inductive of the original reactance of the line where the TCSC is placed.

Obviously, the reactance of the TCSC is flexible and can be optimally set for each plausible wind scenario (Case C). On the contrary, Case B is a specific setting of Case C, imposing a fixed series compensation instead of an optimal one for each scenario.

A comprehensive analysis of the numerical results is given in Paper J2. Accordingly, the following observations are in order:

1. The value of the objective function (5.1) for Case C is comparatively smaller than that of Case B, and the value of these two cases are lower than the value for Case A. This implies that a series capacitive compensation (Cases B and C) is effective with respect to a case without compensation (Case A). Additionally, it is observed that a TCSC (Case C) leads to a better result than a FSC (Case B) due to its higher capability in controlling power flows.

2. For all cases, no load is curtailed due to the comparatively high penalty value in the objective function.

3. In Case A without series compensation, the expected value of wind power spillage ($\widetilde{W}^{\mathrm{SP}}$) as defined by (5.2) is 16.4%. However, in Cases B and C with series compensation, such value is decreased to 13.2% and 11.4%, respectively. This implies that a flexible series compensation (TCSC) is more effective than a fixed series compensation in reducing wind power spillage.

$$\widetilde{W}^{\mathrm{SP}} = \sum_{ks} \rho_s \frac{W_{ks}^{\mathrm{SP}}}{W_{ks}} \tag{5.2}$$

   where W_{ks}^{SP} is as introduced in Section 5.4 and W_{ks} is actual power production of wind farm k in the operating condition involving wind scenario s.

4. The amount of wind power spillage of Case C is comparatively lower than that of the two other cases in all scenarios.

5. The optimal series compensation (Case C) always decreases the wind power spillage with respect to the case without compensation (Case A). However, there is no guarantee to reduce wind power spillage using fixed series compensation (Case B). According to the results obtained, the amount of wind power spillage of Case B is worse than that of Case A in some scenarios, according to Fig. 4 of Paper J2, scenarios 5, 10 and 15.

6. The expected value of active power losses in the network is minimum in Case C with optimal setting of TCSC.

5.5.1 Simulation results for a new case study in which the TCSC is located in another transmission line

In the previously reported simulation results, i.e., results given in Paper J2, transmission line 14-16 has been selected for installing the TCSC since it is a long transmission line connecting the wind farm to the northern part of the system (i.e, buses 14-24). This line is located somewhere in between the two available wind farms. Additionally, the system data of the RTS have been modified in such a way that the system becomes comparatively weak, and thus installing a TCSC in line 14-16 decreases the wind power spillage significantly. However, note that if the location of TCSC is changed, this TCSC may not be effective in decreasing the wind

power spillage. Thus, to identify the best location of a TCSC in a given system is a complex problem that is outside the scope of this work, and such location is one of the inputs to the model proposed in this chapter.

Nevertheless, to verify that the proposed OPF model works well regardless the location of the TCSC, we report below a new case study in which the TCSC is located in line 11-14 of the considered test system. However, to highlight the effectiveness of the TCSC in decreasing the wind power spillage, we have also modified the system data with respect to the data reported in the original case (the one described in Paper J2). These modifications are provided in Tables 5.1 and 5.2. Note that all the notations have been defined in Paper J2.

Table 5.1: Modification to network data for the case in which the TCSC is located in line 11-14

Transmission line (n, m)	l_{nm} [miles]	r_{nm} [p.u.]	x_{nm} [p.u.]	b_{nm} [p.u.]	$\overline{S}_{nm}$ [p.u.]
11-14	280	0.0540	0.4180	0.0088	2.3
14-16	107	0.0200	0.2356	0.0204	2.1

Table 5.2: Modification to load data for the case in which the TCSC is located in line 11-14 [p.u.]

Load (d)	Location [Bus]	L_d^{P} [p.u.]	L_d^{Q} [p.u.]
9	10	2.425	0.600

The numerical results for this new case (in which TCSC is located in line 11-14) are given in Table 5.3, whose structure is similar to that of Table IV of Paper J2. Rows 2, 3 and 4 of Table 5.3, refer to Case A (no FACTS device installed), Case B (an installed fixed series capacitor in line 11-14) and Case C (an installed TCSC in line 11-14 with optimal setting), respectively. Similarly to the results in Table IV of Paper J2, the results in the Table 5.3 allows concluding that the optimal operation of the TCSC significantly decreases the wind power spillage with respect to a case in which either no TCSC or a fixed series capacitor is installed.

Table 5.3: Numerical results for the case in which no devise /a FSC/ a TCSC is located in line 11-14

	The value of objective function (1) [p.u.]	Expected value of unserved load ($\widetilde{L}^{\mathrm{SH}}$) [p.u.]	Expected value of wind power spillage percentage ($\widetilde{W}^{\mathrm{SP}}$) [%]	Expected value of active power loss ($\widetilde{P}^{\mathrm{L}}$) [p.u.]	CPU time [second]
Case A	163.6	0	18.3	1.11	38.1
Case B	158.2	0	17.7	1.22	45.0
Case C	106.5	0	11.9	1.16	73.8

5.6 The continuation of the work: ac unit commitment with FACTS devices under wind power uncertainty

In this chapter, an OPF model with FACTS devices has been proposed to minimize the amount of wind power spillage in the system. The system operator runs the proposed model which is formulated as a two-stage stochastic programming problem after the last market floor. In other words, the first-stage of the proposed OPF, "prior to uncertainty realization", takes place after closing the last market, i.e., the balancing or real-time market. This work can be continued considering the day-ahead market as the first-stage of the problem, and therefore, dealing with the stochastic form of a network-constrained unit commitment (UC) problem. Note that the objective of such UC problem is to determine the least-cost commitment and dispatch of generating units to serve the load in a power system with high penetration of wind power. This new research work aims to incorporate FACTS devices into the formulation of a network-constrained UC problem under wind power uncertainty which allows us to study the impacts of such devises on improving the UC outcomes, e.g., reducing the dispatch cost of generating units.

Unlike most unit commitment studies that consider dc representation of transmission system (dc-UC), in this new work, ac network representation should be taken into account (ac-UC). The simplifications considered in the dc-UC problems, i.e., the exclusion of ac constraints are not acceptable when operating conditions become increasingly stressed due to the increasing wind production. Additionally, the effectiveness of FACTS devices becomes observable dealing with these ac constraints, e.g., voltage magnitude and reactive power constraints. However, an ac-UC problem contains nonlinear power flow equations, constraints and also a set of binary variables to determine on/off status of units, which makes the type of such optimization problem to be mixed-integer non-linear, and thus very hard to solve. Therefore, the key requirement to carry out the new research work is to find a solution strategy for the ac-UC problem under wind power uncertainty. Accordingly, an efficient solution approach based on Benders' decomposition is proposed in Chapter 6. The final step will be incorporating FACTS devices into the proposed formulation of such ac-UC problem.

Chapter 6

AC Unit Commitment under Wind Power Uncertainty: A Benders' Decomposition Approach

In this chapter, an efficient solution approach based on Benders' decomposition is proposed to solve a network-constrained ac unit commitment (ac-UC) problem under wind power uncertainty.

6.1 Introduction

6.1.1 Motivation

Unit commitment (UC) is a crucial short-term decision-making problem in power system operations, whose objective is to determine the least-cost commitment and dispatch of generating units to serve the load. The deterministic form of the UC problem and its solution strategies are extensively documented in the literature, e.g., [67,68]. However, the recent increase of stochastic production units, especially wind power, in generation portfolios calls for a stochastic form of the UC problem, instead of a deterministic one. Moreover, a precise modeling of the physical laws characterizing this problem is needed as increasing wind power production generally results in stressed operating conditions. Hence, the need for an ac modeling arises.

6.1.2 Literature Review

Large-scale integration of wind power increases significantly the level of uncertainty [50], hence the need of a stochastic UC approach. The stochastic UC problem was first studied in mid 90's [69, 70]. More recent works include [51, 71, 72]. These approaches embed a dc representation of transmission system, rendering a mixed-integer linear UC problem (network-constrained dc-UC problem), which is generally tractable [73–76]. It is worth mentioning that due to the simplifications

considered in the dc-UC problems, i.e., the exclusion of voltage magnitude and reactive power constraints, an ex-post verification is required to check that the results obtained are implementable. A UC problem including an ac network representation (network-constrained ac-UC problem) provides a comparatively more precise description of power system operations, particularly as operating conditions become increasingly stressed due to increasing wind production. However, the ac unit commitment (ac-UC) problem is mixed-integer non-linear, and thus hard to solve. In the technical literature, there are few works addressing the ac-UC problem. Reference [77] proposes an approach based on Benders' decomposition to solve an ac network-constrained hydrothermal scheduling problem. A security-constrained ac-UC problem is proposed in [78], whose objective is to minimize the system's operating cost while maintaining appropriate security. The heuristic technique proposed in [78] decomposes the original problem into a master problem representing an ac-UC problem under a normal operating condition, and a subproblem checking security constraints. Note that wind power uncertainty is not modeled either in [77] or [78]. Reference [79] formulates a security-constrained stochastic ac-UC problem under wind power uncertainty, and discusses potential solution techniques, but numerical results are not reported.

This chapter proposes a network-constrained ac-UC problem in which the wind power uncertainty is characterized by a set of suitable scenarios. To cope with wind power uncertainty, a two-stage stochastic programming model is considered, whose first-stage represents the day-ahead market, and whose second-stage represents the real-time operating conditions involving wind power realizations.

6.1.3 Contributions

Considering the context above, the contributions of this work are threefold:

1. To propose a stochastic network-constrained ac-UC problem for a system with significant wind power production using a two-stage model, whose first-stage describes the day-ahead market, and whose second-stage represents the real-time operation involving wind scenarios.

2. To decompose the proposed ac-UC problem by scenario and time period, which ease the computational burden.

3. To implement Benders' decomposition, which allows decomposing the original mixed-integer and non-linear ac-UC problem to (i) a mixed-integer linear master problem, and (ii) a set of non-linear, but continuous subproblems.

Note that in the rest of this chapter the terms "dc-UC" and "ac-UC" refer to "network-constrained dc-UC" and "network-constrained ac-UC" problems, respectively.

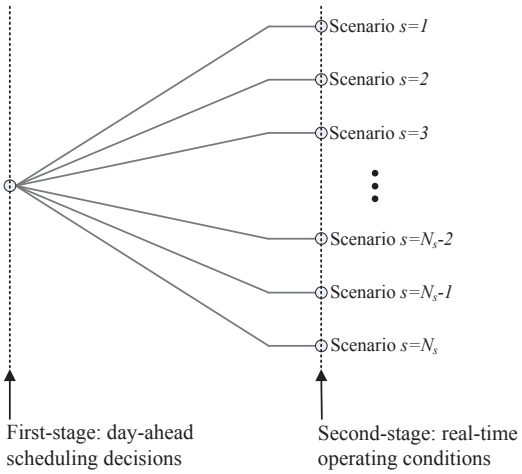

Figure 6.1: Two-stage stochastic decision framework of the proposed ac-UC problem.

6.2 Ac-UC Model

6.2.1 Stochastic Framework

Fig. 6.1 depicts the two-stage stochastic framework considered in this chapter. Note that these two stages are simultaneously considered. The first-stage includes the scheduling decisions made at the day-ahead market. Such decisions are adapted to any wind production realization in the second-stage, where the real-time operating conditions corresponding to individual wind scenarios are represented. This way, prior to the uncertainty realization in the second-stage, the system is optimally prepositioned via scheduling decisions in the first-stage. Therefore, the first-stage decisions are scenario-independent, while each second-stage decision adapts to the operating conditions of the corresponding wind power realization. Further details on the two-stage stochastic programming model used in this chapter can be found in [80].

The proposed ac-UC problem clears the day-ahead market while considering all plausible real-time operating conditions. Therefore, the scheduling decisions made at the first-stage (day-ahead market) are consistent with those conditions. Since operating limits are enforced explicitly at the second-stage for all plausible operating conditions, the resulting schedule is both optimal and consistent with real-time operating conditions.

6.2.2 Modeling Assumptions

For the sake of clarity, the modeling assumptions considered in this work are listed as follows:

1. The first-stage of the proposed UC problem (that represents the day-ahead market) embodies a dc network representation, while the second-stage (that represents the real-time operation) embeds an ac one. This assumption is consistent with the functioning of most real-world electricity markets.

2. For the sake of simplicity, only wind power uncertainty is taken into account. However, other uncertainties can be incorporated into the model. The uncertainty of wind power production is modeled through a set of plausible scenarios based on the available forecasted data.

3. The minimum up-time and minimum down-time constraints of thermal units are not considered in this work. To consider them, additional binary variables are required [81].

4. A number of units are available to provide reserve.

5. The wind power production cost is assumed to be nil.

6. All loads are assumed to be inelastic.

7. Wind farms of Type 3 DFIG and Type 4 full converter are able to provide voltage support in steady-state and dynamically [82]. However, for the sake of simplicity, we assume unit power factor for all wind farms.

8. The security constraints are not modeled in this work. However, such constraints can be easily incorporated in the proposed framework.

6.2.3 Formulation

The detailed formulation of the considered two-stage ac-UC problem is provided in Paper J3 through sets of equations (1)-(3). The outputs of the proposed ac-UC problem are of two types, first-stage (day-ahead market) and second-stage (real-time operation). Variables pertaining to the first-stage are:

C_{it}^{SU} Start-up cost of unit i in period t.

P_{it}^{DA} Active power scheduled for unit i in period t.

W_{kt}^{DA} Active power scheduled for wind farm k in period t.

$\theta_{nt}^{\mathrm{DA}}$ Voltage angle at node n in period t at the scheduling stage.

Additionally, variables corresponding to the second-stage include:

L_{dts}^{SH} Involuntarily active load shedding of load d in period t and scenario s.

Q_{its} Reactive power output of unit i in period t and scenario s.

r_{its} Reserve deployed by unit i in period t and scenario s.

W_{kts}^{SP} Wind power spillage of wind farm k in period t and scenario s.

v_{nts} Voltage magnitude at node n in period t and scenario s.

θ_{nts} Voltage angle at node n in period t and scenario s.

Equation (6.1) demonstrates the objective function of the proposed ac-UC problem problem which represent the system expected cost. The first two terms of (6.1) correspond to the system cost at scheduling time (first-stage), while the other two terms refer to the expected cost in real-time operation (second-stage). The first term represents the start-up cost of the units, the second one refers to their production cost, the third term represents the reserve deployment cost, and the last one is the load curtailment cost.

$$\underset{\Xi}{\text{Minimize}} \quad \left\{ \sum_{t(i\in\mathcal{G})} \left[C_{it}^{\mathrm{SU}} + C_i P_{it}^{\mathrm{DA}}\right] + \sum_{s} \rho_s \left[\sum_{t(i\in\mathcal{G})} C_i \; r_{its} + \sum_{t(d\in\mathcal{D})} V_d^{\mathrm{SH}} L_{dts}^{\mathrm{SH}} \right] \right\} \tag{6.1}$$

where C_i is marginal cost of the energy offered by unit i, ρ_s is probability of scenario s and V_d^{SH} is value of load shed for load d.

In addition, the objective function (6.1) is subject to two sets of constrains, first-stage and second-stage constraints. These constraints have been fully described in Paper J3 by the sets of equations (2) and (3). It is worth mentioning that the status of generating unit i is determined via the binary variable u_{it} that is equal to 1 if unit i is scheduled to be committed in period t and equal to 0 if it is not. The other optimization variables considered in the formulation of the proposed ac-UC problem are continuous.

This is very important to note that the proposed ac-UC problem is mixed-integer, nonlinear and thus non-convex, a difficult problem to solve. The next section proposes a solution strategy based on Benders' decomposition to solve such a problem.

6.3 Benders' solution

For solving the proposed ac-UC problem which is a mixed-integer nonlinear programming problem, there is no reliable off-the-shelf solver available. To make this problem efficiently solvable, Benders' decomposition is applied, whose advantages are as follows:

1. To transform the proposed mixed-integer and nonlinear ac-UC problem to (i) a mixed-integer and linear master problem (first-stage), and (ii) a set of nonlinear, but continuous subproblems (second-stage). Note that the optimal solution of each subproblem and master problem can be obtained through available solvers.

2. To decompose the second-stage of the UC problem by scenario and time period. This makes the ac-UC problem computationally tractable, if even a large number of wind power scenarios are considered.

Note that further explanations regarding the proposed solution strategy such as introducing the complicating variables of the problem, discussing on the convexification issues, describing the heuristic temporal decomposition technique, formulating the subproblems and the master problem, and finally presenting the Benders' algorithm are provided in detail in Paper J3.

6.4 Results and discussions

This section evaluates the numerical results obtained for a case study based on the IEEE one-area 24-node reliability test system (RTS) [66]. The detailed description of the considered test system is provided in Paper J3. Note that in this study, a daily time horizon (time periods t_1 to t_{24}) is considered. Three different cases are analyzed in the simulation:

Case A) This case refers to a dc-UC problem, where both stages embody a dc representation of the network. This problem is directly solved using a mixed-integer linear solver.

Case B) This case refers to an ac-UC problem based on model (1)-(3) given in Paper J3, and solved by the proposed Benders' algorithm. The voltage magnitude of each node is enforced to be within 0.9 p.u. and 1.1 p.u.

Case C) This case is similar to Case B, but constraints on the voltage magnitude of nodes are relaxed. In this case, the voltage magnitude of nodes can lie within 0.5 p.u. and 1.5 p.u. Although this case is not realistic, it is considered for illustrative purposes.

Table 6.1 mathematically characterizes the non-decomposed dc-UC problem (Case A), the non-decomposed ac-UC problem, and the decomposed ac-UC problem (Cases B and C).

A comprehensive analysis of the numerical results is reported in Paper J3. Accordingly, the most important observations are as follows:

Table 6.1: The mathematical characteristics of each case

Problem	Formulation (see Paper J3)	Type of optimization model	Binary variables included?	Available solver	Case
Non-decomposed dc-UC	Combination of (1), (2) and (9)	MILP[a]	Yes	CPLEX [83]	A
Non-decomposed ac-UC	Combination of (1), (2), and (3)	MINLP[b]	Yes	No off-the -shelf solver	-
Decomposed ac-UC	Benders' algorithm (depicted in Fig. 2) including subproblems (5) and master problem (7)	NLP[c] (subproblems)	No	CONOPT [84]	B and C
		MILP (master problem)	Yes	CPLEX [83]	

[a] Mixed-integer linear programming
[b] Mixed-integer non-linear programming
[c] Non-linear programming (continuous)

1. The expected cost in Case A (dc-UC problem) is comparatively smaller than that of Cases B and C (ac-UC problems). The reason of this is that the ac-UC problem enforces more realistic constraints than those of the dc-UC one. Also, the expected cost of Case B is comparatively higher than that of Case C, where voltage magnitude constraints are not tightly enforced.

2. The dc-UC and ac-UC problems yield different commitment status for the generating units. According to Fig. 4 of Paper J3, generating units 22 and 23 are decommitted in Case A (dc-UC problem), while they are committed in peak hours of Case B (ac-UC problem). Similarly, generating unit 9 is committed in time periods 1 and 2 of Case B.

3. In addition to the commitment status of generating units, the dispatch results of committed units from the dc-UC and ac-UC formulations are different. For example in Cases A and B, generating unit 32 is scheduled in peak hour t_{20} 3.2 p.u. and 2.5 p.u., respectively.

4. The reason for these differences is the constraints that are not modeled in the dc-UC formulation (Case A), i.e., reactive power constraints and voltage magnitude constraints. For example, the numerical results of Case B (ac-UC problem) illustrate that the voltage magnitudes of node 6 within different scenarios and time periods are mostly equal to its upper bound, i.e., 1.1 p.u. However, the results obtained by dc-UC model (Case A) misrepresents such constraint, since it does not consider the voltage magnitude bounds. In addition to those constraints, power losses in the network is the other reason of differences, as it is modeled in the ac-UC problem (Case B), but it is not in the dc-UC problem (Case A).

5. According to Fig. 4 of Paper J3, although both Cases B and C solve ac-UC problems, different bounds on voltage magnitude constraints render slightly

different results. For example, the comparatively small generating unit 15 is fully committed in Case C, while it is fully decommitted in Case B. On the other hand, the comparatively large generating unit 9 is not committed in Case C for time periods t_1 and t_2, while it is in Case B. These differences allow concluding that the voltage magnitude constraint may potentially alter the commitment results.

To summarize, this chapter has proposed an efficient solution approach based on Benders' decomposition to solve an ac-UC problem under wind power uncertainty. The numerical results obtained validate the well-functioning of the proposed approach.

6.5 Future work: adding FACTS devices to the formulation of the ac-UC problem under wind uncertainty

As mentioned in Section 5.6, after proposing a solution strategy for the ac-UC problem under wind power uncertainty, the next step will be evaluating the effectiveness of FACTS devices in improving the outcomes of such problem.

Incorporating FACTS devices into the proposed formulation of ac-UC problem under wind uncertainty is quite straightforward, and will only slightly changes the equations provided in Paper J3. Similar to Chapter 5 (Paper J2), FACTS devices are only considered in the second-stage of the proposed formulation since they are fast enough to be adjusted to any desirable value within their lower and upper bounds in seconds. To explain the required modification of the proposed ac-UC formulation, the thyristor controlled series capacitor (TCSC) is selected among the available types of FACTS devices, and the injection model is used for its modeling.

Therefore, a new variable x^{tcsc}_{nmts}, the reactance of the TCSC installed in transmission line (n,m) in period t and scenario s, will be added to the set of equations (3) of Paper J3. Similar to equation (11) of Paper J2, a new constraint will also be added to the set of equation (3) to enforce that the reactance of the TCSC lies within its lower and upper bounds. The new variable x^{tcsc}_{nmts} will change the definition of Functions $P_{nmts}(\mathbf{v}, \boldsymbol{\theta})$, $Q_{nmts}(\mathbf{v}, \boldsymbol{\theta})$ and $S_{nmts}(\mathbf{v}, \boldsymbol{\theta})$ used in equations (3a), (3b) and (3m) in a way to be dependent on $\mathbf{x^{tcsc}}$ as well, i.e., the new notations for these functions will be $P_{nmts}(\mathbf{v}, \boldsymbol{\theta}, \mathbf{x^{tcsc}})$, $Q_{nmts}(\mathbf{v}, \boldsymbol{\theta}, \mathbf{x^{tcsc}})$ and $S_{nmts}(\mathbf{v}, \boldsymbol{\theta}, \mathbf{x^{tcsc}})$. The definitions of these new functions are exactly similar to equations (24)-(33) of Paper J2 with this difference that all the equation will be for "each time period t and each scenario s" instead of only for "each scenario s", i.e., the subscript "s" in all the notations should be changed to "ts", for instance, θ_{ns} will change to θ_{nts} or v_{ns} will change to v_{nts}.

After applying the above modifications in order to incorporate TCSC into the ac-UC formulation (or any other type of FACTS devices), the problem should be solved using the Benders' solution proposed in this chapter (Paper J3). Unfortunately, due to the time limitation, we couldn't find the opportunity to carry out the simulations

based on the modified stochastic ac-UC problem considering FACTS devices, and this task will be considered as the future work of this chapter. The main objective is to study the impacts of such devices on improving the ac-UC outcomes, e.g., reducing the dispatch cost of generating units especially when the system is stressed (i.e., the UC constraints are mostly active).

Chapter 7

Conclusions and Future Work

In this final chapter, the key conclusions are drawn, and ideas for future research work are outlined.

7.1 Conclusions

This thesis work has focused on two main topics: (i) rotor angle stability and (ii) system operation under wind uncertainty. Within this scope, the following conclusions can be drawn:

1. **Applications of trajectory sensitivity analysis to determine the impacts of system parameters on the rotor angle stability**
   Using analytical formulation of trajectory sensitivity analysis, an approach has been proposed to find the suitable locations of series and shunt compensators in order to improve the transient stability, and also enhance the damping of small signal oscillations of power system. This approach is based on calculation of trajectory sensitivities of the rotor angles of generators with respect to some parameters of interest, e.g. reactances of transmission lines for series compensations and injected reactive power into the grid nodes for shunt compensation. The proposed approach not only has determined the most effective locations to install series/shunt compensators, but also explained why installing such compensators in certain locations could worsen the power system stability. Additionally, dynamic sensitivities of rotor angles with respect to the inertia of generators have been calculated to evaluate the impacts of inertia reduction of generators on the transient stability of the system. The inertia reduction can be the result of penetrating high amount of wind power into the power system. The results obtained have shown that depending on the type and location of the disturbance and also the location of inertia reduction, the transient stability is either improved or weakened. Regarding the computational time viewpoint, the proposed methods are more efficient compared to the similar works which used numerical formulation of TSA since

solving the TSA equations with the analytical method needs fewer number of time domain simulations. Three case systems IEEE 3-machine 9-bus, IEEE 10-machine 39-bus and Nordic-32 have been considered in this study, and the numerical results have demonstrated validity, accuracy and efficiency of the proposed approaches.

2. **Minimizing wind power spillage using an OPF with FACTS devices**
A methodology has been provided to minimize wind power spillage using an OPF with FACTS devices. In addition, total active power loss has been minimized and load shedding has been avoided as well. Among FACTS devices, TCSC has been selected for this study. The uncertainty of wind power production has been modeled through a number of plausible scenarios. The conclusions drawn from this work are listed below:

   a) A series compensation may reduce the wind power spillage, unserved load, and total active power losses of the network.

   b) Prior to wind uncertainty realization, the system is prepositioned using the proposed methodology to optimally cope with the wind production realizations.

   c) Optimal reactance setting of the TCSC needs to be determined for each wind scenario. According to the results obtained, for each scenario, the optimal utilization of the TCSC (optimal reactance setting) is effective to decrease wind power spillage; however, a FSC is not necessarily effective.

   d) Optimal setting of the TCSC reactance across all scenarios is not constant, and it does not necessarily equal its upper or lower bound. For the case of this study, such optimal setting depends on the inputs from the market and the system constraints.

3. **AC unit commitment under wind power uncertainty: a benders' decomposition approach**
An efficient solution approach based on Benders' decomposition has been proposed to solve a network-constrained ac unit commitment (ac-UC) problem under wind power uncertainty. The UC problem considered has been formulated as a two-stage stochastic programming model, whose first-stage refers to the day-ahead market, while the second-stage represents the real-time operation involving wind scenarios. Note that the type of such problem is mixed-integer and nonlinear, whose optimal solution is complicated in general to be found. In addition, such a network-constrained ac-UC problem may become computationally intractable considering a very large number of scenarios to model uncertainties of the available wind power resources. The proposed approach allows decomposing this problem into a mixed-integer linear master problem and a set of non-linear but continuous subproblems, one per scenario

and time period. Note that there is no reliable off-the-shelf solver available for a MINLP problem, while MILP and NLP problems are both solvable using available commercial solvers. The numerical results obtained validate the well-functioning of the proposed approach.

We point out that the commitment status and dispatch results of generating units obtained by the dc and ac formulations might be different. The reasons for the differences are (i) the constraints that are not modeled in the dc-UC formulation, i.e., reactive power and voltage magnitude constraints, and (ii) power losses which are not considered in the dc-UC formulation. It is also pointed out that the tightness level of voltage magnitude constraint in the ac-UC problem may potentially alter the commitment results.

7.2 Future work

The ideas that can be considered as the future work for this thesis are listed below:

1. The proposed methods can be applied to larger or more realistic test systems considering different contingencies and operational situations for more accurate evaluation of their validity, efficiency and accuracy.

2. The developed methods can be extended to include other types of FACTS devices and also HVDC systems.

3. A more precise and effective approach based on TSA can be developed considering both the mechanical power and inertia of generators as system parameters to determine the impacts of replacing a fuel-based generator by its equivalent wind power on the system stability. Another idea is to consider the detailed dynamic model of such wind generator in the commercial software for the verifications of the results.

4. Application of TSA can also be used for tuning the parameters of FACTS controllers. In this vein, the detailed model of FACTS devices equipped with their controllers should be implemented, and the controller parameters that need to be tuned are considered as the system parameters in the corresponding TSA-based study. In this way, the impact of each controller parameter on the system stability is determined which is the basic requirement for such tuning.

5. In part II of this thesis, stochastic programming is used to deal with optimization problems under uncertainty while the proposed models can also be formulated and solved using robust optimization instead in the future work. Additionally, the results obtained from both methodologies can be compared in order to determine the pros and cons of each approach.

6. A stochastic dc unit commitment problem in a large-scale power system can be computationally intractable since it needs to consider a very large number

of scenarios for modeling the uncertainty of the available wind producers. Another future work can be solving such a dc-UC problem using the proposed approach in Chapter 6 based on Benders' decomposition for the case where the problem cannot be solved directly with the available commercial solvers.

7. FACTS devices can also be incorporated into the proposed ac-UC problem under wind power uncertainty in Chapter 6. This allows studying the impacts of such devises on improving the ac-UC outcomes, e.g., reducing the dispatch cost of generating units especially when the system is stressed (i.e., the UC constraints are mostly active).

Bibliography

[1] J. M. Morales, A. J. Conejo, H. Madsen, P. Pinson, and M. Zugno, *Integrating Renewables in Electricity Markets: Operational Problems*, vol. 205. Springer US, Boston, MA, 2014.

[2] D. S. Kirschen and G. Strbac, *Fundamentals of Power System Economics*. Chichester, West Sussex, England ; Hoboken, NJ: Wiley, first ed., May 2004.

[3] IEA, *Lessons from Liberalised Electricity Markets*. Paris: Organisation for Economic Co-operation and Development, Dec. 2005.

[4] H. Bahar and J. Sauvage, "Cross-border trade in electricity and the development of renewables-based electric power," OECD trade and environment working papers, Organisation for Economic Co-operation and Development, Paris, Apr. 2013.

[5] "Renewables 2013 global status report," tech. rep., Renewable Energy Policy Network for the 21st Century (REN21), June 2013.

[6] N. G. Hingorani and L. Gyugyi, *Understanding FACTS: Concepts and Technology of Flexible AC Transmission Systems*. New York: Wiley-IEEE Press, 1 edition ed., Dec. 1999.

[7] P. Pourbeik, P. Kundur, and C. Taylor, "The anatomy of a power grid blackout - root causes and dynamics of recent major blackouts," *IEEE Power and Energy Magazine*, vol. 4, pp. 22–29, Sept. 2006.

[8] P. Kundur, J. Paserba, V. Ajjarapu, G. Andersson, A. Bose, C. Canizares, N. Hatziargyriou, D. Hill, A. Stankovic, C. Taylor, T. Van Cutsem, and V. Vittal, "Definition and classification of power system stability IEEE/CIGRE joint task force on stability terms and definitions," *IEEE Transactions on Power Systems*, vol. 19, pp. 1387–1401, Aug. 2004.

[9] P. Kundur, *Power System Stability and Control*. McGraw-Hill Education, Jan. 1994.

[10] L. Rouco and I. Perez-Arriaga, "Multi-area analysis of small signal stability in large electric power systems by SMA," *IEEE Transactions on Power Systems*, vol. 8, pp. 1257–1265, Aug. 1993.

[11] M. Gibbard, N. Martins, J. J. Sanchez-Gasca, N. Uchida, V. Vittal, and L. Wang, "Recent applications of linear analysis techniques," *IEEE Transactions on Power Systems*, vol. 16, pp. 154–162, Feb. 2001.

[12] J. Rueda, D. Colome, and I. Erlich, "Assessment and enhancement of small signal stability considering uncertainties," *IEEE Transactions on Power Systems*, vol. 24, pp. 198–207, Feb. 2009.

[13] G. Angelidis and A. Semlyen, "Improved methodologies for the calculation of critical eigenvalues in small signal stability analysis," *IEEE Transactions on Power Systems*, vol. 11, pp. 1209–1217, Aug. 1996.

[14] G. Maria, C. Tang, and J. Kim, "Hybrid transient stability analysis [power systems]," *IEEE Transactions on Power Systems*, vol. 5, pp. 384–393, May 1990.

[15] A. A. Fouad and S. E. Stanton, "Transient stability of a multi-machine power system. part II: critical transient energy," *IEEE Transactions on Power Apparatus and Systems*, vol. PAS-100, pp. 3417–3424, July 1981.

[16] A. Fouad, V. Vittal, and T. K. Oh, "Critical energy for direct transient stability assessment of a multimachine power system," *IEEE Transactions on Power Apparatus and Systems*, vol. PAS-103, pp. 2199–2206, Aug. 1984.

[17] T. Athay, R. Podmore, and S. Virmani, "A practical method for the direct analysis of transient stability," *IEEE Transactions on Power Apparatus and Systems*, vol. PAS-98, pp. 573–584, Mar. 1979.

[18] M. Laufenberg and M. A. Pai, "A new approach to dynamic security assessment using trajectory sensitivities," *IEEE Transactions on Power Systems*, vol. 13, pp. 953–958, Aug. 1998.

[19] A. Zamora-Cárdenas and C. R. Fuerte-Esquivel, "Multi-parameter trajectory sensitivity approach for location of series-connected controllers to enhance power system transient stability," *Electric Power Systems Research*, vol. 80, pp. 1096–1103, Sept. 2010.

[20] M. Pavella, D. Ernst, and D. Ruiz-Vega, *Transient Stability of Power Systems: A Unified Approach to Assessment and Control*. Springer, Oct. 2000.

[21] S. C. Savulescu, *Real-Time Stability Assessment in Modern Power System Control Centers*. Hoboken, N.J: Wiley-IEEE Press, 1 edition ed., Feb. 2009.

[22] D. Ruiz-Vega and M. Pavella, "A comprehensive approach to transient stability control part 1: near optimal preventive control," in *IEEE Power Engineering Society General Meeting, 2003*, vol. 3, pp. –, July 2003.

[23] D. Ruiz-Vega and M. Pavella, "A comprehensive approach to transient stability control. II. open loop emergency control," *IEEE Transactions on Power Systems*, vol. 18, pp. 1454–1460, Nov. 2003.

[24] Y. Xue, T. Van Cutsem, and M. Ribbens-Pavella, "Real-time analytic sensitivity method for transient security assessment and preventive control," *Generation, Transmission and Distribution, IEE Proceedings C*, vol. 135, pp. 107–117, Mar. 1988.

[25] Y. Xue, T. Van Cutsem, and M. Ribbens-Pavella, "A simple direct method for fast transient stability assessment of large power systems," *IEEE Transactions on Power Systems*, vol. 3, pp. 400–412, May 1988.

[26] I. Hiskens and M. A. Pai, "Trajectory sensitivity analysis of hybrid systems," *IEEE Transactions on Circuits and Systems I: Fundamental Theory and Applications*, vol. 47, pp. 204–220, Feb. 2000.

[27] D. Z. Fang and Q. Yi-fei, "A new trajectory sensitivity approach for computations of critical parameters," *Electric Power Systems Research*, vol. 77, pp. 303–307, Mar. 2007.

[28] T. B. Nguyen, M. A. Pai, and I. A. Hiskens, "Sensitivity approaches for direct computation of critical parameters in a power system," *International Journal of Electrical Power & Energy Systems*, vol. 24, pp. 337–343, June 2002.

[29] M. A. Pai and T. B. Nguyen, "Trajectory sensitivity theory in nonlinear dynamical systems: Some power system applications," in *Stability and Control of Dynamical Systems with Applications* (D. Liu and P. J. Antsaklis, eds.), Control Engineering, pp. 271–292, BirkhÃ¤user Boston, Jan. 2003.

[30] I. Hiskens and J. Alseddiqui, "Sensitivity, approximation, and uncertainty in power system dynamic simulation," *IEEE Transactions on Power Systems*, vol. 21, no. 4, pp. 1808–1820, 2006.

[31] T. Nguyen and M. A. Pai, "Dynamic security-constrained rescheduling of power systems using trajectory sensitivities," *IEEE Transactions on Power Systems*, vol. 18, pp. 848–854, May 2003.

[32] M. Ghandhari, G. Andersson, and I. Hiskens, "Control lyapunov functions for controllable series devices," *IEEE Transactions on Power Systems*, vol. 16, pp. 689–694, Nov. 2001.

[33] M. Ghandhari, G. Andersson, M. Pavella, and D. Ernst, "A control strategy for controllable series capacitor in electric power systems," *Automatica*, vol. 37, pp. 1575–1583, Oct. 2001.

[34] M. H. Haque, "Improvement of first swing stability limit by utilizing full benefit of shunt FACTS devices," *IEEE Transactions on Power Systems*, vol. 19, pp. 1894–1902, Nov. 2004.

[35] E. Gholipour and S. Saadate, "Improving of transient stability of power systems using UPFC," *IEEE Transactions on Power Delivery*, vol. 20, pp. 1677–1682, Apr. 2005.

[36] J. Zhao, A. Ishigame, S. Kawamoto, and T. Taniguchi, "Structural control of electric power networks for transient stability," *IEEE Transactions on Power Systems*, vol. 9, pp. 1575–1581, Aug. 1994.

[37] K. N. Shubhanga and A. Kulkarni, "Application of structure preserving energy margin sensitivity to determine the effectiveness of shunt and series FACTS devices," *IEEE Transactions on Power Systems*, vol. 17, pp. 730–738, Aug. 2002.

[38] D. Chatterjee and A. Ghosh, "Transient stability assessment of power systems containing series and shunt compensators," *IEEE Transactions on Power Systems*, vol. 22, pp. 1210–1220, Aug. 2007.

[39] M. Farsangi, Y. H. Song, and K. Lee, "Choice of FACTS device control inputs for damping interarea oscillations," *IEEE Transactions on Power Systems*, vol. 19, pp. 1135–1143, May 2004.

[40] Y. Tang and A. P. S. Meliopoulos, "Power system small signal stability analysis with FACTS elements," *IEEE Transactions on Power Delivery*, vol. 12, pp. 1352–1361, July 1997.

[41] M. Noroozian and G. Andersson, "Damping of inter-area and local modes by use of controllable components," *IEEE Transactions on Power Delivery*, vol. 10, pp. 2007–2012, Oct. 1995.

[42] B. Kumar, S. Singh, and S. Srivastava, "Placement of FACTS controllers using modal controllability indices to damp out power system oscillations," *IET Generation, Transmission Distribution*, vol. 1, pp. 209–217, Mar. 2007.

[43] H. Okamoto, A. Kurita, and Y. Sekine, "A method for identification of effective locations of variable impedance apparatus on enhancement of steady-state stability in large scale power systems," *IEEE Transactions on Power Systems*, vol. 10, pp. 1401–1407, Aug. 1995.

[44] R. Rouco and F. L. Pagola, "An eigenvalue sensitivity approach to location and controller design of controllable series capacitors for damping power system oscillations," *IEEE Transactions on Power Systems*, vol. 12, pp. 1660–1666, Nov. 1997.

[45] "The iberian peninsula electricity exchange, omie, 2013 [online]. available: http://www.omie.es/," 2013.

[46] "The dannish energy agency, 2013 [online]. available: http://www.ens.dk/."

[47] "The nordic electricity exchange, nordpool [online]. available: http://www.nordpoolspot.com/."

[48] "Pennsylvania- new jersey- maryland interconnection, pjm [online]. available: http://www.pjm.com/."

[49] "Iso-new england [online]. available: http://www.iso-ne.com/."

[50] A. J. Conejo, M. Carrión, and J. M. Morales, *Decision Making Under Uncertainty in Electricity Markets*. International Series in Operations Research & Management Science, New York, NY, USA: Springer, 2010.

[51] J. M. Morales, A. J. Conejo, and J. Perez-Ruiz, "Economic valuation of reserves in power systems with high penetration of wind power," *IEEE Transactions on Power Systems*, vol. 24, pp. 900–910, May 2009.

[52] J. M. Morales, A. J. Conejo, K. Liu, and J. Zhong, "Pricing electricity in pools with wind producers," *IEEE Transactions on Power Systems*, vol. 27, pp. 1366–1376, Aug. 2012.

[53] M. Ghofrani, A. Arabali, M. Etezadi-Amoli, and M. Fadali, "A framework for optimal placement of energy storage units within a power system with high wind penetration," *IEEE Transactions on Sustainable Energy*, vol. 4, pp. 434–442, Apr. 2013.

[54] A. M. Geoffrion, "Generalized benders decomposition," *Journal of Optimization Theory and Applications*, vol. 10, pp. 237–260, Oct. 1972.

[55] M. Ghandhari, "Dynamic analysis of power systems, part II," *KTH*, Tech. Rep., 2007.

[56] J. Machowski and J. R. Bumby, *Power System Dynamics and Stability*. John Wiley & Sons, Oct. 1997.

[57] P. W. Sauer and M. A. Pai, *Power System Dynamics and Stability*. Prentice Hall, 1998.

[58] K. Brenan, S. Campbell, and L. Petzold, *Numerical Solution of Initial-Value Problems in Differential-Algebraic Equations*. Classics in Applied Mathematics, Society for Industrial and Applied Mathematics, Jan. 1995.

[59] E. A. Zamora-Càrdenas and C. R. Fuerte-Esquivel, "Computation of multiparameter sensitivities of equilibrium points in electric power systems," *Electric Power Systems Research*, vol. 96, pp. 246–254, Mar. 2013.

[60] R. Sadikovic, P. Korba, and G. Andersson, "Application of FACTS devices for damping of power system oscillations," in *Power Tech, 2005 IEEE Russia*, pp. 1–6, June 2005.

[61] M. A. Pai, *Energy Function Analysis for Power System Stability*. Springer, Aug. 1989.

[62] M. Stubbe and M. Amorouayeche, *Long Term Dynamics: Final report. Phase II*. CIGRE, 1995.

[63] A. J. Conejo, E. Castillo, R. Minguez, and R. Garcia-Bertrand, *Decomposition Techniques in Mathematical Programming: Engineering and Science Applications*. Berlin; New York: Springer, 2006 edition ed., Jan. 2006.

[64] S. N. Singh and A. K. David, "Optimal location of FACTS devices for congestion management," *Electric Power Systems Research*, vol. 58, pp. 71–79, June 2001.

[65] M. Noroozian and G. Andersson, "Power flow control by use of controllable series components," *IEEE Transactions on Power Delivery*, vol. 8, pp. 1420–1429, July 1993.

[66] C. Grigg, P. Wong, P. Albrecht, R. Allan, M. Bhavaraju, R. Billinton, Q. Chen, C. Fong, S. Haddad, S. Kuruganty, W. Li, R. Mukerji, D. Patton, N. Rau, D. Reppen, A. Schneider, M. Shahidehpour, and C. Singh, "The IEEE reliability test system-1996. a report prepared by the reliability test system task force of the application of probability methods subcommittee," *IEEE Transactions on Power Systems*, vol. 14, pp. 1010–1020, Aug. 1999.

[67] R. Baldick, "The generalized unit commitment problem," *IEEE Transactions on Power Systems*, vol. 10, pp. 465–475, Feb. 1995.

[68] F. Zhuang and F. D. Galiana, "Towards a more rigorous and practical unit commitment by Lagrangian relaxation," *IEEE Trans. Power Syst.*, vol. 3, pp. 763–773, May 1988.

[69] S. Takriti, J. Birge, and E. Long, "A stochastic model for the unit commitment problem," *IEEE Transactions on Power Systems*, vol. 11, pp. 1497–1508, Aug. 1996.

[70] P. Carpentier, G. Gohen, J.-C. Culioli, and A. Renaud, "Stochastic optimization of unit commitment: a new decomposition framework," *IEEE Transactions on Power Systems*, vol. 11, pp. 1067–1073, May 1996.

[71] F. Bouffard, F. D. Galiana, and A. J. Conejo, "Market-clearing with stochastic security-part i: formulation," *IEEE Transactions on Power Systems*, vol. 20, pp. 1818–1826, Nov. 2005.

[72] F. Bouffard, F. D. Galiana, and A. J. Conejo, "Market-clearing with stochastic security-part II: case studies," *IEEE Transactions on Power Systems*, vol. 20, pp. 1827–1835, Nov. 2005.

[73] Q. Wang, J. Wang, and Y. Guan, "Price-based unit commitment with wind power utilization constraints," *IEEE Transactions on Power Systems*, vol. 28, pp. 2718–2726, Aug. 2013.

[74] A. Kalantari, J. Restrepo, and F. Galiana, "Security-constrained unit commitment with uncertain wind generation: The loadability set approach," *IEEE Transactions on Power Systems*, vol. 28, pp. 1787–1796, May 2013.

[75] A. Tuohy, P. Meibom, E. Denny, and M. O'Malley, "Unit commitment for systems with significant wind penetration," *IEEE Transactions on Power Systems*, vol. 24, pp. 592–601, May 2009.

[76] J. Wang, M. Shahidehpour, and Z. Li, "Security-constrained unit commitment with volatile wind power generation," *IEEE Transactions on Power Systems*, vol. 23, pp. 1319–1327, Aug. 2008.

[77] W. Sifuentes and A. Vargas, "Hydrothermal scheduling using benders decomposition: Accelerating techniques," *IEEE Transactions on Power Systems*, vol. 22, pp. 1351–1359, Aug. 2007.

[78] Y. Fu, M. Shahidehpour, and Z. Li, "Security-constrained unit commitment with AC constraints," *IEEE Transactions on Power Systems*, vol. 20, pp. 1001–1013, May 2005.

[79] C. Murillo-Sanchez, R. Zimmerman, C. Lindsay Anderson, and R. Thomas, "Secure planning and operations of systems with stochastic sources, energy storage, and active demand," *IEEE Transactions on Smart Grid*, vol. 4, pp. 2220–2229, Dec. 2013.

[80] A. J. Conejo, M. Carrión, and J. M. Morales, *Decision Making Under Uncertainty in Electricity Markets*. International Series in Operations Research & Management Science, New York, NY, USA: Springer, 2010.

[81] J. Ostrowski, M. F. Anjos, and A. Vannelli, "Tight mixed integer linear programming formulations for the unit commitment problem," *IEEE Trans. Power Syst.*, vol. 27, pp. 39–46, Feb. 2012.

[82] S. Muller, M. Deicke, and R. W. De Doncker, "Doubly fed induction generator systems for wind turbines," *IEEE Ind. Appl. Mag.*, vol. 8, pp. 26–33, May 2002.

[83] CPLEX, GAMS. The Solver Manuals. GAMS/CPLEX [Online]. Available: http://www.gams.com/, 2010.

[84] A. Drud, "GAMS/CONOPT. Bagsvaerd, Denmark: ARKI Consulting and Development," [Online]. Available: http://www.gams.com/, 1996.

Paper J1

Using Trajectory Sensitivity Analysis to Find Suitable Locations of Series Compensators for Improving Rotor Angle Stability

Electric Power Systems Research 111 (2014) 1–8

Contents lists available at ScienceDirect

Electric Power Systems Research

journal homepage: www.elsevier.com/locate/epsr

Using trajectory sensitivity analysis to find suitable locations of series compensators for improving rotor angle stability

Amin Nasri*, Robert Eriksson, Mehrdad Ghandhari

Department of Electric Power System, KTH Royal Institute of Technology, 10044 Stockholm, Sweden

ARTICLE INFO

Article history:
Received 14 October 2013
Received in revised form 23 January 2014
Accepted 27 January 2014
Available online 21 February 2014

Keywords:
Trajectory sensitivity analysis (TSA)
Transient stability
Small signal stability
Flexible AC transmission system (FACTS) devices
Critical clearing time (CCT)

ABSTRACT

This paper proposes an approach based on trajectory sensitivity analysis (TSA) to find most suitable placement of series compensators in the power system. The main objective is to maximize the benefit of these devices in order to enhance the rotor angle stability. This approach is formulated as a two-stage problem, whose first-stage describes prior to fault occurrence and whose second-stage represents the power system behavior involving a set of severe faults. The first-stage focuses on small signal stability, while the second-stage deals with transient stability of power system. In this vein, the trajectory sensitivities of the rotor angles of generators with respect to the reactances of transmission lines are calculated. Two equivalent rotor angles are introduced to find stability indices corresponding to the first- and the second-stage of the proposed approach. Numerical results from IEEE 10-machine 39-bus test system demonstrate the usefulness of the proposed method.

1. Introduction

1.1. Motivation and aim

Deregulation in electricity markets, increasing electricity demands and high penetration of renewable energy sources have increased the power transactions within and between regions in today's power systems. The installation of new transmission lines cannot be carried out easily because of its heavy costs and environmental concerns. As a result, this competitive environment pushes the existing transmission systems to be operated close to their critical conditions which may result in higher risk of transient instability. Moreover, small signal oscillations occur more frequently in a heavy-loaded interconnected power system. In this situation, rotor angle stability would be one of the main concerns of the power system operators.

Series flexible AC transmission systems (FACTS) devices, e.g., Thyristor Controlled Series Capacitor (TCSC), can have a significant impact on operational flexibility and controllability of the power system. They can manipulate the reactance of transmission lines and control the power flow through lines in a way to increase the transient stability margins. These devices, equipped with the proper controller, can also be used to improve the small signal stability. Since the impact of these compensators on the system stability is strongly dependent on their locations, it is required to provide useful information to the system planners regarding the best possible locations to install them. In this paper, an effective approach is proposed to identify the most suitable placement of series compensators for improving both the transient and small signal stability of the power system.

1.2. Literature review

Assessment of rotor angle stability is essential to study the dynamic behavior of the power system. Time domain simulation is the traditional way for transient stability assessment which has two main disadvantageous, namely time-consuming computation requirement and incapability to provide any information regarding the stability margin [1]. The other method which has been widely used for this purpose is transient energy function (TEF) method [2–4]. The significant advantage of this method is its capability to provide a stability index [1]. Several methodologies have been proposed based on the sensitivity of TEF to determine the effectiveness of FACTS devices in improving the transient stability. For instance, [5] proposes a methodology based on sensitivities of the critical energy of post-fault system with respect to some system parameters, e.g., reactance of the lines for series compensations and injected reactive power into nodes for shunt compensations. A structure preserving energy margin sensitivity based analysis is carried out in [6] for placement of series and shunt FACTS devices.

* Corresponding author. Tel.: +46 707 305063; fax: +46 8 790 6510.
E-mail addresses: amin.nasri@ee.kth.se, amin.nasri@gmail.com (A. Nasri), robert.eriksson@ee.kth.se (R. Eriksson), mehrdad.ghandhari@ee.kth.se (M. Ghandhari).

0378-7796/$ – see front matter © 2014 Elsevier B.V. All rights reserved.
http://dx.doi.org/10.1016/j.epsr.2014.01.022

Despite all the advantages of the TEF based methods, the main shortcoming of them is their high complexity in the following situations: (i) considering differential-algebraic equation (DAE) models of power systems, (ii) dealing with the detailed models of the system's components, and (iii) when a number of system's parameters have to be taken into account for the sensitivity analysis [7–9].

Applications of trajectory sensitivity analysis (TSA) have been introduced as an alternative to overcome the mentioned shortcoming of the TEF based method [7]. Ref. [10] uses TSA to calculate the critical values of some power system parameters, e.g., fault clearing time and mechanical input power of generators. The proposed method in [10] is based on the computation of the norm of trajectory sensitivities of rotor angles and speeds of generators with respect to the parameters of interest. Ref. [8] discusses the application of TSA to power systems containing series and shunt compensators. A transient stability index is introduced based on a numerical estimation of TSA, and is calculated for the power system with different locations of series and shunt compensators. Ref. [11] identifies the optimal location and proper design of the TCSC-controller with the help of TSA for a power system involving several fault conditions. Using numerical formulation of TSA, considering the compensators' models in the study and simulating the power system for all the possible locations of compensators causes high computational burden for the proposed method in [8,11]. Ref. [9] develops a multi-parameter trajectory sensitivity approach to find the best locations of series compensators in order to improve the transient stability. An index of proximity to instability is determined based on the norm of trajectory sensitivities of the rotor angles and the speeds of generators with respect to the transmission line susceptances. Using the analytical formulation of TSA in [9] and also in the current paper, the cumbersome computational process becomes much simpler compared to the numerical method which is used in [8,11]. As it is explained completely in [9], the analytical formulation of TSA reduces the required number of time domain simulations from $(n_l+1)\times n_z$ to n_z for a power system with n_l transmission lines and n_z fault scenarios. Compared to [9], the method proposed in this paper is also capable to determine the transmission lines on which the installed compensators could have an opposite effect on the system stability. The latter will be addressed in details in this paper.

In the technical literature, there are also some works focusing on suitable placement of FACTS devices for improving small signal stability, e.g., [12,13] which propose controllability indices in order to find such a placement. Ref. [14] uses an eigenvalue sensitivity approach to determine the transmission line whose reactance modulation would be more effective to damp out the oscillatory modes of interest. It is important to note that, in previous literature, there is no thorough placement approach considering both the transient and small signal stability improvements, and such approach is addressed in this paper.

1.3. Contributions

Considering the works analyzed in the literature review, the contributions of this paper are threefold:

1. To propose a novel approach based on analytical formulation of TSA for suitable placement of series compensators in order to improve both the transient and small signal stability of the power system.
2. To formulate the proposed approach as a two-stage problem analyzing the pre-fault and post-fault behavior of power system.
3. To demonstrate the conditions where installing series compensators in the transmission lines deteriorates the power system stability.

1.4. Paper organization

The rest of this paper is organized as follows: Section 2 presents how to formulate the TSA technique. Section 3 explains the application of TSA for transient and small signal stability assessments. Section 4 proposes an approach for suitable placement of series compensators in order to improve rotor angles stability. Section 5 provides results from a case study, and finally Section 6 provides a number of relevant conclusions.

2. Trajectory sensitivity

2.1. Power system modeling and analytical formulation of trajectory sensitivity

Power systems can be modeled by the following differential algebraic equations [15]

$$\dot{x} = f(x, y; \lambda) \tag{1}$$

$$0 = g(x, y; \lambda) \tag{2}$$

$$x(t_0) = x_0, \quad y(t_0) = y_0 \tag{3}$$

where x is a vector containing the dynamic states, y is a vector of algebraic states and λ is a vector of system parameters. Rotor angles of the generators (δ), magnitude and angle of bus voltages and reactances of the transmission lines are the examples of the dynamic states, algebraic states and parameters of the power system, respectively. Vectors x_0 and y_0 are the initial conditions of dynamic and algebraic states. Function f is the set of differential equations which model the dynamics of equipments such as generators. The algebraic equations g consist of the network equations based on Kirchhoff's current law, i.e. the sum of all current (or powers) flowing into each bus must be equal to zero. To write the equations in a more organized way, vectors of $\underline{x}$ and $\underline{f}$ are defined as follows:

$$\underline{x} = \begin{bmatrix} x \\ \lambda \end{bmatrix}, \quad \underline{f} = \begin{bmatrix} f \\ 0 \end{bmatrix} \tag{4}$$

and therefore

$$\dot{\underline{x}} = \underline{f}(\underline{x}, y) \tag{5}$$

$$0 = g(\underline{x}, y) \tag{6}$$

To calculate the trajectory sensitivities analytically, the derivatives of (5), (6) are calculated with respect to $\underline{x}_0$

$$\dot{\underline{x}}_{\underline{x}_0} = \underline{f}_{\underline{x}}(t)\underline{x}_{\underline{x}_0} + \underline{f}_y(t)y_{\underline{x}_0} \tag{7}$$

$$0 = g_{\underline{x}}(t)\underline{x}_{\underline{x}_0} + g_y(t)y_{\underline{x}_0} \tag{8}$$

The initial conditions for $\underline{x}_{\underline{x}_0}$ and $y_{\underline{x}_0}$ are obtained by differentiating (3) with respect to $\underline{x}_0$. It is obvious that the initial value for the trajectory sensitivities of dynamic states is an identity matrix. Using this identity matrix, the initial values for the trajectory sensitivities of algebraic states can be also computed from (8).

$$\underline{x}_{\underline{x}_0}(t_0) = I, \quad y_{\underline{x}_0}(t_0) = -(g_y(t_0))^{-1} g_{\underline{x}_0}(t_0) \tag{9}$$

where $\underline{f}_{\underline{x}}$, $\underline{f}_y$, $g_{\underline{x}}$ and g_y are time varying functions which are calculated along the system trajectories. To find the trajectory sensitivities, the DAEs (5)–(8) should be solved simultaneously considering the initial conditions described above. The solution method is explained in detail in the next section.

2.2. Trapezoidal approach for trajectory sensitivity computation

The trapezoidal numerical integration approach introduces two sets of algebraic difference equations (10) and (11) which are coupled to the original DAEs (5)–(8) as follows [15]:

$$0 = \begin{bmatrix} F_1(\cdot) \\ F_2(\cdot) \end{bmatrix} = \begin{bmatrix} \frac{\eta}{2}\underline{f}(\underline{x}^{k+1}, \underline{y}^{k+1}) - \underline{x}^{k+1} + \frac{\eta}{2}\underline{f}(\underline{x}^{k}, \underline{y}^{k}) + \underline{x}^{k} \\ g(\underline{x}^{k+1}, \underline{y}^{k+1}) \end{bmatrix} \tag{10}$$

$$0 = \begin{bmatrix} F_3(\cdot) \\ F_4(\cdot) \end{bmatrix} = \begin{bmatrix} \underline{x}_{\underline{x}_0}^{k+1} - \underline{x}_{\underline{x}_0}^{k} - \frac{\eta}{2}(\underline{f}_{\underline{x}}^{k}\underline{x}_{\underline{x}_0}^{k} + \underline{f}_{\underline{y}}^{k}\underline{y}_{\underline{x}_0}^{k} + \underline{f}_{\underline{x}}^{k+1}\underline{x}_{\underline{x}_0}^{k+1} + \underline{f}_{\underline{y}}^{k+1}\underline{y}_{\underline{x}_0}^{k+1}) \\ g_{\underline{x}}^{k+1}\underline{x}_{\underline{x}_0}^{k+1} + g_{y}^{k+1}\underline{y}_{\underline{x}_0}^{k+1} \end{bmatrix} \tag{11}$$

where η is the integration time-step, and the superscript k indexes the time instant t_k. Note that (10) is a set of implicit non-linear algebraic equations which is solved using Newton–Raphson iterative algorithm. The set of equation (10) has the form $F(\varkappa) = 0$ which is solved iteratively based on

$$\varkappa_{i+1} = \varkappa_i - F_{\varkappa}(\varkappa_i)^{-1} F(\varkappa_i) \tag{12}$$

where $F_{\varkappa}$ is the Jacobian of F with respect to $\varkappa$, and the index i is the Newton–Raphson iteration step. So, the solution to the non-linear set of equations (10) is obtained by solving the following linear problem

$$\begin{bmatrix} \underline{x}^{k+1} \\ y^{k+1} \end{bmatrix}_i = \begin{bmatrix} \underline{x}^{k} \\ y^{k} \end{bmatrix}_i - \underbrace{\begin{bmatrix} \frac{\eta}{2}\underline{f}_{\underline{x}}^{k+1} - I & \frac{\eta}{2}\underline{f}_{y}^{k+1} \\ g_{\underline{x}}^{k+1} & g_{y}^{k+1} \end{bmatrix}_i^{-1}}_{F_{\varkappa}} \begin{bmatrix} F_1(\cdot) \\ F_2(\cdot) \end{bmatrix}_i \tag{13}$$

Once (13) has converged, the trajectory sensitivities are calculated by rearranging the set of linear equations (11) as given in (14)

$$\begin{bmatrix} \underline{x}_{\underline{x}_0}^{k+1} \\ y_{\underline{x}_0}^{k+1} \end{bmatrix} = \underbrace{\begin{bmatrix} \frac{\eta}{2}\underline{f}_{\underline{x}}^{k+1} - I & \frac{\eta}{2}\underline{f}_{y}^{k+1} \\ g_{\underline{x}}^{k+1} & g_{y}^{k+1} \end{bmatrix}^{-1}}_{F_{\varkappa}} \begin{bmatrix} -\frac{\eta}{2}(\underline{f}_{\underline{x}}^{k}\underline{x}_{\underline{x}_0}^{k} + \underline{f}_{y}^{k}\underline{y}_{\underline{x}_0}^{k}) - \underline{x}_{\underline{x}_0}^{k} \\ 0 \end{bmatrix} \tag{14}$$

Note that the coefficient matrix in the right side of (14) is exactly the same Jacobian used in solving final iteration of (13).

2.3. Numerical formulation of trajectory sensitivity analysis

To calculate the trajectory sensitivity of state variable x to the parameter λ with a numerical formulation of TSA, a small perturbation of $\Delta\lambda$ over the nominal parameter λ_0 should be considered such that $\lambda = \lambda_0 + \Delta\lambda$. So, the numerical estimation of sensitivity is defined as

$$x_{\lambda} = \frac{x(\lambda) - x(\lambda_0)}{\Delta\lambda} \tag{15}$$

Obviously, the TSA calculation for a system with n_{λ} number of parameters, using numerical formulation, needs to $(n_{\lambda} + 1)$ number of time domain simulations.

3. Transient and small signal stability assessment using trajectory sensitivity analysis

Power systems may become transiently unstable after being subjected to large disturbances. The result of transient instability appears in the form of increasing rotor angles of some generators which leads to their loss of synchronism with other generators. Under small disturbances, rotor angle's oscillations show if the system is small signal stable or not. If their oscillation are positively damped and decay with time, the power system is stable. Otherwise, there will be a negative damping in electromechanical oscillation which results in oscillatory instability.

Therefore, it is possible to check both the transient and small signal stability using rotor angles of generators (dynamic states δ). To improve the transient stability, power system parameters can be controlled (if applicable) in a way to have positive effects on the variation of rotor angles of generators when the system is subjected to a fault, and prevent power system from being transiently unstable. These parameters can also be controlled for improving the power oscillation damping, and ensuring the small signal stability of power system.

Reactance of transmission line is one of the parameters which can have a considerable effect on the rotor angle stability of power system. Nowadays with the presence of series FACTS devices, it is possible to dynamically change the reactance of the transmission lines, control the power flows through lines, and improve the rotor angle stability of power system. Due to the heavy costs of these devices, it is necessary to find the appropriate locations to install minimum numbers of them required for the stability enhancement. In this paper, trajectory sensitivities of rotor angles of generators to the reactances of transmission lines are used for suitable placement of series compensators. Eqs. (16) and (17) show power system parameters considered in this study and trajectory sensitivities of dynamical states to such parameters as described above.

$$\lambda = [\, x_{L_1} \quad \cdots \quad x_{L_l} \quad \cdots \quad x_{L_{n_l}} \,] \tag{16}$$

$$\frac{\partial\delta}{\partial\lambda} = \begin{bmatrix} \frac{\partial\delta_1}{\partial x_{L_1}} & \cdots & \frac{\partial\delta_1}{\partial x_{L_l}} & \cdots & \frac{\partial\delta_1}{\partial x_{L_{n_l}}} \\ \vdots & \vdots & \vdots & \vdots & \\ \frac{\partial\delta_i}{\partial x_{L_1}} & \cdots & \frac{\partial\delta_i}{\partial x_{L_l}} & \cdots & \frac{\partial\delta_n}{\partial x_{L_{n_l}}} \\ \vdots & \vdots & \vdots & \vdots & \\ \frac{\partial\delta_n}{\partial x_{L_1}} & \cdots & \frac{\partial\delta_n}{\partial x_{L_l}} & \cdots & \frac{\partial\delta_n}{\partial x_{L_{n_l}}} \end{bmatrix} \tag{17}$$

where x_{L_l} is the reactance of the lth transmission line, n_l is the number of lines, δ_i is the rotor angle of the ith generator, and n is the number of generators.

4. Suitable placement of series compensators to improve rotor angle stability

In this section, a method is proposed to find the suitable placement of series compensators for improving rotor angle stability. Rotor angle stability is divided to two categories, small signal stability and transient stability. The time framework of this study is characterized as follows:

1. Before fault occurrence ($t_0 < t < t_f^-$): this time frame pertains to small signal stability enhancement since there is no disturbance in the system, and linearization is permissible for the purpose of analysis.
2. After fault occurrence ($t_f^+ < t < t_{end}$): this time frame is concerned with transient stability improvement since the power system is subjected to several large disturbances.

4.1. Small signal stability improvement ($t_0 < t < t_f^-$)

Despite the fact that before fault occurrence power system works in its operating point with fixed state and algebraic variables, the trajectory sensitivities will oscillate around their operating points as a result of non-zero initial values described in (9) until their steady-state values will be reached. The trajectory sensitivities are computed based on (14) with this explanation that matrices $\underline{f}_{\underline{x}}$, $\underline{f}_{\underline{y}}$, $g_{\underline{x}}$ and g_y are time-invariant since there is no change in the system. Eq. (18) describes the evolution of the trajectory sensitivities $\underline{x}_{\underline{x}_0}$, $y_{\underline{x}_0}$ within this time frame $(t_0 - t_f^-)$ [15,16].

$$\begin{bmatrix} \underline{x}_{\underline{x}_0}^{k+1} \\ y_{\underline{x}_0}^{k+1} \end{bmatrix} = \underbrace{\begin{bmatrix} \frac{\eta}{2}\underline{f}_{\underline{x}}^0 - I & \frac{\eta}{2}\underline{f}_{\underline{y}}^0 \\ g_{\underline{x}}^0 & g_y^0 \end{bmatrix}^{-1}}_{F_{\chi}} \begin{bmatrix} -\frac{\eta}{2}(\underline{f}_{\underline{x}}^0 \underline{x}_{\underline{x}_0}^k + \underline{f}_{\underline{y}}^0 y_{\underline{x}_0}^k) - \underline{x}_{\underline{x}_0}^k \\ 0 \end{bmatrix} \tag{18}$$

These oscillations show how sensitive state and algebraic variables are to the system parameters under assumption that the system is subjected to a very small disturbance such that the state and algebraic variables can be considered constant. In this section, an algorithm is proposed for suitable placement of series compensators to enhance the small signal stability of the system.

4.1.1. Definition of equivalent angle δ_{eq_s}

An equivalent rotor angle δ_{eq_s} is defined based on the modal analysis corresponding to the mode of interest. The mode of interest ϑ_i which is the one with poorest damping and a low frequency is determined from eigenvalues of the following matrix:

$$A = \underline{f}_{\underline{x}} - \underline{f}_{\underline{y}} g_y^{-1} g_{\underline{x}} \tag{19}$$

where $\underline{f}_{\underline{x}}$, $\underline{f}_{\underline{y}}$, $g_{\underline{x}}$ and g_y were defined in (7) and (8). The right eigenvector of A matrix corresponding to the eigenvalue ϑ_i is calculated satisfying (20)

$$AV_i^r = \vartheta i V_i^r \tag{20}$$

Note that V_r^i is a column vector of order $n_x \times 1$, where n_x is a number of state variables. Those arrays of the vector which are corresponding to the rotor angles of the generators δ_i are selected, and their imaginary part with respect to their real part are shown as a compass plot. Based on this compass plot, generators are divided to two groups, namely A_s and B_s, which are oscillating against each other. The definition of this equivalent angle is as follows

$$M_{A_s} = \sum_{i \in A_s} M_i, \quad M_{B_s} = \sum_{j \in B_s} M_j \tag{21}$$

$$\delta_{A_s} = M_{A_s}^{-1} \sum_{i \in A_s} M_i \delta_i, \quad \delta_{B_s} = M_{B_s}^{-1} \sum_{j \in B_s} M_j \delta_j \tag{22}$$

$$\delta_{eq_s} = \delta_{A_s} - \delta_{B_s} \tag{23}$$

where M_i is the inertia of the ith generator. According to this definition, the trajectory sensitivity of the equivalent angle to the reactances of transmission lines is as follows:

$$\frac{\partial \delta_{eq_s}}{\partial x_{L_l}} = \frac{\partial \delta_{A_s}}{\partial x_{L_l}} - \frac{\partial \delta_{B_s}}{\partial x_{L_l}} \tag{24}$$

where

$$\frac{\partial \delta_{A_s}}{\partial x_{L_l}} = M_{A_s}^{-1} \sum_{i \in A_s} M_i \frac{\partial \delta_i}{\partial x_{L_l}}, \quad \frac{\partial \delta_{B_s}}{\partial x_{L_l}} = M_{B_s}^{-1} \sum_{j \in B_s} M_j \frac{\partial \delta_j}{\partial x_{L_l}} \tag{25}$$

4.1.2. The proposed algorithm for suitable placement of series compensators to improve small signal stability

- Trajectory sensitivities of rotor angles with respect to the reactances of transmission lines are calculated solving (18) for $t_0 < t < t_f^-$.
- According to Section 4.1.1, trajectory sensitivities of the equivalent angle δ_{eq_s} with respect to the reactances of transmission lines are plotted using the obtained data in the previous step. The normalized first-cycle peak value of these trajectory sensitivities are determined. The transmission lines with the most positive peak values are the most effective locations to install series compensators in order to shift the critical eigenvalue to the left-half plane, increase the system damping, and therefore improve the small signal stability.

4.2. Transient stability improvement ($t_f^+ < t < t_{end}$)

To find the trajectory sensitivities after fault occurrence, the sets of Eqs. (13) and (14) should be solved simultaneously.

4.2.1. Definition of equivalent angle δ_{eq_t}

In this section, an equivalent angle is introduced for transient stability assessment. To define this angle, generators are separated to two groups A_t and B_t, depending if their rotor angles (δ) after fault occurrence are accelerating or decelerating, respectively. Note that the rotor angles of generators are plotted in the center of inertia (COI) reference. Then, these two groups are replaced by a single machine equivalent system. The equivalent angle δ_{eq_t} includes all the rotor angles and is defined as follows [17]

$$M_{A_t} = \sum_{i \in A_t} M_i, \quad M_{B_t} = \sum_{j \in B_t} M_j \tag{26}$$

$$\delta_{A_t} = M_{A_t}^{-1} \sum_{i \in A_t} M_i \delta_i, \quad \delta_{B_t} = M_{B_t}^{-1} \sum_{j \in B_t} M_j \delta_j \tag{27}$$

$$\delta_{eq_t} = \delta_{A_t} - \delta_{B_t} \tag{28}$$

According to this definition, the trajectory sensitivity of this equivalent angle to the reactances of transmission lines is as follows:

$$\frac{\partial \delta_{eq_t}}{\partial x_{L_i}} = \frac{\partial \delta_{A_t}}{\partial x_{L_i}} - \frac{\partial \delta_{B_t}}{\partial x_{L_i}} \tag{29}$$

where

$$\frac{\partial \delta_{A_t}}{\partial x_{L_i}} = M_{A_t}^{-1} \sum_{i \in A_t} M_i \frac{\partial \delta_i}{\partial x_{L_i}}, \quad \frac{\partial \delta_{B_t}}{\partial x_{L_i}} = M_{B_t}^{-1} \sum_{j \in B_t} M_j \frac{\partial \delta_j}{\partial x_{L_i}} \tag{30}$$

4.2.2. The proposed algorithm for suitable placement of series compensators to improve transient stability

- A set of most severe faults with the following clearing times are selected.

$$t_{cl_z} = t_{cc_z} - \varepsilon \tag{31}$$

  where t_{cl_z} and t_{cc_z} are the clearing time (CT) and critical clearing time (CCT) of the zth fault, respectively, and ε is a positive small number (1 ms in this study).
- For each fault:
  1. (13) and (14) are solved simultaneously using the λ vector introduced in (16), and all the dynamic and algebraic variables and their trajectory sensitivities with respect to the parameter

vector λ are calculated. Final simulation time t_{end} should be large enough to cover the first swing (5 s in this study).

2. Based on the obtained data for the rotor angles (δ) of the generators, they are divided to A_t and B_t groups as explained in Section 4.2.1.
3. The matrix of trajectory sensitivities of dynamical states (17) is obtained, and based on the definition of δ_{eq_t}, trajectory sensitivities of δ_{eq_t} with respect to the reactances of transmission lines are computed.
4. The first-swing peak to peak value of trajectory sensitivity of δ_{eq_t} to each transmission line and its sign after fault occurrence are determined. Note that if a trajectory sensitivity curve is increasing (decreasing) after fault occurrence, its peak to peak value is positive (negative).
5. A normalized index of trajectory sensitivity ($\widehat{S}_{zl}$) is calculated for each transmission line which shows the effectiveness of that line for improving the transient stability. The definition of $\widehat{S}_{zl}$ is as follows:

$$\widehat{S}_{zl} = \frac{S_{zl}}{\overline{S}_z} \cdot \frac{x_{L_l}}{\overline{x}_L} \quad \forall l \in L, \quad \forall z \in Z \tag{32}$$

$$S_{zl} = \overset{pp}{\max}\left(\frac{\partial \delta_{eq_t}}{\partial x_{L_l}}\right) \quad \forall l \in L, \forall z \in Z \tag{33}$$

where z is the index of faults; l is the index of transmission lines; L is the set of transmission lines; Z is the set of selected severe faults; $\widehat{S}_{zl}$ is the normalized index of trajectory sensitivity corresponding to transmission line l and fault z; S_{zl} is the index of trajectory sensitivity corresponding to transmission line l and fault z; $\overline{S}_z$ is the maximum value of S_{zl} among the transmission lines for fault z; $\overline{x_L}$ is the maximum value of x_{L_l} among the transmission lines; $\overset{pp}{\max}(\cdot)$ gives the first-swing peak to peak value of a function; $\partial\delta_{eq_t}/\partial x_{L_l}$ is the trajectory sensitivity of the equivalent rotor angle δ_{eq_t} with respect to the reactance of lth transmission line.

Note that the term $x_{L_l}/x_{L_l}^{\max}$ in (32) is because of the practical limitation of each line, and gives a higher weight to those lines with larger values of reactance and therefore larger possible amount of series compensation.

- Finally

1. The transmission lines with the largest positive values of total trajectory sensitivity indices (T_l^S) are selected as the most suitable places to install series compensator for improving the transient behavior of the power system

$$T_l^S = \sum_{z \in Z} p(z)\widehat{S}_{zl} \quad \forall l \in L, \quad \forall z \in Z \tag{34}$$

where T_l^S is the total trajectory sensitivity index corresponding transmission line l; $p(z)$ is a function which determines the degree of importance of each fault. For instance, this function could be a combination of the occurrence probability, degree of severity, and etc.

5. Simulation and results

The IEEE 10-machine 39-bus test systems is used to evaluate the proposed approach. Fig. 1 shows the single line diagram of this test system. The system data is taken from [18]. All the generators are represented by the classical model.

Table 1
Oscillatory modes of the system.

Mode no	Eigenvalue	Oscillating generators
1	$0 \pm 0.5811i$ (Hz)	Gen1 vs other generators

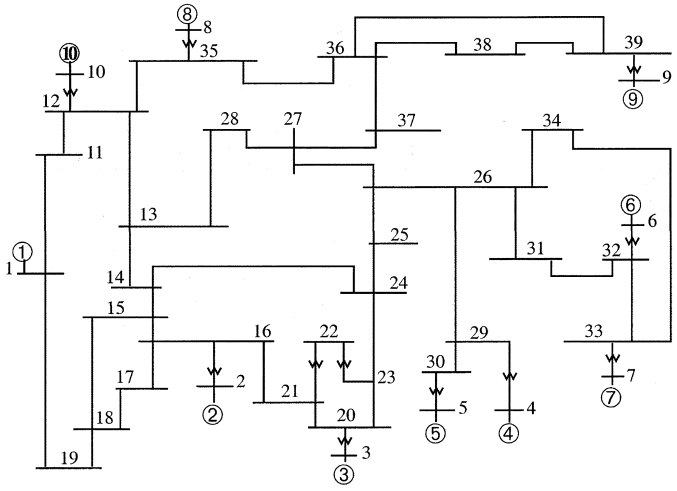

Fig. 1. IEEE 39-bus 10-machine test system.

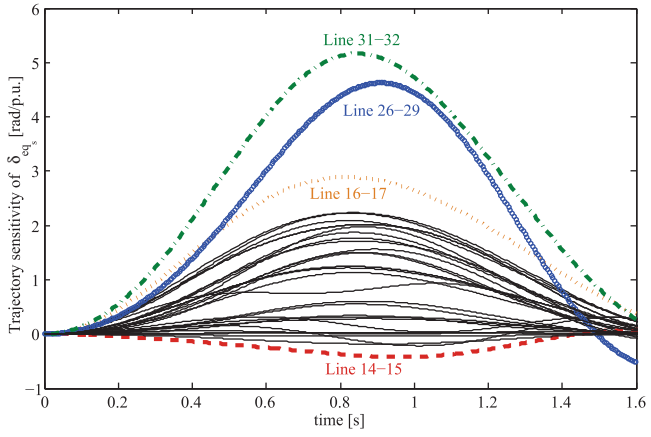

Fig. 2. Trajectory sensitivities of δ_{eq_s} to the reactances of transmission lines – before fault occurrence.

The system mode with poorest damping and low frequency is determined using the A matrix introduced in (19) and is given in Table 1. The modal analysis corresponding to this mode shows that generator 1 oscillates against the rest of generators. The equivalent angle is defined based on (23) considering generator 1 as the B_s group and the rest of generators as the A_s group. Eq. (18) is solved using the system parameters introduced in (16), and the trajectory sensitivities of the equivalent angle δ_{eq_s} to the reactances of different transmission lines are determined based on (24). Fig. 2 shows the first-cycle oscillation of these trajectory sensitivities. Fig. 3 demonstrates the normalized first-cycle peak values of these trajectory sensitivities. It can be seen that Line 31–32, Line 26–29 and Line 16–17 have the largest positive peak values, respectively, and therefore, are the most suitable places to install series compensators. Fig. 3 also shows that series compensation of transmission Line 14–15 may have a slightly negative effect on the mode of interest, and can deteriorate the small signal stability.

5.1. Transient stability improvement

Table 2 shows the set of chosen severe faults to be applied to this test system. Note that all the selected faults occur at $t_f = 2$ s.

When a fault occurs in the system, generators are divided to two transient groups as mentioned in Section 4.2.1. Fig. 4 shows the rotor angles of generators in center of inertia reference for Fault $z = 4$. It is observed that after fault occurrence, the generator 1 is

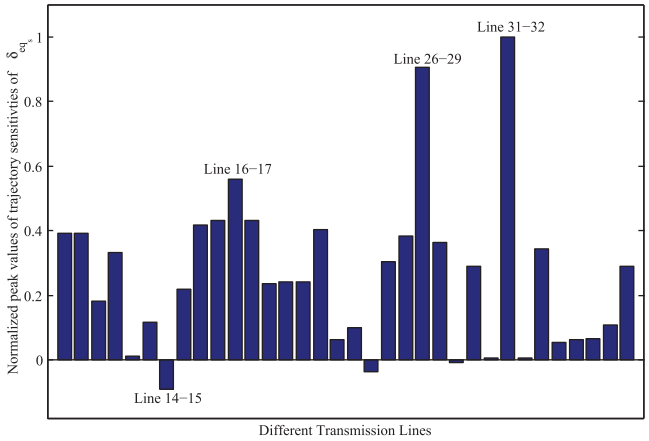

Fig. 3. Trajectory sensitivities of δ_{eq_s} to the reactances of transmission lines – normalized first-cycle peak value

Table 2
List of selected faults.

Name	Fault location	Clearing time (CT) (ms)
Fault $z=1$	Line 35–36 close to bus 36	152
Fault $z=2$	Line 36–37 close to bus 36	147
Fault $z=3$	Line 36–38 close to bus 36	150
Fault $z=4$	Line 36–38 close to bus 38	148
Fault $z=5$	Line 36–39 close to bus 36	153
Fault $z=6$	Line 36–39 close to bus 39	133
Fault $z=7$	Line 38–39 close to bus 38	141
Fault $z=8$	Line 38–39 close to bus 39	126

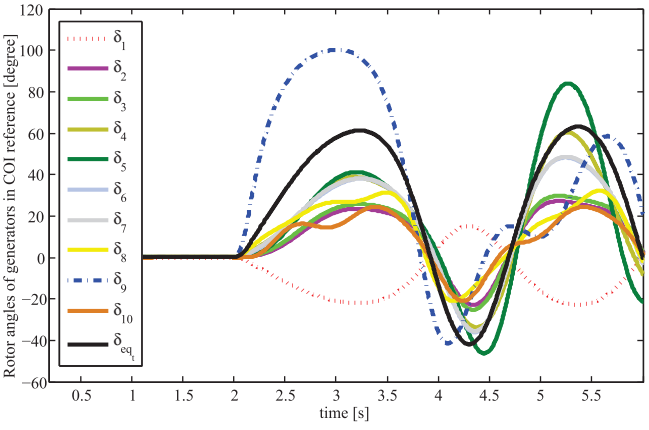

Fig. 4. Rotor angles of the generators and the equivalent angle (δ_{eq_t}) – fault $z=4$.

decelerating while the rest of generators are accelerating. For this fault, generator 1 is selected as the B_t group and the rest of generators as the A_t group. The equivalent rotor angle δ_{eq_t} is calculated using (28), and is also depicted in Fig. 4. The trajectory sensitivities

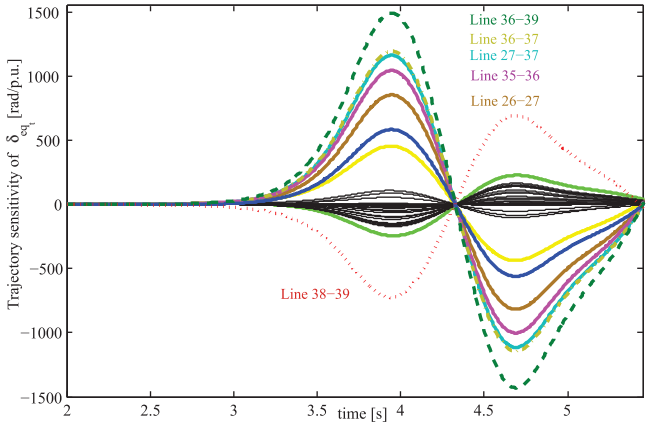

Fig. 5. Trajectory sensitivities of δ_{eq_t} to the reactances of transmission lines – fault $z=4$.

of δ_{eq_t} with respect to the reactances of transmission lines are calculated according to (29) and shown in Fig. 5. It is observed that Line 36–39, Line 36–37, Line 27–37, Line 35–36 and Line 26–27 have the largest positive values of indices of trajectory sensitivities (S_{zl}) while Line 38–39 has the most negative value of such index. Note that the effect of each transmission line on the transient stability depends on the amplitude and sign of its corresponding index of trajectory sensitivity (S_{zl}). It can be written based on the trajectory sensitivities

$$\Delta\delta_{eq_t} \approx \left(\frac{\partial\delta_{eq_t}}{\partial x_{L_l}}\right)\Delta x_{L_l} \tag{35}$$

As series capacitor is going to be installed in the transmission lines, Δx_{L_l} is negative, and since δ_{eq_t} increases rapidly after occurring fault which is visible from Fig. 4, the value of trajectory sensitivity of δ_{eq_t} with respect to the reactance of the transmission line should be positive to make $\Delta\delta_{eq_t}$ negative, decrease δ_{eq_t}, and enhance transient stability of the system. Thus, the amplitude of S_{zl} shows how sensitive δ_{eq_t} is to the reactances of the transmission line l, and its sign determines if putting series capacitor in that line has positive or negative effect on the transient stability. For instance, installing series capacitor in Line 38–39 not only cannot improve transient stability for this fault but also may have a large negative effect because of its large negative value of index of trajectory sensitivity. Between the transmission lines with positive effects, Line 36–39, Line 36–37, Line 27–37, Line 35–36 and Line 26–27 may have better impact on the transient stability of the system, respectively. Note that to find the most effective place to install the series compensator, the normalized indices of trajectory sensitivity ($\widehat{S}_{zl}$) should be calculated. Table 3 gives such indices for transmission line l considering fault z. It should be mentioned that the values of $\widehat{S}_{zl}$ are different from the values of S_{zl}. For instance, in case of fault $z=4$, Fig. 4 depicts that Line 36–37 is a more sensitive place compared to Line 35–36 due to its larger value of S_{zl},

Table 3
Normalized indices of trajectory sensitivities $\widehat{S}_{zl}$.

$\widehat{S}_{zl}$	Line 11–12 $l=1$	Line 26–27 $l=21$	Line 27–37 $l=26$	Line 35–36 $l=30$	Line 36–37 $l=31$	Line 36–38 $l=32$	Line 36–39 $l=33$	Line 38–39 $l=34$
$z=1$	−0.125	0.107	0.275	–	0.235	0.249	0.456	0.221
$z=2$	−0.139	0.109	0.248	0.403	–	0.274	0.500	0.242
$z=3$	−0.126	0.111	0.274	0.408	0.235	–	0.692	0.208
$z=4$	−0.102	0.081	0.217	0.359	0.188	–	1.000	−0.119
$z=5$	−0.093	0.090	0.226	0.342	0.193	0.374	–	0.242
$z=6$	−0.086	0.064	0.165	0.283	0.141	0.503	–	0.242
$z=7$	−0.089	0.081	0.213	0.369	0.183	0.384	1.000	–
$z=8$	−0.129	0.097	0.240	0.415	0.204	0.623	1.000	–

Table 4
Total trajectory sensitivity indices T_l^S.

	Line 11–12 l = 1	Line 26–27 l = 21	Line 27–37 l = 26	Line 35–36 l = 30	Line 36–37 l = 31	Line 36–38 l = 32	Line 36–39 l = 33	Line 38–39 l = 34
T_l^S	−6240	5169	12,966	18,223	9656	17,462	32,889	7125

but according to Table 4, Line 35–36 is a more suitable place to install the device. This is because of larger reactance of Line 35–36 compared to Line 36–37 and the term $x_{L_l}/\overline{x_L}$ in (32).

The final step is to combine all the results, and choose the most suitable place to install the compensator. This decision is strongly dependent on the definition of $p(z)$ as a function fault z. For example, assuming the same probability of occurrence for difference faults, and only considering the severity of them, $p(z)$ may have this structure

$$p(z) = \frac{1}{CT(z)} \quad \forall z \in Z \tag{36}$$

Note that the procedures to define $p(z)$ function is outside the scope of this work.

Considering the structure for $p(z)$ as introduced in (36), and using (34), the total trajectory sensitivity indices (T_l^S) corresponding to transmission line l are calculated, and given in Table 4. According to this table, installing series compensator in Line 36–39 has much better effect on the transient stability compared to the other transmission lines.

5.2. Simulation with commercial software

To verify the results, commercial software, SIMPOW® 11, is used to simulate the test system containing a series compensator in different locations. Regarding small signal stability improvement, a Thyristor Controlled Series Capacitor (TCSC) is placed in different transmission lines, and the mode of interest is obtained for each new location as shown in Table 5. Note that the modeling of TCSC is based on the method described in [19]. As expected, the installation of TCSC in Line 31–32, 26–29 and 16–17 are more effective in shifting the mode of interest to the left-half plane, and therefore improving the system damping and small signal stability. It is also observed that putting TCSC in Line 14–15 makes the system unstable.

The next step is to check the correctness of the results obtained for transient stability enhancement. In this vein, a Fixed Series Capacitor (FSC) is installed in different transmission lines, and for each location, the new CCTs of the selected faults are calculated via time domain simulation. The reactance of FSC is set to 50% capacitive of the original reactance of the line where the FSC is placed. Table 6 shows the difference-value (Δ_{zl}^{CCT}) between the new and old CCTs of the selected fault z after series compensation of transmission line l. It can be seen that the results are consistent with the normalized indices of trajectory sensitivities shown in Table 3. As expected, Line 36–39 has the best impacts on the transient stability of the system, and the other lines may improve or worsen the transient stability depending on the fault location. To illustrate positive and negative impacts of transmission line's series compensation on the transient stability, Fig. 6 shows the rotor angle of generator 9, δ_9, which is the weakest generator corresponding to fault $z = 4$, for 50% capacitive compensations of Line 36–39 and Line 38–39. As it was expected from Table 3, capacitive compensation of Line 36–39 improves the transient stability while such compensation of Line 38–39 make the system unstable.

Table 5
The mode of interest for different locations of TCSC.

TCSC location	Mode of interest
Without any TCSC	0.0000 ± 0.5811i (Hz)
TCSC installed in transmission Line 14–15	0.0074 ± 0.5809i (Hz)
TCSC installed in transmission Line 16–17	−0.0509 ± 0.5821i (Hz)
TCSC installed in transmission Line 26–29	−0.0868 ± 0.5817i (Hz)
TCSC installed in transmission Line 31–32	−0.0944 ± 0.5820i (Hz)

Obviously, the ideal case is when one specific transmission line is selected as the most suitable place to install the series compensator for both the transient and small signal stability improvements. Otherwise, the final placement decision is made depending on how the system operator weights the importance of these stabilities. For the test system used in this study, Table 4 concludes that Line 36–39 is the best location to install the series compensator if the transient stability enhancement is the main goal. Additionally, Fig. 2 depicts that Line 31–32 is the best place for installing the series compensator if the small signal stability improvement is the main objective. For the future work, a new index may also be proposed considering both small signal and transient stability improvements with different weighting factors to determine the suitable placement of FACTS devices.

Regarding the range of validity of the results reported in the paper, note that the trajectory sensitivities are obtained through a linearization around the dynamic trajectories of state and algebraic variables of the power system. These dynamic trajectories are dependent on the current operating point of the system (initial condition), and obviously, if the operating point changes, similar results cannot be guaranteed. Note that in cases in which TSA is used to provide a first-order approximation of the system trajectories after series compensations of the transmission lines, the amount of this series compensation, Δx_{L_l}, should be small; otherwise, the accuracy of estimation is not acceptable [15]. In other words, (35) provides a precise approximation of $\Delta\delta_{eq_t}$ only for small values of series compensation, Δx_{L_l}. However, the limitation above is not the case of this paper, in which non-linear simulations are used to determine the trajectories of power system after series compensation as shown in Fig. 6. Pursuing clarity, the TSA approach is only used in this paper to find the transmission line with the highest amount of trajectory sensitivity, $\partial\delta_{eq_t}/\partial x_{L_l}$. Therefore, the results obtained are valid for any feasible amount of series compensation, Δx_{L_l}.

Regarding the computational burden, calculating these sensitivities based on the numerical formulation of TSA described in

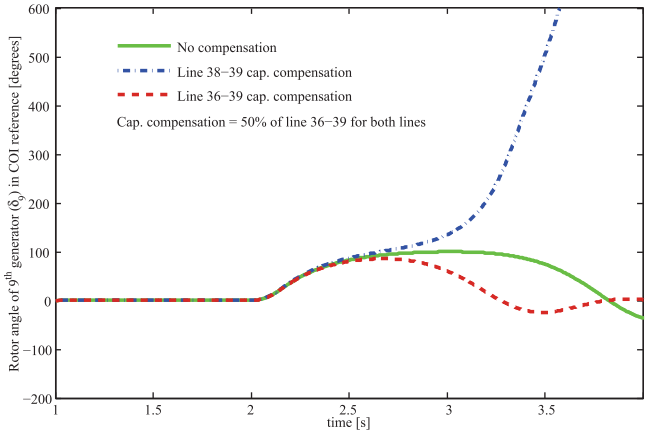

Fig. 6. Rotor angle of generator 9, δ_9, for different compensation scenarios considering fault $z = 4$.

Table 6
Δ_{zl}^{CCT} after series capacitive compensation of different transmission lines.

Δ_{zl}^{CCT}	Line 11–12 l = 1 (ms)	Line 26–27 l = 21 (ms)	Line 27–37 l = 26 (ms)	Line 35–36 l = 30 (ms)	Line 36–37 l = 31 (ms)	Line 36–38 l = 32 (ms)	Line 36–39 l = 33 (ms)	Line 38–39 l = 34 (ms)
z = 1	−4	+3	+9	–	+9	+10	+17	+6
z = 2	−3	+3	+6	+9	–	+7	+15	+5
z = 3	−3	+3	+8	+11	+8	–	+22	+5
z = 4	−3	+2	+6	+8	+6	–	+35	-4
z = 5	−3	+3	+8	+11	+8	+15	–	+8
z = 6	−2	+2	+4	+6	+4	+16	–	+6
z = 7	−2	+2	+5	+8	+5	+10	+32	–
z = 8	−3	+2	+4	+6	+4	+13	+32	–

Section 2.3 needs to run $(n_l + 1) \times n_z$ time domain simulations to find the nominal and perturbed trajectories for a power system with n_l lines (possible places to install series compensator) and n_z fault scenarios. Using analytical formulation of TSA, only n_z time domain simulations are required. For the IEEE 39-bus 10-machine test system used in this paper which has 46 lines and 8 fault scenarios, the required number of time domain simulations has been reduced from 376 ($(n_l + 1) \times n_z$) to 8 (n_z), because of the analytical formulation of TSA. Even though, the placement studies are normally carried out offline, and not based on real-time data of the system, the proposed method simplifies significantly the cumbersome computational process of placement procedure for the larger power systems.

6. Conclusion

A novel approach is proposed based on the trajectory sensitivity analysis to find the suitable locations of series compensators in order to improve the transient stability, and also enhance the damping of small signal oscillations of power system. In this method, trajectory sensitivities of the rotor angles of the generators with respect to the reactances of transmission lines are calculated for the pre-fault and post-fault systems considering the most severe contingencies. The proposed approach not only finds the most effective locations to install series compensators, but also demonstrates why installing series compensators in the transmission lines cannot always improve the power system stability. The numerical result on the IEEE 3-machine 9-bus and IEEE 10-machine 39-bus systems show validity, accuracy and efficiency of the proposed approach. Future research may extend this technique to cover the other types of FACTS devices.

References

[1] G.A. Maria, C. Tang, J. Kim, Hybrid transient stability analysis [power systems], IEEE Transactions on Power Systems 5 (1990) 384–393.
[2] A.A. Fouad, S.E. Stanton, Transient stability of a multi-machine power system. Part II. Critical transient energy, Power Engineering Review PER-1 (1981) 3417–3424.
[3] T. Athay, P. Podmore, S. Virmani, A practical method for the direct analysis of transient stability, IEEE Transactions on Power Apparatus and Systems PAS-98 (1979) 573–584.
[4] A.A. Fouad, V. Vittal, T.K. Oh, Critical energy for direct transient stability assessment of a multimachine power system, IEEE Transactions on Power Apparatus and Systems PAS-103 (1981) 2199–2206.
[5] A. Ishigame, S. Kawamoto, T. Taniguchi, Structural control of electric power networks for transient stability, IEEE Transactions on Power Systems 9 (1994) 1575–1581.
[6] K.N. Shubhanga, A.M. Kulkarni, Application of structure preserving energy margin sensitivity to determine the effectiveness of shunt and series facts devices, IEEE Transactions on Power Systems 17 (2002) 730–738.
[7] M.J. Laufenberg, M.A. Pai, A new approach to dynamic security assessment using trajectory sensitivities, IEEE Transactions on Power Systems 13 (1998) 953–958.
[8] D. Chatterjee, A. Ghosh, Transient stability assessment of power systems containing series and shunt compensators, IEEE Transactions on Power Systems 22 (2007) 1210–1220.
[9] A. Zamora-Cardenas, C.R. Fuerte-Esquivel, Multi-parameter trajectory sensitivity approach for location of series-connected controllers to enhance power system transient stability, Electric Power Systems Research 80 (2010) 1096–1103.
[10] D.Z. Fang, Q. Yi-fei, A new trajectory sensitivity approach for computations of critical parameters, Electric Power Systems Research 77 (2007) 303–307.
[11] D. Chatterjee, A. Ghosh, TCSC control design for transient stability improvement of a multi-machine power system using trajectory sensitivity, Electric Power Systems Research 77 (2007) 470–483.
[12] H. Okamoto, A. Kurita, Y. Sekine, A method for identification of effective locations of variable impedance apparatus on enhancement of steady-state stability in large scale power systems, IEEE Transactions on Power Systems 10 (1995) 1401–1407.
[13] B.K. Kuma, S.N. Singh, S.C. Srivastava, Placement of facts controllers using modal controllability indices to damp out power system oscillations, IET Generation, Transmission & Distribution 1 (2007) 209–217.
[14] L. Rouco, F.L. Pagola, An eigenvalue sensitivity approach to location and controller design of controllable series capacitors for damping power system oscillations, IEEE Transactions on Power System 12 (1997) 1660–1666.
[15] I.A. Hiskens, M.A. Pai, Trajectory sensitivity analysis of hybrid systems, IEEE Transactions on Power System 47 (2000) 204–220.
[16] A. Zamora-Crdenas, C.R. Fuerte-Esquivel, Computation of multi-parameter sensitivities of equilibrium points in electric power systems, Electric Power Systems Research 3 (2013) 246–254.
[17] M. Pavella, D. Ernst, D. Ruiz-Vega, Transient Stability of Power Systems: A Unified Approach to Assessment and Control, Kluwer Academic Publishers, Boston/Dordrecht/London, 2000.
[18] M.A. Pai, Energy Function Analysis for Power System Stability, Kluwer Academic Publishers, Boston/Dordrecht/London, 2007.
[19] A. Nasri, R. Eriksson, M. Ghandhari, Appropriate placement of series compensators to improve small signal stability of power system, Energy Conference and Exhibition, ENERGYCON (2012) 421–426.

Paper J2

Minimizing Wind Power Spillage Using an OPF with FACTS Devices

Minimizing Wind Power Spillage Using an OPF With FACTS Devices

Amin Nasri, *Student Member, IEEE*, Antonio J. Conejo, *Fellow, IEEE*, S. Jalal Kazempour, *Member, IEEE*, and Mehrdad Ghandhari, *Senior Member, IEEE*

***Abstract*—This paper proposes an optimal power flow (OPF) model with flexible AC transmission system (FACTS) devices to minimize wind power spillage. The uncertain wind power production is modeled through a set of scenarios. Once the balancing market is cleared, and the final values of active power productions and consumptions are assigned, the proposed model is used by the system operator to determine optimal reactive power outputs of generating units, voltage magnitude and angles of buses, deployed reserves, and optimal setting of FACTS devices. This system operator tool is formulated as a two-stage stochastic programming model, whose first-stage describes decisions prior to uncertainty realization, and whose second-stage represents the operating conditions involving wind scenarios. Numerical results from a case study based on the IEEE RTS demonstrate the usefulness of the proposed tool.**

***Index Terms*—FACTS devices, optimal power flow (OPF), stochastic programming, thyristor controlled series capacitor (TCSC), wind power spillage.**

I. Introduction

A. Motivation and Aim

OVER the last decade, the share of wind power in the generation portfolio of power systems has significantly grown. However, the inherent variability of wind power and also the technical constraints due to long-distance power transmission may limit the integration of wind power production into the system. On the other hand, flexible AC transmission systems (FACTS) devices can significantly improve the operational flexibility and help integrating increasing amounts of wind power.

In a power system with significant penetration of wind power, e.g., the system of Denmark with 3951 MW of wind capacity (29.1% of the installed capacity) and the system of Spain with 22 213 MW of wind capacity (21.7% of the installed capacity), transmission flexibility is very important [1]–[3].

Manuscript received May 25, 2013; revised October 12, 2013 and November 25, 2013; accepted January 07, 2014. Date of publication January 29, 2014; date of current version August 15, 2014. The work of A. Nasri was supported by Erasmus Mundus Joint Doctorate in Sustainable Energy Technologies and Strategies. Paper no. TPWRS-00662-2013.

A. Nasri and M. Ghandhari are with KTH Royal Institute of Technology, Stockholm, Sweden (e-mail: Amin.Nasri@ee.kth.se; Mehrdad.Ghandhari@ee.kth.se).

A. J. Conejo is with the Universidad de Castilla–La Mancha, Ciudad Real, Spain (e-mail: Antonio.Conejo@uclm.es).

S. J. Kazempour is with Johns Hopkins University, Baltimore, MD 21218 USA (e-mail: skazemp1@jhu.edu).

Digital Object Identifier 10.1109/TPWRS.2014.2299533

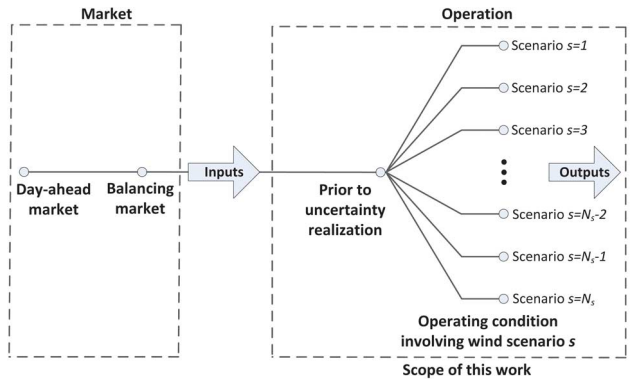

Fig. 1. Decision framework of the proposed model.

The fast operation of FACTS devices makes them appropriate tools to cope with the deviations of wind power production by altering the reactance of transmission lines and/or nodal voltages. To this end, the optimal setting of such devices needs to be determined per wind scenario, which results in reduced wind power spillage. Wind power spillage refers to the amount of the wind power production which is not used due to technical reasons, e.g., insufficient transmission capacity.

This paper proposes an optimal power flow (OPF) model with FACTS devices based on a two-stage stochastic programming problem to optimally determine the setting of such devices. The main objective is to minimize wind power spillage, while the second priority is to minimize active power losses in the network.

B. Decision Framework

The framework considered consists of two consecutive stages as depicted in Fig. 1: market and operation.

1) Market: By noon of day $D-1$ the "day-ahead market" for day D is cleared and preliminary values for active power productions and consumptions are determined. Then, about 1 hour prior to power delivery, the "balancing market" (also called "real-time market") is cleared and "final" values for active power productions and consumptions are assigned to each generating unit and to each demand, respectively. The balancing market adjusts the results of the day-ahead market and compensates deviations. Note that this framework is consistent with most real-world markets [2]–[6]. Note also that this market stage is outside the scope of this work; however, its final outcomes are in fact the inputs for the OPF problem considered in this paper. Such inputs are:

a) power production of generating unit i (P_i^{fix});

b) active power consumption by load d (L_d^{P});
c) maximum downward reserve of active power that can be provided by generating unit i (R_i^{D});
d) maximum upward reserve of active power that can be provided by generating unit i (R_i^{U});
e) power production of wind farm k as dispatched in the market (W_k^{fix}).

2) Operation: After clearing the balancing market, the proposed OPF model is used by the system operator to minimize wind power spillage. It is important to note that the OPF proposed does not represent the market stages, i.e., the system operator runs such an OPF after closing the last market, i.e., the balancing or real-time market. Thus, the time frame of this OPF spans from the closing of the balancing market to power delivery. In most real-world electricity markets, this time period is smaller than one hour. This model is cast as a two-stage stochastic programming problem in which the first-stage refers to the decisions "prior to uncertainty realization", while the second-stage represents the "operating conditions involving wind scenarios". In the first-stage, the market operator makes "scheduling decisions" appropriate for any plausible wind production scenario, while in the second-stage, "operating decisions" corresponding to each individual scenario are made.

The outputs of the proposed model are of two types, first-stage and second-stage. Variables pertaining to the first-stage are:

a) voltage magnitude at bus n prior to uncertainty realization (v_n^0);
b) voltage angle at bus n prior to uncertainty realization (θ_n^0);
c) scheduled reactive power output of generating unit i prior to uncertainty realization (Q_i^0).

Additionally, variables corresponding to the second-stage include:

a) voltage magnitude at bus n in the operating condition involving wind scenario s (v_{ns});
b) voltage angle at bus n in the operating condition involving wind scenario s (θ_{ns});
c) Reactance of the thyristor controlled series capacitor (TCSC) installed in transmission line (n, m) in the operating condition involving wind scenario s (x_{nms}^{tcsc});
d) deployed reserve of active power by generating unit i in the operating condition involving wind scenario s (r_{is});
e) deployed reserve of reactive power by generating unit i in the operating condition involving wind scenario s (q_{is});
f) wind power spillage of wind farm k in the operating condition involving wind scenario s (W_{ks}^{SP});
g) involuntarily active load shedding of load d in the operating condition involving wind scenario s (L_{ds}^{SH}).

Regarding the scheduling decisions made in the first-stage of the proposed model, note that the first-stage variables constitute *here-and-now* decisions, i.e., scenario-independent decisions that are made before the realization of any scenario, but they are adapted to all the scenarios. On the other hand, the second-stage variables constitute *wait-and-see* decisions, i.e., decisions which are related to the operating conditions involving each wind power production scenario.

Note that if the wind power production realizes in a scenario different that any of the considered ones, the closest scenario to the wind power realization is selected. Alternatively, an additional OPF can be run with the most likely wind production scenario to derive appropriate adjustments to the settings.

C. Literature Review and Contributions

Power systems with significant penetration of wind power need to be flexible to cope with uncertainties in wind generation. In [7], a network-constrained market clearing model for systems with a significant wind penetration is provided. In [8], a pricing scheme is proposed for a market with wind producers using a two-stage stochastic programming problem.

Reference [9] provides a technique to manage energy storage systems to maximize wind power utilization over a scheduling period. In [10], a comprehensive study is carried out for the Croatian power system to analyze the potential of hydro-power plants to work as storage if significant wind production is integrated.

FACTS devices are effective tools to improve power system flexibility. In [11], an OPF model is proposed to increase the available transfer capacity of the power network using diverse FACTS devices. Reference [12] uses a heuristic technique to determine optimal location and setting of various types of FACTS devices to improve the system loadability. In [13], an OPF-based security-constrained re-dispatching model is proposed to resolve system congestion and security issues using FACTS devices.

In the technical literature, few works are available in which the maximization of wind power integration is sought using FACTS devices. Some of those studies pertain to the optimal placement of FACTS devices in a power system with high penetration of the wind power. In this vein, [14] introduces a long-term techno-economic method for allocating FACTS devices to facilitate wind power integration. In addition, [15] presents a methodology for optimal placement of FACTS devices to maximize wind power integration by increasing the transfer capability of a weak transmission system.

Some other studies analyze diverse impacts of FACTS devices on the grid functionality in the presence of significant renewable energy resources. For example, [16] analyzes how the large-scale integration of the wind power affects the security indices of a power system with FACTS devices. In addition, [17] evaluates the capability of FACTS devices to prevent voltage collapse and under-voltage trippings while integrating wind power in a weak network. In the same vein, [18] proposes some design features of FACTS devices to maintain or even to improve the grid functionality of a power system with significant integration of renewable energy resources.

The works available in the technical literature focusing on the optimal setting of FACTS devices in a power system with significant wind power integration are limited. Reference [19] proposes a methodology to determine the optimal setting of FACTS devices to fully utilize the existing transmission capacity in the presence of intermittent and/or variable energy resources, e.g., wind farms. The proposed approach consists of a two-stage control scheme that determines the optimal setting of FACTS de-

vices using a database obtained by a collection of offline simulations. Compared to [19], the method proposed in this paper does not require offline database covering all the potential variations of the loads and/or the generations. On the contrary, this paper models the wind power production uncertainty using a set of plausible scenarios based on forecasted values within one hour of power delivery. Thus, the computational burden is reduced, and the results are generally more precise since the forecasted values are related to the current operating condition.

Considering the literature review above, the contributions of this paper are threefold:

1) To propose an OPF model with FACTS devices, compatible with the structure of most real-world electricity markets, whose objective is minimizing wind power spillage. This OPF model is run by the system operator once the final values of the active power productions and consumptions are assigned after market clearing.
2) To model the uncertainty of wind power production through a set of plausible wind power scenarios and to formulate the proposed OPF model using a two-stage stochastic programming problem.
3) To derive the optimal deployment of active and reactive power reserves, and to optimally identify the FACTS device settings corresponding to each wind scenario, which result in minimum wind power spillage.

D. Paper Organization

The rest of this paper is organized as follows. Section II presents the modeling features and assumptions of the proposed OPF model, and its formulation. Section III provides results from a realistic case study. Section IV provides a number of relevant conclusions. Finally, some mathematical definitions are provided in an Appendix.

II. AC OPF Model

A. Notation

The main notation used in this paper is provided below, while other symbols are defined as required. The following notational observations are in order:

a) All constants and variables are expressed in per-unit.
b) Symbols $\mathbf{v}$, $\boldsymbol{\theta}$ and $\mathbf{x^{tcsc}}$ written in bold without index, are vector forms of variables. For example, symbol $\boldsymbol{\theta}$ represents the vector of all voltage angles.

1) Indices:

n, m	Indices for system buses.
s	Index for wind power scenarios.
k	Index for wind farms.
d	Index for demands.
i	Index for generating units.

2) Sets:

Ξ	Set of optimization variables.
$\mathcal{K}$	Set of wind farms.
$\mathcal{D}$	Set of demands.
$\mathcal{G}$	Set of generating units.
Ω_n	Set of system buses adjacent to bus n.

Sets $\mathcal{K}$, $\mathcal{D}$ and $\mathcal{G}$ include subscript n if referring to the set of wind farms, demands and units, respectively, located at bus n.

3) Constants:

ρ_s	Probability of scenario s.
L_d^{P}	Active power consumption by load d.
L_d^{Q}	Reactive power consumption by load d.
P_i^{fix}	Power production of generating unit i as dispatched in the market.
W_{ks}	Power production of wind farm k in the operating condition involving wind scenario s.
W_k^{fix}	Power production of wind farm k as dispatched in the market.
$\underline{x}_{nm}^{\mathrm{tcsc}}$	Lower bound of the reactance of the TCSC installed between buses n and m.
$\overline{x}_{nm}^{\mathrm{tcsc}}$	Upper bound of the reactance of the TCSC installed between buses n and m.
$\underline{v}_n$	Lower bound of the voltage magnitude at bus n.
$\overline{v}_n$	Upper bound of the voltage magnitude at bus n.
$\overline{Q}_i$	Maximum reactive power production of generating unit i.
$\underline{Q}_i$	Maximum reactive power consumption of generating unit i.
R_i^{D}	Maximum downward reserve of active power that can be provided by unit i.
R_i^{U}	Maximum upward reserve of active power that can be provided by unit i.
Q_i^{D}	Maximum downward reserve of reactive power that can be provided by unit i.
Q_i^{U}	Maximum upward reserve of reactive power that can be provided by unit i.
α_k^{SP}	Weighting factor associated with wind power spillage of wind farm k.
α_d^{SH}	Weighting factor associated with unserved active load d.
α_{nm}^{L}	Weighting factor associated with active power loss of the transmission line (n, m).
Y_{nm}	Admittance magnitude of transmission line (n, m).
ϕ_{nm}	Admittance angle of transmission line (n, m).
l_{nm}	Length of transmission line (n, m).
r_{nm}	Resistance of transmission line (n, m).
x_{nm}	Reactance of transmission line (n, m).
b_{nm}	Shunt conductance of transmission line (n, m).
$\overline{S}_{nm}$	Capacity of transmission line (n, m).

4) Variables:

v_n^0	Voltage magnitude at bus n prior to uncertainty realization.
θ_n^0	Voltage angle at bus n prior to uncertainty realization.
Q_i^0	Scheduled reactive power production of generating unit i prior to uncertainty realization.
v_{ns}	Voltage magnitude at bus n in the operating condition involving wind scenario s.
θ_{ns}	Voltage angle at bus n in the operating condition involving wind scenario s.
x_{nms}^{tcsc}	Reactance of the TCSC installed in transmission line (n,m) in the operating condition involving wind scenario s.
r_{is}	Deployed reserve of active power by generating unit i in the operating condition involving wind scenario s.
q_{is}	Deployed reserve of reactive power by generating unit i in the operating condition involving wind scenario s.
W_{ks}^{SP}	Wind power production spillage of wind farm k in the operating condition involving wind scenario s.
L_{ds}^{SH}	Involuntarily active load shedding of load d in the operating condition involving wind scenario s.

5) Functions:

$S_{nm}^0(.)$	Scheduled apparent power for transmission line (n,m) prior to uncertainty realization.
$S_{nms}(.)$	Apparent power through transmission line (n,m) in the operating condition involving wind scenario s.
$P_{nms}^{\text{L}}(.)$	Active power loss of transmission line (n,m) in the operating condition involving wind scenario s.
$P_{nms}^{\text{inj}}(.)$	Active power injection of the TCSC installed in transmission line (n,m) into bus n in the operating condition involving wind scenario s.
$Q_{nms}^{\text{inj}}(.)$	Reactive power injection of the TCSC installed in transmission line (n,m) into bus n in the operating condition involving wind scenario s.
$P_{nm}^0(.)$	Scheduled active power flow from bus n to bus m prior to uncertainty realization.
$Q_{nm}^0(.)$	Scheduled reactive power flow from bus n to bus m prior to uncertainty realization.
$P_{nms}(.)$	Active power flow from bus n to bus m in the operating condition involving wind scenario s.
$Q_{nms}(.)$	Reactive power flow from bus n to bus m in the operating condition involving wind scenario s.

The mathematical definition of all functions above are given in the Appendix.

B. Modeling Features and Assumptions

The assumptions considered in this paper are as follows:

1) A detailed ac representation of the transmission system is embedded within the considered OPF model.
2) For the sake of simplicity, only wind power production uncertainty is taken into account. However, other uncertainties such as generators' availability can be incorporated into the model. The uncertainty of wind power production is modeled through a set of plausible wind power scenarios based on the available forecasted data prior to running the proposed OPF. Note that scenario generation techniques are beyond of the scope of this paper.
3) The proposed OPF model is run after clearing the last market (e.g., the balancing or real-time market). This implies that the active power productions of all generating units have been dispatched, and are fixed at the time of running the proposed OPF model. In fact, the values of active power productions and consumptions provided by the market clearing process are the inputs of the proposed OPF model, whose mechanisms for minimizing wind power spillage are a) optimal setting of the FACT devices, and b) optimal deployment of active and reactive power reserves. Therefore, since the decisions obtained with the proposed OPF model do not change the cleared quantities in the market, a financial analysis is not generally required.
4) Wind power production of each farm corresponding to each scenario remains fixed over the time period considered. However, note that the proposed model can be run using a variety of study horizons (e.g., from one hour to several minutes prior to power delivery) and of time steps (e.g., from ten minutes to one minute). The longer the study horizon to be analyzed, the higher the wind uncertainty and the larger the number of wind scenarios to be considered. In other words, if the study horizon is one hour, a comparatively larger number of wind scenarios needs to considered, which may result in an array to different FACTS settings. If, on the other hand, the study horizon is just ten minutes, few wind scenarios need to be considered, which generally results in a single FACTS setting.
5) The power factors of wind producers are considered to be equal to one.
6) Among the available FACTS devices, the thyristor controlled series capacitor (TCSC) is selected in this paper. However, the proposed methodology can be straightforwardly extended to consider any other type of FACTS devices.
7) The injection model of the TCSC [20] and [21] is used in this paper since it provides an appropriate representation of TCSC functioning and can be easily incorporated into an OPF formulation.

C. Formulation

The considered two-stage OPF problem is formulated as follows:

$$\underset{\Xi}{\text{Minimize}} \sum_s \rho_s \left[\sum_{k\in\mathcal{K}} \alpha_k^{\text{SP}} W_{ks}^{\text{SP}} + \sum_{d\in\mathcal{D}} \alpha_d^{\text{SH}} L_{ds}^{\text{SH}} + \sum_{n(m\in\Omega_n)} \alpha_{nm}^{\text{L}} P_{nms}^{\text{L}}(\mathbf{v},\boldsymbol{\theta},\mathbf{x}^{\mathbf{tcsc}}) \right]. \quad (1)$$

The main goal of objective function (1) is to minimize wind power spillage, while the second priority is to minimize active power losses in the network. In addition, load shedding is also considered in (1) to avoid load curtailment. Thus, this objective function consists of three terms: 1) wind power spillage, 2) unserved load, and 3) active power losses in the network. Weighting factors α_k^{SP}, α_d^{SH} and α_{nm}^{L} specify the degree of importance of their corresponding terms.

Objective function (1) is subject to constraints (2)–(20). Note that constraints (2)–(8) pertain to the first-stage (prior to uncertainty realization), while constraints (9)–(20) refer to the second-stage (operating conditions):

$$\sum_{i\in\mathcal{G}_n} P_i^{\text{fix}} + \sum_{k\in\mathcal{K}_n} W_k^{\text{fix}} - \sum_{d\in\mathcal{D}_n} L_d^{\text{P}} = \sum_{m\in\Omega_n} P_{nm}^0(\mathbf{v},\boldsymbol{\theta}) \quad \forall n \quad (2)$$

$$\sum_{i\in\mathcal{G}_n} Q_i^0 - \sum_{d\in\mathcal{D}_n} L_d^{\text{Q}} = \sum_{m\in\Omega_n} Q_{nm}^0(\mathbf{v},\boldsymbol{\theta}) \quad \forall n. \quad (3)$$

Constraints (2) and (3) represent the active and the reactive power balance at each bus prior to uncertainty realization:

$$\underline{Q}_i \le Q_i^0 \le \overline{Q}_i \quad \forall i\in\mathcal{G} \quad (4)$$

$$\underline{v}_n \le v_n^0 \le \overline{v}_n \quad \forall n \quad (5)$$

$$-\pi \le \theta_n^0 \le \pi \quad \forall n \quad (6)$$

$$\theta_{n=1}^0 = 0 \quad (7)$$

$$S_{nm}^0(\mathbf{v},\boldsymbol{\theta}) \le \overline{S}_{nm} \quad \forall n, \forall m\in\Omega_n. \quad (8)$$

Constraints (4)–(6) enforce the lower and upper bounds of reactive power production of generating units, and voltage magnitudes and angles of buses. Constraint (7) sets $n = 1$ as the reference bus. Finally, limits on transmission line capacities are enforced through (8):

$$\sum_{i\in\mathcal{G}_n} r_{is} + \sum_{k\in\mathcal{K}_n} \left(W_{ks} - W_k^{\text{fix}} - W_{ks}^{\text{SP}}\right) + \sum_{d\in\mathcal{D}_n} L_{ds}^{\text{SH}} = \sum_{m\in\Omega_n} P_{nms}(\mathbf{v},\boldsymbol{\theta},\mathbf{x}^{\mathbf{tcsc}}) - \sum_{m\in\Omega_n} P_{nm}^0(\mathbf{v},\boldsymbol{\theta}) \quad \forall n, \forall s \quad (9)$$

$$\sum_{i\in\mathcal{G}_n} q_{is} = \sum_{m\in\Omega_n} Q_{nms}(\mathbf{v},\boldsymbol{\theta},\mathbf{x}^{\mathbf{tcsc}}) - \sum_{m\in\Omega_n} Q_{nm}^0(\mathbf{v},\boldsymbol{\theta}) \quad \forall n, \forall s. \quad (10)$$

Similarly to (2) and (3), constraints (9) and (10) represent active and the reactive power balances for the operating conditions (second-stage) at each bus and for each scenario. Note that such balance constraints enforce that the unexpected deviations of wind production are met with wind power spillage, and/or load curtailment, and/or reserve deployment. Note also that unlike in the first-stage, TCSCs may alter the power flows of the second-stage, i.e., $P_{nms}(\mathbf{v},\boldsymbol{\theta},\mathbf{x}^{\mathbf{tcsc}})$ and $Q_{nms}(\mathbf{v},\boldsymbol{\theta},\mathbf{x}^{\mathbf{tcsc}})$. It is important to note that a TCSC is adjusted to any desirable value within its lower and upper bounds in seconds. Therefore, the optimal setting of such devise is only considered in the second-stage of the proposed model:

$$\underline{x}_{nm}^{\text{tcsc}} \le x_{nms}^{\text{tcsc}} \le \overline{x}_{nm}^{\text{tcsc}} \quad \forall n, \forall m\in\Omega_n, \forall s \quad (11)$$

$$0 \le L_{ds}^{\text{SH}} \le L_d^{\text{P}} \quad \forall d\in\mathcal{D}, \forall s \quad (12)$$

$$0 \le W_{ks}^{\text{SP}} \le W_{ks} \quad \forall k\in\mathcal{K}, \forall s \quad (13)$$

$$-R_i^{\text{D}} \le r_{is} \le R_i^{\text{U}} \quad \forall i\in\mathcal{G}, \forall s \quad (14)$$

$$-Q_i^{\text{D}} \le q_{is} \le Q_i^{\text{U}} \quad \forall i\in\mathcal{G}, \forall s \quad (15)$$

$$\underline{Q}_i \le q_{is} + Q_i^0 \le \overline{Q}_i \quad \forall i\in\mathcal{G}, \forall s \quad (16)$$

$$\underline{v}_n \le v_{ns} \le \overline{v}_n \quad \forall n, \forall s \quad (17)$$

$$-\pi \le \theta_{ns} \le \pi \quad \forall n, \forall s \quad (18)$$

$$\theta_{(n=1)s} = 0 \quad \forall s \quad (19)$$

$$S_{nms}(\mathbf{v},\boldsymbol{\theta},\mathbf{x}^{\mathbf{tcsc}}) \le \overline{S}_{nm} \quad \forall n, \forall m\in\Omega_n, \forall s. \quad (20)$$

Constraints (11) enforce that the reactance of each TCSC lies within its lower and upper bounds. Constraints (12)–(15) bound the values of unserved loads, wind power spillage, and deployed active and reactive reserves. Constraints (16) ensure the feasibility of the reactive power production of each generating unit. Finally, constraints (17)–(20) are similar to (5)–(8), but for the operating conditions (second-stage).

Note that the optimization variables of problem (1)–(20) are in the set below:

$$\Xi = \left\{ v_n^0, \theta_n^0, Q_i^0, v_{ns}, \theta_{ns}, x_{nms}^{\text{tcsc}}, W_{ks}^{\text{SP}}, L_{ds}^{\text{SH}}, r_{is}, q_{is} \right\}.$$

Finally, note also that the proposed optimization problem (1)–(20) is non-linear and non-convex, but continuous. However, it is important to note that as the number of scenarios increases, the objective function of the considered model convexifies since such objective function represents the expectation over a discrete number of scenarios. In other words, as this discrete number of scenarios increases, the scenario diversity increases, and the diversity of the single-scenario objective functions increases as well, which result in a smoothing effect leading to the convexification of the objective function [22]. This effect has been verified numerically through simulations. However, the non-convex feasibility region of the considered problem remains as such, i.e., non-convex, due to the nature of the AC power flow equations. Nevertheless, numerical simulations indicate that the convexifying effect over the objective function (not over the constraints) of an increasing number of scenarios is significant and leads to increasingly well-behaved problems.

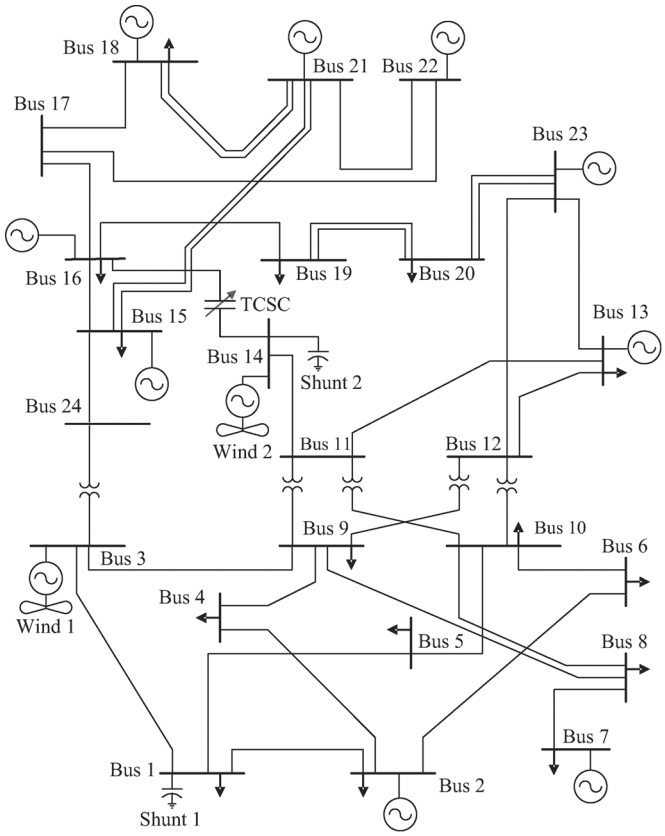

Fig. 2. IEEE one-area reliability test system (RTS).

TABLE I
NETWORK DATA

Transmission line (n,m)	l_{nm} [miles]	r_{nm} [p.u.]	x_{nm} [p.u.]	b_{nm} [p.u.]	$\overline{S}_{nm}$ [p.u.]
1-3	55	0.0546	0.2112	0.0572	2.3
3-9	62	0.0616	0.2380	0.0161	1.6
7-8	16	0.0159	0.0614	0.0166	4.0
6-10	16	0.0139	0.0605	2.4590	2.5
10-11	0	0.0023	0.0839	0.0000	3.0
11-14	144	0.0270	0.2090	0.0176	2.3
12-23	266	0.0496	0.3864	0.0508	5.0
13-23	238	0.0444	0.3460	0.0454	5.0
14-16	188	0.0350	0.4123	0.0117	2.1
15-24	179	0.0335	0.2595	0.0218	5.0

III. CASE STUDY

This section presents numerical results for a case study based on the IEEE one-area reliability test system (RTS) depicted in Fig. 2 [23].

A. Data

The network data such as l_{nm}, r_{nm}, x_{nm}, b_{nm} and $\overline{S}_{nm}$ are those reported in [23], except the ones given in Table I.

In addition, data for generating units and loads are given in Tables II and III, respectively.

Two wind farms ($k = 1$ and $k = 2$) are considered and located at buses 3 and 14. The power production of wind farms as dispatched in the market (W_k^{fix} for $k = 1$, and $k = 2$) are equal to 2.6 p.u. and 2.0 p.u., respectively. Their production uncertainty is modeled through the 25 scenarios shown in Fig. 3.

TABLE II
DATA FOR GENERATING UNITS

Generator (i)	Location [Bus]	P_i^{fix} [p.u.]	R_i^{D} [p.u.]	R_i^{U} [p.u.]	$\underline{Q}_i$ [p.u.]	$\overline{Q}_i$ [p.u.]	Q_i^{D} [p.u.]	Q_i^{U} [p.u.]
1-2	2	0.10	0.03	0.03	0.00	0.10	0.05	0.05
3-4	2	0.76	0.02	0.02	-0.25	0.30	0.15	0.15
5-7	7	1.00	0.40	0.40	0.00	0.60	0.30	0.30
8-10	13	1.97	1.00	1.00	0.00	0.80	0.40	0.40
11-15	15	0.18	0.10	0.10	0.00	0.06	0.03	0.03
16	16	1.00	0.50	0.50	-0.50	0.80	0.40	0.40
17	18	0.00	0.00	0.00	-0.50	0.80	0.40	0.40
18	21	3.80	0.00	0.00	-0.50	2.00	1.00	1.00
19-24	22	3.80	0.00	0.00	-0.50	2.00	1.00	1.00
25	23	0.50	0.50	0.50	-0.10	0.16	0.16	0.16
26-27	23	0.50	0.50	0.50	-0.50	0.80	0.40	0.40
28	23	1.80	0.70	0.70	-0.25	1.50	0.75	0.75

TABLE III
LOAD DATA

Load (d)	Location [Bus]	L_d^{P} [p.u.]	L_d^{Q} [p.u.]
1	1	0.705	1.432
2	2	0.000	0.000
3	4	1.410	0.225
4	5	1.065	0.210
5	6	2.490	0.420
6	7	1.875	2.784
7	8	2.565	0.525
8	9	2.625	0.540
9	10	2.925	0.600
10	13	3.975	3.289
11	15	4.755	0.960
12	16	1.500	0.300
13	18	4.995	1.020
14	19	2.715	0.555
15	20	1.920	0.390

The probabilities of all the scenarios (ρ_s) are identical and equal to 0.04.

Moreover, since the power factors of the wind plants are considered to be equal to one, two shunt admittances of j2 p.u. and j0.25 p.u. are connected to buses 1 and 14, respectively, for improving the voltage profile.

The lower and upper limits of bus voltage magnitude are 0.9 p.u. and 1.1 p.u., respectively, for all buses.

Finally, the values for weighting factors α_k^{SP}, α_d^{SH} and α_{nm}^{L} in the objective function (1) are considered 100, 1000 and 1, respectively. Note that these factors are chosen to weight in a different manner each term included in the objective function. This way the degree of importance of each term is properly represented. This value selection implies that the optimization priorities are 1) avoiding load shedding, 2) minimizing wind power spillage, and 3) minimizing active power losses in the network.

B. Cases Considered

In this study three different cases are analyzed:

Case A) No FACTS device is installed in the system (no series compensation).

Case B) A single fixed series capacitor (FSC) is installed in transmission line (14,16), whose reactance is capacitive

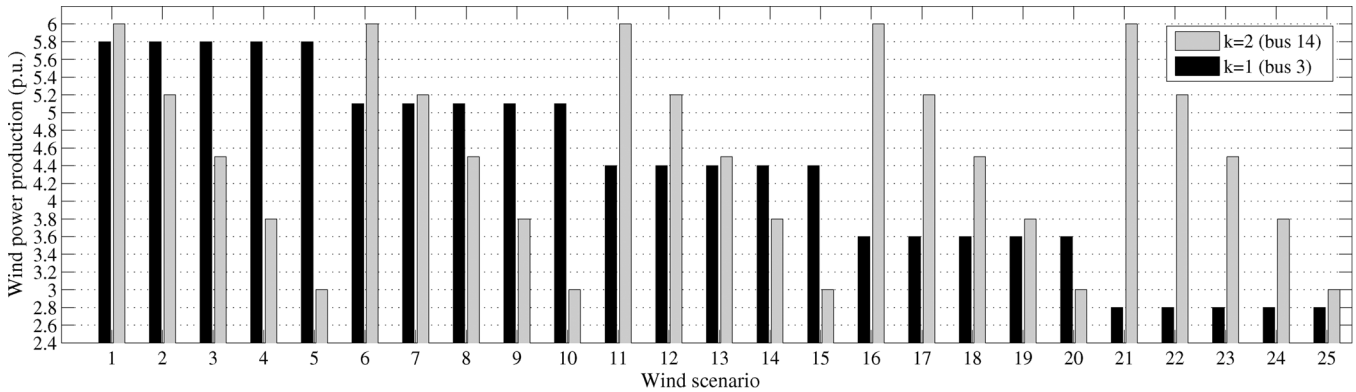

Fig. 3. Wind power scenarios.

TABLE IV
NUMERICAL RESULTS FOR CASES CONSIDERED

	The value of objective function (1) [p.u.]	Expected value of unserved load ($\widetilde{L}^{\mathrm{SH}}$) [p.u.]	Expected value of wind power spillage percentage ($\widetilde{W}^{\mathrm{SP}}$) [%]	Expected value of active power loss ($\widetilde{P}^{\mathrm{L}}$) [p.u.]	CPU time [second]
Case A	146.5	0	16.4	1.13	29.4
Case B	117.6	0	13.2	1.32	28.9
Case C	101.8	0	11.4	1.09	65.5

and equal to 80% of the original reactance of the line, i.e., 0.32 p.u.

Case C) A single TCSC is installed in transmission line (14,16). The limitation of the effective reactance of the TCSC is set to 80% capacitive (0.32 p.u.) and 50% inductive (-0.20 p.u.) of the original reactance of the line where the TCSC is placed.

Note that the reactance of the TCSC is flexible and can be optimally set for each plausible wind scenario (Case C). On the contrary, Case B is a specific setting of Case C, imposing a fixed series compensation instead of an optimal one for each scenario.

The corresponding numerical results are given in the next subsection.

C. Numerical Results

The numerical results for the three cases considered are given in Table IV. Rows 2, 3, and 4 refer to Cases A, B, and C, respectively. In addition, column 2 provides the value of objective function (1).

Expected value of unserved load as expressed by (21), is given in the third column of Table IV.

The fourth column of Table IV gives the expected value of wind power spillage in percentage as defined by (22).

Finally, the expected value of total active power losses in the network is given in the fifth column of Table IV based on (23):

$$\widetilde{L}^{\mathrm{SH}} = \sum_{ds} \rho_s L_{ds}^{\mathrm{SH}} \tag{21}$$

$$\widetilde{W}^{\mathrm{SP}} = \sum_{ks} \rho_s \frac{W_{ks}^{\mathrm{SP}}}{W_{ks}} \tag{22}$$

$$\widetilde{P}^{\mathrm{L}} = \sum_{n(m\in\Omega_n)s} \frac{1}{2}\rho_s P_{nms}^{\mathrm{L}}(\mathbf{v}, \boldsymbol{\theta}, \mathbf{x}^{\mathbf{tcsc}}). \tag{23}$$

According to Table IV, the following observations are in order:

1) The value of the objective function for Case C is comparatively smaller than that of Case B, and the value of these two cases are lower than the value for Case A. This implies that a series capacitive compensation (Cases B and C) is effective with respect to a case without compensation (Case A). Additionally, it is observed that a TCSC (Case C) leads to a better result than an FSC (Case B) due to its higher capability in controlling power flows.
2) For all cases, no load is curtailed due to the comparatively high value of the weighting factor α_d^{SH}.
3) In Case A without series compensation, the expected value of wind power spillage is 16.4%. However, in Cases B and C with series compensation, such value is decreased to 13.2% and 11.4%, respectively. This implies that a flexible series compensation (TCSC) is more effective than a fixed series compensation in reducing wind power spillage.
4) Fig. 4 depicts the amount of wind power spillage per scenario and for each case. Accordingly, the amount of wind power spillage of Case C is comparatively lower than that of the two other cases in all scenarios.
5) Based on Fig. 4, the optimal series compensation (Case C) always decreases the wind power spillage with respect to the case without compensation (Case A). However, there is no guarantee to reduce wind power spillage using fixed series compensation (Case B). For instance, the amount of wind power spillage of Case B is worse than that of Case A in scenarios 5, 10 and 15.
6) According to the fifth column of Table IV, the expected value of active power losses in the network is minimum in Case C with optimal setting of TCSC.

If a TCSC is used to reduce wind power spillage, its optimal reactance needs to be determined. Table V illustrates the optimal reactance setting of the TCSC for each scenario as obtained solving problem (1)–(20).

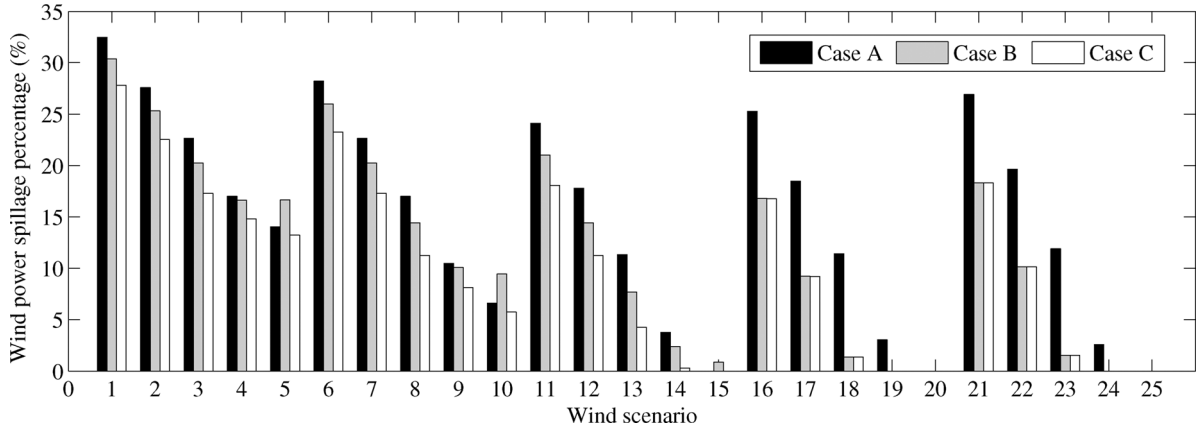

Fig. 4. Percentage of wind power spillage per scenario and for each case.

TABLE V
OPTIMAL REACTANCE SETTING OF TCSC PER SCENARIO (CASE C)

s	x^{tcsc}_{nms} [p.u.]	s	x^{tcsc}_{nms} [p.u.]	s	x^{tcsc}_{nms} [p.u.]	s	x^{tcsc}_{nms} [p.u.]	s	x^{tcsc}_{nms} [p.u.]
$s1$	0.261	$s6$	0.261	$s11$	0.261	$s16$	0.256	$s21$	0.248
$s2$	0.261	$s7$	0.261	$s12$	0.261	$s17$	0.256	$s22$	0.248
$s3$	0.261	$s8$	0.261	$s13$	0.261	$s18$	0.256	$s23$	0.248
$s4$	0.131	$s9$	0.131	$s14$	0.131	$s19$	0.185	$s24$	0.198
$s5$	-0.200	$s10$	-0.200	$s15$	-0.003	$s20$	0.096	$s25$	0.119

According to Table V, the optimal setting of the TCSC reactance across scenarios does not necessarily equal either its upper bound ($\overline{x}^{\text{tcsc}}_{nm} = 0.32$ p.u.) or its lower bound ($\underline{x}^{\text{tcsc}}_{nm} = -0.20$ p.u.). In fact, it is optimally determined considering the inputs from the market (P^{fix}_i, L^{P}_d, R^{D}_i,R^{U}_i, and W^{fix}_k) and system's constraints, e.g., limits on voltage angles and magnitudes, and the capacities of the transmission lines. To illustrate the concepts of the first- and the second-stage variables, as an example, Fig. 5 shows the scheduled decisions for the reactive power production of generating unit 27 prior to the uncertainty realization (Q^0_{27}) and also the reactive power production of such a generator in the operating condition involving wind scenario s ($Q^0_{27} + q_{27s}$). These results are depicted for two cases: Case A in which no FACTS device is installed, and Case C in which one TCSC is installed.

D. Computational Issues

Optimization problem (1)–(20) is solved using CONOPT [24] under GAMS [25] on a Sun Fire X4600M2 with 8 Quad-Core processors clocking at 2.9 GHz and 256 GB of RAM. Since the model is continuous, but non-convex, suitable initial points need to be used. Among different initial points checked, starting points $\mathbf{v} = 1$, $\boldsymbol{\theta} = 0$ and $\mathbf{x}^{\mathbf{tcsc}} = \overline{x}^{\text{tcsc}}_{nm}$ show the best performance in finding the optimal solution. The initial point that achieves in the best performance is the one that provides the smallest value for the objective function (1) with the lowest computational time.

The computational times required for solving the proposed model are provided in the last column of Table IV. Among the cases considered, the time to solve Case C is comparatively higher. Note that these times are small enough and appropriate for the considered problem. However, the proposed OPF model may become computationally intractable if applied to a large-scale power system considering many scenarios. In that case, the use of parallelization and/or decomposition techniques may significantly reduce the computational time.

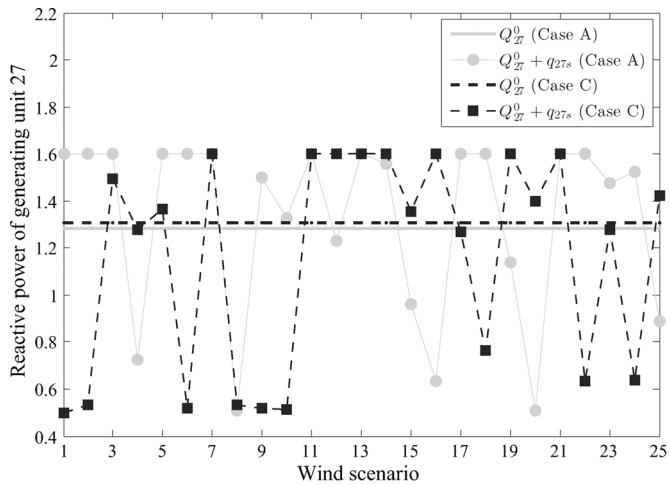

Fig. 5. Reactive power production of generating unit 27 prior to and after uncertainty realization.

IV. CONCLUSION

This paper provides a methodology to minimize wind power spillage using an OPF with FACTS devices. In addition, total active power losses is minimized and load shedding is avoided as well. Among FACTS devices, FSC and TCSC are selected for this study. The uncertainty of wind power production is modeled through a number of plausible scenarios. The conclusions drawn from this work are listed as follows:

1) A series compensation may reduce the wind power spillage, unserved load, and total active power losses of the network.
2) Prior to uncertainty realization, the system is prepositioned to optimally cope with the wind production realizations.
3) For each scenario, the optimal utilization of the TCSC (optimal reactance setting) is effective to decrease wind power spillage; however, an FSC is not necessarily effective.
4) Optimal reactance setting of the TCSC needs to be determined for each wind scenario.

5) Optimal setting of the TCSC reactance across all scenarios is not constant, and it does not necessarily equal its upper or lower bound. Such optimal setting depends on the inputs from the market and the system constraints.

APPENDIX

This Appendix provides the mathematical definition of all functions used throughout the paper. Functions $P^0_{nm}(\mathbf{v},\boldsymbol{\theta})$ and $Q^0_{nm}(\mathbf{v},\boldsymbol{\theta})$ used in (2) and (3) are mathematically formulated as follows:

$$P^0_{nm}(\mathbf{v},\boldsymbol{\theta}) = Y_{nm}\left[{v_n^0}^2\cos(\phi_{nm}) - v_n^0 v_m^0\cos\left(\theta_n^0-\theta_m^0-\phi_{nm}\right)\right] \quad \forall n,\forall m\in\Omega_n \tag{24}$$

$$Q^0_{nm}(\mathbf{v},\boldsymbol{\theta}) = -Y_{nm}\left[{v_n^0}^2\sin(\phi_{nm}) + v_n^0 v_m^0\sin\left(\theta_n^0-\theta_m^0-\phi_{nm}\right)\right] \quad \forall n,\forall m\in\Omega_n. \tag{25}$$

Considering (24) and (25), function $S^0_{nm}(\mathbf{v},\boldsymbol{\theta})$ used in (8) is

$$S^0_{nm}(\mathbf{v},\boldsymbol{\theta}) = \sqrt{P^{0^2}_{nm}(\mathbf{v},\boldsymbol{\theta}) + Q^{0^2}_{nm}(\mathbf{v},\boldsymbol{\theta})} \quad \forall n,\forall m\in\Omega_n. \tag{26}$$

Similarly to (24)–(26), functions $P_{nms}(\mathbf{v},\boldsymbol{\theta},\mathbf{x^{tcsc}})$, $Q_{nms}(\mathbf{v},\boldsymbol{\theta},\mathbf{x^{tcsc}})$ and $S_{nms}(\mathbf{v},\boldsymbol{\theta},\mathbf{x^{tcsc}})$ used in (9), (10) and (20) corresponding to the operating conditions (second-stage) are mathematically formulated as follows:

$$P_{nms}(\mathbf{v},\boldsymbol{\theta},\mathbf{x^{tcsc}}) = Y_{nm}\left[v_{ns}^2\cos(\phi_{nm}) - v_{ns}v_{ms}\cos(\theta_{ns}-\theta_{ms}-\phi_{nm})\right] - P^{\text{inj}}_{nms}(\mathbf{v},\boldsymbol{\theta},\mathbf{x^{tcsc}}) \quad \forall n,\forall m\in\Omega_n,\forall s \tag{27}$$

$$Q_{nms}(\mathbf{v},\boldsymbol{\theta},\mathbf{x^{tcsc}}) = -Y_{nm}\left[v_{ns}^2\sin(\phi_{nm}) + v_{ns}v_{ms}\sin(\theta_{ns}-\theta_{ms}-\phi_{nm})\right] - Q^{\text{inj}}_{nms}(\mathbf{v},\boldsymbol{\theta},\mathbf{x^{tcsc}}) \quad \forall n,\forall m\in\Omega_n,\forall s \tag{28}$$

$$S_{nms}(\mathbf{v},\boldsymbol{\theta},\mathbf{x^{tcsc}}) = \sqrt{P^2_{nms}(\mathbf{v},\boldsymbol{\theta},\mathbf{x^{tcsc}}) + Q^2_{nms}(\mathbf{v},\boldsymbol{\theta},\mathbf{x^{tcsc}})} \quad \forall n,\forall m\in\Omega_n,\forall s \tag{29}$$

where functions $P^{\text{inj}}_{nms}(\mathbf{v},\boldsymbol{\theta},\mathbf{x^{tcsc}})$ and $Q^{\text{inj}}_{nms}(\mathbf{v},\boldsymbol{\theta},\mathbf{x^{tcsc}})$ used in (27) and (28) pertain to the injection model of TCSC [20] and [21], and are defined as follows:

$$P^{\text{inj}}_{nms}(\mathbf{v},\boldsymbol{\theta},\mathbf{x^{tcsc}}) = v_{ns}^2\Delta G_{nms} - v_{ns}v_{ms}\times\left[\Delta G_{nms}\cos(\theta_{ns}-\theta_{ms}) + \Delta B_{nms}\sin(\theta_{ns}-\theta_{ms})\right] \quad \forall n,\forall m\in\Omega_n,\forall s \tag{30}$$

$$Q^{\text{inj}}_{nms}(\mathbf{v},\boldsymbol{\theta},\mathbf{x^{tcsc}}) = -v_{ns}^2\Delta B_{nms} - v_{ns}v_{ms}\times\left[\Delta G_{nms}\sin(\theta_{ns}-\theta_{ms}) - \Delta B_{nms}\cos(\theta_{ns}-\theta_{ms})\right] \quad \forall n,\forall m\in\Omega_n,\forall s \tag{31}$$

where

$$\Delta G_{nms} = \frac{x^{\text{tcsc}}_{nms}r_{nm}\left(x^{\text{tcsc}}_{nms}-2x_{nm}\right)}{\left[r_{nm}^2+x_{nm}^2\right]\left[r_{nm}^2+(x_{nm}-x^{\text{tcsc}}_{nms})^2\right]} \quad \forall n,\forall m\in\Omega_n,\forall s \tag{32}$$

$$\Delta B_{nms} = \frac{-x^{\text{tcsc}}_{nms}\left(r_{nm}^2-x_{nm}^2+x^{\text{tcsc}}_{nms}x_{nm}\right)}{\left[r_{nm}^2+x_{nm}^2\right]\left[r_{nm}^2+(x_{nm}-x^{\text{tcsc}}_{nms})^2\right]} \quad \forall n,\forall m\in\Omega_n,\forall s. \tag{33}$$

Clearly, (30)–(33) correspond to those buses connected to a transmission line with a TCSC.

Finally, the value of $P^{\text{L}}_{nms}(\mathbf{v},\boldsymbol{\theta},\mathbf{x^{tcsc}})$ used in (1) and (23) is calculated as follows:

$$P^{\text{L}}_{nms}(\mathbf{v},\boldsymbol{\theta},\mathbf{x^{tcsc}}) = P_{nms}(\mathbf{v},\boldsymbol{\theta},\mathbf{x^{tcsc}}) + P_{mns}(\mathbf{v},\boldsymbol{\theta},\mathbf{x^{tcsc}}) \quad \forall n,\forall m\in\Omega_n,\forall s. \tag{34}$$

ACKNOWLEDGMENT

A. Nasri has been awarded an Erasmus Mundus Ph.D. Fellowship. He would like to express his gratitude towards all partner institutions within the program as well as the European Commission for their support.

REFERENCES

[1] The Red Eléctrica de España, REE, 2013 [Online]. Available: http://www.ree.es/
[2] The Iberian Peninsula Electricity Exchange, OMIE, 2013 [Online]. Available: http://www.omie.es/
[3] The Dannish Energy Agency, 2013 [Online]. Available: http://www.ens.dk/
[4] The Nordic Electricity Exchange, NordPool [Online]. Available: http://www.nordpoolspot.com/
[5] Pennsylvania-New Jersey-Maryland Interconnection, PJM [Online]. Available: http://www.pjm.com/
[6] ISO-New England [Online]. Available: http://www.iso-ne.com/
[7] J. M. Morales, A. J. Conejo, and J. Pérez-Ruiz, "Economic valuation of reserves in power systems with high penetration of wind power," *IEEE Trans. Power Syst.*, vol. 24, no. 2, pp. 900–910, May 2009.
[8] J. M. Morales, A. J. Conejo, K. Liu, and J. Zhong, "Pricing electricity in pools with wind producers," *IEEE Trans. Power Syst.*, vol. 27, no. 3, pp. 1366–1376, Aug. 2012.
[9] M. Ghofrani, A. Arabali, M. Etezadi-Amoli, and M. S. Fadali, "A framework for optimal placement of energy storage units within a power system with high wind penetration," *IEEE Trans. Sustain. Energy*, vol. 4, no. 2, pp. 434–442, Apr. 2013.
[10] T. Capuder, H. Pandžic, L. Kuzle, and D. Škrlec, "Specifics of integration of wind power plants into the Croatian transmission network," *Appl. Energy*, vol. 101, pp. 142–150, Jan. 2013.
[11] Y. Xiao, Y. H. Song, C. C. Pérez-Ruiz, and Y. Z. Sun, "Available transfer capability enhancement using FACTS devices," *IEEE Trans. Power Syst.*, vol. 18, no. 1, pp. 305–312, Feb. 2003.
[12] S. Gerbex, R. Cherkaoui, and A. J. Germond, "Optimal location of multi-type FACTS devices in a power system by means of genetic algorithms," *IEEE Trans. Power Syst.*, vol. 16, no. 3, pp. 537–544, Aug. 2001.
[13] R. Zérate-Miñano, A. J. Conejo, and F. Milano, "OPF-based security redispatching including FACTS devices," *IET Gen., Transm., Distrib.*, vol. 2, no. 6, pp. 821–833, Nov. 2008.
[14] F. B. Alhasawi and J. V. Milanovic, "Techno-economic contribution of FACTS devices to the operation of power systems with high level of wind power integration," *IEEE Trans. Power Syst.*, vol. 27, no. 3, pp. 1414–1421, Aug. 2012.
[15] A. D. Shakib, E. Sphair, and G. Balzer, "Optimal location of series FACTS devices to control line overloads in power systems with high wind feeding," in *Proc. IEEE Bucharest PowerTech*, Jun. 2009, pp. 1–7.
[16] M. J. Hossain, H. R. Pota, M. A. Mahmud, and R. A. Ramos, "Investigation of the impacts of large-scale wind power penetration on the angle and voltage stability of power systems," *IEEE Syst. J.*, vol. 6, no. 1, pp. 76–84, Mar. 2012.
[17] M. Narimani and R. K. Varma, "Application of static VAR compensator (SVC) with fuzzy controller for grid integration of wind farm," in *Proc. Canadian Conf. Electrical and Computer Engineering (CCECE)*, May 2010, pp. 1–6.

[18] R. Grunbaum, "FACTS for grid integration of wind power," in *Proc. IEEE PES Innovative Smart Grid Technologies Conf. Europe (ISGT Europe)*, Oct. 2010, pp. 1–8.
[19] R. Yang and G. Hug-Glanzmann, "Optimal usage of transmission capacity with FACTS devices in the presence of wind generation: A two-stage approach," in *Proc. IEEE Power and Energy Society General Meeting*, Jul. 2012, pp. 1–7.
[20] S. N. Singh and A. K. David, "Optimal location of FACTS devices for congestion management," *Elect. Power Syst. Res.*, vol. 58, no. 2, pp. 71–79, Jun. 2001.
[21] M. Noroozian and G. Anderson, "Power flow control by use of controllable series components," *IEEE Trans. Power Del.*, vol. 8, no. 3, pp. 1420–1429, Jul. 1993.
[22] D. P. Bertsekas and N. R. Sandell, "Estimates of the duality gap for large-scale separable nonconvex optimization problems," in *Proc. 21st IEEE Conf. Decision and Control*, Miami Beach, FL, USA, Dec. 1982, pp. 782–785.
[23] Reliability System Task Force, "The IEEE reliability test system 1996: A report prepared by the reliability test system task force of the application of probability methods subcommittee," *IEEE Trans. Power Syst.*, vol. 14, no. 3, pp. 1010–1020, Aug. 1999.
[24] A. S. Drud, GAMS/CONOPT. Bagsvaerd, Denmark, ARKI Consulting and Development, 1996 [Online]. Available: http://www.gams.com/
[25] A. Brooke, D. Kendrick, A. Meeraus, R. Raman, and R. E. Rosenthal, GAMS, a User's Guide, GAMS Development Corp.. Washington, DC, USA, Dec. 1998 [Online]. Available: http://www.gams.com/

Amin Nasri (S'11) received the M.Sc. degree in electrical engineering from Sharif University of Technology, Tehran, Iran, in 2008. He is pursuing the Erasmus Mundus Joint Doctorate in sustainable energy technologies and strategies (SETS) hosted by Comillas Pontifical University, Spain; Royal Institute of Technology, Sweden; and Delft University of Technology, The Netherlands. He is currently pursuing the Ph.D. degree in the Division of Electric Power Systems, School of Electrical Engineering at KTH Royal Institute of Technology.

His research interests include power system operation, dynamics, stability and control, and FACTS.

Antonio J. Conejo (F'04) received the M.S. degree from the Massachusetts Institute of Technology, Cambridge, MA, USA, in 1987, and the Ph.D. degree from the Royal Institute of Technology, Stockholm, Sweden, in 1990.

He is currently a full Professor at the University of Castilla–La Mancha, Ciudad Real, Spain. His research interests include control, operations, planning and economics of electric energy systems, as well as statistics and optimization theory and its applications.

S. Jalal Kazempour (S'08–M'14) received the B.Sc. degree from the University of Tabriz, Tabriz, Iran, in 2006, the M.Sc. degree from Tarbiat Modares University, Tehran, Iran, in 2009, and the Ph.D. degree from the University of Castilla–La Mancha, Ciudad Real, Spain, in 2013, all in electrical engineering.

He is currently a postdoctoral fellow at the Whiting School of Engineering, Department of Mechanical Engineering, Johns Hopkins University, Baltimore, MD, USA. His research interests include electricity markets, optimization and its applications to energy systems.

Mehrdad Ghandhari (SM'14) received the M.Sc. and Ph.D. degrees in electrical engineering from Royal Institute of Technology (KTH), Stockholm, Sweden, in 1995 and 2000, respectively.

He is currently a full Professor at KTH. His research interests include power system dynamics, stability and control, and FACTS and HVDC systems.

Paper J3

Network-constrained AC Unit Commitment under Uncertainty: A Benders' Decomposition Approach

Network-constrained AC Unit Commitment under Uncertainty: A Benders' Decomposition Approach

Amin Nasri, *Student Member, IEEE*, S. Jalal Kazempour, *Member, IEEE*,
Antonio J. Conejo, *Fellow, IEEE*, and Mehrdad Ghandhari, *Senior Member, IEEE*,

***Abstract*—This paper proposes an efficient solution approach based on Benders' decomposition to solve a network-constrained ac unit commitment problem under uncertainty. The wind power production is the only source of uncertainty considered in this paper, which is modeled through a suitable set of scenarios. The proposed model is formulated as a two-stage stochastic programming problem, whose first-stage refers to the day-ahead market, and whose second-stage represents real-time operation. The proposed Benders' approach allows decomposing the original problem, which is mixed-integer non-linear and generally intractable, into a mixed-integer linear master problem and a set of non-linear, but continuous subproblems, one per scenario. In addition, to temporally decompose the proposed ac unit commitment problem, a heuristic technique is used to relax the inter-temporal ramping constraints of the generating units. Numerical results from a case study based on the IEEE one-area reliability test system (RTS) demonstrate the usefulness of the proposed approach.**

***Index Terms*—Network-constrained ac unit commitment, Wind power uncertainty, Stochastic programming, Benders' decomposition.**

I. Introduction

A. Motivation

Unit commitment (UC) is a crucial short-term decision-making problem in power system operations, whose objective is to determine the least-cost commitment and dispatch of generating units to serve the load. The deterministic form of the UC problem and its solution strategies are extensively documented in the literature, e.g., [1]–[3]. However, the recent increase of stochastic production units, especially wind power, in generation portfolios calls for a stochastic form of the UC problem, instead of a deterministic one. Moreover, a precise modeling of the physical laws characterizing this problem is needed as increasing wind power production generally results in stressed operating conditions. Hence, the need for an ac modeling arises.

The work of A. Nasri is supported by Erasmus Mundus Joint Doctorate in Sustainable Energy Technologies and Strategies. The work of S. J. Kazempour was supported by the US National Science Foundation under grant ECCS 1230788.

A. Nasri and M. Ghandhari are with KTH Royal Institute of Technology, Stockholm, Sweden, (e-mails: Amin.Nasri@ee.kth.se, and Mehrdad.Ghandhari@ee.kth.se)

S. J. Kazempour is with Johns Hopkins University, Baltimore, MD 21218 USA (e-mail: skazemp1@jhu.edu).

A. J. Conejo is with The Ohio State University, Columbus, OH 43210 USA (e-mail: conejonavarro.1@osu.edu).

B. Literature Review and Contributions

Large-scale integration of wind power increases significantly the level of uncertainty [4], hence the need of a stochastic UC approach. The stochastic UC problem was first studied in mid 90's [5], [6]. More recent works include [7]–[9]. These approaches embed a dc representation of transmission system, rendering a mixed-integer linear UC problem (network-constrained dc-UC problem), which is generally tractable [10]–[13]. It is worth mentioning that due to the simplifications considered in the dc-UC problems, i.e., the exclusion of voltage magnitude and reactive power constraints, an ex-post verification is required to check that the results obtained are implementable.

A UC problem including an ac network representation (network-constrained ac-UC problem) provides a comparatively more precise description of power system operations, particularly as operating conditions become increasingly stressed due to increasing wind production. However, the ac unit commitment (ac-UC) problem is mixed-integer non-linear, and thus hard to solve. In the technical literature, there are few works addressing the ac-UC problem. Reference [14] proposes an approach based on Benders' decomposition to solve an ac network-constrained hydrothermal scheduling problem. A security-constrained ac-UC problem is proposed in [15], whose objective is to minimize the system's operating cost while maintaining appropriate security. The heuristic technique proposed in [15] decomposes the original problem into a master problem representing an ac-UC problem under a normal operating condition, and a subproblem checking security constraints. Note that wind power uncertainty is not modeled either in [14] or [15]. Reference [16] formulates a security-constrained stochastic ac-UC problem under wind power uncertainty, and discusses potential solution techniques, but numerical results are not reported.

This paper proposes a network-constrained ac-UC problem in which the wind power uncertainty is characterized by a set of suitable scenarios. To cope with wind power uncertainty, a two-stage stochastic programming model is considered, whose first-stage represents the day-ahead market, and whose second-stage represents the real-time operating conditions involving wind power realizations.

Considering the context above, the contributions of this paper are threefold:

1) To propose a stochastic two-stage network-constrained ac-UC problem for a system with significant wind power production.

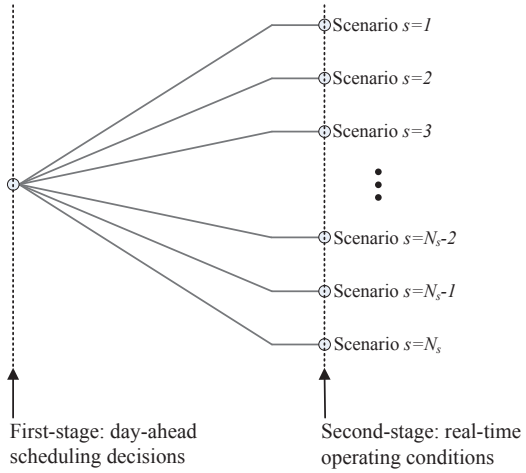

Fig. 1: Two-stage stochastic decision framework of the proposed ac-UC problem.

2) To decompose the proposed network-constrained ac-UC problem by scenario and time period, which ease the computational burden.
3) To implement Benders' decomposition, which requires iteratively solving (i) a mixed-integer linear master problem, and (ii) a set of non-linear, but continuous subproblems.

Note that in the rest of this paper the terms "dc-UC" and "ac-UC" refer to "network-constrained dc-UC" and "network-constrained ac-UC" problems, respectively.

II. AC-UC MODEL

A. Stochastic Framework

Fig. 1 depicts the two-stage stochastic framework considered in this paper. Note that these two stages are simultaneously considered. The first-stage includes the scheduling decisions made at the day-ahead market. Such decisions are adapted to any wind production realization in the second-stage, where the real-time operating conditions corresponding to individual wind scenarios are represented. This way, prior to the uncertainty realization in the second-stage, the system is optimally prepositioned via scheduling decisions in the first-stage. Therefore, the first-stage decisions are scenario-independent, while each second-stage decision adapts to the operating conditions of the corresponding wind power realization. Further details on the two-stage stochastic programming model used in this paper can be found in [4].

The proposed ac-UC problem clears the day-ahead market while considering all plausible real-time operating conditions. Therefore, the scheduling decisions made at the first-stage (day-ahead market) are consistent with those conditions. Since operating limits are enforced explicitly at the second-stage for all plausible operating conditions, the resulting schedule is both optimal and consistent with real-time operating conditions.

B. Modeling Assumptions

For the sake of clarity, the modeling assumptions considered in this work are listed as follows:

1) The first-stage of the proposed UC problem (that represents the day-ahead market) embodies a dc network representation, while the second-stage (that represents the real-time operation) embeds an ac one. This assumption is consistent with the functioning of most real-world electricity markets.
2) For the sake of simplicity, only wind power uncertainty is taken into account. However, other uncertainties can be incorporated into the model. The uncertainty of wind power production is modeled through a set of plausible scenarios based on the available forecasted data.
3) The minimum up-time and minimum down-time constraints of thermal units are not considered in this paper. To consider them, additional binary variables are required [17].
4) A number of units are available to provide reserve.
5) The wind power production cost is assumed to be nil.
6) All loads are assumed to be inelastic.
7) Wind farms of Type 3 DFIG and Type 4 full converter are able to provide voltage support in steady-state and dynamically [18]. However, for the sake of simplicity, we assume unit power factor for all wind farms.
8) The security constraints are not modeled in this work. However, such constraints can be easily incorporated in the proposed framework.

C. Notation

The main notation used is defined below. All variables and constants are expressed in per-unit. Symbols $\mathbf{v}$ and $\boldsymbol{\theta}$ written in bold without index are vector forms of the nodal voltage magnitude and the nodal voltage angles, respectively.

Indices:

d	Index for loads.
i	Index for generating units.
k	Index for wind farms.
n/m	Indices for system nodes.
s	Index for wind power scenarios.
t	Index for time periods.

Sets:

$\mathcal{D}$	Set of loads.
$\mathcal{G}$	Set of generating units.
$\mathcal{K}$	Set of wind farms.
Ω_n	Set of nodes adjacent to node n.

Sets $\mathcal{K}$, $\mathcal{D}$ and $\mathcal{G}$ include subscript n if referring to the set of wind farms, loads and generating units, respectively, located at node n.

Continuous Variables:

C_{it}^{SU}	Start-up cost of unit i in period t.
P_{it}^{DA}	Active power scheduled for unit i in period t.
W_{kt}^{DA}	Active power scheduled for wind farm k in period t.

$\theta_{nt}^{\mathrm{DA}}$ Voltage angle at node n in period t at the scheduling stage.
L_{dts}^{SH} Involuntarily active load shedding of load d in period t and scenario s.
Q_{its} Reactive power output of unit i in period t and scenario s.
r_{its} Reserve deployed by unit i in period t and scenario s.
W_{kts}^{SP} Wind power spillage of wind farm k in period t and scenario s.
v_{nts} Voltage magnitude at node n in period t and scenario s.
θ_{nts} Voltage angle at node n in period t and scenario s.

Note that the first four variables pertain to the first-stage.

Binary Variables:

u_{it} 0/1 variable that is equal to 1 if unit i is scheduled to be committed in period t.

Constants:

ρ_s Probability of scenario s.
λ_i^{SU} Start-up cost of unit i.
C_i Marginal cost of the energy offered by unit i.
L_{dt}^{P} Active power consumed by load d in period t.
L_{dt}^{Q} Reactive power consumed by load d in period t.
$\overline{P}_i$ Active power capacity of unit i.
$\underline{P}_i$ Minimum active power output of unit i.
P_i^{ini} Initial active power output of unit i.
$\overline{Q}_i$ Reactive power capacity of unit i.
$\underline{Q}_i$ Minimum reactive power output of unit i.
R_i^{U} Maximum up-reserve that can be deployed by unit i.
R_i^{D} Maximum down-reserve that can be deployed by unit i.
R_i^{+} Maximum Ramp-up rate of unit i.
R_i^{-} Maximum Ramp-down rate of unit i.
r_i^{ini} Initial reserve deployed by unit i.
$\overline{S}_{nm}$ Capacity of transmission line (n,m).
u_i^{ini} Initial commitment status of unit i.
V_d^{SH} Value of load shed for load d.
W_{kts} Wind power production realization of farm k in period t and scenario s.
$\overline{W}_{kt}^{\mathrm{DA}}$ Maximum power production of wind farm k in period t that can be scheduled at the scheduling stage. It is assumed to be equal to the expected power production, i.e., $\overline{W}_{kt}^{\mathrm{DA}} = \sum_s \rho_s W_{kts},\ \forall k, \forall t$.
x_{nm} Reactance of transmission line (n,m).
Y_{nm} Admittance magnitude of transmission line (n,m).
ϕ_{nm} Admittance angle of transmission line (n,m).

Functions:

$P_{nmt}^{\mathrm{DA}}(.)$ Scheduled active power through transmission line (n,m) in period t.
$P_{nmts}(.)$ Active power through transmission line (n,m) in period t and scenario s.
$Q_{nmts}(.)$ Reactive power through transmission line (n,m) in period t and scenario s.
$S_{nmts}(.)$ Apparent power through transmission line (n,m) in period t and scenario s.

The mathematical definitions of the functions above are given in Appendix A.

D. Formulation

The considered two-stage ac-UC problem is formulated as (1)-(3). Objective function (1) represents the system's expected cost, and is subject to first-stage constraints (2) and second-stage constraints (3). The optimization variables of the ac-UC problem (1)-(3) are the elements of the set:

$$\Xi^{\mathrm{UC}} = \{\theta_{nt}^{\mathrm{DA}}, C_{it}^{\mathrm{SU}}, P_{it}^{\mathrm{DA}}, W_{kt}^{\mathrm{DA}}, u_{it}, v_{nts}, \theta_{nts}, r_{its}, Q_{its}, W_{kts}^{\mathrm{SP}}, L_{dts}^{\mathrm{SH}}\}.$$

Note that the mathematical definitions of the functions used in (2) and (3) are given in Appendix A.

The objective function is:

$$\underset{\Xi^{\mathrm{UC}}}{\text{Minimize}} \quad \sum_{(i\in\mathcal{G})t} \left[C_{it}^{\mathrm{SU}} + C_i P_{it}^{\mathrm{DA}}\right] + \sum_s \rho_s \left[\sum_{(i\in\mathcal{G})t} C_i\ r_{its} + \sum_{(d\in\mathcal{D})t} V_d^{\mathrm{SH}} L_{dts}^{\mathrm{SH}}\right] \tag{1}$$

The first two terms of (1) correspond to the system's cost at scheduling time (first-stage), while the other two terms refer to the expected cost in real-time operation (second-stage). The first term represents the start-up cost of the units, the second one refers to their production cost, and the third term represents the reserve deployment cost. Note that the reserve deployment cost (third term) refers to the production cost of the additional energy produced in real-time operation to offset the energy imbalance occurred due to wind power variability. This term is in fact the product of the generating unit's marginal cost and the production increment from day-ahead to real-time operation. Finally, the last term of (1) is the load curtailment cost.

The first-stage constraints are:

$$\sum_{i\in\mathcal{G}_n} P_{it}^{\mathrm{DA}} + \sum_{k\in\mathcal{K}_n} W_{kt}^{\mathrm{DA}} - \sum_{d\in\mathcal{D}_n} L_{dt}^{\mathrm{P}} = \sum_{m\in\Omega_n} P_{nmt}^{\mathrm{DA}}(\boldsymbol{\theta}) \quad \forall n, \forall t \tag{2a}$$

$$\underline{P}_i u_{it} \leq P_{it}^{\mathrm{DA}} \leq \overline{P}_i u_{it} \qquad \forall i \in \mathcal{G}, \forall t \qquad (2b)$$
$$0 \leq W_k^{\mathrm{DA}} \leq \overline{W}_{kt}^{\mathrm{DA}} \qquad \forall k \in \mathcal{K}, \forall t \qquad (2c)$$
$$-R_i^- \leq \left[P_{i(t=1)}^{\mathrm{DA}} - P_i^{\mathrm{ini}}\right] \leq R_i^+ \qquad \forall i \in \mathcal{G} \qquad (2d)$$
$$-R_i^- \leq \left[P_{it}^{\mathrm{DA}} - P_{i(t-1)}^{\mathrm{DA}}\right] \leq R_i^+ \qquad \forall i \in \mathcal{G}, \forall t > 1 \qquad (2e)$$
$$-\pi \leq \theta_{nt}^{\mathrm{DA}} \leq \pi \qquad \forall n, \forall t \qquad (2f)$$
$$\theta_{(n=1)t}^{\mathrm{DA}} = 0 \qquad \forall t \qquad (2g)$$
$$P_{nmt}^{\mathrm{DA}}(\boldsymbol{\theta}) \leq \overline{S}_{nm} \qquad \forall n, \forall m \in \Omega_n, \forall t \qquad (2h)$$
$$C_{i(t=1)}^{\mathrm{SU}} \geq \lambda_i^{\mathrm{SU}} \left[u_{i(t=1)} - u_i^{\mathrm{ini}}\right] \qquad \forall i \in \mathcal{G} \qquad (2i)$$
$$C_{it}^{\mathrm{SU}} \geq \lambda_i^{\mathrm{SU}} \left[u_{it} - u_{i(t-1)}\right] \qquad \forall i \in \mathcal{G}, \forall t > 1 \qquad (2j)$$
$$C_{it}^{\mathrm{SU}} \geq 0 \qquad \forall i \in \mathcal{G}, \forall t. \qquad (2k)$$

Constraints (2a) represent the active power balance at scheduling time at each node and for each time period. Constraints (2b) and (2c) enforce the lower and upper bounds for active power production of generating units and wind farms, respectively. Constraints (2d) and (2e) ensure that the hourly changes of scheduled power do not violate the ramp-rate limits. Constraints (2f) enforce lower and upper bounds of voltage angles. Constraints (2g) set $n = 1$ as the reference node. The capacity of each transmission line is enforced through (2h). Constraints (2j)-(2k) allow calculating the start-up cost of the units.

The second-stage constraints are:

$$\sum_{i \in \mathcal{G}_n} (P_{it}^{\mathrm{DA}} + r_{its}) + \sum_{k \in \mathcal{K}_n} \left(W_{kts} - W_{kts}^{\mathrm{SP}}\right) - \sum_{d \in \mathcal{D}_n} (L_{dt}^{\mathrm{P}} - L_{dts}^{\mathrm{SH}}) = \sum_{m \in \Omega_n} P_{nmts}(\mathbf{v}, \boldsymbol{\theta}) \ \forall n, \forall t, \forall s \qquad (3a)$$
$$\sum_{i \in \mathcal{G}_n} Q_{its} - \sum_{d \in \mathcal{D}_n} L_{dt}^{\mathrm{Q}} = \sum_{m \in \Omega_n} Q_{nmts}(\mathbf{v}, \boldsymbol{\theta}) \qquad \forall n, \forall t, \forall s \qquad (3b)$$
$$0 \leq L_{dts}^{\mathrm{SH}} \leq L_{dt}^{\mathrm{P}} \qquad \forall d \in \mathcal{D}, \forall t, \forall s \qquad (3c)$$
$$0 \leq W_{kts}^{\mathrm{SP}} \leq W_{kts} \qquad \forall k \in \mathcal{K}, \forall t, \forall s \qquad (3d)$$
$$-R_i^{\mathrm{D}} \leq r_{its} \leq R_i^{\mathrm{U}} \qquad \forall i \in \mathcal{G}, \forall t, \forall s \qquad (3e)$$
$$\underline{P}_i u_{it} \leq \left[r_{its} + P_{it}^{\mathrm{DA}}\right] \leq \overline{P}_i u_{it} \qquad \forall i \in \mathcal{G}, \forall t, \forall s \qquad (3f)$$
$$\underline{Q}_i u_{it} \leq Q_{its} \leq \overline{Q}_i u_{it} \qquad \forall i \in \mathcal{G}, \forall t, \forall s \qquad (3g)$$
$$-R_i^- \leq \left[\left(P_{i(t=1)}^{\mathrm{DA}} + r_{i(t=1)s}\right) - \left(P_i^{\mathrm{ini}} + r_i^{\mathrm{ini}}\right)\right] \leq R_i^+ \qquad \forall i \in \mathcal{G}, \forall s \qquad (3h)$$
$$-R_i^- \leq \left[\left(P_{it}^{\mathrm{DA}} + r_{its}\right) - \left(P_{i(t-1)}^{\mathrm{DA}} + r_{i(t-1)s}\right)\right] \leq R_i^+ \qquad \forall i \in \mathcal{G}, \forall t > 1, \forall s \qquad (3i)$$
$$\underline{v}_n \leq v_{nts} \leq \overline{v}_n \qquad \forall n, \forall t, \forall s \qquad (3j)$$
$$-\pi \leq \theta_{nts} \leq \pi \qquad \forall n, \forall t, \forall s \qquad (3k)$$
$$\theta_{(n=1)ts} = 0 \qquad \forall t, \forall s \qquad (3l)$$
$$S_{nmts}(\mathbf{v}, \boldsymbol{\theta}) \leq \overline{S}_{nm} \qquad \forall n, \forall m \in \Omega_n, \forall t, \forall s. \qquad (3m)$$

Constraints (3a) and (3b) represent the active and reactive power balance in real-time operation at each node and for each time period and scenario. Active power balance constraints (3a) enforce that the deviations of wind production are met with reserve deployment of generating units, and/or wind power spillage of farms, and/or curtailment of loads. Constraints (3c)-(3g) bound the value of unserved load, wind power spillage, active power reserve deployed, total active power production and reactive power production of generating units, respectively. Constraints (3h) and (3i) enforce ramp-rate limits. Constraints (3j) enforce the lower and upper bounds of nodes' voltage magnitude. Finally, constraints (3k)-(3m) are similar to (2f)-(2h), but for real-time operation.

Finally, note that the proposed ac-UC problem (1)-(3) is mixed-integer, non-linear and generally intractable. To make it solvable, Benders' decomposition is applied as described in the next section.

III. Benders' Solution

This section proposes a solution strategy based on Benders' decomposition to solve problem (1)-(3).

A. Complicating Variables and Convexification

If first-stage variables P_{it}^{DA} and u_{it} are fixed to given values in problem (1)-(3), this problem decomposes into (i) a scenario-independent mixed-integer linear problem (representing the first-stage), and (ii) a set of non-linear continuous problems, one per scenario (representing the second-stage). Therefore, P_{it}^{DA} and u_{it} are complicating variables, and Benders' decomposition can be potentially applied [19].

Although the original ac-UC problem (1)-(3) is non-convex and Benders' decomposition is not generally applicable, if the number of wind power scenarios is large enough, the objective function (1) as a function of the complicating variables convexifies as shown in [20]. In other words, the objective function of an expected value stochastic programming problem convexifies as the number of scenarios increases. The reason of this is that the objective function represents the expectation over a number of scenarios. Thus, as the number of scenarios increases, the diversity of objective functions increases, while the weight of each single-scenario decreases. This results in a smoothing effect leading to the convexification of the expected value objective function. This convexification allows a successful implementation of Benders' decomposition.

Benders' convergence is guaranteed if the objective function of the original problem projected on the subspace of the complicating variables has a convex envelope. The proposed ac-UC problem (1)-(3) is "sufficiently" convexified by considering a large enough number of scenarios, and our numerical analysis confirms the well-functioning of the proposed decomposition algorithm. Nevertheless, convergence cannot be generally guaranteed for the considered problem.

Finally, note that the asymptotic convexification yielded by increasing the number of scenarios is not a heuristic, provided that a large-enough number of scenarios is considered.

B. Decomposition by Scenario and Time Period

Fixing the complicating variables P_{it}^{DA} and u_{it} to given values decomposes the ac-UC problem (1)-(3) by scenario. However, the ramping constraints (3h) and (3i), which links time periods, impede the ac-UC problem to decompose by time period.

In general, an appropriate balance is needed between model accuracy and computational burden. To this end, a heuristic technique is used in this paper to decompose the proposed ac-UC problem by time period. This technique allows reducing the computational burden, but at the potential cost of introducing imprecision in the final solution. According to this heuristic technique, the inter-temporal ramping constraints (3h) and (3i) are relaxed and enforced just locally. That is, at time t, ramping limits are enforced with respect to time $t-1$, and time periods are processed successively from the first to the last one. However, note that if needed, a reduced number of hours (e.g., 3 or 4) may be processed at the same time, which may be helpful for periods with high increase/decrease in demand and/or renewable production levels. Our extensive numerical simulations show that the results obtained with and without such a heuristic technique are close enough.

The formulation of Benders' master problem and subproblems are provided in the next subsections.

C. Subproblem

The subproblem for scenario s and time period t is formulated as (4) below. All variables pertain to Benders' iteration ν.

$$\Big\{\underset{\Xi_{ts}^{\mathrm{SP}}}{\text{Minimize}} \quad Z_{ts}^{(\nu)} = \sum_{i\in\mathcal{G}} C_i\ r_{its}^{(\nu)} + \sum_{d\in\mathcal{D}} V_d^{\mathrm{SH}} L_{dts}^{\mathrm{SH}^{(\nu)}} \tag{4a}$$

$$\text{subject to}$$

$$(3) \tag{4b}$$

$$P_{it}^{\mathrm{DA}^{(\nu)}} = P_{it}^{\mathrm{DA,fixed}} \qquad \forall i\in\mathcal{G} \tag{4c}$$

$$u_{it}^{(\nu)} = u_{it}^{\mathrm{fixed}} \qquad \forall i\in\mathcal{G} \tag{4d}$$

$$\Big\} \quad \forall t, \forall s.$$

Objective function (4a) represents total operation costs in real time operation. Constraint (4b) comprises the second-stage constraints. Constraints (4c) and (4d) fix the values of the complicating variables to given values obtained from the solution of the master problem. The formulation of the master problem is provided in the next subsection.

Reactive power constraints (3g) and voltage magnitude constraints (3j) are enforced in each subproblem (4), while similar constraints are not enforced in the master problem. Thus, the fixed values in (4c) and (4d) obtained from the master problem may make subproblems (4) infeasible. To prevent infeasibility, a number of non-negative slack variables are included in the reactive power and voltage magnitude constraints, along with penalties in the objective function (4a) [19], [21]. Thus, the always-feasible form of (4) is (5) below:

$$\Big\{\underset{\Xi_{ts}^{\mathrm{SP}}}{\text{Minimize}} \quad Z_{ts}^{(\nu)} = \sum_{i\in\mathcal{G}} C_i\ r_{its}^{(\nu)} + \sum_{d\in\mathcal{D}} V_d^{\mathrm{SH}} L_{dts}^{\mathrm{SH}^{(\nu)}} + \sum_{i\in\mathcal{G}} h^{\mathrm{Q}}\left(\underline{Q}_{its}^{\mathrm{aux}^{(\nu)}} + \overline{Q}_{its}^{\mathrm{aux}^{(\nu)}}\right) + \sum_{n} h^{\mathrm{v}}\left(\underline{v}_{nts}^{\mathrm{aux}^{(\nu)}} + \overline{v}_{nts}^{\mathrm{aux}^{(\nu)}}\right) \tag{5a}$$

$$\text{subject to}$$

$$(3a)-(3f),(3h),(3i),(3k)-(3m) \tag{5b}$$

$$\left(\underline{Q}_i - \underline{Q}_{its}^{\mathrm{aux}^{(\nu)}}\right) u_{it} \le Q_{its}^{(\nu)} \le \left(\overline{Q}_i + \overline{Q}_{its}^{\mathrm{aux}^{(\nu)}}\right) u_{it} \qquad \forall i\in\mathcal{G} \tag{5c}$$

$$\left(\underline{v}_n - \underline{v}_{nts}^{\mathrm{aux}^{(\nu)}}\right) \le v_{nts}^{(\nu)} \le \left(\overline{v}_n + \overline{v}_{nts}^{\mathrm{aux}^{(\nu)}}\right) \quad \forall n \tag{5d}$$

$$\underline{Q}_{its}^{\mathrm{aux}^{(\nu)}} \ge 0, \quad \overline{Q}_{its}^{\mathrm{aux}^{(\nu)}} \ge 0 \qquad \forall i\in\mathcal{G} \tag{5e}$$

$$\underline{v}_{nts}^{\mathrm{aux}^{(\nu)}} \ge 0, \quad \overline{v}_{nts}^{\mathrm{aux}^{(\nu)}} \ge 0 \qquad \forall n \tag{5f}$$

$$P_{it}^{\mathrm{DA}^{(\nu)}} = P_{it}^{\mathrm{DA,fixed}} \quad : \mu_{its}^{\mathrm{P}^{(\nu)}} \qquad \forall i\in\mathcal{G} \tag{5g}$$

$$u_{it}^{(\nu)} = u_{it}^{\mathrm{fixed}} \quad : \mu_{its}^{\mathrm{u}^{(\nu)}} \qquad \forall i\in\mathcal{G} \tag{5h}$$

$$\Big\} \quad \forall t, \forall s.$$

The optimization variables pertaining to each subproblem (5) are the elements of the set:

$$\Xi_{ts}^{\mathrm{SP}} = \{Z_{ts}^{(\nu)}, P_{it}^{\mathrm{DA}^{(\nu)}}, u_{it}^{(\nu)}, v_{nts}^{(\nu)}, \theta_{nts}^{(\nu)}, r_{its}^{(\nu)}, Q_{its}^{(\nu)}, W_{kts}^{\mathrm{SP}^{(\nu)}}, L_{dts}^{\mathrm{SH}^{(\nu)}}, \underline{Q}_{its}^{\mathrm{aux}^{(\nu)}}, \overline{Q}_{its}^{\mathrm{aux}^{(\nu)}}, \underline{v}_{nts}^{\mathrm{aux}^{(\nu)}}, \overline{v}_{nts}^{\mathrm{aux}^{(\nu)}}\}.$$

Note that $\underline{Q}_{its}^{\mathrm{aux}^{(\nu)}}$, $\overline{Q}_{its}^{\mathrm{aux}^{(\nu)}}$, $\underline{v}_{nts}^{\mathrm{aux}^{(\nu)}}$ and $\overline{v}_{nts}^{\mathrm{aux}^{(\nu)}}$ are non-negative slack variables, while h^{Q} and h^{v} are large enough positive constants.

Note also that u_{it} is a continuous variable in each subproblem (5), while it is a binary variable in the original problem (1)-(3) and the master problem (7). Thus, each subproblem (5) is continuous and non-linear.

The complicating variables are fixed through constraints (5g) and (5h), whose dual variables, $\mu_{its}^{\mathrm{P}^{(\nu)}}$ and $\mu_{its}^{\mathrm{u}^{(\nu)}}$, provide sensitivities to be used in building Benders' cuts for the master problem. These sensitivities are obtained as follows:

$$\mu_{it}^{\mathrm{P}^{(\nu)}} = \sum_{s} \rho_s\ \mu_{its}^{\mathrm{P}^{(\nu)}} \qquad \forall i\in\mathcal{G}, \forall t \tag{6a}$$

$$\mu_{it}^{\mathrm{u}^{(\nu)}} = \sum_{s} \rho_s\ \mu_{its}^{\mathrm{u}^{(\nu)}} \qquad \forall i\in\mathcal{G}, \forall t. \tag{6b}$$

In addition, the following value is calculated to be used in (6d) and master problem (7):

$$Z^{(\nu)} = \sum_{ts} \rho_s\ Z_{ts}^{(\nu)}. \tag{6c}$$

The upper bound for the optimal value of objective function of the original problem (1)-(3) at iteration ν is obtained as:

$$Z_{up}^{(\nu)} = Z^{(\nu)} + \sum_{(i\in\mathcal{G})t} \left[C_{it}^{\mathrm{SU,fixed}} + C_i P_{it}^{\mathrm{DA,fixed}}\right], \tag{6d}$$

where the value of $C_{it}^{\mathrm{SU,fixed}}$ is calculated using fixed values for u_{it}^{fixed}.

D. Master problem

The master problem corresponding to the original problem (1)-(3) is formulated as (7) below. All variables refer to Benders' iteration ν. The objective function (7a) corresponds to (1), where $\alpha^{(\nu)}$ represents the expected cost in real-time operation.

$$\underset{\Xi^{\mathrm{MP}}}{\text{Minimize}} \quad Z_{down}^{(\nu)} = \sum_{(i\in\mathcal{G})t} \left[C_{it}^{\mathrm{SU}^{(\nu)}} + C_i P_{it}^{\mathrm{DA}^{(\nu)}} \right] + \alpha^{(\nu)} \tag{7a}$$

subject to:

$$Z^{(\mathrm{j})} + \sum_{(i\in\mathcal{G})t} \mu_{it}^{\mathrm{P}^{(j)}} \left(P_{it}^{\mathrm{DA}^{(\nu)}} - P_{it}^{\mathrm{DA}^{(\mathrm{j})}} \right) + \sum_{(i\in\mathcal{G})t} \mu_{it}^{\mathrm{u}^{(j)}} \left(u_{it}^{(\nu)} - u_{it}^{(j)} \right) \leq \alpha^{(j)} \quad j = 1, ..., \nu-1 \tag{7b}$$

$$\alpha^{(\nu)} \geq \alpha^{\mathrm{down}} \tag{7c}$$

$$\text{(2a), (2c)} - \text{(2k)} \tag{7d}$$

$$P_{it}^{\mathrm{DA}^{(\nu)}} + \left[\max_s \; r_{its}^{(\nu-1)} \right] u_{it}^{(\nu)} \leq \overline{P}_i \; u_{it}^{(\nu)} \quad \forall i \in \mathcal{G}, \forall t \tag{7e}$$

$$P_{it}^{\mathrm{DA}^{(\nu)}} + \left[\min_s \; r_{its}^{(\nu-1)} \right] u_{it}^{(\nu)} \geq \underline{P}_i \; u_{it}^{(\nu)} \quad \forall i \in \mathcal{G}, \forall t. \tag{7f}$$

Master problem (7) is mixed-integer linear, and its optimization variables are the elements of the set:

$$\Xi^{\mathrm{MP}} = \{ Z_{down}^{(\nu)}, \theta_{nt}^{\mathrm{DA}^{(\nu)}}, C_{it}^{\mathrm{SU}^{(\nu)}}, P_{it}^{\mathrm{DA}^{(\nu)}}, W_{kt}^{\mathrm{DA}^{(\nu)}}, u_{it}^{(\nu)}, \alpha^{(\nu)} \}.$$

Constraints (7b) are Benders' cuts, which are generated one per iteration. Note that the feasibility cuts are not required in the master problem because always-feasible subproblems (5) are used within the proposed Benders' algorithm. This "trick" has proven to be computationally efficient. Constraint (7c) imposes a lower bound on $\alpha^{(\nu)}$ to accelerate convergence. Constraint (7d) enforce all first-stage constraints, except (2b). Instead of (2b), constraints (7e) and (7f) are included in the master problem to improve convergence. Note that $\max_s \; r_{its}^{(\nu-1)}$ and $\min_s \; r_{its}^{(\nu-1)}$ are parameters obtained from the solution of the subproblems in the previous iteration. In fact, in addition to the Benders' cuts (7b), constraints (7e) and (7f) further link the master problem and the subproblems.

The value of objective function (7a), i.e., $Z_{down}^{(\nu)}$, is a lower bound for the optimal value of the objective function of problem (1)-(3). The solution of the master problem (7) updates the values of complicating variables.

E. Benders' Algorithm

The proposed Benders' algorithm is as follows:

1) **Input:** a small tolerance ε to control convergence, and initial guesses of the complicating variables, $P_{it}^{\mathrm{DA}^0}$ and $u_{it}^0 \;\; \forall i \in \mathcal{G}, \forall t$.
2) **Initialization:** Set $\nu = 1$, $Z_{down}^{(\nu)} = -\infty$, $P_{it}^{\mathrm{DA,fixed}} = P_{it}^{\mathrm{DA}^0}$ and $u_{it}^{\mathrm{fixed}} = u_{it}^0 \;\; \forall i \in \mathcal{G}, \forall t$.
3) **Initial scenario:** Consider scenario $s = 1$.
4) **Initial time period:** Consider time period $t = 1$.
5) **Subproblem solution:** Solve (5) for scenario s and time period t and calculate $Z_{ts}^{(\nu)}$.
6) **Next time period:** Consider the next time period, and repeat step 5. If all time periods have been considered, go to the next step.
7) **Next scenario:** Consider the next scenario, and repeat steps 4 to 6. If all scenarios have been considered, go to the next step.
8) **Convergency check:** If $|Z_{up}^{(\nu)} - Z_{down}^{(\nu)}| \leq \varepsilon$, the optimal solution with a level of accuracy ε has been obtained. Otherwise, calculate $Z^{(\nu)}$ and the sensitivities to build the next Benders' cut. Then, set $\nu \longleftarrow \nu + 1$.
9) **Master problem solution:** Solve (7), calculate $Z_{down}^{(\nu)}$ and update the values of complicating variables. Then, continue in step 3.

The flowchart of the proposed Benders' algorithm is depicted in Fig. 2.

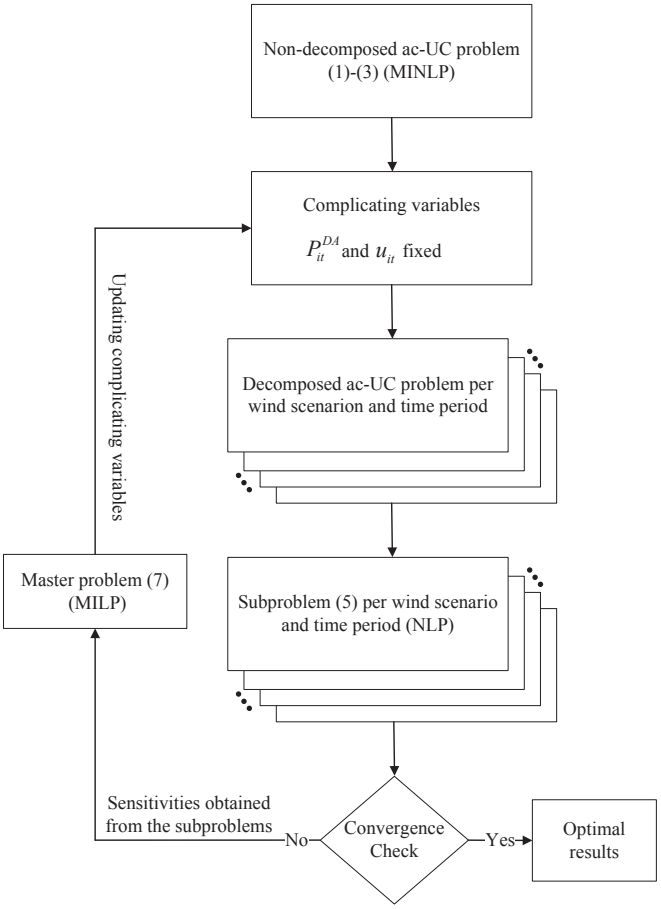

Fig. 2: Flowchart of the proposed Benders' algorithm.

IV. Case Study

This section presents numerical results for a case study based on the IEEE one-area 24-node reliability test system (RTS) [22]. In this study, a daily time horizon (time periods t_1 to t_{24}) is considered. Under the per-unit system used, 1 p.u. of power is equivalent to 100 MW.

TABLE I: Network data

Transmission line (n,m)	1-3	3-9	6-10	10-11	11-14	14-16
$\overline{S}_{nm}$ [p.u.]	2.3	1.6	2.5	3.0	2.3	2.1

A. Data

Network data $\overline{S}_{nm}$ are those reported in [22], except the ones given in Table I. In addition, data for generating units are given in Table II. Note that generating units 1, 2, 5 and 6 do not provide reserve. Note also that to highlight voltage issues, the synchronous condenser connected to node 14 in [22] is removed.

Hourly active and reactive loads are those given in [22] multiplied by the hourly load factors provided in Table III. Accordingly, time period t_{20} is the peak hour.

Two wind farms located at nodes 3 and 14 are considered, whose installed capacities are 2.85 p.u. and 2.96 p.u., respectively. Total wind capacity (i.e., 5.81 p.u.) is 13.71% of the total installed capacity (42.36 p.u.). The wind power production uncertainties are characterized through 40 scenarios, as illustrated in Fig. 3, whose upper plot corresponds to the farm located at node 3, and whose lower plot refers to the farm located at node 14. Note that each dot illustrates the wind production level of the corresponding farm for a given time period under a particular scenario. In other words, each scenario of any of the two plots contains 24 dots indicating the wind production levels of the corresponding farm over 24 time periods. These 40 scenarios have been derived from historical data, and accurately represent the uncertainty without making the considered problem computationally intractable. The corresponding probabilities (ρ_s) are given in Table IV. Based on the scenarios considered, the expected total wind power production over the 24 time periods is 1.72 p.u. (i.e., 29.60% of the total wind capacity).

The value of load shedding for all demands (V_d^{SH}) is considered 10000 \$/p.u. Finally, tolerance ε required for convergence check is set to 0.3% of the value of the objective function (expected cost).

B. Cases Considered

Three different cases are analyzed:

Case A) This case refers to a dc-UC problem, where both stages embody a dc representation of the network. This problem is directly solved using a mixed-integer linear solver.

Case B) This case refers to an ac-UC problem based on model (1)-(3) solved by the proposed Benders' algorithm. The voltage magnitude of each node is enforced to be within 0.9 p.u. and 1.1 p.u.

Case C) This case is similar to Case B, but constraints on the voltage magnitude of nodes are relaxed. In this case, the voltage magnitude of nodes can lie within 0.5 p.u. and 1.5 p.u. Although this case is not realistic, it is considered for illustrative purposes.

Table V mathematically characterizes the non-decomposed dc-UC problem (Case A), the non-decomposed ac-UC problem, and the decomposed ac-UC problem (Cases B and C).

TABLE II: Data for generating units

Unit (i)	node	$\underline{P}_i$ [p.u.]	$\overline{P}_i$ [p.u.]	$\underline{Q}_i$ [p.u.]	$\overline{Q}_i$ [p.u.]	R_i^{U}, R_i^{D} [p.u.]	R_i^{+}, R_i^{-} [p.u.]	C_i [$\frac{\$}{\text{p.u.}}$]	λ_i^{SU} [\$]	u_i^{ini}	P_i^{ini} [p.u.]	r_i^{ini} [p.u.]
1,2	1	0.100	0.200	0.00	0.10	0.000	0.100	1109	300	1	0.20	0.00
3,4	1	0.152	0.760	-0.25	0.30	0.100	0.500	1246	400	1	0.76	0.00
5,6	2	0.100	0.200	0.00	0.10	0.000	0.100	1109	300	1	0.20	0.00
7,8	2	0.152	0.760	-0.25	0.30	0.100	0.500	1246	400	1	0.76	0.00
9	7	0.800	3.500	-0.25	1.50	1.000	2.500	1720	100	0	0.00	0.00
10,11	7	0.150	1.000	0.00	0.60	0.550	0.850	1660	275	1	0.55	0.45
12-14	13	0.620	1.970	0.00	0.80	0.450	1.150	1408	300	1	1.97	0.00
15-19	15	0.024	0.120	0.00	0.06	0.096	0.096	2141	400	0	0.00	0.00
20	15	0.500	1.550	-0.50	0.80	0.450	1.000	1592	200	1	1.10	0.45
21	16	0.500	1.550	-0.50	0.80	0.450	1.000	1592	200	1	1.10	0.45
22	18	1.000	4.000	-0.50	2.00	1.500	2.800	1917	250	0	0.00	0.00
23	21	1.000	4.000	-0.50	2.00	1.500	2.800	1917	250	0	0.00	0.00
24-29	22	0.000	0.500	-0.10	0.16	0.150	0.500	0	100	1	0.50	0.00
30,31	23	0.500	1.550	-0.50	0.80	0.450	1.000	1592	200	1	1.10	0.45
32	23	0.800	3.500	-0.25	1.50	1.000	2.500	1720	100	0	0.00	0.00

TABLE III: Load factor corresponding to each time period

Time period	t_1	t_2	t_3	t_4	t_5	t_6	t_7	t_8	t_9	t_{10}	t_{11}	t_{12}
Load factor	0.75	0.70	0.65	0.60	0.62	0.63	0.65	0.68	0.70	0.72	0.75	0.78
Time period	t_{13}	t_{14}	t_{15}	t_{16}	t_{17}	t_{18}	t_{19}	t_{20}	t_{21}	t_{22}	t_{23}	t_{24}
Load factor	0.80	0.85	0.85	0.90	0.92	0.95	0.98	1.00	0.97	0.93	0.91	0.92

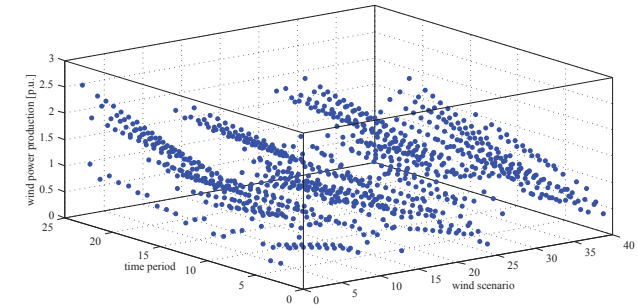

(a)

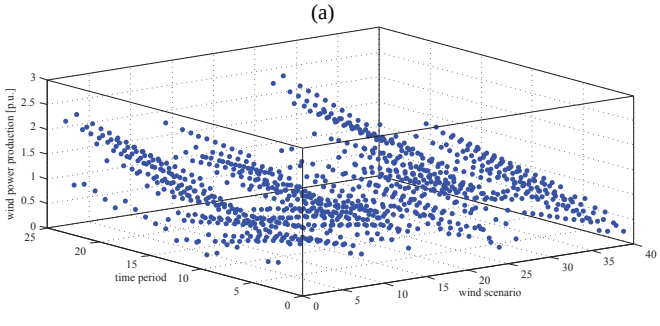

(b)

Fig. 3: Wind power scenarios of the farm (a) located at node 3, (b) and of that located at node 14.

Note that the non-decomposed dc-UC problem (Case A) includes the dc version of ac constraints (3), which is given in Appendix B as constraints (9).

The corresponding numerical results are given and analyzed in the next subsection.

TABLE V: The mathematical characteristics of each UC problem

Problem	Formulation	Type of optimization model	Binary variables included?	Available solver	Case
Non-decomposed dc-UC	Combination of (1), (2), and (9)	MILP[a]	Yes	CPLEX [23]	A
Non-decomposed ac-UC	Combination of (1), (2), and (3)	MINLP[b]	Yes	No off-the-shelf solver	-
Decomposed ac-UC	Benders' algorithm (depicted in Fig. 2) including subproblems (5) and master problem (7)	NLP[c] (subproblems)	No	CONOPT [24]	B and C
		MILP (master problem)	Yes	CPLEX [23]	

[a]Mixed-integer linear programming
[b]Mixed-integer non-linear programming
[c]Non-linear programming (continuous)

TABLE IV: The probability of each scenario (ρ_s)

s	ρ_s	s	ρ_s	s	ρ_s	s	ρ_s	s	ρ_s	s	ρ_s	s	ρ_s	s	ρ_s
s_1	0.01	s_6	0.03	s_{11}	0.05	s_{16}	0.01	s_{21}	0.03	s_{26}	0.01	s_{31}	0.02	s_{36}	0.03
s_2	0.01	s_7	0.03	s_{12}	0.05	s_{17}	0.01	s_{22}	0.04	s_{27}	0.01	s_{32}	0.02	s_{37}	0.03
s_3	0.01	s_8	0.03	s_{13}	0.01	s_{18}	0.02	s_{23}	0.04	s_{28}	0.01	s_{33}	0.02	s_{38}	0.04
s_4	0.02	s_9	0.04	s_{14}	0.01	s_{19}	0.02	s_{24}	0.05	s_{29}	0.01	s_{34}	0.02	s_{39}	0.04
s_5	0.02	s_{10}	0.04	s_{15}	0.01	s_{20}	0.03	s_{25}	0.05	s_{30}	0.01	s_{35}	0.02	s_{40}	0.04

TABLE VI: Numerical results for Cases A-C

	Expected cost [$]	CPU time [minute]
Case A	638537.8	70
Case B	651909.9	194
Case C	650368.9	159

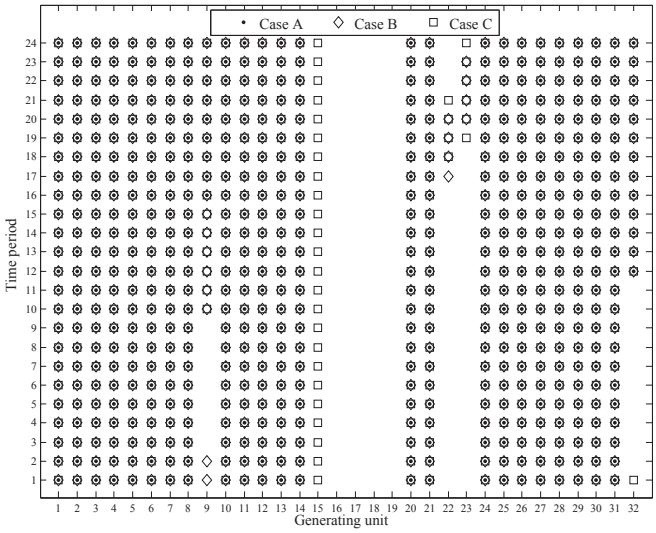

Fig. 4: Commitment status of the units for Cases A-C

C. Numerical Results

The expected cost, i.e., the value of objective function (1), for the three cases considered are given in the second column of Table VI. Additionally, the commitment status of the units are depicted in Fig. 4. Note that for all cases, neither load curtailment nor wind power spillage occurs.

According to Table VI and Fig. 4, the following observations are in order:

1) The expected cost in Case A (dc-UC problem) is comparatively smaller than that of Cases B and C (ac-UC problems). The reason of this is that the ac-UC problem enforces more realistic constraints than those of the dc-UC one. Also, the expected cost of Case B is comparatively higher than that of Case C, where voltage magnitude constraints are not tightly enforced.
2) The dc-UC and ac-UC problems yield different commitment status for the generating units. According to Fig. 4, generating units 22 and 23 are decommitted in Case A (dc-UC problem), while they are committed in peak hours of Case B (ac-UC problem). Similarly, generating unit 9 is committed in time periods 1 and 2 of Case B.
3) In addition to the commitment status of generating units, the dispatch results of committed units from the dc-UC and ac-UC formulations are different. For example in Cases A and B, generating unit 32 is scheduled in peak hour t_{20} 3.2 p.u. and 2.5 p.u., respectively.
4) The reason for these differences is the constraints that are not modeled in the dc-UC formulation (Case A), i.e., reactive power constraints (3g) and voltage magnitude constraints (3j). For example, the numerical results of Case B (ac-UC problem) illustrate that the voltage magnitudes of node 6 within different scenarios and time periods are mostly equal to its upper bound, i.e., 1.1 p.u. However, the results obtained by dc-UC model (Case A) misrepresents such constraint, since it does not consider the voltage magnitude bounds. In addition to constraints (3g) and (3j), power losses in the network is the other reason of differences, as it is modeled in the ac-UC problem (Case B), but it is not in the dc-UC problem (Case A).
5) According to Fig. 4, although both Cases B and C solve ac-UC problems, different bounds on voltage magnitude constraints (3j) render slightly different results. For example, the comparatively small generating unit 15 is fully committed in Case C, while it is fully decommitted in Case B. On the other hand, the comparatively large generating unit 9 is not committed in Case C for time periods t_1 and t_2, while it is in Case B. These differences allow concluding that the voltage magnitude constraint may potentially alter the commitment results.

Finally, Fig. 5 illustrates the evolution of Benders' algorithm in Case B (ac-UC problem). This algorithm converges in iteration 25, where the difference between $Z_{up}^{(\nu)}$ (upper curve) and

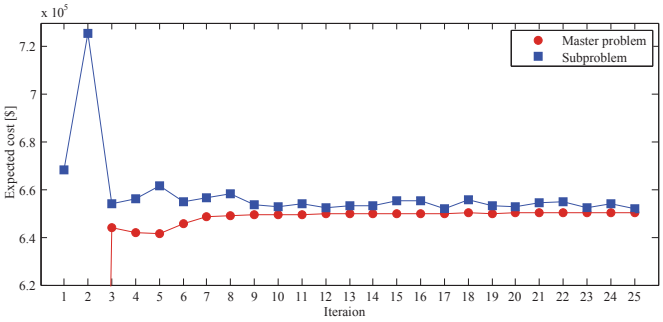

Fig. 5: Evolution of Benders' algorithm in Case B

$Z_{down}^{(\nu)}$ (lower curve) is smaller than the considered tolerance.

D. Computational, Optimality and Implementation Issues

Each subproblem (5) is solved using CONOPT [24] under GAMS [25], while the master problem (7) is solved using CPLEX 12.1 [23] under GAMS [25], both on a Sun Fire X4600M2 with 8 Quad-Core processors clocking at 2.9 GHz and 256 GB of RAM.

The following computational, optimality and implementation issues are in order:

- We report that we have verified the well-functioning of the heuristic technique explained in Section III-B. To this end, the expected cost for dc-UC problem is obtained using the proposed Benders' algorithm. Its difference with respect to that of Case A (the non-decomposed solution) is verified to be smaller than 0.2%.
- The computational times required for solving different instances are provided in the last column of Table VI. The computational time to solve Case B is comparatively higher. Note that both Cases B and C are solved iteratively, however the constraints of Case B are tighter. On the other hand, Case A is solved in a non-iterative way, thus its computational time is comparatively smaller.
- To speed-up convergence, suitable values for constants α^{down}, h^{Q} and h^{v} need to be derived. In this paper, the values considered are -10^8, 10^3 and 10^3, respectively, obtained through a try-and-error analysis. Note that too large values of constants h^{Q} and h^{v} may lead to convergence fluctuations, while comparatively small values may lead to infeasible solutions.
- Note that the original ac-UC problem (1)-(3) is non-convex, and since the number of scenarios cannot be increased beyond a limit to ensure computational tractability, the result obtained may not be a global optimal. To overcome such issue, a multi-start decomposition approach is used [26]. Accordingly, the proposed decomposition problem is solved several times considering diverse initial points, and finally the one leading to the smallest value for the objective function (1) is selected. Among the diverse initial solutions checked, the flat start, i.e., $\mathbf{v} = 1$ and $\boldsymbol{\theta} = 0$, shows the best performance.
- To assess the effect of the considered tolerance ε on the solution obtained, the proposed decomposition algorithm has been re-run considering a smaller value for ε, i.e., 0.1%. The total cost of operation has not significantly changed: \$651304.6 for ε=0.1% and \$651909.9 for ε=0.3% (Case B). However, the number of iterations required for the convergence of Benders' algorithm and therefore the CPU time increases significantly with ε=0.1%.
- Note that reducing the number of scenarios is computationally appropriate if decomposition techniques are not used, while a larger number of scenarios is generally better if decomposition techniques are used. It is important to note that using a larger number of scenarios generally results in higher accuracy.
- Note that in the decomposed cases considered (Cases B and C), the number of subproblems is 960 (40×24), being each of them comparatively small. The CPU time needed to solve each subproblem is about to 2% of the total time, which is reasonable. This means that the computational time may not significantly increase if a comparatively larger system is considered provided that the number of scenarios is reduced. However, to tackle case studies pertaining to real-world systems with thousands of nodes and lines and a large number of scenarios, the following additional alternatives are also available:
  - To use a supercomputer,
  - To implement parallelization techniques [27],
  - To apply appropriate techniques to simplify the network [28] and/or to reduce the number of scenarios [29],
  - To decompose the UC problem by area [30].

V. Conclusions

This paper proposes an efficient solution approach based on Benders' decomposition to solve a network-constrained ac-UC problem under uncertainty. The proposed approach allows decomposing such problem, which is mixed-integer non-linear and generally intractable, into a mixed-integer linear master problem and a set of non-linear but continuous subproblems, one per scenario and time period. Note that there is no off-the-shelf solver available for a MINLP problem, while MILP and NLP problems are both solvable using available commercial solvers. The numerical results obtained validate the well-functioning of the proposed approach.

We point out that the commitment status and dispatch results of generating units obtained by the dc and ac formulations might be different. The reasons for the differences are (i) the constraints that are not modeled in the dc-UC formulation, i.e., reactive power and voltage magnitude constraints, and (ii) power losses which are not considered in the dc-UC formulation. It is also pointed out that the tightness level of voltage magnitude constraint in the ac-UC problem may potentially alter the commitment results.

Appendix A

This appendix provides the functions used in this paper. Function $P_{nmt}^{\text{DA}}(\boldsymbol{\theta})$ used in equations (2a) and (2h) is mathematically formulated below:

$$P^{\mathrm{DA}}_{nmt}(\boldsymbol{\theta}) = \frac{1}{x_{nm}}\left(\theta^{\mathrm{DA}}_{nt} - \theta^{\mathrm{DA}}_{mt}\right) \quad \forall n, \forall m \in \Omega_n, \forall t. \tag{8a}$$

Functions $P_{nmts}(\mathbf{v}, \boldsymbol{\theta})$, $Q_{nmts}(\mathbf{v}, \boldsymbol{\theta})$ and $S_{nmts}(\mathbf{v}, \boldsymbol{\theta})$ used in equations (3a), (3b) and (3m) are mathematically formulated below:

$$P_{nmts}(\mathbf{v}, \boldsymbol{\theta}) = Y_{nm}[v^2_{nts}\cos(\phi_{nm}) - v_{nts}v_{mts} \cos(\theta_{nts} - \theta_{mts} - \phi_{nm})] \quad \forall n, \forall m \in \Omega_n, \forall t, \forall s \tag{8b}$$

$$Q_{nmts}(\mathbf{v}, \boldsymbol{\theta}) = -Y_{nm}[v^2_{nts}\sin(\phi_{nm}) + v_{nts}v_{mts} \sin(\theta_{nts} - \theta_{mts} - \phi_{nm})] \quad \forall n, \forall m \in \Omega_n, \forall t, \forall s \tag{8c}$$

$$S_{nmts}(\mathbf{v}, \boldsymbol{\theta}) = \sqrt{P^2_{nmts}(\mathbf{v}, \boldsymbol{\theta}) + Q^2_{nmts}(\mathbf{v}, \boldsymbol{\theta})} \quad \forall n, \forall m \in \Omega_n, \forall t, \forall s. \tag{8d}$$

APPENDIX B

The dc version of ac constraints (3) included in the non-decomposed dc-UC problem (Case A of Section IV-B) is provided below:

$$\sum_{i \in \mathcal{G}_n}(P^{\mathrm{DA}}_{it} + r_{its}) + \sum_{k \in \mathcal{K}_n}\left(W_{kts} - W^{\mathrm{SP}}_{kts}\right) - \sum_{d \in \mathcal{D}_n}(L^{\mathrm{P}}_{dt} - L^{\mathrm{SH}}_{dts}) = \frac{1}{x_{nm}}(\theta_{nts} - \theta_{mts}) \ \forall n, \forall t, \forall s \tag{9a}$$

$$(3c) - (3f), (3h), (3i), (3k), (3l) \tag{9b}$$

$$\frac{1}{x_{nm}}(\theta_{nts} - \theta_{mts}) \leq \overline{S}_{nm} \quad \forall n, \forall m \in \Omega_n, \forall t, \forall s. \tag{9c}$$

REFERENCES

[1] R. Baldick, "The generalized unit commitment problem," *IEEE Trans. Power Syst.*, vol. 10, pp. 465–475, Feb. 1995.

[2] F. Zhuang and F. D. Galiana, "Towards a more rigorous and practical unit commitment by Lagrangian relaxation," *IEEE Trans. Power Syst.*, vol. 3, pp. 763–773, May 1988.

[3] N. J. Redondo and A. J. Conejo, "Short-term hydro-thermal coordination by Lagrangian relaxation: solution of the dual problem," *IEEE Trans. Power Syst.*, vol. 14, pp. 89–95, Feb. 1999.

[4] A. J. Conejo, M. Carrión, and J. M. Morales, *Decision Making Under Uncertainty in Electricity Markets*. International Series in Operations Research & Management Science, New York, NY, USA: Springer, 2010.

[5] S. Takriti, J. R. Birge, and E. Long, "A stochastic model for the unit commitment problem," *IEEE Trans. Power Syst.*, vol. 11, pp. 1497–1508, Aug. 1996.

[6] P. Carpentier, G. Gohen, J.-C. Culioli, and A. Renaud, "Stochastic optimization of unit commitment: a new decomposition framework," *IEEE Trans. Power Syst.*, vol. 11, pp. 1067–1073, May 1996.

[7] J. M. Morales, A. J. Conejo, and J. Perez-Ruiz, "Economic valuation of reserves in power systems with high penetration of wind power," *IEEE Trans. Power Syst.*, vol. 24, pp. 900–910, May 2009.

[8] F. Bouffard, F. D. Galiana, and A. J. Conejo, "Market-clearing with stochastic security–Part I: Formulation," *IEEE Trans. Power Syst.*, vol. 20, pp. 1818–1826, Nov. 2005.

[9] F. Bouffard, F. D. Galiana, and A. J. Conejo, "Market-clearing with stochastic security–Part II: Case studies," *IEEE Trans. Power Syst.*, vol. 20, pp. 1827–1835, Nov. 2005.

[10] Q. Wang, J. Wang, and Y. Guan, "Price-based unit commitment with wind power utilization constraints," *IEEE Trans. Power Syst.*, vol. 28, pp. 2718–2726, Aug. 2013.

[11] A. Kalantari, J. F. Restrepo, and F. D. Galiana, "Security-constrained unit commitment with uncertain wind generation: The loadability set approach," *IEEE Trans. Power Syst.*, vol. 28, pp. 1787–1796, May 2013.

[12] A. Tuohy, P. Meibom, E. Denny, and M. O'Malley, "Unit commitment for systems with significant wind penetration," *IEEE Trans. Power Syst.*, vol. 24, pp. 592–601, May 2009.

[13] J. Wang, M. Shahidehpour, and Z. Li, "Security-constrained unit commitment with volatile wind power generation," *IEEE Trans. Power Syst.*, vol. 23, pp. 1319–1327, Aug. 2008.

[14] W. S. Sifuentes and A. Vargas, "Hydrothermal scheduling using Benders decomposition: Accelerating techniques," *IEEE Trans. Power Syst.*, vol. 22, pp. 1351–1359, Aug. 2007.

[15] Y. Fu, M. Shahidehpour, and Z. Li, "Security-constrained unit commitment with AC constraints," *IEEE Trans. Power Syst.*, vol. 20, pp. 1001–1013, May 2005.

[16] C. E. Murillo-Sanchez, R. D. Zimmerman, C. L. Anderson, and R. J. Thomas, "Secure planning and operations of systems with stochastic sources, energy storage, and active demand," *IEEE Transactions on Smart Grid*, vol. 4, pp. 2220–2229, Dec. 2013.

[17] J. Ostrowski, M. F. Anjos, and A. Vannelli, "Tight mixed integer linear programming formulations for the unit commitment problem," *IEEE Trans. Power Syst.*, vol. 27, pp. 39–46, Feb. 2012.

[18] S. Muller, M. Deicke, and R. W. De Doncker, "Doubly fed induction generator systems for wind turbines," *IEEE Ind. Appl. Mag.*, vol. 8, pp. 26–33, May 2002.

[19] A. J. Conejo, E. Castillo, R. Minguez, and R. Garcia-Bertrand, *Decomposition Techniques in Mathematical Programming: Engineering and Science Applications*. Heidelberg, Germany: Springer, 2006.

[20] D. P. Bertsekas and N. R. Sandell, "Estimates of the duality gap for large-scale separable nonconvex optimization problems," in *21st IEEE Conference on Decision and Control*, vol. 21, pp. 782–785, Dec. 1982.

[21] T. N. Santos and A. L. Diniz, "Feasibility and optimality cuts for the multistage Benders decomposition approach: Application to the network constrained hydrothermal scheduling," in *IEEE Power Energy Society General Meeting, 2009. PES '09*, pp. 1–8, July 2009.

[22] Reliability System Task Force, "The IEEE reliability test system-1996. a report prepared by the reliability test system task force of the application of probability methods subcommittee," *IEEE Trans. Power Syst.*, vol. 14, pp. 1010–1020, Aug. 1999.

[23] CPLEX, GAMS. The Solver Manuals. GAMS/CPLEX [Online]. Available: http://www.gams.com/, 2010.

[24] A. S. Drud, "GAMS/CONOPT. Bagsvaerd, Denmark: ARKI Consulting and Development," [Online]. Available: http://www.gams.com/, 1996.

[25] A. Brooke, D. Kendrick, A. Meeraus, R. Raman, and R. E. Rosenthal, "GAMS, a User's Guide. Washington, DC: GAMS Development Corp.," [Online]. Available: http://www.gams.com/, Dec. 1998.

[26] R. Mínguez, F. Milano, R. Zárate-Miñano, and A. J. Conejo, "Optimal network placement of SVC devices," *IEEE Trans. Power Syst.*, vol. 22, pp. 1851–1860, Nov. 2007.

[27] A. Papavasiliou and S. S. Oren, "Multiarea stochastic unit commitment for high wind penetration in a transmission constrained network," *Oper. Res.*, vol. 61, pp. 578–592, May 2013.

[28] X. Cheng and T. J. Overbye, "PTDF-based power system equivalents," *IEEE Trans. Power Syst.*, vol. 20, pp. 1868–1876, Nov. 2005.

[29] J. M. Morales, S. Pineda, A. J. Conejo, and M. Carrión, "Scenario reduction for futures market trading in electricity markets," *IEEE Trans. Power Syst.*, vol. 24, pp. 878–888, May 2009.

[30] A. Ahmadi-Khatir, A. J. Conejo, and R. Cherkaoui, "Multi-area unit scheduling and reserve allocation under wind power uncertainty," *IEEE Trans. Power Syst.*, vol. 29, pp. 1701–1710, July 2014.

Amin Nasri (S'11) received his M.Sc. degree in Electrical Engineering from Sharif University of Technology, Tehran, Iran, in 2008. He is currently pursuing the Erasmus Mundus Joint Doctorate in Sustainable Energy Technologies and Strategies (SETS) in the Division of Electric Power Systems, School of Electrical Engineering at KTH Royal Institute of Technology.

His research interests include power system operation, dynamics, stability and control, and FACTS.

S. Jalal Kazempour (S'08-M'14) received the B.Sc. degree in Electrical Engineering from University of Tabriz, Tabriz, Iran, in 2006, the M.Sc. degree from Tarbiat Modares University, Tehran, Iran, in 2009, and the Ph.D. degree from the University of Castilla-La Mancha, Ciudad Real, Spain, in 2013. He is currently a postdoctoral fellow at the Whiting School of Engineering, Department of Mechanical Engineering, Johns Hopkins University, Baltimore, MD, USA.

His research interests include electricity markets, optimization and its applications to energy systems.

Antonio J. Conejo (F'04) received the M.S. degree from MIT, Cambridge, Massachusetts, US, in 1987, and the Ph.D. degree from the Royal Institute of Technology, Stockholm, Sweden, in 1990. He is currently a full professor at The Ohio State University, Columbus, Ohio, US.

His research interests include control, operations, planning, economics and regulation of electric energy systems, as well as statistics and optimization theory and its applications.

Mehrdad Ghandhari (SM'14) received the M.Sc. and Ph.D. degrees in electrical engineering from Royal Institute of Technology (KTH), Stockholm, Sweden, in 1995, and 2000, respectively.

He is currently a full Professor at KTH. His research interests include power system dynamics, stability and control, and FACTS and HVDC systems.

Paper C1

Multi-Parameter Trajectory Sensitivity Approach To Analyze the Impacts of Wind Power Penetration on Power System Transient Stability

http : //www.cigre.org

AORC Technical meeting 2014

"No.1045"

Multi-parameter trajectory sensitivity approach to analyze the impacts of wind power penetration on power system transient stability

A. Nasri **H. Chamorro** **M. Ghandhari**
KTH Royal Institute of Technology
Sweden

SUMMARY

In the most real-world power systems, the share of wind power penetration in total installed generation capacity is rapidly increasing. This large-scale integration of wind power into an electric power system poses challenges to the power system operators and planners. One of the main challenges is to maintain sufficient margins for transient stability. High penetration of wind power causes reduction of the total kinetic energy stored in through rotating masses since wind generators are decoupled from the grid by power electronic converters, and therefore, cannot contribute to the inertia of the grid. The resulting reduction of grid inertia may cause higher risk of transient instability. In this paper, trajectory sensitivity analysis (TSA) technique is used to determine the impacts of decreasing inertia of different generating units on the transient stability of power system. Numerical results from IEEE 10-machine 39-bus test system demonstrate the usefulness of the proposed approach.

KEYWORDS

Trajectory Sensitivity Analysis (TSA) – Transient Stability – Inertia – Wind Power Generation – Critical Clearing Time (CCT)

1. Introduction

Over the last decade, the share of renewable energy resources in the generation portfolio of power systems has been significantly grown. Among those resources, the wind power is relatively cheap, and technologically mature. In the real-world power systems, wind generation is growing at the rate of 30% annually, and therefore, these resources will substitute gradually the conventional fuel-based generating units. This results in reduction of the total kinetic energy stored in power systems through rotating masses since wind generators are decoupled from the grid by power electronic converters, and cannot contribute to the inertia of the grid. The resulting reduction of grid inertia may cause higher risk of transient instability. This papers aims to analyze the impacts of inertia reduction on the transient stability of power system.

Assessment of transient stability is essential to study the dynamic behavior of the power system. Time domain simulation is the traditional way for transient stability assessment which has two main disadvantageous: (i) time-consuming computation requirement and (ii) incapability to provide any information regarding the stability margin [1]. The other method which has been widely used for this purpose is transient energy function (TEF) method [2, 3]. The significant advantage of this method is its capability to provide a stability index [1]. However, despite all the advantages of the TEF based methods, the main shortcoming of them is their high complexity after considering differential-algebraic equation (DAE) models of power systems, dealing with the detailed models of the system's components, taking into account a number of system's parameters for the sensitivity analysis [4]. Applications of trajectory sensitivity analysis (TSA) have been introduced as an alternative to overcome the mentioned shortcoming of the TEF based method [5]. Using TSA, it is possible to calculate the sensitivity of power system trajectories with respect to some system parameters, e.g., reactances of transmission line, mechanical power and inertial of generators, and to determine how effective a certain parameter is for the transient stability enhancement. Reference [6] uses TSA to calculate the critical values of some power system parameters, e.g., fault clearing time and mechanical input power of generators. In [7], trajectory sensitivities of rotor angles of generators are calculated with respect to the reactances of different transmission lines in order to find the most suitable placement of series compensators for improving transient stability of power system.

In the technical literature, there are some works focusing on the impacts of large-scale integration of wind power on the transient stability. Reference [8] uses extended equal area criterion approach, and considers different wind power generator models as well as different penetration level to study the characteristic of power transient stability for large scale wind power integration. The detailed models of onshore and offshore wind farms are provided in [9] in order to evaluate transient stability of the system through iterative time-domain simulation.

There are also some limited works in the literature studying the impact of inertia variation on the system stability. An eigenvalue sensitivity analysis with respect to the inertia of generators is carried out in [10] in order to determine the impacts of increased penetration of wind generation on small signal stability of power system. However, there is no sensitivity-based analysis focusing on the transient stability of a power system with high amount of wind power generation.

In this paper, trajectory sensitivity analysis (TSA) technique is used to determine the impacts of reducing inertia of different generating units on the transient stability. In this vein, the trajectory sensitivities of the rotor angles with respect to the inertia of generators are calculated in the presence of the most severe disturbances. An equivalent rotor angle is introduced depending if the rotor angles of generators are accelerating or decelerating after the event of fault. A methodology is proposed based on the trajectory sensitivities of this equivalent angle in order to determine how reducing the inertia of generators, which can be the result of providing electrical power from wind generator instead of the conventional resources, affects the transient stability. Numerical results from IEEE 9-machine 39-bus test system demonstrate the usefulness of the proposed method.

2. Trajectory sensitivity analysis

Power systems can be modeled by the following differential algebraic equations [11]

$$\begin{aligned} \dot{x} &= f(x, y; \lambda) \\ 0 &= g(x, y; \lambda) \end{aligned} \tag{1}$$

$$\mathrm{x}(\mathrm{t}_0) = x_0, \quad y(t_0) = y_0 \tag{2}$$

where x is a vector containing the dynamic states, y is a vector of algebraic states and λ is a vector of system parameters. Vectors x_0 and y_0 are the initial conditions of dynamic and algebraic states. Function f is the set of differential equations which model dynamics of equipments such as generators. The algebraic equations g consist of the network equations based on Kirchhoff's current law, i.e. the sum of all current (or powers) flowing into each bus must be equal to zero. To write the equations in a more organized way, vectors of $\underline{x}$ and $\underline{f}$ are defined as follows

$$\underline{x} = \begin{bmatrix} x \\ \lambda \end{bmatrix} \qquad \underline{f} = \begin{bmatrix} f \\ 0 \end{bmatrix} \tag{3}$$

And therefore,

$$\begin{aligned} \dot{\underline{x}} &= f(\underline{x}, y) \\ 0 &= g(\underline{x}, y) \end{aligned} \tag{4}$$

To calculate the trajectory sensitivities, the derivatives of (4) are calculated with respect to $\underline{x}_0$

$$\begin{aligned} \dot{\underline{x}}_{\underline{x}_0} &= \underline{f}_{\underline{x}}(t)\underline{x}_{\underline{x}_0} + \underline{f}_y(t) y_{\underline{x}_0} \\ 0 &= g_{\underline{x}}(t)\underline{x}_{\underline{x}_0} + g_y(t) y_{\underline{x}_0} \end{aligned} \tag{5}$$

The initial conditions for set of equation (5) obtained by differentiating (2) with respect to $\underline{x}_0$

$$\dot{\underline{x}}_{\underline{x}_0}(t_0) = I, \qquad y_{\underline{x}_0}(t_0) = (g_y(t_0))^{-1} g_{\underline{x}}(t_0) \tag{6}$$

To find the trajectory sensitivities, the DAEs (4) and (5) are solved simultaneously with the initial conditions described using trapezoidal numerical integration approach [11].

3. Transient stability assessment using trajectory sensitivity analysis

The result of transient instability appears in the form of increasing rotor angles of some generators which leads to their loss of synchronism with other generators. So, it is possible to use the dynamic trajectory of the rotor angles of generator to analyse the transient stability of the system. Since this study is focusing on the reduction of the effective inertia of the system after high penetration of wind power, the inertia of generators are selected as the system parameters to be considered in the sensitivity analysis. Note that to assess the transient stability in the presence of wind farms, trajectory sensitivity of rotor angle of generator i, δ_i, with respect to inertia of generator j, H_j, is calculated. Equations (7) and (8) show power system parameters considered in this study and trajectory sensitivities of dynamical states to such parameters as described above.

$$\lambda = [H_1 ... H_j ... H_n] \tag{7}$$

$$\frac{\partial \delta}{\partial \lambda}=\begin{bmatrix} \frac{\partial \delta_1}{\partial H_1} \cdots \frac{\partial \delta_1}{\partial H_j} \cdots \frac{\partial \delta_1}{\partial H_n} \\ \bullet \quad \bullet \quad \bullet \\ \frac{\partial \delta_i}{\partial H_1} \cdots \frac{\partial \delta_i}{\partial H_j} \cdots \frac{\partial \delta_i}{\partial H_n} \\ \bullet \quad \bullet \quad \bullet \\ \frac{\partial \delta_n}{\partial H_1} \cdots \frac{\partial \delta_n}{\partial H_j} \cdots \frac{\partial \delta_n}{\partial H_n} \end{bmatrix} \tag{8}$$

Where H_j and δ_i are inertia and rotor angle of generator j and i, respectively, n is the number of generating units, and λ s the vector of system parameters. Note also that, in a large scale power system, it is very time-consuming to check all the rotor angles of generators in order to assess the transient stability of the system. Hence, an equivalent angle is introduced to simplify evaluation of the transient stability. To define this angle, generators are separated to two groups A and B depending if their rotor angles (δ) after fault occurrence are accelerating or decelerating, respectively. Note that the rotor angles of generators are plotted in the center of inertia (COI) reference. Then, these two groups are replaced by a single machine equivalent system. The equivalent angle δ_{eq} includes all the rotor angles and is defined as follows

$$M_A=\sum_{i\in A} M_i, \quad M_B=\sum_{i\in B} M_i \tag{9}$$

$$\delta_A=M_A^{-1}\sum_{i\in A} M_i\delta_i, \quad \delta_B=M_B^{-1}\sum_{i\in B} M_i\delta_i \tag{10}$$

$$\delta_{eq}=\delta_A-\delta_B \tag{11}$$

According to this definition, the trajectory sensitivity of this equivalent angle to the inertia of generators is as follows:

$$\frac{\partial \delta_{eq}}{\partial H_j}=\frac{\partial \delta_A}{\partial H_j}-\frac{\partial \delta_B}{\partial H_j} \tag{12}$$

Where

$$\frac{\partial \delta_A}{\partial H_j}=M_A^{-1}\sum_{i\in A} M_i\frac{\partial \delta_i}{\partial H_j}, \quad \frac{\partial \delta_B}{\partial H_j}=M_B^{-1}\sum_{i\in A} M_i\frac{\partial \delta_i}{\partial H_j} \tag{13}$$

Finally, a normalized index of trajectory sensitivity ($\hat{S}_{zl}$) is defined which shows the impact of inertia reduction of generator j on the transient stability of the system corresponding to fault z:

$$\hat{S}_{zj}=\frac{S_{zj}}{\overline{S}_z} \quad \forall j\in G, \ \ \forall z\in Z \tag{14}$$

$$S_{zj}=\overset{pp}{\max}\left(\frac{\partial \delta_{eq}}{\partial H_j}\right) \quad \forall j\in G, \ \forall z\in Z \tag{15}$$

Where z is the index of fault; j is the index of generator; Z is the set of faults under study; G is the set of generators; S_{zj} is the index of trajectory sensitivity corresponding to the inertia of generator j and fault z, $\overline{S}_z$ is the maximum value of S_{zj} among all the generators for fault z and $\overset{pp}{\max}(\cdot)$ gives the first-swing peak to peak value of a function.

4. Simulation results

The IEEE 10-machine 39-bus test systems is used for simulation. Fig. 1 shows the single line diagram of this test system. The system data is taken from [12]. All the generators are represented by the classical model.

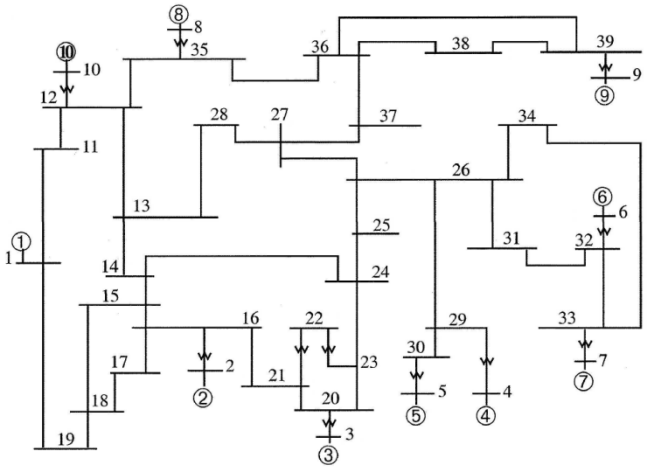

Figure 1. IEEE 10-machine 39-bus test system

Table 1 shows the list of faults selected to be applied to this test system.

Table 1. List of selected faults

Name	Fault location	Clearing time (CT) (ms)
Fault *z=1*	Line 33-34 close to bus 34	195
Fault *z=2*	Line 38-39 close to bus 39	125
Fault *z=3*	Line 15-16 close to bus 16	202

When a fault occurs in the system, if the system remains stable, the rotor angles of generators begin to oscillate around the post-fault operating point. In order to analyze the first-swing transient stability assessment, generators are divided to two transient groups *A* and *B* as mentioned in Section. 3. Fig. 2 depicts the rotor angles of the generators in the COI reference when Fault *z=1* occurs. It is obvious from first swing of the oscillations that the rotor angle of generator *i=1* is decelerating while the rotor angle of other generators are accelerating. Hence, generator *i=1* is placed in group *A* while the rest form group *B*. After this classification, the equivalent angle δ_{eq} is obtained according to (11), and plotted as well, see Fig. 2. The next step is to calculate the trajectory sensitivities of this equivalent angle, based on (12), with respect to the inertia of different generators. Fig. 3 shows such sensitivities after Fault *z=1* happens. As it can be seen from this figure, the generators *j=7, 6, 5, 4, 9, 3, 2* and *8* have the most negative indices of trajectory sensitivity (S_{zj}), respectively, while the generator *j=1* has a positive value for such an index. Equation (15) can explicitly explain how these sensitivities can be used for transient stability assessment.

$$\Delta\delta_{eq} \cong \left(\frac{\partial\delta_{eq}}{\partial H_j}\right)\Delta H_j \qquad (15)$$

In case of Fault *z=1*, it is observed from Fig. 2 that δ_{eq} is drastically increasing, and if it violates a certain limit, the system becomes unstable. In order to improve the transient stability, the steep slope of increasing δ_{eq} should be reduced, i.e., $\Delta\delta_{eq}$ should be negative. According to (15), to have a negative value of $\Delta\delta_{eq}$, $\partial\delta_{eq} / \partial H_i$ should be positive if ΔH_j is negative (reduction of inertia), and vice versa.

Accordingly, inertia reduction of generators *j=7, 6, 5, 4, 9, 3, 2* and *8* have the worst impact on the transient stability, respectively, while such a reduction in generator *j=1* improves the transient stability of this test system corresponding to *z=1*. The same analysis has been carried out for another two severe faults described in Table 1, and the normalized indices of trajectories sensitivities introduced by

(14) are obtained and given in Table 2. Each row of the Table is related to one fault, and shows the trajectory sensitivities of the equivalent rotor angle with respect to the inertia of different generators.

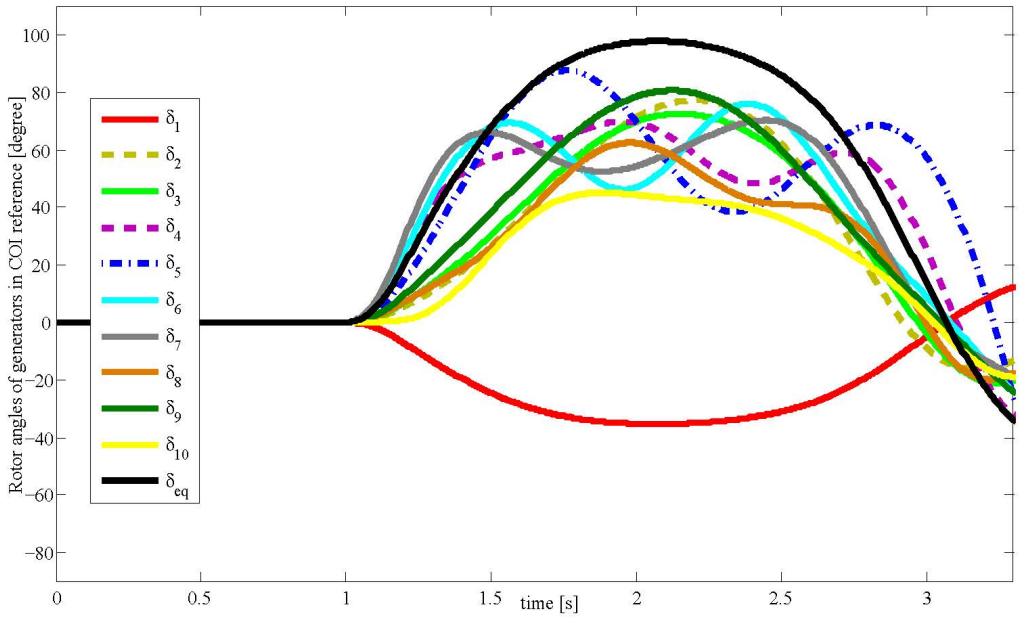

Figure 2. Rotor angles of the generators and the equivalent angle (δ_{eq})- Fault *z=1*

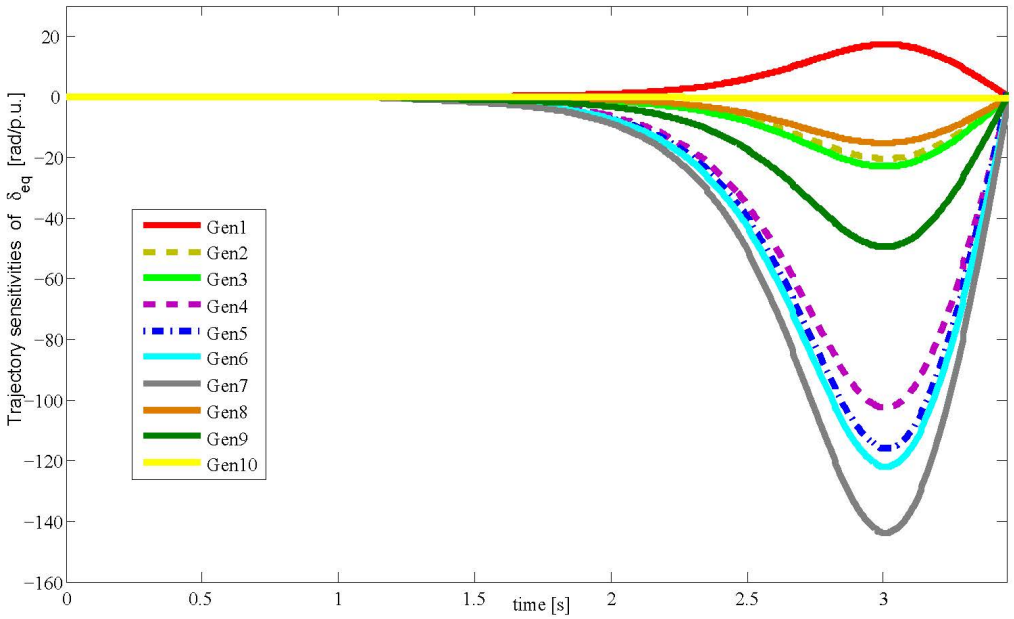

Figure 3. Trajectory sensitivities of δ_{eq} to the inertia of generators- Fault *z=1*

Table 2. Normalized indices of trajectory sensitivities $\hat{S}_{zj}$

$\hat{S}_{zj}$	Gen *j=1*	Gen *j=2*	Gen *j=3*	Gen *j=4*	Gen *j=5*	Gen *j=6*	Gen *j=7*	Gen *j=8*	Gen *j=9*	Gen *j=10*
z=1	0.1200	-0.1420	-0.1601	-0.7129	-0.8067	-0.8485	-1.0000	-0.1064	-0.3446	-0.0032
z=2	0.0053	0.0224	0.0235	0.0292	0.0307	0.0301	0.0300	0.0102	-1.0000	0.0268
z=3	0.0600	-1.0000	-0.5457	-0.1499	-0.1759	-0.1404	-0.1451	-0.0569	-0.1304	-0.0047

To verify the results, commercial software, SIMPOW®11, is used to simulate the test system after inertia reduction. The new critical clearing times of the selected faults after a fixed reduction of inertia in different generators are calculated, and given in Table 3. The new CCTs are precisely matching the

sensitivity values provided in Table 2. For instance, in case of Fault *z=1*, the inertia reduction of generator *j=1* improves slightly the transient stability while the same reduction in the other generators worsen the transient stability. Additionally, the obtained results show that reducing the inertia does not always worsen the transient stability while the general belief is the opposite.

Table 3. New CCTs of the selected faults after inertia reduction of different generators

tcc^{new}	Gen *j=1*	Gen *j=2*	Gen *j=3*	Gen *j=4*	Gen *j=5*	Gen *j=6*	Gen *j=7*	Gen *j=8*	Gen *j=9*	Gen *j=10*
z=1	198	193	193	182	181	181	177	194	189	195
z=2	126	126	126	126	126	126	126	126	100	126
z=3	203	173	186	198	198	198	198	201	199	201

4. Conclusion

In this paper, a sensitivity based analysis has been carried out to find the impacts of inertia reduction of generators on the transient stability of the power system. The inertia reduction can be the result of penetrating high amount of wind power into the power system. Trajectory sensitivity analysis technique has been used to calculate the dynamic sensitivities of equivalent rotor angles of the system with respect to the inertia of generators. It has been shown that the inertia reduction does not always cause transient stability deterioration. Depending of the type and location of the disturbance and also the location of inertia reduction, the transient stability is either improved or weaken. The future study is to consider both the mechanical power and inertia of the generators in the sensitivity analysis, and also to consider the detailed model of wind power for verification of the results.

5. References

[1] G.A. Maria, C. Tang, J. Kim, Hybrid transient stability analysis [power systems], IEEE Transactions on Power Systems 5 (1990) 384–393.

[2] A.A. Fouad, S.E. Stanton, Transient stability of a multi-machine power system. Part II. Critical transient energy, Power Engineering Review PER-1 (1981)3417–3424.

[3] T. Athay, P. Podmore, S. Virmani, A practical method for the direct analysis of transient stability, IEEE Transactions on Power Apparatus and Systems PAS-98(1979) 573–584.

[4] A. Zamora-Cardenas, C.R. Fuerte-Esquivel, Multi-parameter trajectory sensitivity approach for location of series-connected controllers to enhance power system transient stability, Electric Power Systems Research 80 (2010)1096–1103.

[5] M.J. Laufenberg, M.A. Pai, A new approach to dynamic security assessment using trajectory sensitivities, IEEE Transactions on Power Systems 13 (1998)953–958.

[6] D.Z. Fang, Q. Yi-fei, A new trajectory sensitivity approach for computations of critical parameters, Electric Power Systems Research 77 (2007) 303–307.

[7] A. Nasri, R. Eriksson and M. Ghandhari, Using trajectory sensitivity analysis to find suitable locations of series compensators for improving rotor angle stability, Electric Power System Research, in press.

[8] Y. Chen, G. James, X. Yusheng and F. Zue, Impacts of large scale wind power on power system transient stability, International conference on Electric Utility Deregulation and Restructuring and Power Technologies (DRPT) 277 – 283.

[9] C. Liu, Z. Che, C. Leth Bak, Z. Liu, P. Lund and P. Rønne-Hansen, Transient Stability Assessment of Power System with Large Amount of Wind Power Penetration: the Danish Case Study, IPEC conference on power and energy 461 – 467.

[10] T. Athay, P. Podmore, S. Virmani, Impact of increased penetration of DFIG-based wind turbine generators on transient and small signal stability of power systems, IEEE Transactions on Power System, Volume 24, 1426–1434.

[11] I.A. Hiskens, M.A. Pai, Trajectory sensitivity analysis of hybrid systems, IEEE Transactions on Power System 47 (2000) 204–220.

[12] M.A. Pai, Energy Function Analysis for Power System Stability, Kluwer Academic Publishers, Boston/Dordrecht/London, 2007.

Paper C2

Suitable Placements of Multiple FACTS Devices to Improve the Transient Stability Using Trajectory Sensitivity Analysis

Suitable Placements of Multiple FACTS Devices to Improve the Transient Stability Using Trajectory Sensitivity Analysis

Amin Nasri
Electric Power System Department
KTH Royal Institute of Technology
Stockholm, Sweden
Email: amin.nasri@ee.kth.se

Robert Eriksson
Electric Power System Department
KTH Royal Institute of Technology
Stockholm, Sweden
Email: robert.eriksson@ee.kth.se

Mehrdad Ghandhari
Electric Power System Department
KTH Royal Institute of Technology
Stockholm, Sweden
Email: mehrdad.ghandhari@ee.kth.se

***Abstract*—Trajectory sensitivity analysis (TSA) is used as a tool for suitable placement of multiple series compensators in the power system. The goal is to maximize the benefit of these devices in order to enhance the transient stability of the system. For this purpose, the trajectory sensitivities of the rotor angles of the most critical generators with respect to the reactances of transmission lines are calculated in the presence of the most severe faults. Based on the obtained trajectory sensitivities, a method is proposed to determine how effective the series compensation of each transmission line is for improving the transient stability. This method is applied to the Nordic-32 test system to find the priorities of the transmission lines for installation of several series compensators. Simulation with industrial software shows the validity and efficiency of the proposed method.**

I. Introduction

Transient stability is the ability of power system to keep its synchronism when a large disturbance, such as three phase short circuit, occurs in the system. Nowadays, deregulation in electricity markets, increasing electricity demands and high penetration of renewable energy sources on one hand and economic and environmental constraints on installing new transmission lines and building new power plants on the other hand, have pushed the existing transmission systems to be operated close to their critical conditions. So, there is a higher risk of transient instability in today's heavy-loaded and interconnected power systems.

Series Flexible AC Transmission Systems (FACTS) devices such as Thyristor Controlled Series Compensation (TCSC) can have a significant impact on operational flexibility and controllability of the power system. They can dynamically change the total reactance of transmission lines and control the power flow through lines in a way to increase the transient stability margins and make the system more secure. Since the impact of these compensators on the system's stability is strongly dependent on their locations, there is a great need for developing an analytical tool to provide useful information to the system planners regarding the best possible installation locations of them. In this paper, an effective tool is developed to identify the most suitable placement of multiple series compensators for improving transient stability.

Assessment of rotor angle stability is essential to study the dynamic behaviour of the power system. Time domain simulation is the traditional way for transient stability assessment which has two main disadvantages, namely time-consuming computation requirement and incapability to provide any information regarding the stability margin [1]. The other method which has been widely used for this purpose is transient energy function (TEF) method, see [2], [3], and [4]. The significant advantage of this method is its capability to provide a stability index [1]. Several methodologies have been proposed based on the sensitivity of TEF to determine the effectiveness of FACTS devices to improve system's transient stability, see [5], and [6]. Despite all the advantages of the TEF based methods, the main shortcoming of them is their high complexity in the following situations: (i) considering differential-algebraic equation (DAE) models of power systems, (ii) dealing with the detailed models of the system's components, (iii) when a number of system's parameters have to be taken into account for the sensitivity analysis [7].

Applications of trajectory sensitivity analysis (TSA) have been introduced as an alternative to overcome the mentioned shortcoming of the TEF based method [8]. Reference [9] has used TSA to calculate the critical values of some power system's parameters such as fault clearing time, mechanical input power of generators, etc. Their method is based on the computation of the norm of trajectory sensitivities of rotor angles and speeds of generators with respect to the parameters of interest. Reference [10] has discussed the application of TSA to power systems containing series and shunt compensators. A transient stability index has been introduced based on the numerical formulation of TSA and has been calculated for the power system with different locations of series and shunt compensators. Using numerical formulation of TSA, considering the compensators' models in the study and simulating the power system for all the possible locations of compensators has caused high computational burden in their proposed method. Reference [7] has developed a multi-parameter trajectory sensitivity approach to find the best locations of series compensators in order to improve

978-1-4799-1255-1/13/$31.00 ©2013 IEEE

the transient stability. An index of proximity to instability has been determined based on the norm of the trajectory sensitivities of the rotor angles and the speeds of generators with respect to the transmission line susceptances. Using the analytical formulation of TSA in the last mentioned paper and also in the current article, the cumbersome computational process becomes much simpler compared to the methodologies based on the numerical estimation of TSA. The latter will be explained later.

In this paper, a novel method is proposed based on TSA to determine the most appropriate places of series compensations to amend the transient stability of power system. Trajectory sensitivities of the rotor angles of critical generators are computed directly to the reactance of different transmission lines considering the most severe contingencies. The obtained sensitivity curves show perfectly the effect of each transmission line's reactance on the rotor angle's trajectory of each generator, and can be used to identify the the most effective locations to install series compensators for transient stability improvement. The proposed methodology also shows why putting series compensator in one transmission line has a positive and in the other line has a negative effect on the system's stability. The way to carry out the multiple placement is coordinated since the previously installed FACTS devices are considered for each new compensator's allocation. Finally, the authors believe that the proposed method is computationally efficient since analytical formulation of TSA are used and suitable system's parameters are chosen. The system under considerations is Nordic-32 test system.

II. Power system modeling and trajectory sensitivity analysis

As explained comprehensively by [11], power systems can be modeled by the following differential algebraic equations

$$\dot{\underline{x}} = \underline{f}(\underline{x}, y) \tag{1}$$

$$0 = \begin{cases} g^-(\underline{x}, y) & s(\underline{x}, y) < 0 \\ g^+(\underline{x}, y) & s(\underline{x}, y) > 0 \end{cases} \tag{2}$$

$$\underline{x} = \begin{bmatrix} x \\ \lambda \end{bmatrix} \qquad \underline{f} = \begin{bmatrix} f \\ 0 \end{bmatrix} \tag{3}$$

$$\underline{x}(t_0) = \underline{x}_0, \; y(t_0) = y_0 \tag{4}$$

where x is a vector containing the dynamic states, y is a vector of algebraic states and λ is a vector of system parameters. Rotor angles of the generators (δ), magnitude and angle of bus voltages and reactances of the transmission lines are the examples of the dynamic states, algebraic states and parameters of the power system, respectively. x_0 and y_0 are the initial conditions of dynamic and algebraic states. Function f is the set of differential equations which model the dynamics of equipments such as generators. Events such as a three phase short circuit fault occurs when $s(\underline{x}, y) = 0$. The algebraic equations g consist of the network equations based on Kirchhoff's current law, i.e. the sum of all current (or powers) flowing into each bus must be equal to zero, g^- and g^+ show the algebraic equations before and after occurrence of events.

To calculate the trajectory sensitivities analytically, the derivatives of (1), (2) are calculated with respect to $\underline{x}_0$

$$\dot{\underline{x}}_{\underline{x}_0} = \underline{f}_{\underline{x}}(t)\underline{x}_{\underline{x}_0} + \underline{f}_y(t)y_{\underline{x}_0} \tag{5}$$

$$0 = g_{\underline{x}}(t)\underline{x}_{\underline{x}_0} + g_y(t)y_{\underline{x}_0} \tag{6}$$

The system is assumed to be away from the events. The initial conditions for $\underline{x}_{\underline{x}_0}$ and $y_{\underline{x}_0}$ are obtained by differentiating (4) with respect to $\underline{x}_0$. It is clear that the initial value for the trajectory sensitivities of dynamic states is an identity matrix. Using this identity matrix, the initial values for the trajectory sensitivities of algebraic states can be also computed from (6).

$$\underline{x}_{\underline{x}_0}(t_0) = I, \quad y_{\underline{x}_0}(t_0) = -(g_y(t_0))^{-1} g_{\underline{x}_0}(t_0) \tag{7}$$

$\underline{f}_{\underline{x}}$, $\underline{f}_y$, $g_{\underline{x}}$ and g_y are time varying functions which are calculated along the system trajectories. When an event occurs in the system, jump condition should be derived for computation of the trajectory sensitivities which is fully described by [11]. To find the trajectory sensitivities, the DAEs (1)-(2) and (5)-(6) will be solved simultaneously with the initial conditions described above using trapezoidal integration technique.

To calculate the trajectory sensitivity of state variable x to the parameter λ with a numerical formulation of TSA, a small perturbation of $\triangle\lambda$ over the nominal parameter λ_0 should be considered such that $\lambda = \lambda_0 + \triangle\lambda$. So, the numerical estimation of sensitivity is defined as

$$x_\lambda = \frac{x(\lambda) - x(\lambda_0)}{\triangle\lambda} \tag{8}$$

III. Transient stability assessment using trajectory sensitivity analysis

The result of transient instability appears in the form of increasing rotor angles of some generators which leads to their loss of synchronism with other generators. So, monitoring angular swings of generators (dynamic states δ) could be one way to check the transient stability. To improve the transient stability, power system parameters can be controlled (if applicable) in a way to have positive effects on the variation of rotor angles of generators when the system is subjected to a fault and prevent power system from being unstable. Reactance of transmission line is one of these parameters which can have a considerable effect on the stability of power system with controlling power flows in the transmission lines. Nowadays with the presence of FACTS devices, it is possible to control the reactance of transmission lines and improve transient stability of power system. Due to heavy cost of these devices, it is not economical to install several series compensators in a power system, and instead, the optimal locations for installation of these devices should be determined. In this paper, TSA is used to determine the trajectory sensitivities of rotor angles of generators to the reactances of transmission lines. So, the matrices of power system parameters and trajectory sensitivities of dynamical states for this study are as follows

$$\lambda = [x_{L_1} x_{L_j} ... x_{L_{n_l}}] \tag{9}$$

$$\frac{\partial \delta}{\partial \lambda} = \begin{bmatrix} \frac{\partial \delta_1}{\partial x_{L_1}} & \frac{\partial \delta_1}{\partial x_{L_k}} & \cdots & \frac{\partial \delta_1}{\partial x_{L_{n_l}}} \\ \frac{\partial \delta_2}{\partial x_{L_1}} & \frac{\partial \delta_2}{\partial x_{L_k}} & \cdots & \frac{\partial \delta_2}{\partial x_{L_{n_l}}} \\ . & . & . & . \\ . & . & . & . \\ . & . & . & . \\ \frac{\partial \delta_n}{\partial x_{L_1}} & \frac{\partial \delta_n}{\partial x_{L_k}} & \cdots & \frac{\partial \delta_n}{\partial x_{L_{n_l}}} \end{bmatrix} \tag{10}$$

where δ_i is the rotor angle of the i^{th} generator, n is the number of generators, x_{L_k} is the reactance of the $\mathrm{k^{th}}$ transmission line, and n_l is the number of lines. The matrix (10) is a part of solution to the (5) described in Section II.

IV. Appropriate placement of series compensators to improve the transient stability

The proposed algorithm for appropriate placement of multiple series compensators to improve transient stability is as follows

1) Most severe faults with the following clearing times are selected.

$$t_{cl_i} = t_{cc_i} - \varepsilon \tag{11}$$

where t_{cl_i} and t_{cc_i} are the clearing time and critical clearing time (CCT) of the i^{th} fault respectively, and ε is a positive small number (1 ms in this paper).

2) For each fault:
   2.1) (1)-(2) and (5)-(6) are solved simultaneously using the mentioned λ vector and all the dynamic and algebraic variables and their trajectory sensitivities with respect to the parameter vector λ are calculated. Simulation time does not need to be so long (first swing only).
   2.2) Based on the obtained data, the rotor angles (δ) of the generators are depicted in center of inertia (COI) reference and only the most critical generators (close to instability) will be selected. These generators are divided into A and D groups depending if their rotor angles (δ) after fault occurrence are accelerating or decelerating, respectively.
   2.3) The matrix of trajectory sensitivities of dynamical states (10) corresponding to the most critical generators is obtained and trajectory sensitivities of δ_i with respect to the reactances of different transmission lines are computed.
   2.4) A normalized index of trajectory sensitivity ($\widehat{\mathrm{S}}_{\mathrm{zk}}$) is calculated for each transmission line which shows the effectiveness of that line for improving the transient stability. The definition of $\widehat{\mathrm{S}}_{\mathrm{zk}}$ is as follows

$$\widehat{\mathrm{S}}_{\mathrm{zk}} = \frac{\mathrm{S}_{\mathrm{zk}}}{\mathrm{S}_{\mathrm{zk}}^{\max}} \cdot \frac{\mathrm{x}_{\mathrm{L_k}}}{\mathrm{x}_{\mathrm{L_k}}^{\max}} \quad \forall \mathrm{k} \in \mathrm{L}, \forall \mathrm{z} \in \mathrm{Z} \tag{12}$$

$$\mathrm{S}_{\mathrm{zk}} = \mathrm{PP_T}\ \{\mathrm{M_A^{-1}} \sum_{\mathrm{i \in A}} \mathrm{M_i} \frac{\partial \delta_{\mathrm{i}}}{\partial \mathrm{x}_{\mathrm{L_k}}} - \mathrm{M_D^{-1}} \sum_{\mathrm{j \in D}} \mathrm{M_j} \frac{\partial \delta_{\mathrm{j}}}{\partial \mathrm{x}_{\mathrm{L_k}}}\} \quad \forall k \in L, \forall z \in Z \tag{13}$$

$$M_A = \sum_{i \in A} M_i \ , \ M_D = \sum_{j \in D} M_j \tag{14}$$

where

$\widehat{\mathrm{S}}_{\mathrm{zk}}$: is the normalized index of trajectory sensitivity corresponding to each transmission line.
$\mathrm{S}_{\mathrm{zk}}^{\max}$: is the maximum value of S_{zk} among all the transmission lines for fault z.
$x_{L_k}^{max}$: is the maximum value of x_{L_k} among all the transmission lines.
S_{zk}: is the index of trajectory sensitivity corresponding to each transmission line.
PP_T: gives the peak-to-peak value of a function for the period T.
M_i: is the inertia of i^{th} generator.
A: is the set of critical generators which accelerate after fault occurrence.
D: is the set of critical generators which decelerate after fault occurrence.
L: is the set of transmission lines.
Z: is the set of selected severe faults.
M_A: is sum of inertia constants of the generators belonging to the set A.
M_D: is sum of inertia constants of the generators belonging to the set D.
$\partial \delta_i / \partial x_{L_k}$: is the trajectory sensitivity of rotor angle of i^{th} generator with respect to the reactance of k^{th} transmission line.

3) The transmission lines with the greatest positive values of total trajectory sensitivity indices ($\mathrm{TS_k}$) are the most appropriate places to install series compensator for improving the transient behavior of the power system corresponding to $p(z)$

$$\mathrm{TS_k} = \sum_{\mathrm{z \in Z}} \mathrm{p(z)} \widehat{\mathrm{S}}_{\mathrm{zk}} \quad \forall \mathrm{k} \in \mathrm{L}, \forall \mathrm{z} \in \mathrm{Z} \tag{15}$$

where

$\mathrm{TS_k}$: is the total trajectory sensitivity index corresponding to each transmission line.
$p(z)$: is a function which determines the degree of importance of each fault. This function could be a combination of the occurrence probability, degree of severity and etc.

4) To find the appropriate location to install the next series compensator, step (1)-(3) are repeated with the following changes

4.1) The system under study is modified considering all the previously specified series compensators installed at their best locations.
4.2) The transmission lines which already have the series compensator are removed from the list of candidate locations to put the new device.
4.3) Set of selected faults and their corresponding $p(z)$ are updated considering the installed devices.

V. Simulation and Results

The test system used in this study is the Cigre Nordic 32-bus test system. The system is shown in Fig. 4. The system data is taken from [12]. The Classical model is used for the generators. Table I shows list of the selected faults which are applied to this test system. When a fault occurs in the system, critical generators are determined and divided to two transient groups as mentioned in Section 4.2.2. Fig. 2 shows the rotor angles of generators in center of inertia reference for fault 3. It is clear that the generators 11 and 12 which are the most critical ones (close to instability) are both accelerating. So, the A and D sets for this fault are as follows

$$A = \{G11,\ G12\}\ ,\quad D = \{\} \tag{16}$$

To find the value of S_{zk} from (13), trajectory sensitivities of rotor angle of $G11$ and $G12$ should be depicted. The trajectory sensitivities of δ_{11} with respect to the reactances of different transmission lines are shown in Fig. 3. This figure shows that L27-12, $\widehat{\text{L}}12-11$, L8-27 and L26-12 have the largest positive peak to peak values and L25-9 has the most negative value of trajectory sensitivities. The symbols Li$-$j and $\widehat{\text{Li}}-$j determines the first and second transmission line connecting bus i^{th} to j^{th}.

It is important to understand the meaning of the peak to

TABLE I
List of selected faults - Nordic 32-bus test system

Name	Fault Location	Clearing Time
Fault 1	Line 4-21 close to bus 4	166 ms
Fault 2	Line 6-22 close to bus 6	220 ms
Fault 3	Line 12-11 close to bus 11	188 ms
Fault 4	Line 17-18 close to bus 17	238 ms
Fault 5	Line 24-9 close to bus 9	265 ms

peak values and their signs after occurring faults. It can be written based on the trajectory sensitivities

$$\triangle\delta_{11} \approx (\frac{\partial\delta_{11}}{\partial x_{L_i}})\triangle x_{L_i} \tag{17}$$

As series capacitor is going to be installed in the transmission lines, $\triangle x_{L_i}$ will be negative and since δ_{11} will also increase rapidly after occurring fault which is visible from Fig. 2, the value of trajectory sensitivity of δ_{11} with respect to the reactance of the transmission line should be positive to make $\triangle\delta_{11}$ negative, decrease δ_{11}, and enhance the transient stability of the system. Thus, absolute peak to peak value of trajectory sensitivity shows how sensitive δ_{11} is to the reactances of the transmission lines and its sign determines if putting series capacitor in that line has positive or negative effect on the transient stability. Since, generator 12 also has a critical condition for this fault, the same analysis has been done for δ_{12}

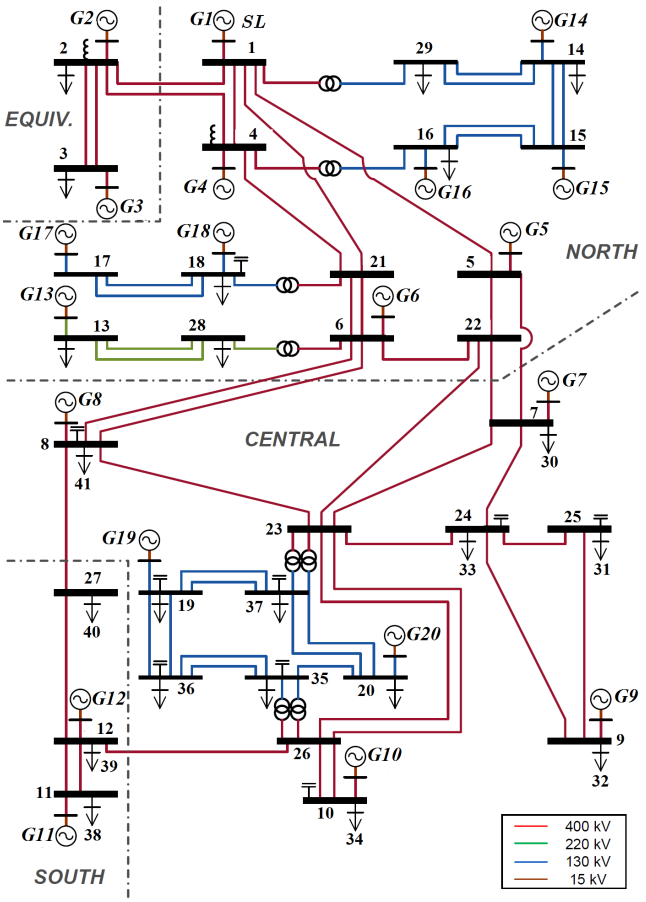

Fig. 1. The Cigre Nordic 32-bus test system

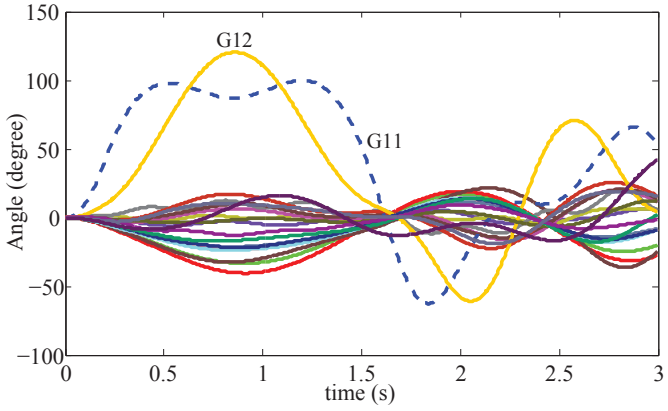

Fig. 2. Rotor angles of generators in center of inertia reference for fault 3

as well, and the values of S_{zk} have been calculated based on (13). Then, $\widehat{S}_{zk}$ which is the normalized index of trajectory sensitivity has been calculated for each transmission lines according to (12). The term $x_{L_k}/x_{L_k}^{max}$ in (12) is because of the practical limitation of each line and gives a higher weight to those lines with larger values of reactance and therefor larger possible amount of series compensation. The similar calculations have been done for the other selected faults, and due to space limitation, only the most important results are given in Table 2 and 3. Table 2 shows the A and D sets for

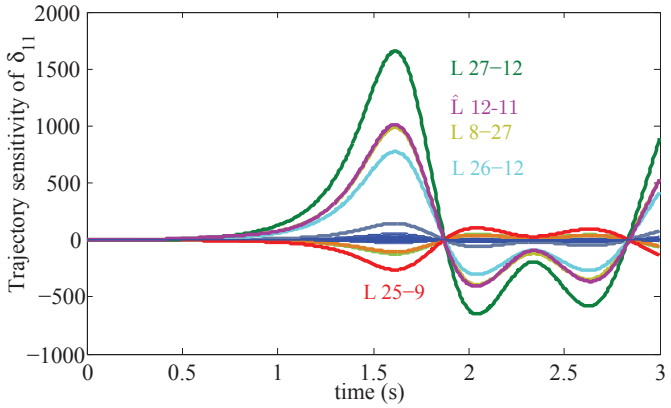

Fig. 3. Trajectory sensitivities of δ_{11} with respect to the reactances of different transmission lines for fault 3

different fault scenarios. As it can be seen in Table 3, for each fault, the first three priorities to install the series device and also the worst one are shown. It should be noted that these values are normalized indices of trajectory sensitivities $\widehat{S}_{zk}$ and are different from S_{zk} values. For instance, in case of fault 3, Fig. 3 depicts that L27-12 is the most sensitive place because it has the highest peak to peak value (S_{zk}), but the most appropriate place to install the device is L26-12 (highest $\widehat{S}_{zk}$ according to the Table 3). This is because of higher reactance of L26-12 compared to L27-12.

TABLE II
SETS A AND D FOR DIFFERENT FAULTS

Fault	1	2	3	4	5
Set A	{G4}	{G13}	{G11, G12}	{G17}	{G9}
Set D	{}	{}	{}	{}	{}

TABLE III
NORMALIZED INDICES OF TRAJECTORY SENSITIVITIES $\widehat{S}_{zk}$

$\widehat{S}_{zk}$	1^{st} priority	2^{nd} priority	3^{rd} priority	Worst place
$\widehat{S}_{1k}$	L4-2:+1.000	L1-4:+0.761	L1-2:+0.251	L22-23:-0.379
$\widehat{S}_{2k}$	L28-13:+1.000	L6-8:+0.336	L22-7:+0.282	L25-9:-0.084
$\widehat{S}_{3k}$	L26-12:+1.000	L8-27:+0.722	L27-12:+0.532	L25-9:-0.062
$\widehat{S}_{4k}$	$\hat{L}$17-18:+1.000	L4-21:+0.027	L1-21:+0.019	L22-23:-0.042
$\widehat{S}_{5k}$	L25-9:+1.000	L24-23:+0.714	L24-25:+0.501	L4-2:-0.067

To verify the results, industrial software SIMPOW®11 is used to simulate the test system in the presence of series compensators. Based on Table 3, it is clear that L26-12, L8-27 and L27-12 are the first priorities to install the series device for Fault 3 and L25-9 is the worst location. Fig. 4 shows the rotor angle of generator 11, δ_{11} which is one of the most critical generators, for the same capacitive compensations of the mentioned lines. As it is expected, capacitive compensation of Line 26-12 has the best improvement of the transient stability while the same compensation of Line 25-9 worsens the transient stability. Then, a fixed series capacitance (in this study, equal to 50% compensation of each transmission line) has been placed in different locations and the new CCTs of the selected faults for most appropriate locations have been calculated by time domain simulations and given in Table 4. It should be mentioned that the CCT values of faults for the system without compensation have been shown in Table 1 as well. It can be seen that the results are consistent with the normalized indices of trajectory sensitivities shown in Table 3. The next step is to combine all the results and choose the most

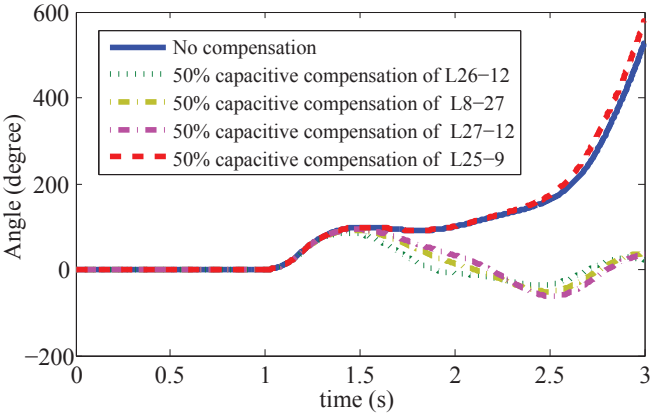

Fig. 4. Rotor angle of generator 11 (δ_{11}) for fault 3

TABLE IV
NEW CCTS OF THE FAULTS AFTER SERIES COMPENSATION OF THE MOST IMPORTANT LINES (MS)

	1^{st} priority	2^{nd} priority	3^{rd} priority	Worst place
Fault 1	L4-2: 175	L1-4: 170	L1-2: 168	L22-23: 164
Fault 2	L28-13: 243	L6-8: 230	L22-7: 228	L25-9: 218
Fault 3	L26-12: 215	L8-27: 202	L27-12: 199	L25-9: 187
Fault 4	$\hat{L}$17-18: 316	L4-21: 239	L1-21: 239	L22-23:237
Fault 5	L25-9: 279	L24-23: 274	L24-25: 270	L4-2: 264

suitable place to install the first compensator. This decision is strongly dependent to the $p(z)$ function corresponding to each fault. For example, assuming the same probability of fault occurrence for difference scenarios and only considering the severity of each fault, $p(z)$ may have this structure

$$p(z) = \frac{1}{CCT(z)} \quad \forall z \in Z \tag{18}$$

This research does not intend to discuss about how to obtain the $p(z)$ function and (15) only recommends a way to incorporate the obtained data for all the fault scenarios and make the best decision about the final location to install the series device.

Considering the $p(z)$ structure introduced in (18) and using (15), the total trajectory sensitivity indices corresponding to different transmission lines, TS_k, have been calculated and are given in Table 5 for the most important lines. According

TABLE V
TOTAL TRAJECTORY SENSITIVITY INDICES TS_k

	1^{st} priority	2^{nd} priority	3^{rd} priority	Worst place
TS_k	L4-2:+6.182	L26-10:+5.071	L17-18:+4.451	L22-23:-1.3836

to the Table 5, Line 4-2 is chosen as the most suitable place to install the first series compensator.

To install the next series device, new CCT values of selected faults in the presence of series compensator installed in Line 4-2 are computed and given in Table 6. As it was expected, the installed device only can improve the CCT value of fault 1, and does not have any considerable effect on the other faults.

TABLE VI
NEW CCT VALUES OF SELECTED FAULTS IN THE PRESENCE OF FIRST COMPENSATOR

	Fault 1	Fault 2	Fault 3	Fault 4	Fault 5
CCT	175 ms	220 ms	188 ms	238 ms	264 ms

Note that Line 4-2 is removed from the list of candidates to put the second device since it has already an installed device. The steps (1)-(3) of the propsed methodology described in Section 4 are repeated with the new situation of the system. Table 7 gives the new values of normalized indices of trajectory sensitivities $\widehat{\mathrm{S}}_{\mathrm{zk}}$ calculated for the placement of the second series compensator. The obtained data depicted in Table 7 determines the first three priorities to install the second series device and also the worst one for each fault. For the final decision about the location of the second device, the $p(z)$ functions of each fault should be updated shown by $\widehat{p}(z)$. It is assumed that for the second device, the probability of fault occurrence is not similar and are according to the Table 8.

TABLE VII
NORMALIZED INDICES OF TRAJECTORY SENSITIVITIES $\widehat{\mathrm{S}}_{\mathrm{zk}}$ - SECOND DEVICE

$\widehat{\mathrm{S}}_{\mathrm{zk}}$	1^{st} priority	2^{nd} priority	3^{rd} priority	Worst place
$\widehat{\mathrm{S}}_{1\mathrm{k}}$	L1-4:+1.000	L2-3:+0.368	L1-2:+0.163	L22-23:-0.432
$\widehat{\mathrm{S}}_{2\mathrm{k}}$	L28-13:+1.000	L6-8:+0.336	L22-7:+0.280	L25-9:-0.083
$\widehat{\mathrm{S}}_{3\mathrm{k}}$	L26-12:+1.000	L8-27:+0.715	L27-12:+0.535	L25-9:-0.064
$\widehat{\mathrm{S}}_{4\mathrm{k}}$	L17-18:+1.000	L4-21:+0.026	L1-5:+0.021	L22-23:-0.032
$\widehat{\mathrm{S}}_{5\mathrm{k}}$	L24-42:+1.000	L25-9:+0.899	L24-23:+0.644	L36-19:-0.034

TABLE VIII
PROBABILITY OF FAULT OCCURRENCE

	Fault 1	Fault 2	Fault 3	Fault 4	Fault 5
$\overline{\mathrm{P}}(\mathrm{z})$	10%	20%	40%	20%	10%

$$\hat{\mathrm{p}}(\mathrm{z}) = \frac{\overline{\mathrm{P}}(\mathrm{z})}{\mathrm{CCT}(\mathrm{z})} \quad \forall \mathrm{z} \in \mathrm{Z} \tag{19}$$

The total trajectory sensitivity indices TS_{k} for the second device are calculated using (19) and (15) and are given in Table 9. This table shows that with this definition of $\widehat{p}(z)$, Line 26-12, Line 8-27 and Line 27-12 are the first priorities and Line 7-23 is the worst location for the placement of second series compensator. These procedures can be repeated to allocate the next series devices.

TABLE IX
TOTAL TRAJECTORY SENSITIVITY INDICES TS_{k} - SECOND DEVICE

	1^{st} priority	2^{nd} priority	3^{rd} priority	Worst place
TS_{k}	L26-12:+2.102	L8-27:+1.565	L27-12:+1.098	L7-23:-0.158

Regarding the computatioal burden, calculating these sensitivities based on the numerical formulation of TSA described in section II needs to run $(n_L + 1) \times n_z$ time domain simulations to find the nominal and perturbed trajectories for a power system with n_L lines (possible places to install series compensator) and n_z fault scenarios. For this test system which has 52 lines and 5 fault scenarios, the required number of time domain simulations has been reduced from 265 ($(n_L+1)\times n_z$) to 5 (n_z) because of the analytical formulation of TSA. For the larger power systems, the proposed method simplifies significantly the cumbersome computational process of placement procedure.

VI. CONCLUSION

A novel method has been proposed based on the trajectory sensitivity analysis (TSA) to find the suitable placement of multiple series compensators in order to improve the transient stability of power system. In this method, trajectory sensitivities of the rotor angles of the most critical generators with respect to the reactances of transmission lines for different fault scenarios have been computed. It has been clarified why putting series compensators in the transmission lines does not always improve the transient stability of power system. Using the analytical formulation of TSA and selecting appropriate system's parameters, the number of required time domain simulations have been reduced significantly. The numerical result on Nordic-32 test system have shown validity, accuracy and efficiency of the proposed approach.

ACKNOWLEDGMENT

Amin Nasri has been awarded an Erasmus Mundus PhD Fellowship. The authors would like to express their gratitude towards all partner institutions within the programme as well as the European Commission for their support.

REFERENCES

[1] G. A. Maria, C. Tang and J. Kim, "Hybrid transient stability analysis [power systems]," *IEEE Trans. on power systems*, vol. 5, no. 2, pp. 384-393, May 1990.

[2] A. A. Fouad, and S. E. Stanton, "Transient stability of a multi-machine power system. part ii. critical transient energy," *IEEE Trans. on power appratus and systems*, vol. PAS-100, no. 7, pp. 3417-3424, Jul. 1981.

[3] T. Athay, P. Podmore, and S. Virmani, "A practical method for the direct analysis of transient stability," *IEEE Trans. on power appratus and systems*, vol. PAS-98, no. 2, pp. 573-584, Mar. 1979.

[4] A. A. Fouad, V. Vittal, and T. K. Oh, "Critical energy for direct transeint stability assessment of a multimachine power system," *IEEE Trans. on power appratus and systems*, vol. PAS-103, no. 8, pp. 2199-2206, Aug. 1984.

[5] J. Zhao, A. Ishigame, S. Kawamoto, and T. Taniguchi "Structural control of electric power networks for transient stability," *IEEE Trans. on power systems*, vol. 9, no. 3, pp. 1575-1581, Aug. 1984.

[6] K. N. Shubhanga, and A. M. Kulkarni, "Application of structure preserving energy margin sensitivity to determine the effectiveness of shunt and series FACTS devices," *IEEE Trans. on power systems*, vol. 17, no. 3, pp. 730-738, Aug. 2002.

[7] A. Zamora-Cárdenas, and C. R. Fuerte-Esquivel, "Multi-parameter trajectory sensitivity approach for location of series-connected controllers to enhance power system transient stability," *Electrical Power and Energy Systems*, vol. 80, no. 9, pp. 1096-1103, Sep. 2010.

[8] M. J. Laufenberg, and M. A. Pai, "A new approach to dynamic security assessment using trajectory sensitivities," *IEEE Trans. on power systems*, vol. 13, no. 3, pp. 953-958, Aug. 1998.

[9] T. B. Nguyen, M. A. Pai, and I. A. Hiskens, "Sensitivity approaches for direct computation of critical parameters in a power system," *International Journal of Electrical Power & Energy Systems*, vol. 24, no. 5, pp. 337-343, Jun. 2002.

[10] D. Chatterjee, and A. Ghosh, "Improvement of transient stability of power system with statcom-controller using trajectory sensitivity," *Electrical Power and Energy Systems*, vol. 33, no. 3, pp. 531-539, Mar. 2011.

[11] I. A. Hiskens, and M. A. Pai, "Trajectory sensitivity analysis of hybrid systems," *IEEE Trans. circuits and systems*, vol. 47, no. 2, pp. 204-220, Feb. 2000.

[12] M. Stubbe, "Long term dynamics phase ii, tf 38-02-08," *Technical report, Cigre*, pp. 1-19, Jun. 1995.

Paper C3

Transient Stability Assessment of Power Systems in the Presence of Shunt Compensators Using Trajectory Sensitivity Analysis

Transient Stability Assessment of Power Systems in the Presence of Shunt Compensators Using Trajectory Sensitivity Analysis

Amin Nasri, *Student Member, IEEE,* Mehrdad Ghandhari, *Member, IEEE,* Robert Eriksson, *Member, IEEE,*

***Abstract*—Trajectory sensitivity analysis (TSA) is used as analysis tool for suitable placement of shunt compensators in the power system. The goal is to maximize the benefit of these devices in order to enhance the transient stability of the system. For this purpose, the trajectory sensitivities of the rotor angles of generators with respect to the reactive power injected into different nodes of the system are calculated in the presence of most probable severe faults. Based on the obtained trajectory sensitivities, a method is proposed to determine how effective the shunt compensation in each node is for improving the transient stability. This method is applied to the IEEE 3-machine 9-bus to find the priorities of system's nodes for installation of shunt compensators. Simulation with industrial software shows the validity and efficiency of the proposed method.**

***Index Terms*—Trajectory Sensitivity Analysis (TSA), Static Synchronous Compensator (STATCOM), Transient Stability, Critical Clearing Time (CCT).**

I. Introduction

TRANSIENT stability is the ability of power system to keep its synchronism when a large disturbance, like three phase short circuit, occurs in the system. Nowadays, deregulation in electricity markets, increasing electricity demands and high penetration of renewable energy sources in one hand and economic and environmental constraints on installing new transmission lines and building new power plants on the other hand, have pushed the existing transmission systems to be operated close to their critical conditions. So, there is a higher risk of transient instability in today's heavy-loaded and interconnected power systems.

Flexible AC Transmission System (FACTS) devices can have a significant impact on operational flexibility and controllability of the power system. Using these devices, the power flow through the system can be controlled dynamically in a way to increase the transient stability margins and make the system more secure. Since the impact of these devices on the system's stability is strongly dependent on their locations, there is a great need for developing an analytical tool to provide useful information to the system planners regarding the best possible installation locations of them. In this paper, an effective tool is developed to identify the most suitable places to install shunt compensators to improve transient stability of power system.

Assessment of rotor angle stability is essential to study the dynamic behaviour of the power system. Time domain simulation is the traditional way for transient stability assessment which has two main disadvantageous, namely time-consuming computation requirement and incapability to provide any information regarding the stability margin [1]. The other method which has been widely used for this purpose is transient energy function (TEF) method [2]–[4]. The significant advantage of this method is its capability to provide a stability index [1]. Several methodologies have been proposed based on the sensitivity of TEF to determine the effectiveness of FACTS devices to improve system's transient stability [5], [6]. Despite all the advantages of the TEF based methods, the main shortcoming of them is their high complexity in the following situations: (i) considering differential-algebraic equation (DAE) models of power systems, (ii) dealing with the detailed models of the system's components, (iii) when a number of system's parameters have to be taken into account for the sensitivity analysis [7]–[11].

Applications of trajectory sensitivity analysis (TSA) have been introduced as an alternative to overcome the mentioned shortcoming of the TEF based method [7]. Ref. [8] has used TSA to calculate the critical values of some power system's parameters such as fault clearing time, mechanical input power of generators, etc. The proposed method in [8] is based on the computation of the norm of trajectory sensitivities of rotor angles and speeds of generators with respect to the parameters of interest. Ref. [9], [10] has discussed the application of TSA to power systems containing series and shunt compensators. A transient stability index has been introduced based on the numerical formulation of TSA and has been calculated for the power system with different locations of series and shunt compensators. Using numerical formulation of TSA, considering the compensators' models in the study and simulating the power system for all the possible locations of compensators has caused high computational burden for the proposed method in [9], [10]. Ref. [11] has developed a multi-parameter trajectory sensitivity approach to find the best locations of series compensators in order to improve the transient stability. An index of proximity to instability has been determined based on the norm of the trajectory sensitivities of the rotor angles and the speeds of generators with respect to the transmission line susceptances. Using the analytical formulation of TSA in [11] and also in this paper, the cumbersome computational process becomes much simpler compared to the numerical method in [8], [9]. The latter will be explained later.

In this paper, a novel method is proposed based on the analytical formulation of TSA to determine the most appropriate places of shunt compensations to amend the transient stability of power system. Trajectory sensitivities of the rotor angles of generators are computed directly with respect to the reactive power injected into different nodes of the system. Based on the obtained trajectory sensitivities, the most effective locations to install shunt compensators are found. The major contribution of this paper is to use the analytical formulation of TSA

A. Nasri, M. Ghandhari and R. Eriksson are with the Department of Electric Power Systems, School of Electrical Engineering at KTH Royal Institute of Technology, Sweden, e-mail: (see http://www.kth.se/en/ees/omskolan/organisation/avdelningar/eps/abouteps).

978-1-4799-1303-9/13/$31.00 ©2013 IEEE

for the suitable placement of shunt compensators in order to enhance the transient stability which is computationally more efficient than the method described in [9,10]. The system under consideration is IEEE 3-machine 9-bus system in this paper.

II. Power system modeling and trajectory sensitivity analysis

As explained comprehensively in [12], power systems can be modeled by the following differential algebraic equations

$$\dot{\underline{x}} = \underline{f}(\underline{x}, y) \tag{1}$$

$$0 = \begin{cases} g^-(\underline{x}, y) & s(\underline{x}, y) < 0 \\ g^+(\underline{x}, y) & s(\underline{x}, y) > 0 \end{cases} \tag{2}$$

$$\underline{x} = \begin{bmatrix} x \\ \lambda \end{bmatrix} \quad \underline{f} = \begin{bmatrix} f \\ 0 \end{bmatrix} \tag{3}$$

$$\underline{x}(t_0) = \underline{x}_0,\ y(t_0) = y_0 \tag{4}$$

where $\underline{x}$ is a vector containing the dynamic states x and the system parameters λ, and y is a vector of algebraic states. Rotor angles of the generators, impedances of the transmission lines and magnitude and angle of bus voltages are the examples of the dynamic states, power system parameters and algebraic states, respectively. $\underline{x}_0$ and y_0 are the initial conditions of the mentioned vectors. Function f is the set of differential equations which model the dynamics of equipments like generators. Events like a three phase short circuit fault occurs when $s(\underline{x}, y) = 0$. The algebraic equations g consist of the network equations based on Kirchhoff's current law, i.e. the sum of all current (or powers) flowing into each bus must be equal to zero, g^- and g^+ show the algebraic equations before and after occurrence of events.

To calculate the trajectory sensitivities analytically, the derivatives of (1), (2) are calculated with respect to $\underline{x}_0$ which contains both the dynamic state's initial conditions and also systems' parameters

$$\dot{\underline{x}}_{\underline{x}_0} = \underline{f}_{\underline{x}}(t)\underline{x}_{\underline{x}_0} + \underline{f}_y(t) y_{\underline{x}_0} \tag{5}$$

$$0 = g_{\underline{x}}(t)\underline{x}_{\underline{x}_0} + g_y(t) y_{\underline{x}_0} \tag{6}$$

The system is assumed to be away from the events. The initial conditions for $\underline{x}_{\underline{x}_0}$ and $y_{\underline{x}_0}$ are obtained by differentiating (3) with respect to $\underline{x}_0$. It is clear that the initial value for the trajectory sensitivities of dynamic states is an identity matrix. Using this identity matrix, the initial values for the trajectory sensitivities of algebraic states can be also computed from (8).

$$\underline{x}_{\underline{x}_0}(t_0) = I, \quad y_{\underline{x}_0}(t_0) = -(g_y(t_0))^{-1} g_{\underline{x}_0}(t_0) \tag{7}$$

$\underline{f}_{\underline{x}}$, $\underline{f}_y$, $g_{\underline{x}}$ and g_y are time varying functions which are calculated along the system trajectories. When an event occurs in the system, jump condition should be derived for computation of the trajectory sensitivities which is fully described in [12]. To find the trajectory sensitivities, the DAEs (1)-(2) and (5)-(6) will be solved simultaneously with the initial conditions described above using trapezoidal integration technique.

To calculate the trajectory sensitivity of state variable x to the parameter λ with a numerical formulation of TSA, a small perturbation of $\triangle\lambda$ over the nominal parameter λ_0 should be considered such that $\lambda = \lambda_0 + \triangle\lambda$. So, the numerical estimation of sensitivity is defined as $x_\lambda = (x(\lambda) - x(\lambda_0))/\triangle\lambda$.

III. Transient stability assessment using trajectory sensitivity analysis

Power systems may become transiently unstable after being subjected to large disturbances. The result of transient instability appears in the form of increasing rotor angles of some generators which leads to their loss of synchronism with other generators. So, monitoring angular swings of generators (or the equivalent angle of all the generators) could be one way to check the transient stability of power system. To improve the transient stability, power system parameters can be controlled (if applicable) in a way to have positive effects on the variation of rotor angles of generators when the system is subjected to a fault and prevent power system from being unstable.

Shunt FACTS devices like Static Synchronous Compensator (STATCOM) are capable of injecting (absorbing) reactive power to (from) the power system's nodes. They can control dynamically the amount of this reactive power injection (absorbtion) so that to improve the rotor angle stability of power system. Due to the heavy costs of these devices, it is necessary to find the appropriate locations to install minimum numbers of them needed for the stability enhancement. In this paper, trajectory sensitivities of rotor angles with respect to the reactive power injected into the different nodes of the system are used for suitable placement of shunt compensators.

So, the matrices of system parameters and trajectory sensitivities of dynamical states to these parameters are as follows

$$\lambda = [Q_{inj_1}\ \ Q_{inj_i}\ \ \cdots\ \ Q_{inj_N}] \tag{8}$$

$$\frac{\partial \delta}{\partial \lambda} = \begin{bmatrix} \frac{\partial \delta_1}{\partial Q_{inj_1}} & \frac{\partial \delta_1}{\partial Q_{inj_i}} & \cdots & \frac{\partial \delta_1}{\partial Q_{inj_N}} \\ \frac{\partial \delta_2}{\partial Q_{inj_1}} & \frac{\partial \delta_2}{\partial Q_{inj_i}} & \cdots & \frac{\partial \delta_2}{\partial Q_{inj_N}} \\ \cdot & \cdot & \cdot & \cdot \\ \cdot & \cdot & \cdot & \cdot \\ \cdot & \cdot & \cdot & \cdot \\ \frac{\partial \delta_n}{\partial Q_{inj_1}} & \frac{\partial \delta_n}{\partial Q_{inj_i}} & \cdots & \frac{\partial \delta_n}{\partial Q_{inj_N}} \end{bmatrix} \tag{9}$$

where Q_{inj_i} is the reactive power injected to the i^{th} node, N is the number of nodes, δ_j is the rotor angle of the j^{th} generator, and n is the number of generators. The matrix (9) is a part of solution to the (5) described in Section II.

IV. Appropriate placement of series compensators to improve transient stability

A. Definition of equivalent angle δ_{eq_t}

In this part, an equivalent angle is defined and the trajectory sensitivity of this angle to the the reactive power injected into the different nodes of the system is introduced for appropriate placement of shunt compensators. To define this angle, machines are separated to two groups named A and B depending if their rotor angles (δ) after fault occurrence, in center of inertia (COI) reference, are accelerating or decelerating, respectively. Then, these two groups are replaced by a single machine equivalent system. The equivalent angle δ_{eq_t} includes all the rotor angles and is defined as follows [13]

$$M_A = \sum_{i \in A} M_i, \quad M_B = \sum_{j \in B} M_j \tag{10}$$

$$\delta_A = M_A^{-1} \sum_{i \in A} M_i \delta_i, \quad \delta_B = M_B^{-1} \sum_{j \in B} M_j \delta_j \tag{11}$$

$$\delta_{eq_t} = \delta_A - \delta_B \tag{12}$$

where M_i and δ_i are the inertia and rotor angle of the i^{th} generator, respectively. According to this definition, the trajectory sensitivity of the equivalent angle to the reactive power injected to different nodes of the system is calculated as follows

$$\frac{\partial \delta_A}{\partial Q_{inj_i}} = M_A^{-1} \sum_{i \in A} M_i \frac{\partial \delta_i}{\partial Q_{inj_i}} \tag{13}$$

$$\frac{\partial \delta_B}{\partial Q_{inj_i}} = M_B^{-1} \sum_{j \in B} M_j \frac{\partial \delta_j}{\partial Q_{inj_i}} \tag{14}$$

$$\frac{\partial \delta_{eq_t}}{\partial Q_{inj_i}} = \frac{\partial \delta_A}{\partial Q_{inj_i}} - \frac{\partial \delta_B}{\partial Q_{inj_i}} \tag{15}$$

B. The proposed algorithm for appropriate placement of shunt compensators to improve transient stability

- Most severe faults with the following clearing times are selected.

$$t_{cl_i} = t_{cc_i} - \varepsilon \tag{16}$$

where t_{cl_i} and t_{cc_i} are the clearing time and critical clearing time (CCT) of the i^{th} fault respectively, and ε is a positive small number (1 ms in this paper).

- For each fault:
  1) (1)-(2) and (5)-(6) are solved simultaneously using the mentioned λ vector and all the dynamic and algebraic variables and their trajectory sensitivities with respect to the parameter vector λ are calculated. Simulation time does not need to be so long (first swing only).
  2) Based on the obtained data for the rotor angles (δ) of the generators, generators are divided to A and B groups which oscillate against each other.
  3) The matrix of trajectory sensitivities of dynamical states (9) is obtained and based on the definition of δ_{eq_t}, trajectory sensitivities of δ_{eq_t} with respect to the reactive power injected into different nodes of the system are computed.
  4) The maximum peak to bottom value of trajectory sensitivity of δ_{eq_t} to each injected reactive power into nodes (except the faulty node) after fault occurrence are determined.
  5) The values obtained in 4) are normalized to their maximum value and are divided to the clearing time of the fault.

- Finally
  1) for each node, sum of normalized trajectory sensitivities of δ_{eq_t} to the injected reactive power into that node for different faults is calculated (data from second step). These results show how effective each node is for improvement of transient stability.
  2) The nodes which have the most positive effects are chosen for installation of shunt compensators.

V. Simulation and results

The IEEE 3-machine 9-bus test system is used to evaluate the proposed algorithms. The system is shown in Fig. 1. The system data is taken from [14]. The reactances of transformers are included in transient reactances of generators. Classical model is used for the generators. Table I shows list of the selected faults which are applied to this test system. When a fault occurs in the system, generators are divided to two transient groups as mentioned in section IV. A. Fig. 2 shows the rotor angles of generators in center of inertia reference for fault 6. It is clear that generators 2 and 3 are accelerating and generator 1 is decelerating. For this fault, generator 1 is selected as the B group and generators 2 and 3 as the A group, and equivalent rotor angle is calculated based on this classification and is also depicted in Fig. 2. The trajectory sensitivities of δ_{eq_t} with respect to the the reactive power injected into different nodes of the system are calculated and shown in Fig. 3. This figure shows that the signs of trajectory sensitivities of δ_{eq_t}, after fault occurrence, with respect to the reactive power injected into different nodes of the system are positive. Nodes 3, 5, 4, 2 and 1 have the largest absolute peak to bottom value of trajectory sensitivities, respectively.
It is so important to understand the meaning of these absolute peak to bottom values and their signs after occurring faults. It can be written based on the trajectory sensitivities

$$\triangle \delta_{eq_t} \approx (\frac{\partial \delta_{eq_t}}{\partial Q_{inj_i}}) \triangle Q_{inj_i} \tag{17}$$

The sign of trajectory sensitivities determines if the reactive power should be injected to or absorbed from different nodes

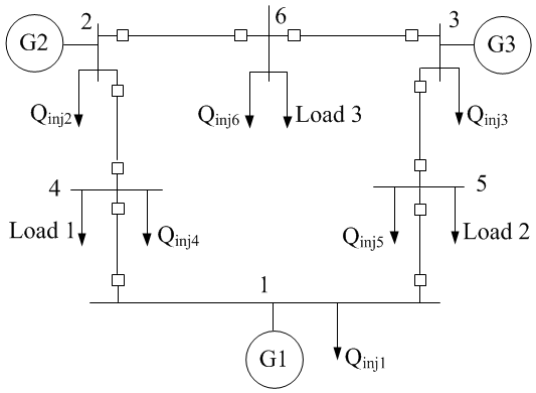

Figure 1. Modified IEEE 9-bus 3-machine test system.

Table I
List of selected faults - IEEE 9-bus 3-machine test system

Name	Fault Location	Clearing Time
Fault 1	Line 1-4 very close to bus 1	143 ms
Fault 2	Line 2-6 very close to bus 2	142 ms
Fault 3	Line 3-5 very close to bus 3	129 ms
Fault 4	Line 4-2 very close to bus 4	202 ms
Fault 5	Line 1-5 very close to bus 5	195 ms
Fault 6	Line 6-3 very close to bus 6	191 ms

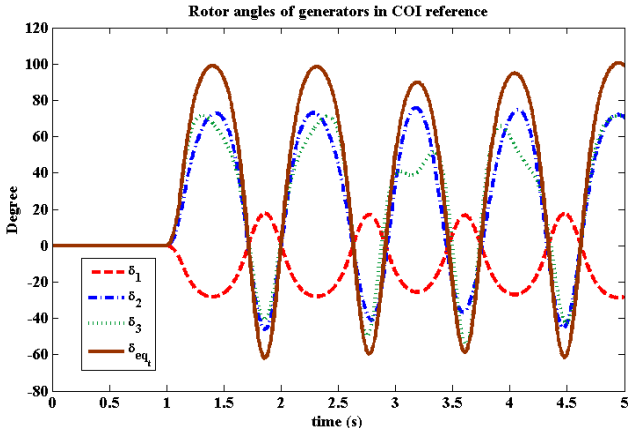

Figure 2. Rotor angles of the generators and the equivalent angle (δ_{eq_t}).

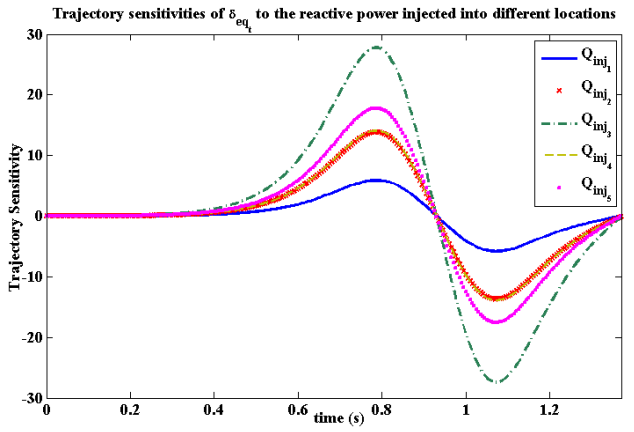

Figure 3. Trajectory sensitivities of δ_{eq_t} to the reactive power injected into the different nodes of the system for Fault 6

of system for the stability enahncement. Since STATCOM is going to be installed in the system, $\triangle Q_{inj_i}$ could be both positive and negative. Due to the sharp increase of δ_{eq_t} after fault occurrence which is visible from Fig. 2, $\triangle\delta_{eq_t}$ should be negative to decrease δ_{eq_t}, and improve the transient stability. For this fault, it can be seen form Fig. 3 that the values of trajectory sensitivities of δ_{eq_t} with respect to the reactive power injected into all the nodes ($\partial\delta_{eq_t}/\partial Q_{inj_i}$) are positive. So, $\triangle Q_{inj_i}$ should be negative to make $\triangle\delta_{eq_t}$ also negative which means that the reactive power should be injected to the nodes after fault occurrence (considering the direction of Q_{inj_i} shown in Fig. 1).

The absolute peak to bottom value of trajectory sensitivities also shows how sensitive δ_{eq_t} is to the shunt compensation in different nodes. For this fault, it means that for the same amount of $\triangle Q_{inj_i}$, there will be larger value of $\triangle\delta_{eq_t}$ when STATCOM is placed at Nodes 3, 5, 4, 2 and 1, respectively. So, the most appropriate place to install the STATCOM to improve the transient stability of this test system corresponding to this fault is node 3. The same calculations are done for the other faults and results are given in Table II. For each fault, computed peak to bottom values of trajectory sensitivities are normalized to their maximum value. Each row corresponding to each fault shows these normalized trajectory sensitivities of δ_{eq_t}. It can be seen that one of the trajectory sensitivities is equal to 1 for each row which shows the most effective place to install shunt compensator for improving the transient stability corresponding to that fault. The next step is to consider clearing time of each fault. For this purpose, all the digits of each row are divided to the clearing time of its corresponding fault. The final step is to calculate the total effect of injecting reactive power into each node on the transient stability for all the selected faults and decide about the best location for installing shunt compensators. According to the obtained results shown in Table III, Node 6 is the best location for installing shunt compensator considering all the selected faults.

Table II
Normalized trajectory sensitivities of δ_{eq_t} for different fault scenarios

	Node 1	Node 2	Node 3	Node 4	Node 5	Node 6
Fault 1	-	0,5493	0,7475	0,9280	**1,0000**	0,7974
Fault 2	0,2870	-	0,9107	0,6517	0,7816	**1,0000**
Fault 3	0,2520	0,6486	-	0,5967	0,6682	**1,0000**
Fault 4	0,3084	0,6820	0,9693	-	0,9324	**1,0000**
Fault 5	0,2853	0,6804	0,9938	0.7448	-	**1,0000**
Fault 6	0,2412	0,5054	**1,0000**	0,5794	0,7016	-

Table III
Total effects of reactive power injection into each node on the transient stability

	Node 1	Node 2	Node 3	Node 4	Node 5	Node 6
Sum	8,2339	18,4217	26,8355	22,9648	26,0348	**30,4884**

To calculate these sensitivities based on the numerical formulation of TSA described in section II, $(n+1)\times n_f$ time domain simulations should be run to to find the nominal and perturbed trajectories for a power system with n nodes (possible places to install shunt compensator) and n_f fault scenarios. For this test system which has 6 nodes and 6 fault scenarios, the required number of time domain simulations has been reduced from 42 ($(n+1)\times n_f$) to 6 (n_f) because of the analytical formulation of TSA. For the large-scale power systems, the proposed method simplifies significantly the cumbersome computational process of placement procedure.

VI. Simulation with Industrial Software

To verify the results, industrial software SIMPOW®11 is used to simulate the test system in the presence of STATCOM. An injection model of STATCOM has been implemented and placed in different locations and the new CCTs of the selected faults have been calculated for each location using time domain simulations. For a better comparison, the STATCOM controller injects dynamically the same amount of reactive power for different placement scenarios. Fig. 4 shows the variation of equivalent rotor angle after fault occurrence at node 6 for different locations of STATCOM. It is clear that the non-compensated system is transiently unstable. As it was expected from Table II, shunt compensation of Nodes 3, 5, 4,

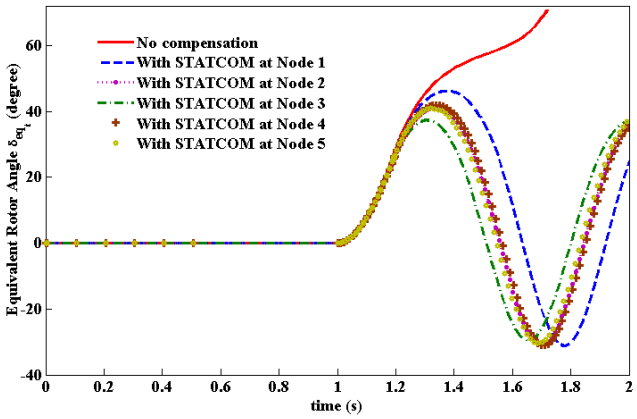

Figure 4. Fault at bus 6 with a clearing time = 193 ms - Equivalent rotor angle, δ_{eq_i}, for different locations of STATCOM

Table IV
Difference between new and old CCTs (ms) of faults after installing STATCOM in different nodes

	Node 1	Node 2	Node 3	Node 4	Node 5	Node 6
Fault 1	-	15	20	22	22	20
Fault 2	6	-	18	10	12	19
Fault 3	4	8	-	7	8	13
Fault 4	11	23	38	-	35	38
Fault 5	12	30	42	33	-	45
Fault 6	10	23	47	23	29	-

2 and 1 have the most positive effects on the transient stability, respectively. Table IV shows the difference between new and old CCTs of all the selected faults corresponding to different location of STATCOM. It can be seen that the results are consistent with the normalized trajectory sensitivities shown in Table II. The results confirms that installing STATCOM at Node 6 has the best total impact on the transient stability.

VII. CONCLUSION

A novel method has been proposed based on the trajectory sensitivity analysis (TSA) to find the suitable locations of shunt compensators in order to improve the transient stability of power system. In this method, trajectory sensitivities of the rotor angles of the generators with respect to the reactive power injected into the different nodes of the system have been computed for different fault scenarios. Using the analytical formulation of TSA and selecting appropriate system's parameters, the number of required time domain simulations have been reduced significantly. Moreover, the proposed method does not need to consider the detailed model of STATCOM for its simulations. The numerical result on the IEEE 3-machine 9-bus system have shown validity, accuracy and efficiency of the proposed approach. The proposed method can also be easily applied to a very large power system assuming the most critical faults are already known. Future research could be the extension of this technique for the placement of multiple FACTS devices with different types to enhance the rotor angle stability and also it's application to a large-scale power system.

ACKNOWLEDGMENT

Amin Nasri has been awarded an Erasmus Mundus PhD Fellowship. The authors would like to express their gratitude towards all partner institutions within the programme as well as the European Commission for their support.

REFERENCES

[1] G. A. Maria, C. Tang, J. Kim, "Hybrid transient stability analysis," *IEEE Trans. on power systems*, vol. 5, pp. 384-393, May 1990.
[2] A. A. Fouad, S. E. Stanton, "Transient Stability of a Multi-Machine Power System. Part II. Critical Transient Energy ," *Power Engineering Review*, vol. PER-1, pp. 3417-3424, July 1981.
[3] T. Athay, P.Podmore, S.Virmani, "A Practical Method for the Direct Analysis of Transient Stability ," *IEEE Trans. on power appratus and systems*, vol. PAS-98, No. 2, pp. 573-584, March/April 1979.
[4] A. A. Fouad, V.Vittal, T. K. Oh, "Critical Energy for Direct Transeint Stability Assessment of a Multimachine Power System," *IEEE Trans. on power appratus and systems*, vol. 103, pp. 2199-2206, August 1984.
[5] A. Ishigame, S. Kawamoto, T. Taniguchi, "Structural control of electric power networks for transient stability," *IEEE Trans. on power systems*, vol. 9, pp. 1575-1581, August 1994.
[6] K. N. Shubhanga, A. M. Kulkarni, "Application of structure preserving energy margin sensitivity to determine the effectiveness of shunt and series FACTS devices," *IEEE Trans. on power systems*, vol. 17, pp. 730-738, August 2002.
[7] M. J. Laufenberg, M. A. Pai, "A new approach to dynamic security assessment using trajectory sensitivities," *IEEE Trans. on power systems*, vol. 13, pp. 953-958, August 1998.
[8] T. B. Nguyen, M. A. Pai, "Sensitivity approaches for direct computation of critical parameters in a power system," *International Journal of Electrical Power & Energy Systems*, vol. 24, pp. 337-343, June 2002.
[9] D. Chatterjee, A. Ghosh, "Transient Stability Assessment of Power Systems Containing Series and Shunt Compensators," *IEEE Trans. on power systems*, vol. 22, pp. 1210-1220, August 2007.
[10] D. Chatterjee, A. Ghosh, "Improvement of transient stability of power system with STATCOM-controller using trajectory sensitivity," *Electrical Power and Energy Systems*, vol. 33, pp. 531-539, January 2011.
[11] A. Zamora-Cárdenas, C. R. Fuerte-Esquivel, "Multi-parametertrajectory sensitivity approach for location of series-connected controllers to enhance power system transient stability," *Electric Power Systems Research*, vol. 80, pp. 1096-1103, March 2010.
[12] I. A. Hiskens, M. A. Pai, "Trajectory sensitivity analysis of hybrid systems," *IEEE Trans. circuits and systems*, vol. 47, February 2000.
[13] M. Pavella, D. Ernst, d. Ruiz-Vega, "Power System System Transient Stability Analysis and Control," *Kluwer Academic Publishers*, 2000.
[14] M. A. Pai, "Energy Function Analysis for Power System Stability," Appendix A, 2007.

Amin Nasri received his M.Sc. degree in Electrical Engineering from the Sharif University of Technology, Tehran, Iran, in 2008. He is pursuing the Erasmus Mundus Joint Doctorate in Sustainable Energy Technologies and Strategies (SETS) hosted by Comillas Pontifical University, Spain; Royal Institute of Technology, Sweden; and Delft University of Technology, Netherlands. He is currently a Ph.D. Student in the Division of Electric Power Systems, School of Electrical Engineering at KTH Royal Institute of Technology.

Mehrdad Ghandhari received the M.Sc., Tech. Lic. and Ph.D. degrees in Electrical Engineering from Royal Institute of Technology, Stockholm, Sweden, in 1995, 1997, and 2000, respectively. He is currently Associate Professor at KTH Royal Institute of Technology.

Robert Eriksson received his M.Sc., Tech. Lic. and Ph.D. degrees in Electrical Engineering from KTH Royal Institute of Technology, Stockholm, Sweden, in 2005, 2008 and 2011 respectively. He is currently a Postdoctoral researcher in the Division of Electric Power Systems, School of Electrical Engineering at KTH Royal Institute of Technology.

Paper C4

Appropriate Placement of Series Compensators to Improve Small Signal Stability of Power System

Appropriate Placement of Series Compensators to Improve Small Signal Stability of Power System

Amin Nasri, *Student Member, IEEE,* Robert Eriksson, *Member, IEEE,* Mehrdad Ghandhari, *Member, IEEE,*

***Abstract*—Series FACTS devices like thyristor controlled series capacitors (TCSC) equipped with appropriate supplementary damping controller can improve the small signal stability of power system if they are located properly. In this paper, trajectory sensitivity analysis (TSA) is used to determine the best locations for installing TCSC to damp out the inter-area mode of oscillation. Based on the modal analysis, an equivalent angle is defined by determining critical and non-critical machines, and then using trajectory sensitivities of this angle with respect to the impedances of the transmission lines; appropriate locations for placing TCSC are found. To verify the accuracy of the proposed method, the residue technique for optimal placement of FACTS devices is also implemented in this paper. Both methods are applied to the IEEE 3-machines 9-buses test system, and the obtained results show the validity and efficiency of the proposed method.**

***Index Terms*—Trajectory sensitivity analysis (TSA), Thyristor Controlled Series Capacitor (TCSC), Small Signal Stability.**

I. Introduction

SMALL signal stability is the ability of the power system to keep its synchronism after being subjected to small disturbances. In a large scale power system, there are several electromechanical oscillations which are usually classified into inter-area modes and local modes. Local modes of oscillation are related to the oscillation of a single generator or a very small group of generators while in the inter-area mode of oscillation, the generators of one area oscillate against generators of another area. Power system stabilizers (PSS) can effectively damp out the local oscillation modes but they are not capable enough to control and damp the inter-area modes of oscillation, which usually take place at lower frequencies, appropriately. On the other hand, Flexible AC Transmission Systems (FACTS) equipped with the proper controller can have a significant impact on the power oscillation damping corresponding to the inter-area modes [1]. Using these devices most effective, it is vital to find the best locations for their installation [2].

Several methods have been proposed for the placement of FACTS devices in the previous literatures. Most of the research in this area have only considered static criterion, for instance, [3] has modified the optimal reactive power dispatch formulation considering FACTS devices as additional parameters and then defined sensitivity indices for optimal placement of FACTS devices to minimize the total system real power loss. In [3], TCSC, Static Var Compensator (SVC), and Thyristor Controlled Phase Angle Regulator (TCPAR) were studied. [4] has derived injection models of TCSC and TCPAR and also introduced the real power flow performance index to find the optimal locations of TCSC and TCPAR for improving Total Transfer Capacity (TTC) of the system. [5] has represented sensitivity index of loading margin with respect to the transmission line impedances and described a method to find the lines for series compensation leading to the largest ATC. In [6], Particle Swarm Optimization (PSO) technique has been used to find number of FACTS devices, their setting and their best places for maximum system loadability and minimum installation cost in the case of using single type and multi type FACTS devices.

There are also some papers which considered dynamic criterion for optimal placement of FACTS devices. For instance, [7] has proposed controllability indices which show the impacts of FACTS devices on the improvement of inter area mode and have been calculated for SVC, TCSC and Unified Power Flow Controller (UPFC). After calculation of these controllability indices for each of FACTS devices in different locations and also for different operating conditions, the optimal places for installation of these devices have been determined. [8] has used an eigenvalue sensitivity approach to find the best locations of controllable series capacitors for damping power system oscillation. The calculated eigenvalue sensitivities are based on the product of the modal controllability of series reactance modulation and the observability factor of the input signal. [9] has applied trajectory sensitivity analysis to the power system for optimal placement of series FACTS devices to improve transient stability of power system. Computed trajectory sensitivities of rotor angles of generators with respect to the impedances of transmission lines show the effect of each transmission lines on the transient stability of power system when subjected to severe faults.

This paper is a continuation of [9] and uses trajectory sensitivity analysis to determine the best locations for installing series compensators to enhance power oscillation damping. It indicates that when there is no fault in the system, the trajectory sensitivities of generators' rotor angles to the impedance of transmission lines can be used as a powerful tool to find the most effective transmission lines for small signal stability improvement. The most important point is that the methods described here and in [9] can be used together as a powerful and efficient tool to analyze the effects of series FACTS devices on both transient and small signal stability of power system and also can be extended in a way to cover the other types of FACTS devices.

A. Nasri, M. Ghandhari and R. Eriksson are with the Department of Electric Power Systems, School of Electrical Engineering at KTH Royal Institute of Technology, Sweden, e-mail: (see http://www.kth.se/en/ees/omskolan/organisation/avdelningar/eps/abouteps).

978-1-4673-1454-1/12/$31.00 © 2012 IEEE

II. Power system modeling and trajectory sensitivity analysis

As explained comprehensively in [10], power systems can be modeled by the following differential algebraic equations

$$\dot{x} = f(x, y; \lambda) \tag{1}$$

$$0 = \begin{cases} g^-(x, y; \lambda) & s(x, y; \lambda) < 0 \\ g^+(x, y; \lambda) & s(x, y; \lambda) > 0 \end{cases} \tag{2}$$

$$x(t_0) = x_0,\ y(t_0) = y_0 \tag{3}$$

Where x are the dynamic states, y are the algebraic states and λ are the parameters of the system. Rotor angles of the generators (δ), magnitude and angle of bus voltages and impedances of the transmission lines are the examples of the dynamic states, algebraic states and parameters of the power system, respectively. x_0 and y_0 are initial conditions of dynamic and algebraic states. Function f is the set of differential equations which model the dynamics of equipments like generators. Events like a three phase short circuit fault occurs when $s(x, y; \lambda) = 0$. The algebraic equations g consist of the network equations based on Kirchhoff's current law, i.e. the sum of all current (or powers) flowing into each bus must be equal to zero, g^- and g^+ show the algebraic equations before and after occurrence of events.

To write the equations in a more organized way, vectors of $\underline{x}$ and $\underline{f}$ are defined as follows

$$\underline{x} = \begin{bmatrix} x \\ \lambda \end{bmatrix} \qquad \underline{f} = \begin{bmatrix} f \\ 0 \end{bmatrix} \tag{4}$$

And therefore

$$\dot{\underline{x}} = \underline{f}(\underline{x}, y) \tag{5}$$

$$0 = \begin{cases} g^-(\underline{x}, y) & s(\underline{x}, y) < 0 \\ g^+(\underline{x}, y) & s(\underline{x}, y) > 0 \end{cases} \tag{6}$$

To calculate the trajectory sensitivities analytically, the derivatives of (5), (6) are calculated with respect to $\underline{x}_0$

$$\dot{\underline{x}}_{\underline{x}_0} = \underline{f}_{\underline{x}}(t)\underline{x}_{\underline{x}_0} + \underline{f}_y(t)y_{\underline{x}_0} \tag{7}$$

$$0 = g_{\underline{x}}(t)\underline{x}_{\underline{x}_0} + g_y(t)y_{\underline{x}_0} \tag{8}$$

where $\underline{x}_{\underline{x}_0}$ and $y_{\underline{x}_0}$ represent the trajectory sensitivities of dynamic and algebraic states with respect to the vector of power system parameters and initial conditions of dynamic states. The system is assumed to be away from the events. It is clear that the initial value for the trajectory sensitivities of dynamic states is an identity matrix. Using this matrix the initial values for the trajectory sensitivities of algebraic states can be also computed.

$$\underline{x}_{\underline{x}_0}(t_0) = I \tag{9}$$

$$y_{\underline{x}_0}(t_0) = -(g_y(t_0))^{-1} g_{\underline{x}_0}(t_0) \tag{10}$$

$\underline{f}_{\underline{x}}$, $\underline{f}_y$, $g_{\underline{x}}$ and g_y are time varying functions which are calculated along the system trajectories. When an event like a short circuit fault occurs in the power system, jump condition should be derived for computation of the trajectory sensitivities which is fully described in [10]. To find the trajectory sensitivities, the differential algebraic equations (5), (6), (7) and (8) should be solved simultaneously with the initial conditions described above.

In this paper, since power system is going to be analyzed before fault occurrence, the system works in its operating point and all the state and algebraic variables are fixed. The trajectory sensitivities are computed using (7) and (8) with the initial condition described in (9) and (10), and as a result of non zero initial values, trajectory sensitivities will oscillate around their operating points. These oscillations exactly show how sensitive are state and algebraic variables to the system parameters for small disturbances in the system and will be used here as a tool for optimal placement of series compensators to improve small signal stability of power system.

III. Small signal stability assessment using trajectory sensitivity analysis

One way to investigate the small signal stability is to monitor rotor angles of generators (dynamic states δ) under small disturbances. If their oscillation are positively damped and decay with time, the power system is stable. Otherwise, there will be a negative damping in electromechanical oscillation which results in oscillatory instability. To improve the small signal stability, power system parameters can be controlled (if applicable) in a way to have positive effects on the power oscillation damping when the system is subjected to small disturbances and prevent power system from being oscillatory unstable. Impedance of transmission line is one of these parameters which can have a considerable effect on the stability of power system by controlling power flows in the transmission lines. Series FACTS devices like TCSC can control the impedance of transmission lines in a way to enhance the small signal stability of power system. Due to heavy cost of these devices, it is not economical to install several TCSCs in a power system, and therefore, the TCSC should be installed in the transmission line whose reactance modulation will be more effective to damp out the oscillatory modes of interest.

Since the goal of this paper is to calculate the trajectory sensitivities of rotor angles of generators to the impedances of transmission line, the matrices of power system parameters and trajectory sensitivities of dynamical states to the system parameters are as follows

$$\lambda = [x_{L_1} x_{L_i} ... x_{L_{n_l}}] \tag{11}$$

$$\frac{\partial \delta}{\partial \lambda} = \begin{bmatrix} \frac{\partial \delta_1}{\partial x_{L_1}} & \frac{\partial \delta_1}{\partial x_{L_i}} & \cdots & \frac{\partial \delta_1}{\partial x_{L_{n_l}}} \\ \frac{\partial \delta_2}{\partial x_{L_1}} & \frac{\partial \delta_2}{\partial x_{L_i}} & \cdots & \frac{\partial \delta_2}{\partial x_{L_{n_l}}} \\ \cdot & \cdot & \cdot & \cdot \\ \cdot & \cdot & \cdot & \cdot \\ \cdot & \cdot & \cdot & \cdot \\ \frac{\partial \delta_n}{\partial x_{L_1}} & \frac{\partial \delta_n}{\partial x_{L_i}} & \cdots & \frac{\partial \delta_n}{\partial x_{L_{n_l}}} \end{bmatrix} \tag{12}$$

where x_{L_i} is the impedance of i^{th} transmission line, n_l is the number of transmission lines, δ_j is the rotor angle of j^{th} generator, and n is the number of generators. The matrix (12) is a part of solution to the equation (7) described in section II.

A. Definition of equivalent angle

In this part, an equivalent angle is defined and the trajectory sensitivity of this angle to the impedances of transmission lines is introduced for appropriate placement of series compensators. The right eigenvector corresponding to the mode of interest of the system has been used to determine how this mode is distributed among different generators of the system. Based on this modal analysis, generators are divided to two groups named A and B which oscillate against each other and then these two groups is replaced by a single machine equivalent system. B group consist of those generators which are more stable compared to the ones in A group. The equivalent angle includes all the rotor angles and is defined as follows [11]

$$M_A = \sum_{i \in A} M_i, \quad M_B = \sum_{j \in B} M_j \tag{13}$$

$$\delta_A = M_A^{-1} \sum_{i \in A} M_i \delta_i, \quad \delta_B = M_B^{-1} \sum_{j \in B} M_j \delta_j \tag{14}$$

$$\delta_{eq} = \delta_A - \delta_B \tag{15}$$

where M_i and δ_i are the inertia and rotor angle of i^{th} generator, respectively. According to this definition, the trajectory sensitivity of the equivalent angle to the impedances of transmission lines is as follows

$$\frac{\partial \delta_{eq}}{\partial x_{L_i}} = \frac{\partial \delta_A}{\partial x_{L_i}} - \frac{\partial \delta_B}{\partial x_{L_i}} \tag{16}$$

where

$$\frac{\partial \delta_A}{\partial x_{L_i}} = M_A^{-1} \sum_{i \in A} M_i \frac{\partial \delta_i}{\partial x_{L_i}} \tag{17}$$

$$\frac{\partial \delta_B}{\partial x_{L_i}} = M_B^{-1} \sum_{j \in B} M_j \frac{\partial \delta_j}{\partial x_{L_i}} \tag{18}$$

B. The proposed algorithm

1) Trajectory sensitivities of rotor angles with respect to the impedances of transmission lines are calculated solving (5), (6), (7) and (8) simultaneously, and without any fault in the system (before fault occurrence time). Simulation time does not need to be so long.
2) System modes can be determined using following A matrix
$$A = \underline{f}_{\underline{x}} - \underline{f}_{\underline{y}} g_y^{-1} g_{\underline{x}} \tag{19}$$
$\underline{f}_{\underline{x}}$, $\underline{f}_{\underline{y}}$, $g_{\underline{x}}$ and g_y were defined in (7) and (8). The mode of interest can be found using the above matrix.
3) The mode of interest which is usually the one with poor damping and lower frequency is chosen. Based on modal analysis, A and B groups of generators are determined. It can be done using right and left eigenvector corresponding to the mode of interest and depicting compass plot.
4) According to (16), trajectory sensitivities of equivalent angle to the impedances of transmission lines are plotted using the obtained data in step 1. The ones which have the maximum positive amplitudes of oscillation are the most effective locations for placement of TCSC to improve the small signal stability.

IV. Optimal placement of TCSC using residue factor

This method is based on the fact that shift of the eigenvalue caused by the TCSC controller is proportional to the magnitude of the corresponding residue. To verify the validity of the proposed algorithm in this paper, the method described in [7] is implemented according to the following procedure to find the best places to install TCSC.

1) Power system is linearized around its operating point and the mode of interest which is going to be improved is determined. The industrial software SIMPOW®11 is used for this simulation [11].
2) TCSC is placed at different transmissions lines and for each location, the power system is linearized around its operating point considering the active power of that line as the input signal and equivalent speed of generators ω_{eq} as the output signal. Equivalent speed can be calculated based on (13)-(15) using generator speeds instead of rotor angles.
3) For each location of TCSC, Residue factor associated with the mode of interest (λ_i) is calculated as follows
$$R_i = |C V_i^r V_i^l B| \tag{20}$$
where C and B are the output and input matrices after linearization, respectively. V_i^r is the i^{th} column of right eigenvector and V_i^l is the i^{th} row of left eigenvector.
4) The transmission line with the maximum positive value of residue is the most suitable place to improve the mode of interest and therefore small signal stability [7].

V. Simulation and results

A. Proposed method implementation

The IEEE 3-machine 9-bus system shown in Fig. 1 is used to evaluate the proposed algorithm, the system data is available in [12]. The reactances of transformers are included in transient reactances of generators. Classical model is used for generators. Table I shows the most important modes of the system based on the linearization around the operating point. The compass plots depicted in Fig. 2 shows that for modes 1 and 2 which are the ones with lower frequencies, generator 1 oscillate against generator 2 and 3. Modes 1 and 2 are selected as modes of interest. Since the goal is to improve the mode of interest, equivalent angle is defined based on (15) considering generator 2 and 3 as the A group and generator 1 as the B group. Equations (5), (6), (7) and (8) are solved simultaneously using system parameters introduced in (11). Figure 3 shows the trajectory sensitivity of the equivalent angle to the impedances of different transmission lines. Table II demonstrates the priorities to install TCSC for improving small signal stability based on the peak values of the calculated trajectory sensitivities. It can be seen that line 3, 6 and 4 have the largest values, respectively and are the best places to install TCSC for improving small signal stability. Table II also shows that putting TCSC in the transmission line 1, 2 and 5 have a negative effect on the mode of interest and can worsen the small signal stability.

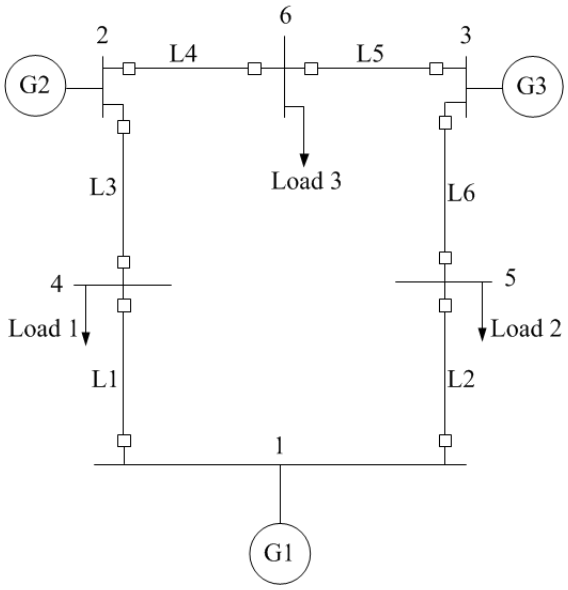

Fig. 1. Modified IEEE 3-machines test system.

TABLE I
Oscillatory modes of the test system

Mode no	Eigenvalue	Oscillating generators
1,2	$0 \pm 1.6339i(Hz)$	Gen1 vs Gen2 and Gen3
3,4	$0 \pm 2.4626i(Hz)$	Gen2 vs Gen3

TABLE II
Trajectory sensitivities of equivalent rotor angle to the impedance of different transmission lines - Peak to bottom values

Line no	**Peak to bottom value**
1	-0.0575
2	-0.0649
3	**2.4623**
4	**0.3873**
5	-0.0605
6	**1.6402**

B. Residue method implementation

Industrial software SIMPOW®11 is used to calculate the absolute value of residue in the presence of TCSC at different transmission lines. First, it is necessary to describe shortly how TCSC has been modeled in this study. Fig. 4 shows a transmission line equipped with a TCSC. The active power flow through transmission line between bus i and bus m when impedance of line is just a reactance is equal to

$$P_{im} = \frac{U_i U_m}{X_{eff}} \sin(\theta_{im}) \tag{21}$$

$$X_{eff} = X_{line} - X_{TCSC} \tag{22}$$

Where, X_{eff} is the value of effective reactance of the transmission line between Bus i and Bus m, X_{line} is the reactance of the transmission line, X_{TCSC} is the reactance of TCSC, U_i and U_m are the voltage magnitude of Bus i and Bus m, and θ_{im} is the angle difference between Bus i and Bus m.

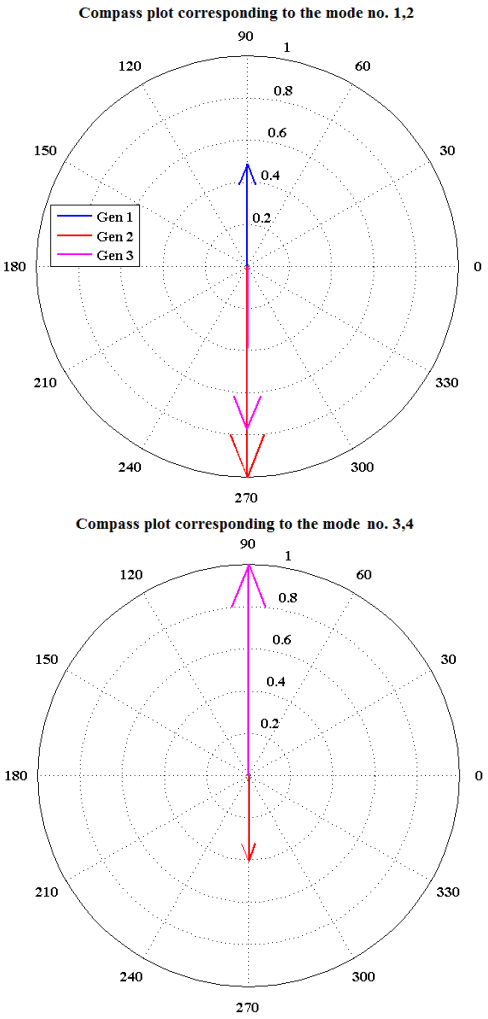

Fig. 2. Compass plot corresponding to the modes no. 1,2 and no. 3,4

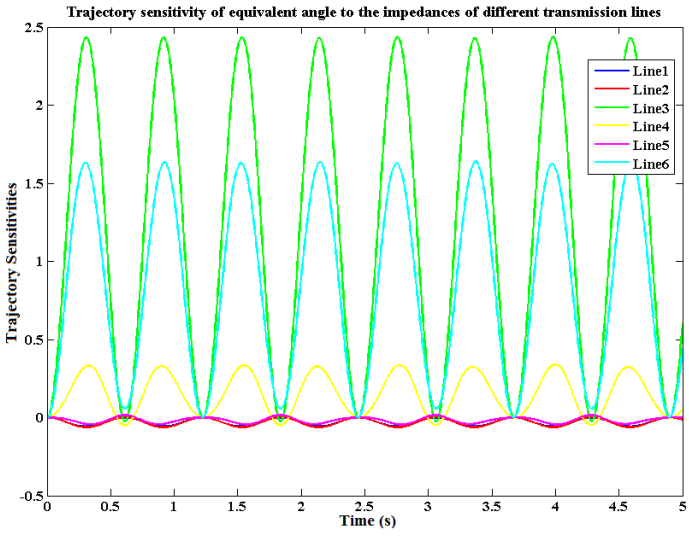

Fig. 3. Trajectory sensitivity of equivalent rotor angle to the impedances of different transmission lines

Since the transmitted active power is inversely proportional

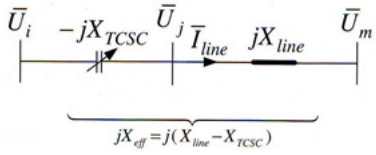

Fig. 4. TCSC steady-state circuit series with a transmission line

to X_{eff}, variation of X_{eff} (due to the TCSC) results in variation of the power flow in the line. Therefore, TCSC can be used as a powerful means for controlling power flows in the transmission lines and for improving power oscillation damping in power systems. X_{TCSC} is

$$X_{TCSC} = X_{TCSC_0} + \triangle X_{TCSC} \tag{23}$$

where X_{TCSC_0} is the TCSC steady state reactance and $\triangle X_{TCSC}$ is the stability control modulation reactance. Controller which is used in this paper is based on the control lyapunov functions defined in [13]. According to these functions

$$\triangle X_{TCSC} = k_{TCSC} \sin(\delta_{eq})\omega_{eq} \tag{24}$$

where k_{TCSC} is a positive gain and ω_{eq} is the equivalent speed of generator.

After implementing TCSC in the industrial software, TCSC is placed in different transmission lines. For each location, the magnitude of residue has been calculated and shown in Table III. The results are very similar to the ones shown in Table II, and Line 3, 6 and 4 are the most effective places to install TCSC for improving small signal stability, respectively. It should be mentioned that this method cannot show the installation locations that have a negative effect on the mode of interest and therefor small signal stability.

TABLE III
Absolute value of residue in the presence of TCSC at different transmission lines

Line no	Residue Index
1	0.0397
2	0.0443
3	**1.6911**
4	**0.2434**
5	0.0338
6	**1.1082**

To verify the correctness of obtained results, the exact changes of mode of interest after installing a TCSC in different transmission lines have been calculated. As it can be seen in Figure 5 and also Table 4, putting TCSC at line 3 can move the mode of interest to the more desires position.

VI. CONCLUSION

This paper proposes a novel method which uses trajectory sensitivity analysis as a tool to determine the effects of changing impedances of different transmission lines on the small signal stability of power system. Using the proposed

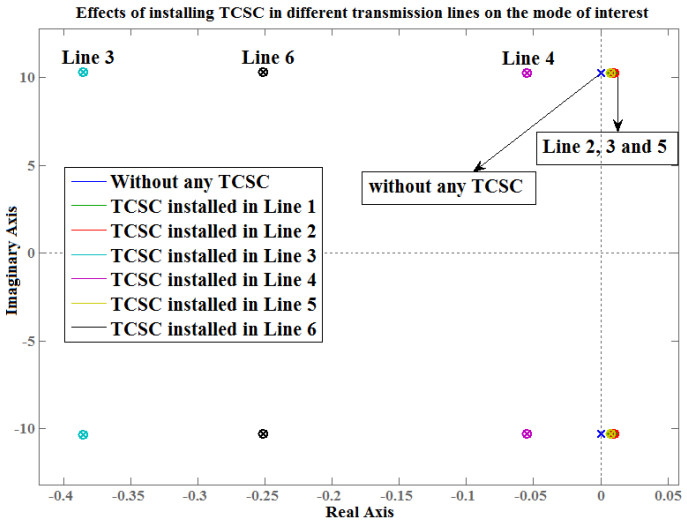

Fig. 5. Effects of installing TCSC in different transmission lines on the mode of interest

TABLE IV
Changes in mode of interest after installing a TCSC in different transmission lines

TCSC Location	Mode of interest
without any TCSC	0.0000 ± 10.2721i
TCSC installed in transmission line 1	0.0076 ± 10.2706i
TCSC installed in transmission line 2	0.0100 ± 10.2704i
TCSC installed in transmission line 3	-0.3853 ± 10.3306i
TCSC installed in transmission line 4	-0.0550 ± 10.2812i
TCSC installed in transmission line 5	0.0089 ± 10.2708i
TCSC installed in transmission line 6	-0.2512 ± 10.3130i

method, it is possible to find the most effective places to install series compensator with just one simulation instead of repetitive simulations, which will reduce significantly the computational cost. It has also been shown that installing series compensators in the transmission lines does not always improve the small signal stability of power system. The proposed method has been applied to the IEEE 3-machine 9-bus system using thyristor controlled series compensator. MATLAB®10b has been used for implementation of the proposed method, and finally results have been verified using industrial software SIMPOW®11. This method can be extended in a way to be applied to the other types of FACTS devices and along with the method described in [9] can be used as a powerful package to analyze the effects of any types of FACTS devices on both small signal and transient stability of power system.

ACKNOWLEDGMENT

Amin Nasri has been awarded an Erasmus Mundus PhD Fellowship. The authors would like to express their gratitude towards all partner institutions within the programme as well as the European Commission for their support.

REFERENCES

[1] M. E. Aboul-Ela, A. A. Salam, J. D. McCalley, J. D. McCalley, J. J. Fouad, "Damping Controller Design for Power System Oscillations Using Global Signals," *IEEE Transactions on Power Systems*, vol. 11, No. 2, pp. 767-773, May 1996.

[2] B. K. Kumar, S. N. Singh, S. C. Srivastava, "Placement of FACTS controllers using modal controllability indices to damp out power system oscillations," *Generation, Transmission and Distribution, IET,*, vol. 1, pp. 209-217, March 2007.

[3] P. Preedavichit, S. C. Srivastava, "Optimal reactive power dispatch considering FACTS devices," *Fourth International Conference on advances in Power System Control, operation and management*, vol. 2, pp. 620-625, November 1997.

[4] K. S. Verma, S. N. Singh, H. O. Gupta, "FACTS devices location for enhancement of total transfer capability," *Power Engineering Society Winter Meeting*, vol. 2, pp. 522-527, January 2001.

[5] E. A. Leonidaki, N. D. Hatziargyriou, G. A. Manos, B. C. Papadias, "A systematic approach for effective location of series compensation to increase available transfer capability," *IEEE Porto Power Tech Conference*, vol. 2, September 2001.

[6] M. Saravanan, S. M. R. Slochanal, P. Venkatesh, P. S. Abraham "Application of PSO technique for optimal location of FACTS devices considering system loadability and cost of installation," *The* 7^{th} *International Power Engineering Conference*, IPEC 2005, vol. 2, pp. 716-721, November 2005.

[7] N. Magaji, M. W. Mustafa,"Optimal location of FACTS devices for damping oscillations using residue factor," *IEEE 2nd International Power and Energy Conference*, PECon 2008, pp. 1339-1344, December 2008.

[8] L. Rouco, F. L. Pagola, "An eigenvalue sensitivity approach to location and controller design of controllable series capacitors for damping power system oscillations," *IEEE Transactions on Power System*, vol. 12, pp. 1660-1666, November 1997.

[9] A. Nasri, M. Ghandhari, R. Eriksson, "Appropriate Placement of Series Compensators to Improve Transient Stability of Power System," *Accepted in IEEE PES Innovative Smart Grid Technologies (ISGT Asia 2012) Conference*, May 2012.

[10] I. A. Hiskens, M. A. Pai, "Trajectory sensitivity analysis of hybrid systems," *IEEE Trans. circuits and systems*, vol. 47, no. 2, February 2000.

[11] SIMPOW: Simulation of Power System, http://simpow.com/index.html

[12] M. A. Pai, "Energy Function Analysis for Power System Stability," Appendix A, 2007.

[13] M. Ghandhari,G. Andersson, M. Pavella, D. Ernst "A control strategy for controllable series capacitor in electric power systems,"*Automatica 37*, pp. 1575-1583, 2001.

Amin Nasri received his M.Sc. degree in Electrical Engineering from the Sharif University of Technology, Tehran, Iran, in 2008. He is pursuing the Erasmus Mundus Joint Doctorate in Sustainable Energy Technologies and Strategies (SETS) hosted by Comillas Pontifical University, Spain; the Royal Institute of Technology, Sweden; and Delft University of Technology, The Netherlands. He is currently a Ph.D. Student in the Division of Electric Power Systems, School of Electrical Engineering at KTH Royal Institute of Technology.

Mehrdad Ghandhari received the M.Sc., Tech. Lic. and Ph.D. degrees in Electrical Engineering from Royal Institute of Technology, Stockholm, Sweden, in 1995, 1997, and 2000, respectively. He is currently Associate Professor at KTH Royal Institute of Technology.

Robert Eriksson received his M.Sc., Tech. Lic. and Ph.D. degrees in Electrical Engineering from KTH Royal Institute of Technology, Stockholm, Sweden, in 2005, 2008 and 2011 respectively. He is currently a Postdoctoral researcher in the Division of Electric Power Systems, School of Electrical Engineering at KTH Royal Institute of Technology.

For KTH Royal Institute of Technology:
DOCTORAL THESIS IN ELECTRICAL ENGINEERING
TRITA-EE 2014:048
www.kth.se

ISSN 1653-5146
ISBN 978-91-7595-302-1